STUDIES IN ENGINE TEST BED AUTOMATION.

by

J.V.Comfort, M.Sc., B.Sc.

A thesis submitted to the University of Warwick for the degree of Doctor of Philosophy.

November 1970.

ABSTRACT.

The work described in this thesis was initiated in response to motivation from the needs of industry, the desire to investigate the performance of a process control computer in a relatively novel application as well as to provide training in methods of research.

Ever-increasing labour costs have caused the automotive and petroleum industries to seek new means of maintaining the throughput of engine testing work. Their task has been made more difficult by the stringent test regulations that have been introduced with the very commendable intention of reducing atmospheric pollution. In consequence, any means by which the efficiency of testing could be improved and the throughput of work increased were deemed worthy of investigation.

Engine testing involves a diversity of simple repetitive operations. These include the collection and processing of data and the execution of logical operations. The digital computer has proved itself to be ideally suited to performing such tasks, but the problem of intsgrating a computer with such an activity remains only partially solved. It is hoped that the work described in this thesis will go some way towards solving this problem.

A description of the instrumentation and interfacing used on the test rig is included together with a description of the program structure and functions. These are not regarded as exemplory but it is hoped that they will aid the identification of the requirements for similar systems.

A linearised mathematical model is developed to represent both the static and dynamic behaviour of the engine and dynamometer. This aspect of the study has provided useful insight into the problems associated with the control of engine test rigs. As a result it has been shown that effective control can be made available without recourse to highly sophisticated techniques.

Optimisation systems as applied to the control of spark timing and mixture strength are considered. The limitations imposed on their operation by the inherent nature of combustion are outlined.

Finally some computer controlled tests that were implemented are described as a means of illustrating the very extensive capabilities of such a system.

ACKNOWLEDGEMENTS.

I should like to acknowledge the advice and assistance given to me by "Shell" Research Ltd., The Ford Motor Co. Ltd. and Crysler U.K. (formerly Rootes Ltd.) Their invaluable help tendered on numerous occasions has enabled me to gain some useful insight into engine testing procedures.

I am also indebted to Mr.T.M.W.Weedon of the B.L.M.C. Group Pollution Research Unit and to my supervisor Dr.M.T.G.Hughes for their advice and recommendations.

Finally, I should like to thank the technicians of the School of Engineering for their assistance and Mrs.C.Allsopp and Mrs.P. Johnson for typing this thesis and reproducing the drawings.

CONTENTS.

Chapter 4.

THE MATHEMATICAL MODELLING STUDY.

Chapter 5.

CONTROL SYSTEMS.

Chapter 6.

PROGRAMS FOR EXPLORATORY COMPUTER CONTROLLED TESTING

Chapter 7.

OPTIMISATION STUDIES.

Chapter 8.

COMPUTER CONTROLLED TESTS.

CHAPTER 1.

INTRODUCTION.

1. Examination of the engine testing activity with special reference to automation.

2. Aims of the research work.

1. Examination of the engine testing activity with special reference to automation.

Internal combustion engine performance evaluation is not generally amenable to analytical treatment and so it must be achieved by experimental running on a test bed. Implicit in the test function is a two-way communication between the engine and the engineer. It is an increase in the efficiency of this communication that this thesis attempts to promote.

Engine testing forms an important part of design, development and production. In production testing the objective is to complete the production operation by making final adjustments and checks to satisfy the product specification. Design and development testing involves more diverse test operations which at times involve a considerably higher degree of test operator participation.

Engine testing, as well as being an important function in manufacture, is also used to evaluate fuel and lubricant performance. The test bed provides simulated service conditions where measurements can be carried out with greater precision.

In the past the communication between the engine and the design, development or production engineer has been achieved by the liberal use of manpower specially trained for the purpose. A more effective use of the human operator is essential for the development of engine testing. This can only be achieved by the delegation of the lower responsibilities of testing to automatic systems and by improving the quality of the test data presented to the engineer.

Employment conditions no longer favour a liberal deployment of manpower for this purpose and the use of automation is therefore essential if the throughput of experimental work is to be increased without the uneconomic duplication of facilities. This factor was largely responsible for the motivation of these studies.

The need for automation in engine testing has been keenly felt by the automotive and petroleum industries for a considerable time, and already a number of computer controlled engine test facilities have been commissioned, mostly in the United States (1). Initial operating experiences with these are favourable, but the lack of operating experience of process control digital computers in this field is restricting the usefulness of such installations, which otherwise appear to offer considerable scope for development.

The advantages offered by computer controlled test facilities are that they can provide higher quality test data in a form which is easily assimilated. Furthermore, the data can be made available within seconds of the completion of a test. This time reduction can lead to more effective utilisation of test facilities. In return it is necessary to standardise engine installation procedures, which in itself is desirable, and to implement more careful planning and specification of tests than is at present associated with manual testing procedures.

Some engine test activities are briefly examined in this thesis in order to indicate the scope for computer control and the problems that exist in its application.

As has already been indicated engine testing forms a significant function in the process of fuel and lubricant development. This is a continual process and it relies on the results of comparative tests which are usually carried out in an adverse environment. Test procedures demand an accurate control of environmental conditions, and often a considerable amount of data acquisition and processing is required. The stabilisation of operating conditions is known to present a real difficulty. A knowledge of typical static and dynamic system transfer characteristics for an engine test bed is therefore desirable in order to provide an indication of the best attainable controlled performance and to suggest practical solutions to the

control problems which are known to exist. For this reason a study was undertaken to develop a mathematical model to represent the most important system transfer functions of a typical engine test bed.

Many engine test activities may be considered as multi-parameter optimisation processes. An example exists in the design of ignition and carburation systems. In practice the cost functions and constraints define exceedingly complex problems which at present are not amenable to mathematical formulation and solution. Practical solutions necessarily involve a reduction of the problem to a scale that can be tackled by the human operator employing experimental methods. Often these are very time consuming. There is scope for a re-appraisal of these problems to utilise advances in electronic instrumentation and the calculating power of the digital computer. The implementation of even the most simple automatic optimisation procedures would save a considerable amount of operator time on some development test procedures.

A recently occurring aspect of engine testing is the quantitative measurement of exhaust gas emissions. In order that vehicles shall be eligible for sale in certain parts of the world exhaust gas emissions must satisfy certain tests. Processing of this test data involves a considerable amount of calculation. An on-line computer controlled test facility can provide the results of a test within seconds of completion, as well as performing routine calibration of the equipment, whereas manual scanning of the data coupled with off-line processing would take several hours to provide comparable results. (2)

Durability testing is another area in which computer control can usefully be applied. Often it is only when the failure of a component is in progress or has just occurred that information is required. The course of events during a failure is often extremely rapid and it is not always within the capability of the human operator to diagnose the conditions of impending component failure and to take appropriate

action. Computer controlled data logging and alarm scanning provides the ideal solution to this problem. Test programs can be designed so as to discard irrelevant data and to increase the rate of data collection in the advent of a suspected imminent failure.

It can be seen that the on-line process control digital computer can justifiably be applied to many facets of engine testing. In particular the computer can aid the design and development processes as well as perform the more mundane testing operations. (3) The application does introduce interfacing problems and the need to re-appraise test procedures in order to exploit fully the new means of solution.

Prior to 1965 automation of engine testing was limited to automatic data logging of endurance tests and simple electromechanical sequencing of test conditions. One of the first on-line computer controlled test facilities was commissioned in the United States in 1966. (1)

2. Aims of the research work.

The general aims of the research work described in this thesis were to examine the problems of communication between the engine and computer in a practical test installation and to demonstrate the feasibility of the computer playing an important part in the engine development process. It was felt that a university provided an ideal environment for a study of this kind compared with an industrial organisation, the latter being restricted by the demands of routine testing. A computer controlled test facility for a single engine was therefore established for this purpose.

CHAPTER 2.

AUTOMATION IN THE AUTOMOTIVE INDUSTRY.

1. Engine test activities.

2. Aims and objectives of tests.

3. Some examples of tests.

4. Projected computer functions.

1. Engine test activities.

Consideration of engine test activities carried out once the engine is installed on the test bed reveals that all types of testing combine the execution of certain basic test operations. These operations are listed:-

1. Setting up operating conditions.
2. Making measurements and collecting data.
3. Processing and presentation of collected data.
4. Execution of decisions based on measurements and processed data.

2. Aims and objectives of tests.

The purposes of testing may be broadly classified as either performance or durability testing. Performance testing is concerned essentially with an examination of the process whereby the chemical energy of the fuel is converted into useful work. The efficiency of this conversion is the chief concern of the test, but it is also necessary for the engine to demonstrate such properties as adequate lubricating oil and coolant flows.

Performance testing is thus characterised by the accumulation of a large quantity of data. The data must be processed and converted into a form which can easily be assimilated by the engineer. This will necessarily involve data reduction, and information of this type is usually presented in the form of graphs. Attempts have been made to automate the processing, conversion and accumulation individually, but only when all three are automated together can any really significant time saving be achieved in the production of the completed results.

The requirements of durability testing are of a different nature since the objectives are concerned with the accumulation of running time.

Data acquisition whilst running is of secondary importance unless relevant to component life and failure. The majority of data is collected when the engine is dismantled for inspection on completion of the test schedule. Less flexibility is required with durability testing. The basic test operations however are still involved.

3. Some examples of tests. (4)

The specification of a typical performance and a typical durability test are examined to establish current practices and to indicate where automation can increase efficiency.

Example 1. To check full throttle power output for an established type of production engine. The objective is to determine the maximum power obtainable from the slowest stable running speed to at least 250 R.P.M. beyond the speed where maximum power is obtainable. The test bed conditions are made to resemble those of service as accurately as possible. The following measurements are taken over the range of speeds at intervals of 500 R.P.M. or less.

1. Air intake temperature.
2. Engine speed with an accuracy of better than ± 0.5%
3. Engine torque " " " " " " ± 1.0%
4. Fuel flow rate " " " " " " ± 2.0%
5. Air flow rate.
6. Sump oil temperature.
7. Water outlet temperature.
8. Optimum ignition timing.

Barometric readings are required before and after the test. At each point the test operator is required to optimise ingition timing and mixture strength to give maximum torque. In addition the speeds for maximum torque and maximum power are determined. The test involves approximately 18 groups of measurements. An average test operator takes 5 minutes to complete the measurements

at each speed. On completion of the test the following data is required in graphical form.

1. Corrected brake horse power v.s. speed.
2. Corrected brake mean effective pressure v.s. speed.
3. Corrected torque v.s. speed.
4. Corrected specific fuel consumption v.s. speed.

The calculations required to present this data require a similar amount of time to the test when executed by hand.

The manual execution of this test schedule is compared with a projected computer controlled execution in order to underline the shortcomings of the manual approach.

The accuracy of the initial mechanical setting up of the engine relies solely on the efficiency of the fitter responsible. A computer generated check list would help to ensure more rigorous observation of setting up procedures and reduce the risk of tests being run under improper operating conditions.

At each speed in the test a two-parameter optimisation process is required. This is followed by the recording of several variables. The recording will invariably include averaging noisy readings by eye. If the optimisation and measurement were executed by a computer a higher output data quality could be achieved by the systematic filtering of measurements. Even the most simple computer controlled optimisation routines can achieve comparable accuracy to the human operator. By a slight re-arrangement of the measurement procedure the corrected results could be made available whilst the test was in progress. A single parameter optimisation process could be used to indicate the speeds at which maximum brake horse power and maximum brake mean effective pressure occur. Furthermore, the computer can be used to check proper operation of the engine during the test and shut down the engine if any impermissible conditions should occur.

Example 2. A 301 hour endurance test. The objective of this test is to prove the durability of engines and components. Initially the engine is run-in and then stripped for inspection. After the test the engine is stripped once again for another comparative examination. External control of oil and water temperatures is required to simulate a severe environment. The measurement of oil leaks is also required.

The test consists of 67 cycles of a 5 hour 50 minute schedule. This schedule is summerised in the table below.

R.P.M.	LOAD.	TIME (minutes)
1000	Nil	10
500 above max. power	full	10
Max. torque	¾ full	10
80% max. power	¾ full	60
40% max. power	full	60
40% max. power	¼ full	10
90% max. power	full	60
Max. torque	¾ full	10
Max. power	full	60
Max. power	¼ full	60 *

* The pressure drop across the oil filter is measured during the last item of the schedule to indicate if a renewal is required.

After each cycle the oil level is checked and a measured amount added to bring the level within the prescribed limits. After every 3rd cycle the engine is allowed to stand for 10 minutes, a measured quantity of oil is added to bring the level up to the full mark and the tappets are adjusted. After every 9th cycle a full throttle power curve is taken, crankcase blowby is measured and compression pressures are checked.

The condition of sparking plugs and contact breaker points are checked and brought within specification. After every 22 cycles the engine oil is changed.

The test schedule requires frequent operator attention to change load and speed conditions. Computer controlled sequencing of the test conditions is all that is required to relieve the test operator of this duty. Several servicing and checking operations are required between the cycles of the schedule. Interfacing these operatings is not considered feasible, but greater consistency would be ensured if the servicing were carried out under the supervision of the computer.

4. Projected computer functions.

In the evolution of the design of an ideal computer controlled test facility capable of performing functions such as those described above it is necessary to design a computer system structure which will perform the following functions:-

1. Simultaneous control of several test cells, performing all present and forseeable test routines with a minimum of direct intervention by the test operator.
2. Acquisition and processing of appropriate test data.
3. Monitoring data for out-of-limit conditions, and the execution of appropriate corrective action.
4. Presentation of test data in an efficient form with the minimum of delay.
5. Provision of instrument calibration and functional checking of test facility operation.
6. Interaction with the test engineer at the highest possible level.

7. To act as a guardian to any test function that it is not feasible to interface and run solely under computer control.

8. To process off-line data. For example, the assembly of new test routines and the maintenance of stores inventories.

9. Permit operator intervention and access to control functions at all levels when they are required.

10. Provide a test program library and storage facilities for other relevant data.

11. Perform other reasonable administrative duties for the test facility.

Two major problems exist in satisfying these requirements, namely the development of a hardware structure and the development of programs to control testing activities. The hardware structure must fulfil the basic function of physically linking the test operator to the engine via the computer. It is the link between the computer and the engine which presents the major problem. In comparison the link between the computer and the human operator is well developed.

In the evolution of a hardware structure it is necessary to consider the extent to which automation is feasible and to decide on the degree of centralisation required. Both will depend on the nature of the test function. At this time when operating experience of computer controlled test installations is minimal a small degree of centralisation is desirable in order to permit operator intervention between the computer and measurement and control actions. This requirement defines the need for local control and measurement units to permit tests to be run without reference to the computer if so desired. The provision of local control loops also relieves the computer of the computation necessary to service these loops, which in a sizeable installation would severely restrict the availability of the computer for other functions.

The two functions of the engine/computer interface are control and measurement. A list of the variables most frequently involved in spark ignition engine testing is given:-

Controls

Throttle opening angle

Air/fuel ratio

Ignition timing

Coolant temperature

Lubricant temperature

Dynamometer load torque

Measurements

Torque

Speed

Fuel flow rate

Air intake flow rate

Air intake temperature

Barometric pressure

Crankcase blowby

Ignition timing

Throttle opening

Coolant temperature

Lubricant temperature

Dynamometer excitation current

Optimum methods of measurement and control of engine variables when interfaced to a computer are by no means established. An objective of this thesis is to examine some methods and to suggest practical solutions to the problems involved.

Relevant experience gained in the chemical process industry can be applied to the development of programs for engine testing. The requirements of engine testing are in comparison more demanding in so much that control functions must be executed more quickly and a highly adaptable program structure is necessary. Program functions fall into 3 categories.

1. Real time executive control of program subroutines.
2. Individual test control involving data acquisition, processing and output.
3. Off-line data processing, including the assembly of new test routines.

Executive control programs are already available for the majority of established process control computers: these have been developed as a result of the needs of the chemical industry. However, few engine test control programs exist. To achieve flexibility new test programs should be as easy as possible to write and correct. This suggests the need for a high-level engine tester's computer language. Such a language cannot be developed without some first hand experience of computer controlled testing to indicate the functional requirements.

CHAPTER 3.

DEVELOPMENT OF THE EXPLORATORY COMPUTER CONTROLLED TEST FACILITY.

1. The structure of the test facility. The test cell, control room and computer laboratory.

2. A description of the engine, dynamometer and process control computer.

3. Instrumentation for the mathematical modelling studies.

4. Further instrumentation to facilitate on-line testing.

The development of the shaft torquemeter and ignition timing control was undertaken jointly with another research student J.Monk.

1. The structure of the test facility.

The choice of engine and dynamometer was made so that the results of the study would be relevant to the automobile industry. For this reason the engine chosen was representative of the design used to power the majority of medium sized British saloon cars. The type of dynamometer chosen for the study is to be found in large numbers in test installations throughout the automobile industry.

A small fast process control digital computer with a general purpose interface was available in the school, and instrumentation was developed to be compatible with this computer interface.

The development of the exploratory test facility proceeded in two stages. Firstly electrical control of engine operation from an adjacent control room was established. This enabled mathematical modelling studies and control system design to be carried out. Secondly computer programs were developed and the appropriate interfacing constructed to enable tests to be run under computer control, the control signals and measurements passing via the control room to the computer. Whilst under computer control the test operator's requirements were communicated to the computer via the on-line typewriter.

The various component parts of the test facility are described:-

The engine test cell.

The engine test cell housed the engine and dynamometer together with their associated transducers and actuators. The test cell was equipped with a cooling water main for the removal of waste heat from the engine and dynamometer. There was a fan driven air supply and extraction system and a compressed air supply to power the dynamometer lubrication and the carburettor float chamber pressure regulator.

The engine control room.

The control room was adjacent to the engine test cell which could be viewed through reinforced windows. The remainder of the engine control and instrumentation equipment was located in the control room. Manual control of all test operations was possible from the control console. Under computer controlled operation the console was wired to the computer interface.

The computer room.

The digital computer and its interface were housed some 250 ft. from the engine in another part of the school. This provided an excellent opportunity to study communication when the engine is remotely situated. Connections between the control console and the computer interface were made via coaxial cables. The on-line peripheral equipment for the computer, consisting of a typewriter, paper tape punch and paper tape reader were also situated in the computer room. Where results were plotted by the computer during a test an analog X-Y recorder in the computer room was connected to the interface for this purpose.

The engine. (Hillman Hunter).

The engine was a 4-cylinder in-line engine with a capacity of 1725 c.c. It has overhead valve gear operated by pushrods. The particular version used was fitted with an aluminium cylinder head and developed a maximum of 80 B.H.P. (gross) at 5000 R.P.M.

The engine mounted on the test stand closely resembled the type fitted to the corresponding production vehicle. Only modifications necessary to mount the engine on the stand and fit the instrumentation and control systems have been carried out. The test cell exhaust system is of corresponding dimensions to that of the vehicle.

The dynamometer. (Heenan and Froude dynamatic.)

The dynamometer was coupled directly to the engine flywheel by a short shaft incorporating rubber universal couplings. Power dissipation was by eddy currents which heat the inner surface of the dynamometer stator. The heat was removed by a constant stream of water pumped between the rotor and stator. The power dissipation rate was controlled by adjusting the excitation current in the field coil. This changed the total flux passing between the rotor and the stator, and the magnitude of the eddy currents. An a.c. tachometer was fitted at the front of the dynamometer to measure rotational speed and a damped spring balance and lever system measured the dynamometer reaction torque. The dynamometer has a maximum power dissipation capability of 200 B.H.P. at 10,000 R.P.M.

The computer. (G.E.C. 90/2).

The computer has a 12-bit word-length with 8K of core store. The central processor operated in the parallel mode and because of the short word length and elaborate addressing facilities most machine instructions occupied two words of the store. Numbers were held in the machine in 2's complement form. The memory cycle time was 1.75 μs.

The interface provided the following facilities:-

Analog inputs. (9 bits plus a sign bit.)

12	± 100 volt/± 10 volt.
5	± 1 volt.
6	± 100 volt.
1	± 250 volt.

The settling time taken by the analog input multiplexor limits the random access sampling rate to a maximum of 100 samples per second.

Analog outputs. (8 bits plus a sign bit.)

6	± 10 volt.

Digital inputs.

8 1-bit inputs in the form of voltage level sensors.

These are referred to as 'S.E.S.' inputs.

Digital outputs.

12 1-bit outputs in the form of relay closures.

Priority interrupt system.

8 levels. The first four levels assigned to:-

1. The input/output buffer associated with the on-line typewriter, the paper tape reader and the paper tape punch.
2. The real time clock.
3. The analog input multiplexor.
4. The digital outputs.

Clock pulse frequencies of 1000 Hz., 100 Hz., 50 Hz. and 10 Hz. were available.

The machine was programmed in the low-level assembly language S.D.S. Symbol. The language has been modified to include mnemonics for the particular interface instructions specific to the machine.

Instrumentation.

An instrumentation voltage range of 0 to +10 volts was chosen for all the analog inputs and outputs from the control console and transducers. This range was chosen for compatibility and to allow the use of linear integrated circuits in the instrumentation. A diagram showing the instrumentation and its availability to the computer and local controls is given in fig. 3.1.

3. Instrumentation for the mathematical modelling study.

The initial instrumentation and control systems were constructed to enable a basic mathematical model of the engine and dynamometer to be developed and experimentally verified. The model was developed to represent the transfer functions between the throttle angle and

dynamometer field current as inputs and the dynamometer speed and coupling shaft torque as outputs. For the modelling study the following instrumentation and control systems were required:-

1. Throttle angular position control.
2. Dynamometer field excitation current control.
3. Dynamometer speed measurement.
4. Coupling shaft torque measurement.

These systems are described in detail below.

Throttle angular position control.

No suitable angular position control for the throttle was found to be available and therefore a special purpose control was designed and constructed. Hydraulic and pneumatic controls were not considered since it was deemed desirable to avoid the need for hydraulic and pneumatic power supplies and the associated electro-hydraulic or electro-pneumatic valves. Three alternative types of electric drive for the throttle spindle were considered, namely a.c. and d.c. servomotors and stepping motors. The servomotors are essentially high speed low torque devices which require a gearbox in order to supply adequate torque for the throttle spindle accelerations. A stepping motor can provide adequate torque with direct coupling. Also, the field control of a stepping motor at low speeds is essentially a switching operation and can be achieved by low power devices. The chief disadvantage with stepping motor actuation is that the output angle is quantised. For the purposes of the investigation it was felt that the simpler drive requirements of the stepping motor warranted its choice.

A 200 steps per revolution stepping motor was used, 45 steps being required to traverse the throttle from fully open to fully closed. The motor output torque was sufficient to accelerate the throttle spindle up to the maximum slewing rate of 200 steps per second within $\frac{1}{2}$ of a step. The closed loop operation of the throttle

dynamometer field current as inputs and the dynamometer speed and coupling shaft torque as outputs. For the modelling study the following instrumentation and control systems were required:-

1. Throttle angular position control.
2. Dynamometer field excitation current control.
3. Dynamometer speed measurement.
4. Coupling shaft torque measurement.

These systems are described in detail below.

Throttle angular position control.

No suitable angular position control for the throttle was found to be available and therefore a special purpose control was designed and constructed. Hydraulic and pneumatic controls were not considered since it was deemed desirable to avoid the need for hydraulic and pneumatic power supplies and the associated electro-hydraulic or electro-pneumatic valves. Three alternative types of electric drive for the throttle spindle were considered, namely a.c. and d.c. servomotors and stepping motors. The servomotors are essentially high speed low torque devices which require a gearbox in order to supply adequate torque for the throttle spindle accelerations. A stepping motor can provide adequate torque with direct coupling. Also, the field control of a stepping motor at low speeds is essentially a switching operation and can be achieved by low power devices. The chief disadvantage with stepping motor actuation is that the output angle is quantised. For the purposes of the investigation it was felt that the simpler drive requirements of the stepping motor warranted its choice.

A 200 steps per revolution stepping motor was used, 45 steps being required to traverse the throttle from fully open to fully closed. The motor output torque was sufficient to accelerate the throttle spindle up to the maximum slewing rate of 200 steps per second within $\frac{1}{2}$ of a step. The closed loop operation of the throttle

control is described with reference to fig. 3.2. The angular position of the throttle spindle was measured by a potentiometer which was directly connected to the spindle. The throttle position as measured by this potentiometer was compared with the demanded position, and if the error exceeded the width of one step a gate was opened to connect the pulse oscillator to the appropriate input of the field drive circuit. The drive circuit commutated the motor field current causing a movement of one step for each input pulse.

Open-loop operation was also available and the throttle could be stepped sequentially in response to the movement of a key switch. The closed loop performance of the control was characterised by velocity limiting and output quantisation. A Nyquist plot showing the closed loop transfer function for 25% of full output amplitude is shown in fig. 3.3.

Dynamometer field excitation current control.

A field excitation current control and a closed loop speed control operating on field current were initially available with the dynamometer. The inputs of these controls were not accessible since they were neither referenced to earth nor floating. This, and the unsatisfactory performance of the speed control led to the decision to replace both the field excitation unit and the speed control with units compatible with the already established instrumentation standards.

The dynamometer field coil when driven from a voltage source had a time constant of approximately 0.5 seconds. For the optimum operation of control systems which operate on engine load torque it is desirable to be able to make changes in this torque as fast as possible. This in turn requires rapid changes in field excitation current which can only be achieved by driving the field coil from a current source. A practical current source must necessarily be limited by amplifier voltage swing and current handling capacity. The design of current source which was

developed had an output voltage swing of ± 60 volts and a maximum output current of 2 amps. The bi-directional output voltage capability was particularly useful in effecting fast reductions in field current. Inputs to this amplifier must be limited so as not to demand a reversal of the field current which the amplifier is capable of providing. (Dynamometers of this type have an inherent rectifying capability in as much as a current passing through them in either direction causes a torque of the same sign.)

The current control amplifier consisted of three parts namely:-

1. An integrated circuit operational amplifier to provide a source of loop gain.
2. A coupling voltage amplification stage.
3. A multiple emitter follower with a current source load to provide the large output current.

A circuit diagram for the amplifier is shown in fig. 3.4.

Speed measurement.

The speed control initially acquired with the dynamometer utilised the existing a.c. tachometer to provide a speed measurement. The same measurement was also used to drive the speed indicator. To make the tachometer output compatible with the chosen instrumentation standards it has been scaled down so that 10 volts corresponds to 5,000 R.P.M.

The rectified a.c. speed signal necessarily contained ripple, and since the acceptable level of ripple for various applications was not known the signal was passed through a variable time constant filter. The circuit diagram for speed measurement scaling and the variable time constant filter is shown in fig. 3.5.

Shaft torquemeter.

A shaft torquemeter was deemed necessary to investigate the interactions between the engine and dynamometer, and to indicate the

response of the engine to fast changes in throttle angle, mixture strength and ignition timing. No existing form of shaft torquemeter was found suitable to instrument the coupling shaft and so a special torquemeter was developed for the purpose.

Due to the short length of the shaft the only practicable method of torque measurement was by measuring shaft strain with strain gauges. The torquemeter employed these connected in a bridge configuration. The torque signal in the form of a voltage analog was transmitted via brass slip rings and silver graphite brushes. The initial design of torquemeter included an integrated circuit amplifier on the shaft to boost the bridge out-of-balance voltage. The power supply for the amplifier and the bridge was also transmitted through slip rings.

The initial design suffered from lack of sensitivity, poor slip-ring noise rejection and amplifier output voltage drift. These shortcomings were emphasized by the low strain levels in the shaft which occur during steady running. The shaft was designed to withstand the high transient torques which occur during load changes, and when the engine is stopped. The transient torques are up to 10 times higher than the maximum torque delivered under steady running conditions.

An improved design of torquemeter was developed to overcome these difficulties. A.c. excitation was applied to the strain gauge bridge to nullify the effects of amplifier drift, and by transmitting the torque signal as a frequency analog superior rejection of slip ring noise was achieved. The operation of the improved design of transducer is described with reference to fig. 3.6.

The voltage supply to the strain gauge bridge was derived from the output of the comparator. The two output voltage levels of the comparator are regulated with zener diodes. When the algebraic sum of the integrator and comparator voltages reached zero the output of the comparator changed sign and the direction of integration was reversed. The rate of integration and hence the output frequency

List of symbols used in the reference to fig. 3.7.

V_{z1} The zener breakdown voltage of Z_1

V_{z2} " " " " " Z_2

V_{z3} " " " " " Z_3

V_{z4} " " " " " Z_4

V_{rz3} The reverse zener voltage of Z_3

V_{rz4} " " " " " Z_4

V_{d1} The forward bias turn-on voltage of D_1

V_{c2} The voltage across the capacitor C_2

was directly proportional to the out of balance of the bridge. This circuit satisfied the requirement for an a.c. bridge supply as well as providing a frequency modulated output. (Oscillation will only be maintained while the rate of change of integrator output voltage is of opposite sign to the bridge supply voltage.) Adjustments were made to the bridge unbalance to bring the oscillation frequency into the range 1-1.3 kHz corresponding to the full range of torque applied in a positive sense. Noise rejection on the power supply slip rings was achieved with a voltage regulator between the slip rings and the measurement circuit. Slip ring noise on the output was further reduced by passing the frequency signal through a first order filter before demodulation.

The demodulation was performed by a high accuracy monostable. The action of the monostable is described with reference to fig. 3.7. At rest the output voltage remained at the positive voltage $V_{z3}+V_{rz4}$. A positive input pulse switched the output to the negative voltage $V_{z4}+V_{rz3}$. Positive feedback via C_2 ensured a fast decisive switching action. (The zener diode Z_2 defined the minimum negative voltage excursion of the non-inverting input of the amplifier). The capacitor C_2 charged through R_2 and V_{c2} approached $V_{z1}+V_{z4}+V_{rz3}$ with a time constant R_2C_2. When the non-inverting amplifier input voltage exceeds V_{d1} the output moved positively again to $V_{z3}+V_{rz4}$.

The high accuracy was achieved by defining the voltage levels with zener diodes and by ensuring decisive initiation and termination of the monostable pulse. The pulse train output of the monostable was filtered with a first order filter with a time constant of 10 milliseconds. The overall accuracy of this torque measurement was limited to 2% of full scale by strain gauge hysteresis.

4. Further Instrumentation to facilitate On-line Testing.

Further instrumentation was developed to provide local controls and measurements for the purposes of local optimisation and exploratory computer-controlled testing. This instrumentation is listed:-

1. Coolant temperature measurement.
2. Lubricant temperature measurement.
3. Fuel flow measurement.
4. Dynamometer torque measurement.
5. Air/fuel ratio control.
6. Ignition timing control.
7. On/off control of starter, ignition, and cold starting device.
8. Oil pressure measurement.

These systems are described in detail below.

Coolant temperature measurement.

In a vehicle closed loop control of coolant temperature is normally provided by a thermostatic valve in the cylinder head outlet pipe. This method of control was not adopted on the test bed since it did not permit adjustment of the setpoint. A negative temperature coefficient thermistor was used to measure the water temperature in the cylinder head outlet pipe. This measurement was employed in the closed loop control of coolant temperature. The control element was a motorised mixing valve which directed part of the flow through a heat-exchanger. When the test rig was under computer control water temperature was monitored for out of limit conditions by sampling the thermistor measurement. The circuit associated with this thermistor which provided an electrical analog of temperature is shown in fig. 3.8. The normal temperature range of the engine gave an output between 2 and 7 volts.

Lubricant temperature measurement.

Under test bed operation there is little or no forced cooling applied to the engine sump. It was therefore necessary to provide

cooling and closed loop control of lubricant temperature. The measurement and control systems were very similar to those applied to the coolant temperature control system. The thermistor probe was situated at the inlet to the main oil gallery.

Fuel flow measurement.

The purpose of measuring fuel flow was to employ the measurement in optimisation processes and the automatic plotting of mixture loops. For this reason a hot-film mass flow measurement system providing a continuous electrical analog of fuel flow rate was chosen. A commercial hot film transducer was acquired and the transducer was fitted between the carburettor float chamber and jet.

The fuel flow meter had a response which extended up to several kHz. In order that pulsations in fuel flow rate should not give rise to aliasing errors when the measurement was sampled by the computer a third order filter was interposed to limit the bandwidth to 5 Hz.

Dynamometer torque measurement.

To provide a mechanically filtered measurement of torque a potentiometer was coupled to the indicator of the dynamometer weighing gear. The output of the potentiometer was scaled to give an electrical analog of torque, +10 volts corresponding to 100 lb_f. ft.

Air/fuel ratio control.

Air/fuel ratio control was achieved by adjusting the pressure applied to the carburettor float chamber. The control was effected by connecting an angular position control to the adjustment spindle of a mechanical pressure regulator. A circuit diagram of the control is given in fig. 3.9. The pressure range corresponding to the 0 to +10 volt input was $\pm$ 7½ inches of water. The pressure regulator was also used to form part of a constant fuel flow rate control loop. The action of the control was to adjust the float chamber pressure in response to the integral of the error between measured and demanded fuel flow rate.

Ignition timing control.

An electronic means of ignition timing and firing was chosen in order to eliminate the mechanical imperfections of the contact breaker system. The electronic system relied on the monitoring of crankshaft rotation by two photoelectric transducers. The monitoring was carried out from an annular plate fitted to the flywheel. The outer rim of the annulus passed through the transducers and was drilled with circular holes on two pitch circles. The outer pitch circle had holes spaced at 1° intervals whilst the inner circle had two holes spaced 180° apart, positioned so that they passed through the transducer 50° B.T.D.C. The timing system is described with reference to fig. 3.10.

A square wave, each cycle of which corresponds to 1° of crankshaft rotation, was derived from the outer transducer and passed via the gate to a 6-bit counter. Pulses from the inner transducer opened the gate to initiate counting.

The count in the register was converted into a voltage in the analog to digital converter, which formed part of the timing system. When this voltage exceeded that of the analog input the comparator changed sign which caused the ignition firing circuit to be triggered. At this stage the counter was reset. To ensure decisive triggering the comparator employed positive d.c. feedback.

The ignition firing circuit operated on the capacitor discharge principle. A standard ignition coil was used as a pulse transformer. The firing system could also be triggered from the contact breaker points when the existing distributor advance characteristic was required.

The system controlled ignition timing over a 64° range, quantised in $\frac{1}{2}^{\circ}$ intervals.

On/off control of ignition, starter and cold starting device.

Circuits were constructed to enable the starter and ignition to be operated from relay closures which form the digital outputs of the computer. A solenoid operated control which also responds to a contact closure brings into operation the cold starting device.

Oil pressure measurement.

A pressure operated switch, of the type normally used to operate a vehicle warning light, is connected so as to provide a 1-bit digital indication of oil pressure for monitoring purposes when the engine is under computer control.

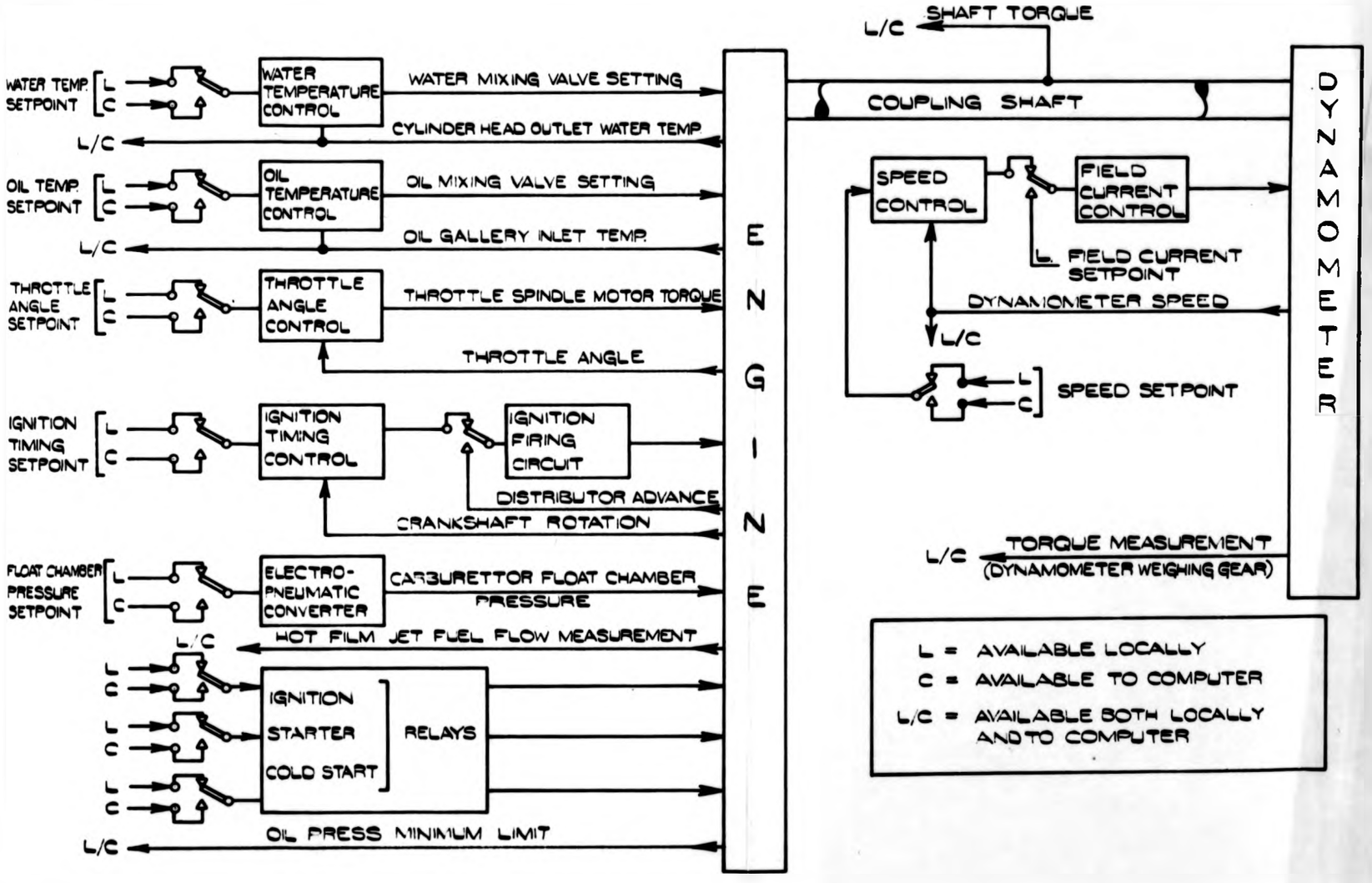

FIG. 3.1 ENGINE / DYNAMOMETER CONTROL SYSTEMS

FIG. 3.2. CLOSED-LOOP THROTTLE ANGLE CONTROL

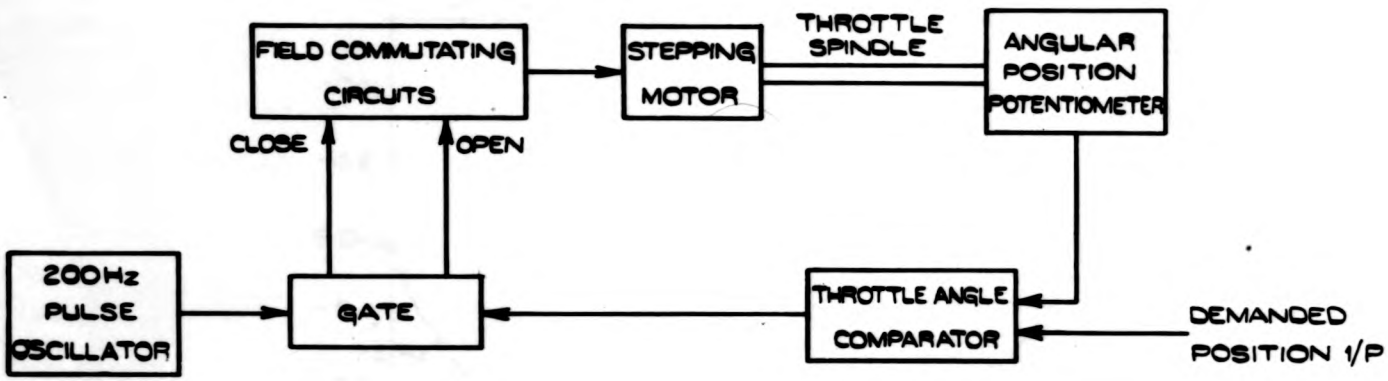

FIG. 3.3 NYQUIST PLOT OF CLOSED LOOP TRANSFER FUNCTION OF THROTTLE CONTROL.

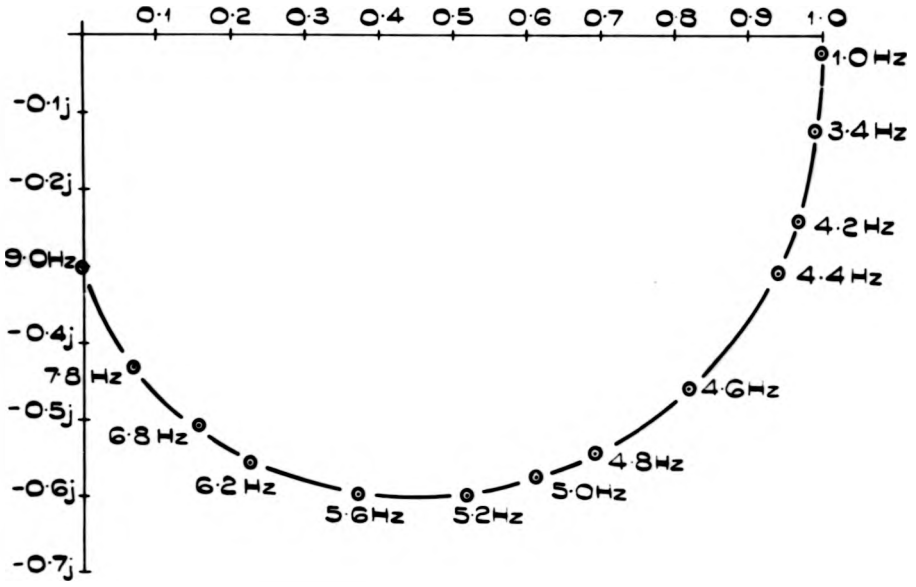

DYNAMOMETER FIELD

Fig. 3.4

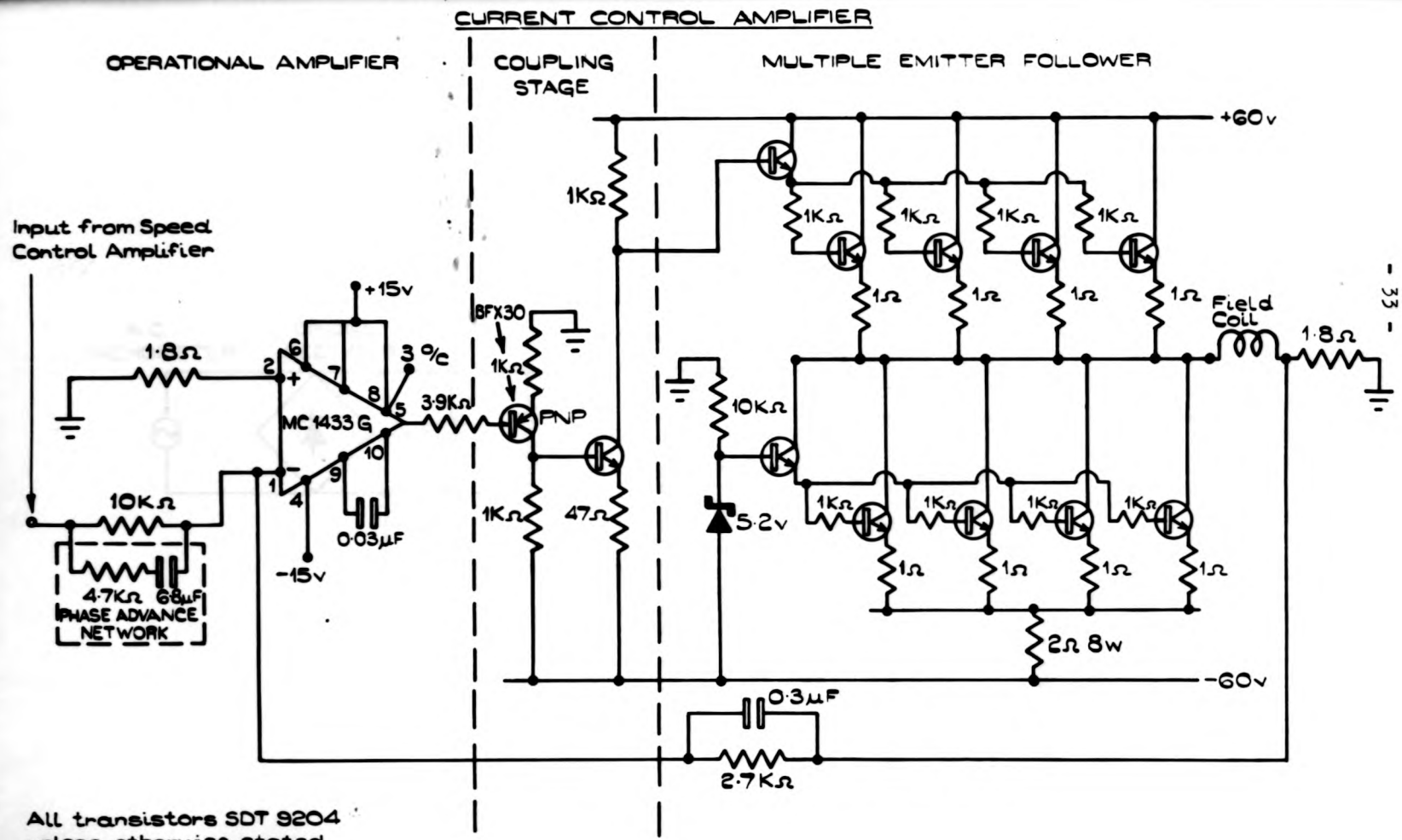

All transistors SDT 9204 unless otherwise stated

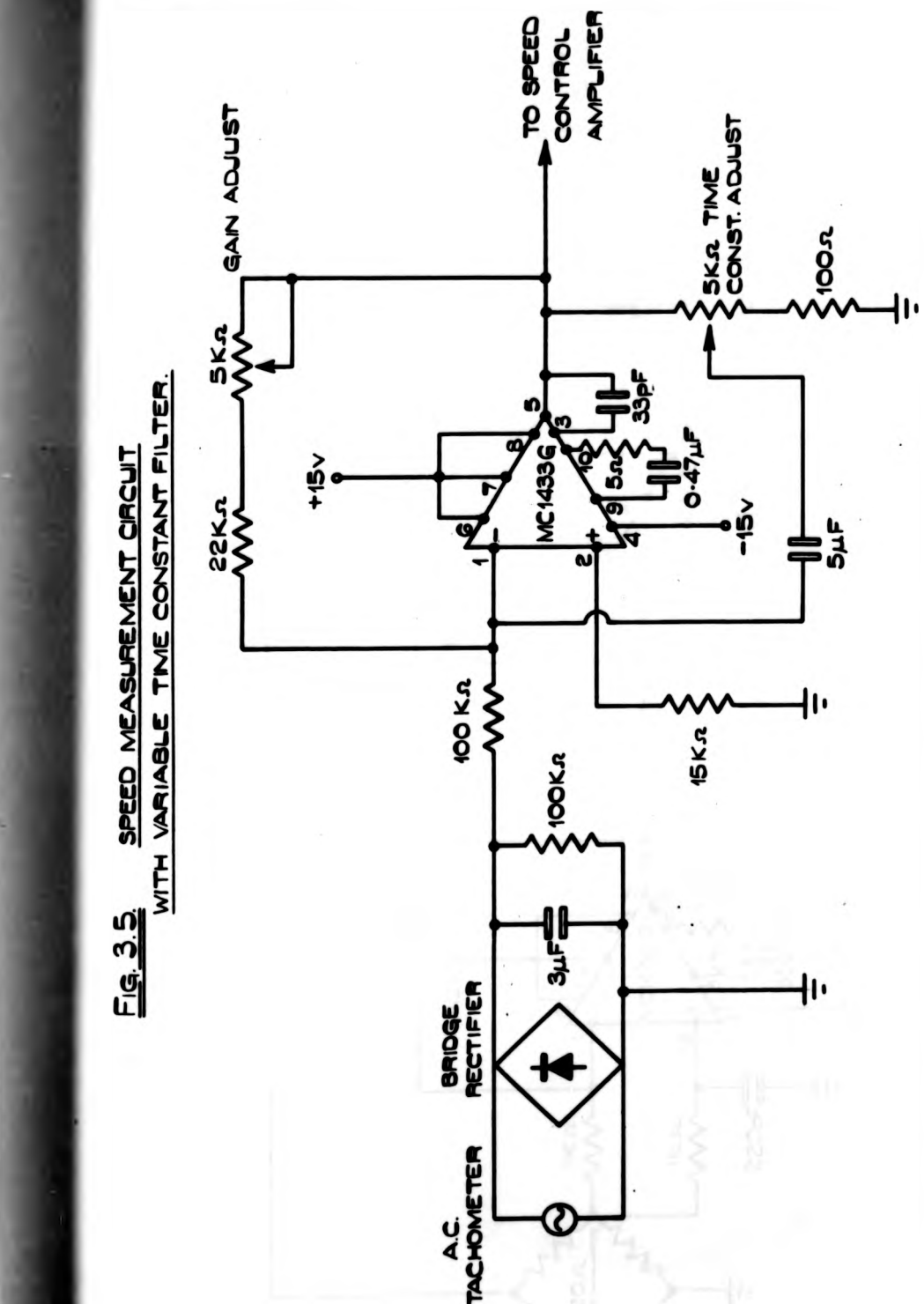

Fig. 3.5 SPEED MEASUREMENT CIRCUIT WITH VARIABLE TIME CONSTANT FILTER.

FIG. 3.6. SHAFT TORQUE TRANSDUCER

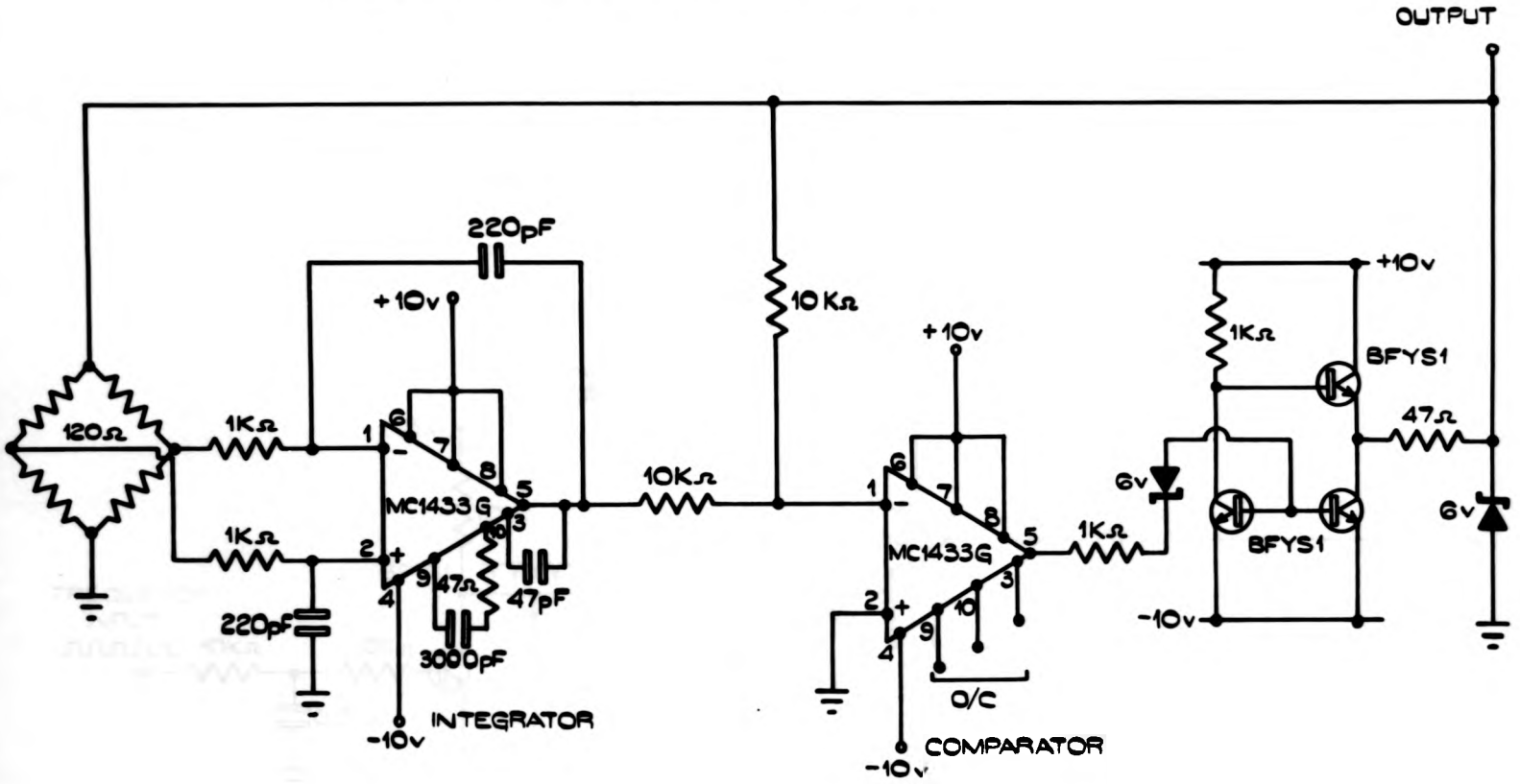

FIG 3.7 HIGH STABILITY MONOSTABLE.

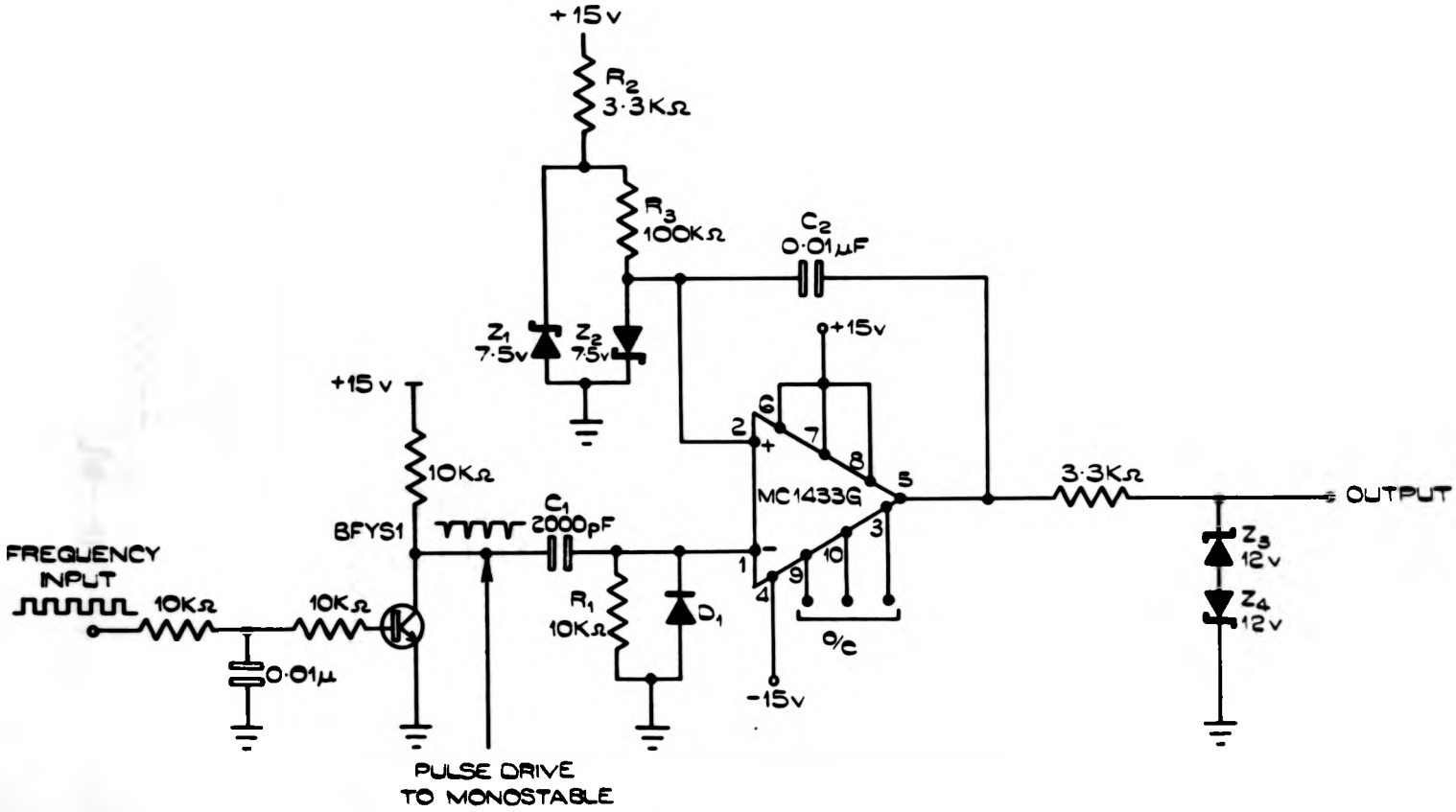

FIG 3.8 TEMPERATURE MEASUREMENT CIRCUITS

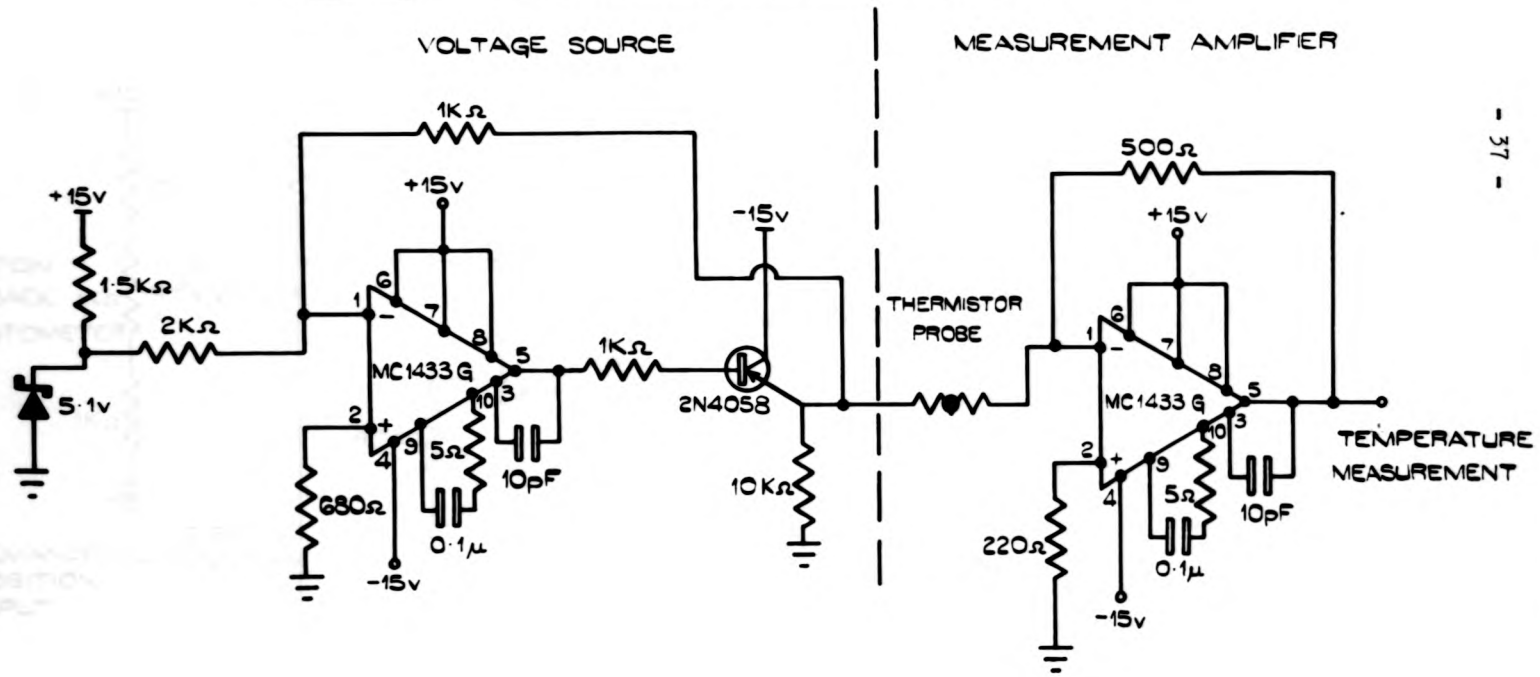

FIG. 3.8 TEMPERATURE MEASUREMENT CIRCUITS

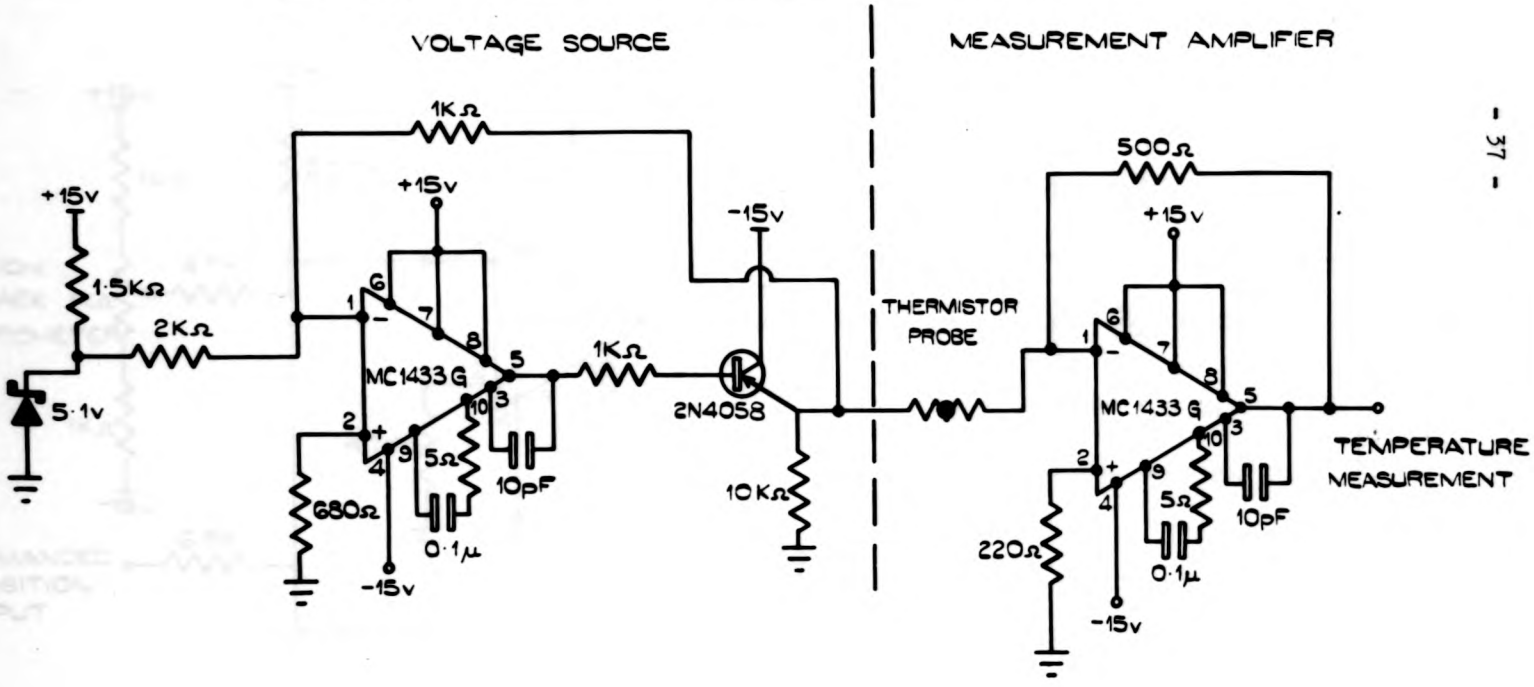

FIG 3.9. ANGULAR POSITION SERVO FOR PRESSURE REGULATOR

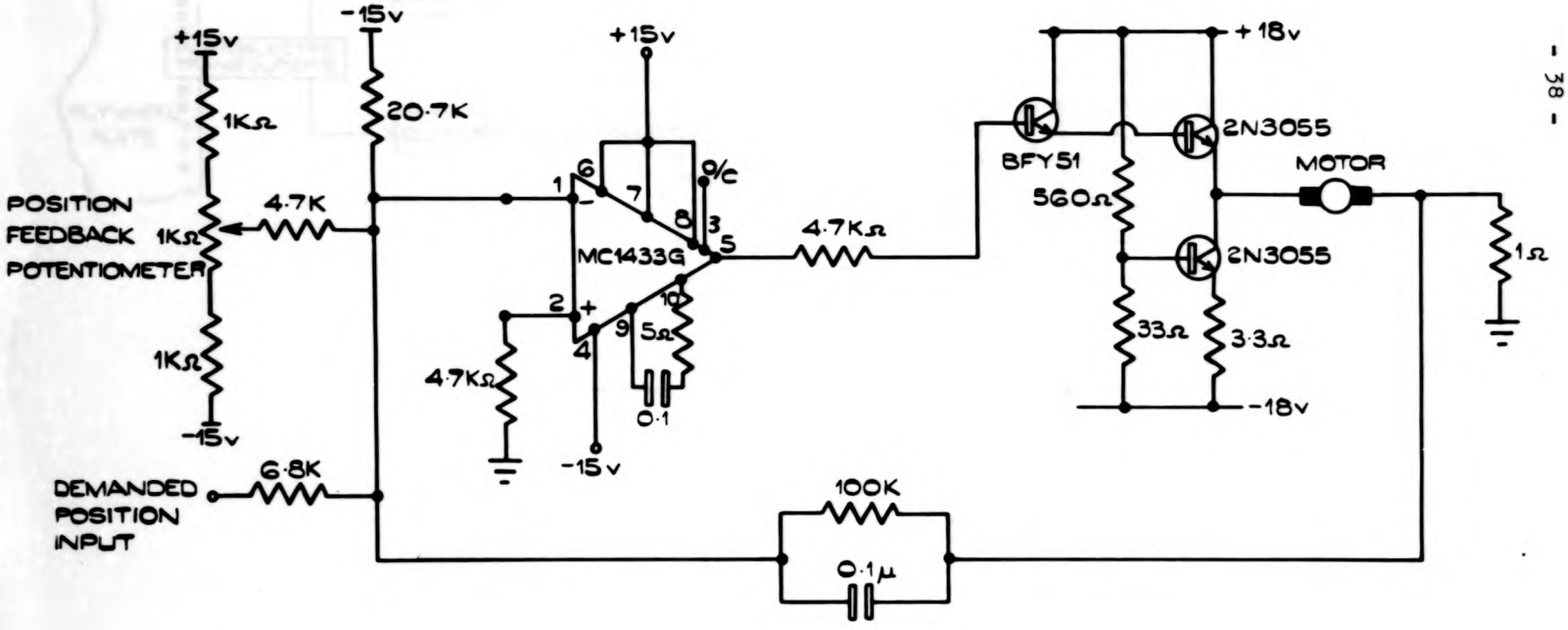

FIG. 3.10. SCHEMATIC OF ELECTRONIC IGNITION CONTROL.

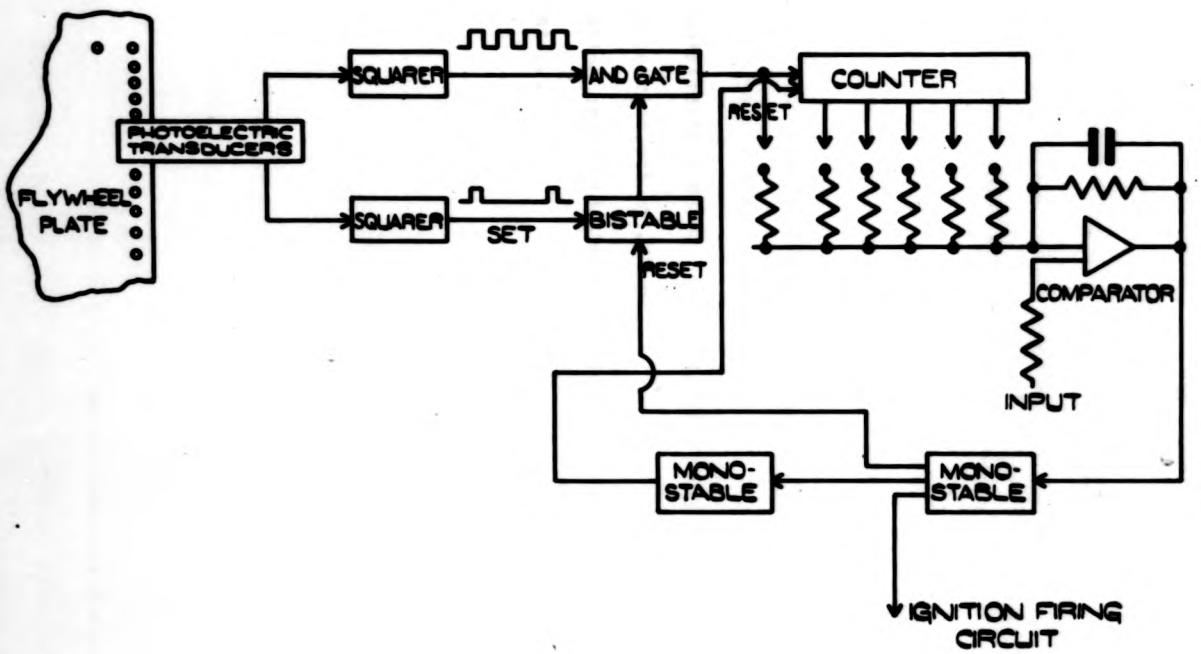

CHAPTER 4.

THE MATHEMATICAL MODELLING STUDY.

1. The scope of the modelling study.
2. The model and its derivation.
3. Experimental verification of the model.
4. Dynamic equations and the analog computer simulation.
5. A comparison of identification methods.
6. Conclusions of the modelling studies.

The derivation of the electrical circuit model and the state space equations was undertaken jointly with J.Monk.

The system identification using pseudo-random binary sequences (P.R.B.S.) was carried out by J.Monk.

The identification using wide-band Gaussian techniques was carried out by P.Wellstead.

1. Scope of the mathematical modelling study.

A mathematical modelling study of the engine and dynamometer was deemed to be of value in promoting an understanding of the interactions of the physical components of the test rig. A lumped electrical circuit form for the model was chosen because of the ease with which the physical components of the system could be associated with the elements of the model. The sampled-data form of representation (5) was not adopted since this form of representation is only valid at a fixed speed. Also most of the variables with which the model was concerned were continuous. Where they were not continuous sampling rates were comparatively high and so the added complexity of this form was not considered justifiable. Subsequently in chapter 7 some effects of sampling are considered. An appropriate form of control strategy for the type of test rig upon which the study is based has been developed from the model. The transfer function of the model between dynamometer field current and speed was utilised in the design of an analog speed control system.

The model represented the small signal transfer functions between throttle angle and dynamometer field current as inputs and shaft torque and dynamometer speed as outputs at an operating point in the middle of the torque speed range.

The theoretical transfer functions of the model at this operating point are compared with those obtained from the rig itself by sinewave testing. The dynamics of the test rig were also identified by two other research students using correlation techniques with P.R.B.S. (6) and wide-band Gaussian inputs. Their results are included for comparison.

2. The Model.

The basis of the electro-mechanical analogy used in the plant model is the formal similarity of the mathematical equations describing the properties of two physically diverse systems. The analogy is defined

in table 4.1. It will be appreciated that the choice of current to represent torque and voltage to represent angular velocity is arbitrary, and could equally well have been reversed, in this case an inductance would be used to represent a moment of inertia and a capacitance compliance. (7)

The model was developed initially to represent the system under steady state conditions about a chosen operating point in the middle of the torque and speed ranges. To extend the model so that it would represent the system under small signal dynamic conditions at this point the energy storage elements and time delays were added. Their interactions and magnitudes were evaluated by structural considerations and dynamics measurements.

The engine torque/speed curves for the full range of throttle servo inputs are given in fig. 4.1. Difficulties were encountered in obtaining the curves in the low speed and high torque regime due to unstable operation, and an explanation of this is presented later in the chapter. The curves in this regime were obtained using a proportional speed control which acted upon the dynamometer field current. The engine is represented by a voltage source, V_E with internal resistance, R_E, shown in fig. 4.2a. The slope of the torque/speed curves remains substantially constant for the full range of throttle settings. V_E is given by the intercept of the tangent to the torque/speed curve with the speed axis. The slope of this tangent equals $-1/R_E$. The model structure is valid throughout the torque/speed range of the engine. At low speeds with large throttle openings the slope of the characteristic changes sign. Under these conditions R_E becomes negative. V_E is a function of throttle opening, which is governed by the input voltage to the throttle servo V_T. The relationship between V_T and V_E is shown in fig. 4.3b. If the low speed high torque regime is excluded the relationship between V_T and V_E is substantially linear.

The dynamometer torque/speed curves are given in fig. 4.1. The small signal model for the dynamometer is given by a resistance R_D in parallel with a current generator I_D, and is given in fig. 4.2b. The values are obtained in a similar manner to those for the engine. The small signal effect of a change in field current I_F is to change the value of I_D. For larger signals it is not possible to make the assumption that R_F is constant and I_D is linearly related to field current. The slope of the tangent to the dynamometer torque/speed curves equals $1/R_d$.

In the analogy the coupling shaft is represented by a short-circuit coupling, as no velocity difference exists across it in the steady state.

Extension to the model to include dynamics.

A consideration of the detailed structure of the engine would lead to a model including energy dissipation elements due to service, pumping thermodynamic and mechanical losses and energy storage elements due to the various reciprocating and rotating parts which would all contribute to the dynamic behaviour. (Service losses are those due to such items as the dynamo and cooling fan drive). Because this would lead to an excessively complicated model the most significant dynamics of the engine were revealed by experimental investigation. This was carried out by decoupling the engine from the shaft connecting it to the dynamometer and obtaining a series of transfer functions between input voltage to the throttle servo and engine speed measured at the flywheel. For this purpose a circuit was constructed which converted the 1° ignition timing pulse rate into a voltage analog of speed. The transfer functions were measured over a range of mean speeds using a digital transfer function analyser (T.F.A.), a typical result is shown in fig. 4.4. Examination of the amplitude plots of the transfer function revealed the dynamics of a predominantly first order system. The phase plots correspond to a first order system with a time delay. The effective time delay was found to be proportional to the inverse

of engine speed and is given by (104/engine speed in r.p.m.) seconds. This would be accounted for by the average time taken to inhale and ignite a charge. The capacitor C_E is introduced into the model to represent the lumped inertia of the engine. Its value was derived from the engine source resistance R_E and the time constant of the first order system representing the engine. The dynamic model of the engine is given in fig. 4.5a.

Examination of the mechanical structure of the dynamometer revealed a large rotor inertia. Energy absorption is carried out by viscous drag between the rotor and stator and by eddy current dissipation in the stator. The rotor inertia, giving the value of C_D was evaluated by carrying out simple mechanical tests. The outer casing of the dynamometer is connected to the weighing gear through a lever arm. The weighing gear is comprised of a spring and dashpot system, connected at one end to the inertial frame of reference and at the other to the lever system. The component values associated with the dynamometer outer casing and weighing gear were evaluated from physical measurement of the spring and lever arm and a step response of the system. Hence C_B, R_B and L_B were determined. The dynamic model of the dynamometer is given in fig. 4.5c.

To complete the model the connecting shaft is represented by an inductor in parallel with a resistor, since it behaves like a torsional spring with internal damping. The shaft stiffness was measured physically, and the internal damping was derived from inspection of the transient response of the anchored shaft attached to the dynamometer rotor. The model of the shaft is shown in fig. 4.5b. Table 4.2 assigns the equivalent electrical values to the model.

3. Experimental verification of the model.

To reduce the order of the model and simplify the problem of comparing the model with the plant the dynamometer casing was clamped to the inertial frame of reference. The simplified form of the model is given in fig. 4.6.

The initial verification of the model was carried out using sine-wave testing techniques. Step responses for the plant were compared with those obtained from the analog computer model.

The measured variables available were dynamometer speed, V_D, and shaft torque, I_S, and the input variables were the voltages applied to the throttle servo, V_T, and the dynamometer field current controller, V_L. Four transfer functions therefore defined the small signal dynamic performance. An algol 60 program was written to calculate the theoretical frequency responses for the model, and these are compared with those obtained with the digital transfer function analyser (T.F.A.) (8) in figs 4.7 and 4.8. Measurements over the range 0.001 to 15Hz were taken with the T.F.A. In this range the experimental and theoretical transfer functions between the throttle servo input and dynamometer speed and shaft torque show favourable agreement. However the responses of shaft torque and dynamometer speed to inputs to the dynamometer field current control show poor agreement. These responses are compared in fig. 8. It was suggested that the extra attenuation at high frequencies of the plant was due to the energy storage elements associated with the magnetic field of the dynamometer casing and rotor. To investigate this, the frequency response between the field current control input voltage and flux was examined using a search coil. This response is given in fig. 4.9. The experimental result has been modified to remove the differentiating action of the search coil. From examination of this response it was deduced that these energy storage elements contributed two cascaded first order lags. The revised model including these lags is shown in fig. 4.10. The revised

frequency responses of shaft torque and dynamometer speed to the input to the dynamometer field current control showed considerably better agreement. These are shown in fig. 4.11.

Step responses for the plant and analog computer model are shown in fig. 4.12. The throttle velocity limit will significantly affect the high frequency components of a large step input, therefore it is difficult to identify the high frequency performance of the rig from these responses.

4. Dynamic equations and analog computer simulation.

The three state variables chosen for the electromechanical model were the engine speed V_F, the dynamometer speed V_D, and the shaft torque I_S.

The state space matrix equation for the system, assuming linear operation is:-

$$\begin{bmatrix} \frac{d}{dt} V_F \\ \frac{d}{dt} V_D \\ \frac{d}{dt} I_S \end{bmatrix} = \begin{bmatrix} -\frac{1}{C_E R_E} & 0 & -\frac{1}{C_E} \\ 0 & -\frac{1}{C_D R_D} & \frac{1}{C_D} \\ \left(\frac{1}{L_S} - \frac{1}{C_E R_E R_S}\right) & \left(\frac{1}{C_D R_D R_S} - \frac{1}{L_S}\right) & \left(\frac{1}{C_E R_S} - \frac{1}{C_D R_S}\right) \end{bmatrix} \begin{bmatrix} V_F \\ V_D \\ I_S \end{bmatrix}$$

$$+ \begin{bmatrix} \frac{1}{R_E C_E} & 0 \\ 0 & -\frac{1}{C_D} \\ \frac{1}{C_E R_E R_S} & \frac{1}{C_D R_S} \end{bmatrix} \begin{bmatrix} V_E \\ I_D \end{bmatrix}$$

Where $V_E = 4.86\, V_T$

and $0.0332 \frac{d^2}{dt^2}(I_D) + 0.713 \frac{d}{dt}(I_D) + I_D = 1.26\, V_L$

V_T = throttle servo input voltage

V_E = engine source voltage

V_L = load current amplifier input voltage

I_D = dynamometer source current

The analogue computer diagram for the above equations is given in fig. 4.13.

5. A comparison of identification methods.

Apart from the identification using sinusoidal and step perturbations the system dynamics were identified using P.R.B.S. and wide band Gaussian perturbations. The experiments with both these forms of perturbation were carried out subsequent to the sinusoidal perturbation experiments and consequently were able to make use of a prior knowledge of the system dynamics.

The results of the P.R.B.S. identification which are presented in the form of impulse responses are shown in fig. 4.14. Where the frequency range of the dynamics were relatively small the P.R.B.S. experiments gave good results. However, where the range of dynamics is larger, computer storage limitations prevented the use of input sequences of sufficient length to enable the impulse responses to be portrayed in adequate detail.

Similar difficulties were experienced with the experiments using wide band Gaussian perturbations. The responses obtained from these experiments, which were conducted at a slightly different operating point are shown in figs. 4.15, 4.16, 4.17, and 4.18. For comparison points obtained from sinusoidal testing with the T.F.A. are included. Again it was not possible in some cases to cover the system dynamics in sufficient detail. The results obtained in these experiments showed good agreement with those obtained by sinusoidal testing.

Sinusoidal testing using the T.F.A. proved to be the most flexible method of identification. However this method did require considerably

more time to execute. At the highest frequencies covered by the identification all the methods gave poor results due to the adverse signal to noise ratio.

6. Conclusions of the modelling studies.

The frequency responses of the model and those obtained from the rig by sinewave testing showed good agreement over the frequency range 0.001 Hz. to 15 Hz. Special equipment, in the form of a digital transfer function analyser, was required to help derive the results quickly. Step response testing gave rapid results when examining the slowest system time constants and was particularly useful in drawing attention to the lead lag in the transfer function between throttle opening and shaft torque.

The steady state model of the system provided a useful means of defining the stability of any operating point in the torque/speed plane. Without closed loop torque or speed control operating on either dynamometer field current or throttle angle there exists at least one unstable operating regime in the torque/speed plane. (In this instance a point is defined as stable if the system returns to that operating point after a slight displacement.)

Consider point P in fig. 4.19. If a slight increase in speed were imposed on the system the dynamometer load torque would exceed the output torque of the engine and the system would return to operation at point P. The same is not true of point Q, since a slight displacement from this point will cause the engine to stall or lead to an increase in speed and to stable operation at point R. The extent of this unstable regime is indicated in fig. 4.20.

The stability of any point may be defined from the values of the circuit elements of the model. An unstable point will occur when the nett conductance of the circuit loop including R_E and R_D becomes negative. Application of this criterion confirms the existence of the unstable regime under open loop operation which is shown in fig. 4.20.

The electrical circuit model also provides a convenient means by which the effect of closed loop controls on the system can be examined. The system has two inputs and two outputs, and consequently four possible single loop control configurations exist. These configurations are examined by firstly considering the effect of an idealised control and then imposing the limitations of a practical control system.

Control of dynamometer speed by the adjustment of dynamometer field current.

In this case the dynamometer in the model is replaced by a voltage source. The value of the voltage corresponds to the speed setpoint. An ideal voltage source has zero driving impedance hence $R_D = 0$ and $\frac{1}{R_D} = \infty$. $\left(\frac{1}{R_E} + \frac{1}{R_D}\right)$ can therefore never become negative and in an idealised case all points in the torque/speed plane are stable. A practical control is limited by the range of dynamometer field currents and by the finite value of R_D which will cause unstable operation at very low speeds where a high torque is developed.

Control of shaft torque by the adjustment of dynamometer field current.

In this case the dynamometer in the model is replaced by a current source. The value of the current corresponds to the torque setpoint. An ideal current source has an infinite driving impedance hence $R_D = \infty$ and $\frac{1}{R_D} = 0$. $\left(\frac{1}{R_E} + \frac{1}{R_D}\right)$ will become negative when $\frac{1}{R_E}$ is negative, and consequently there will be an unstable regime at high speeds and low torques. The area of this regime is larger than that which occurs when no closed loop control is applied. Again the practical control will be limited by the range of dynamometer field currents. The extent of stable operation is shown in fig. 4.21.

Over the range of speeds examined on the exploratory test bed dynamometer field current increases monotonically with speed for constant torque operation. At high speeds however, above those which could be reached on the experimental test bed this will not

be the case (9), and the slope of the dynamometer load lines changes sign. Once this occurs the torque control loop gain is reversed and positive feedback renders the control unstable. The extent of stable operation in these circumstances is bounded by the speed at which this change of sign occurs.

Control of dynamometer speed by the adjustment of throttle angle.

In this case the engine in the model is replaced by a voltage source. The value of this voltage corresponds to the speed setpoint. By similar reasoning to that applied above $\left(\frac{1}{R_E} + \frac{1}{R_D}\right) = \infty$ and all points in the torque/speed plane will be stable. However, since a practical control system must act through R_E the throttle becomes effectively decoupled from the system when $R_E = \infty$, and the loop gain is reversed when R_E changes sign. The area where control is effective is the same as the stable area shown in fig. 4.21.

Control of shaft torque by adjustment of throttle angle.

In this case the engine in the model is replaced by a current source. The value of the current corresponds to the torque setpoint. $\left(\frac{1}{R_E} + \frac{1}{R_D}\right)$ will be positive and all of the torque/speed plane will be stable. Again the practical control system must act through R_E and the throttle becomes similarly decoupled from the system. When $R_E = 0$ the area where control is effective is again the same as the stable area shown in fig. 4.20.

Similar reasoning may be applied to consider the operation of a 2-loop system for the simultaneous control of torque and speed. When R_E becomes infinite the control input connected to the throttle becomes effectively decoupled, and when R_E changes sign the loop is rendered unstable by virtue of positive feedback.

The single loop control of dynamometer speed by the adjustment of field current would therefore appear to be the most useful form of control that can be applied to a test rig of this type. With all other forms of control unstable or inaccessible regimes exist, and

consequently they do not permit a full exploration of the torque/ speed range of the engine.

Mechanical Quantity	Electrical Quantity	Mechanical Units	Electrical Units
Torque	Current	Poundal Feet	Amps
Angular Velocity	Voltage	Radians/ Second	Volts
Inertia	Capaci- tance	$lbm.ft^2$	Farads
Viscous Damping	Resistance	Rads/sec. ft.pdl.	Ohms
Compliance	Inductance	Rads/pdl. ft.	Henrys

Table 4.1. Definition of the analogy.

1 volt = 52.4 rads/sec (10v = 5000 r.p.m.)

1 amp = 322 pdl.ft. (10v = 100 lbf. ft.)

R_E	1.19
C_E	0.447F
L_S	5.32×10^{-4}H
R_S	0.455
C_D	1.38F
R_D	3.00
C_B	7.57×10^{3}F

Table 4.2. Numerical values for the electrical analogy.

FIG. 4.1.

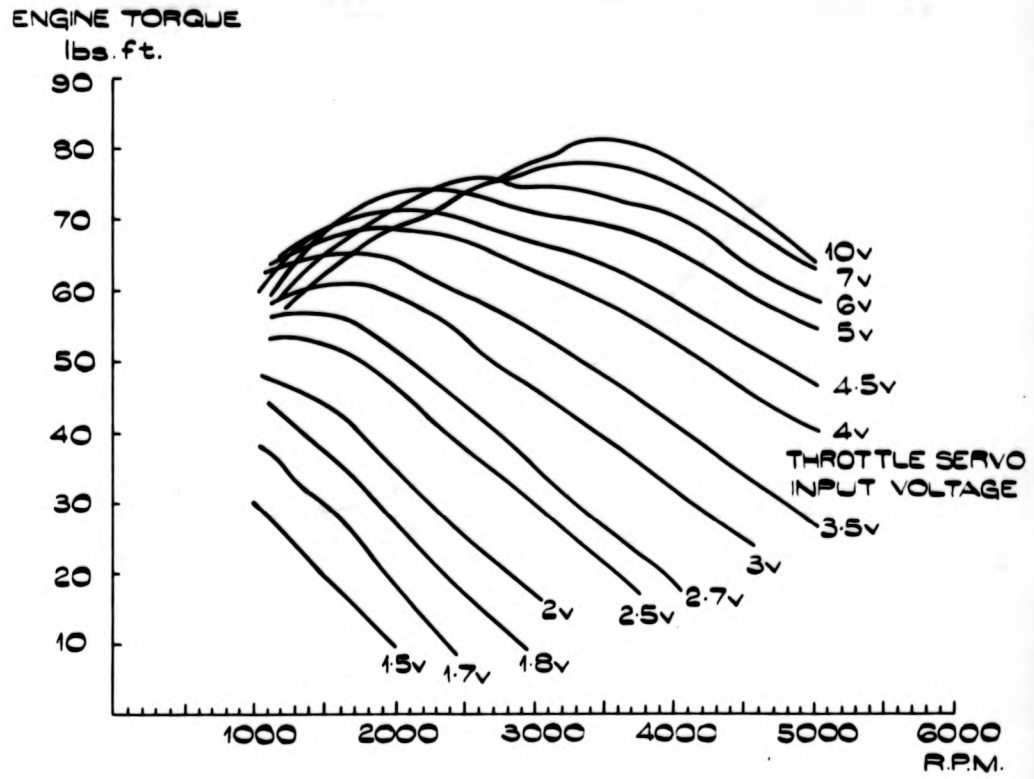
ENGINE TORQUE
lbs.ft.
90
80
70
60
50
40
30
20
10
10v
7v
6v
5v
4·5v
4v
THROTTLE SERVO
INPUT VOLTAGE
3·5v
3v
2·7v
2·5v
2v
1·8v
1·7v
1·5v
1000
2000
3000
4000
5000
6000
R.P.M.

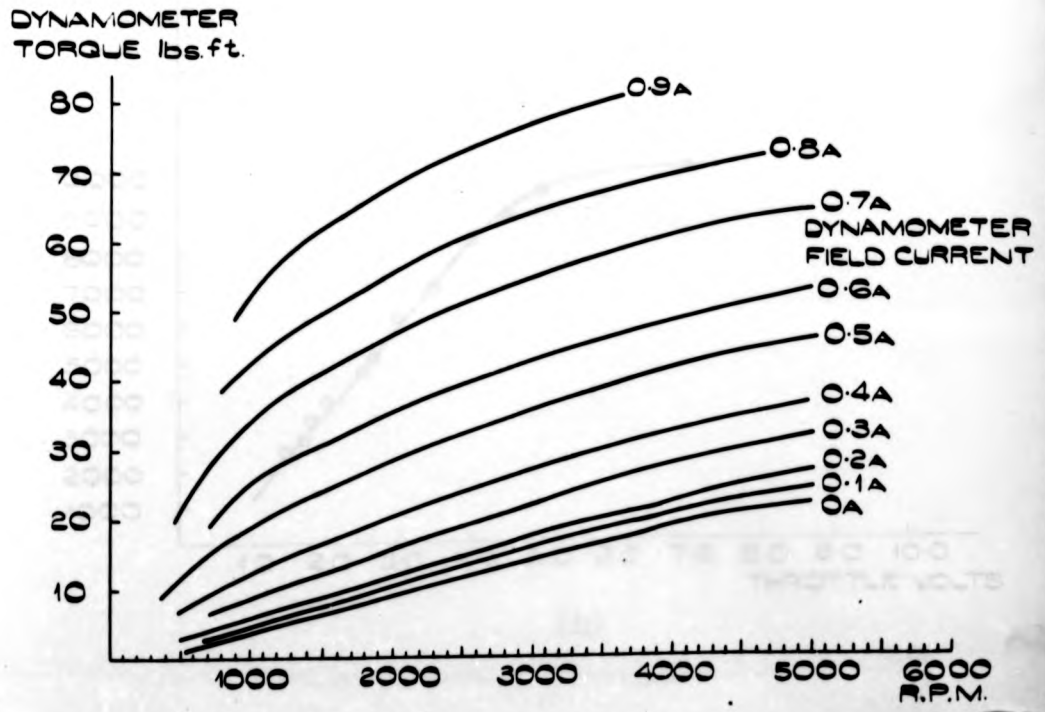
DYNAMOMETER
TORQUE lbs.ft.
80
70
60
50
40
30
20
10
0·9A
0·8A
0·7A
DYNAMOMETER
FIELD CURRENT
0·6A
0·5A
0·4A
0·3A
0·2A
0·1A
0A
1000
2000
3000
4000
5000
6000
R.P.M.

FIG 4.3

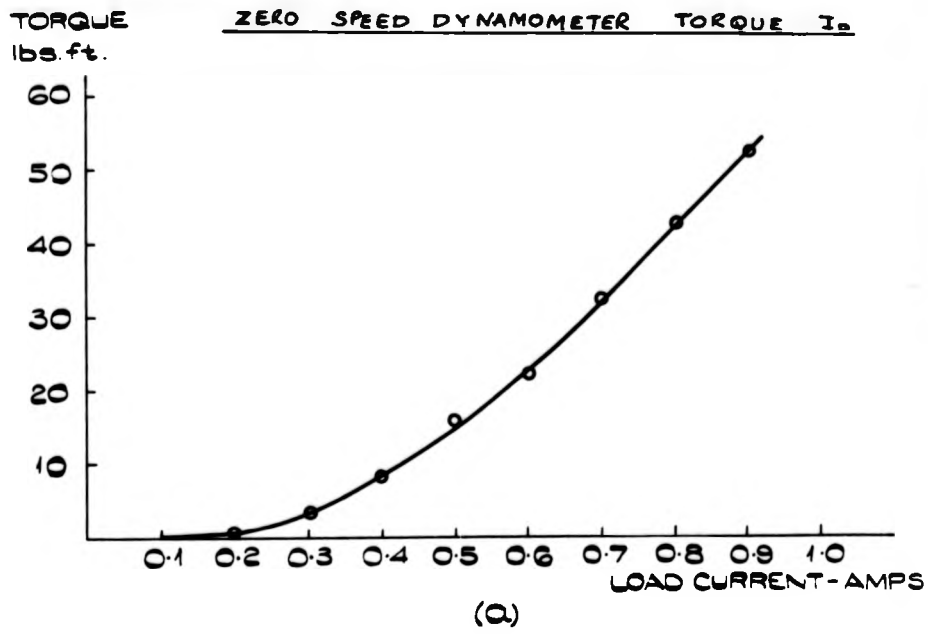
TORQUE
lbs.ft.
ZERO SPEED DYNAMOMETER TORQUE I_a
60
50
40
30
20
10
0·1 0·2 0·3 0·4 0·5 0·6 0·7 0·8 0·9 1·0
LOAD CURRENT - AMPS

(a)

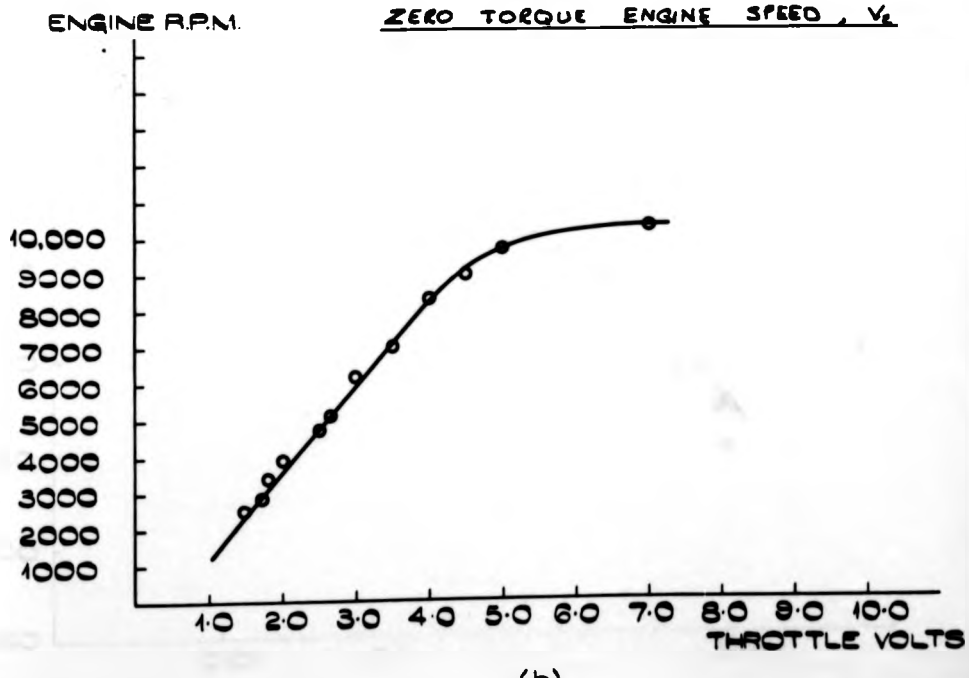
ENGINE R.P.M.
ZERO TORQUE ENGINE SPEED, V_e
10,000
9000
8000
7000
6000
5000
4000
3000
2000
1000
1·0 2·0 3·0 4·0 5·0 6·0 7·0 8·0 9·0 10·0
THROTTLE VOLTS

(b)

FIG 4.3

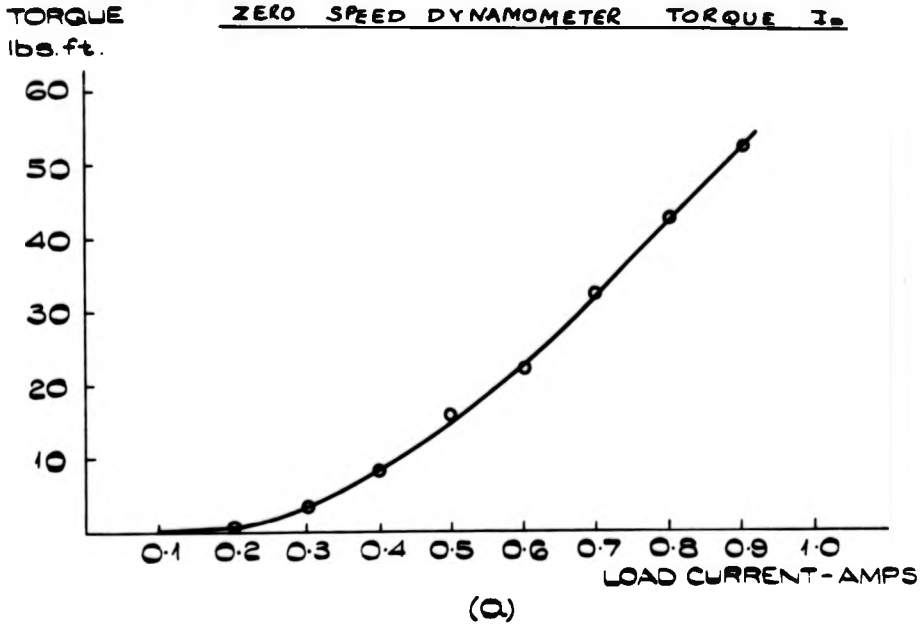
TORQUE
lbs.ft.
ZERO SPEED DYNAMOMETER TORQUE I_0
60
50
40
30
20
10
0·1
0·2
0·3
0·4
0·5
0·6
0·7
0·8
0·9
1·0
LOAD CURRENT - AMPS

(a)

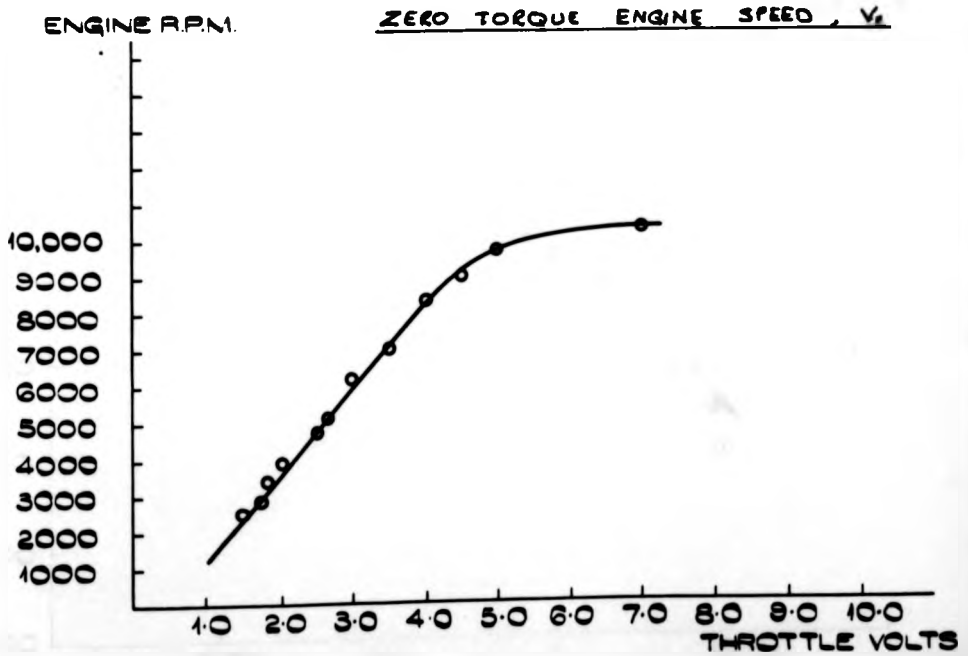
ENGINE R.P.M.
ZERO TORQUE ENGINE SPEED, V_0
10,000
9000
8000
7000
6000
5000
4000
3000
2000
1000
1·0
2·0
3·0
4·0
5·0
6·0
7·0
8·0
9·0
10·0
THROTTLE VOLTS

(b)

FIG 4.4 THROTTLE SPEED DYNAMOMETER DISCONNECTED.

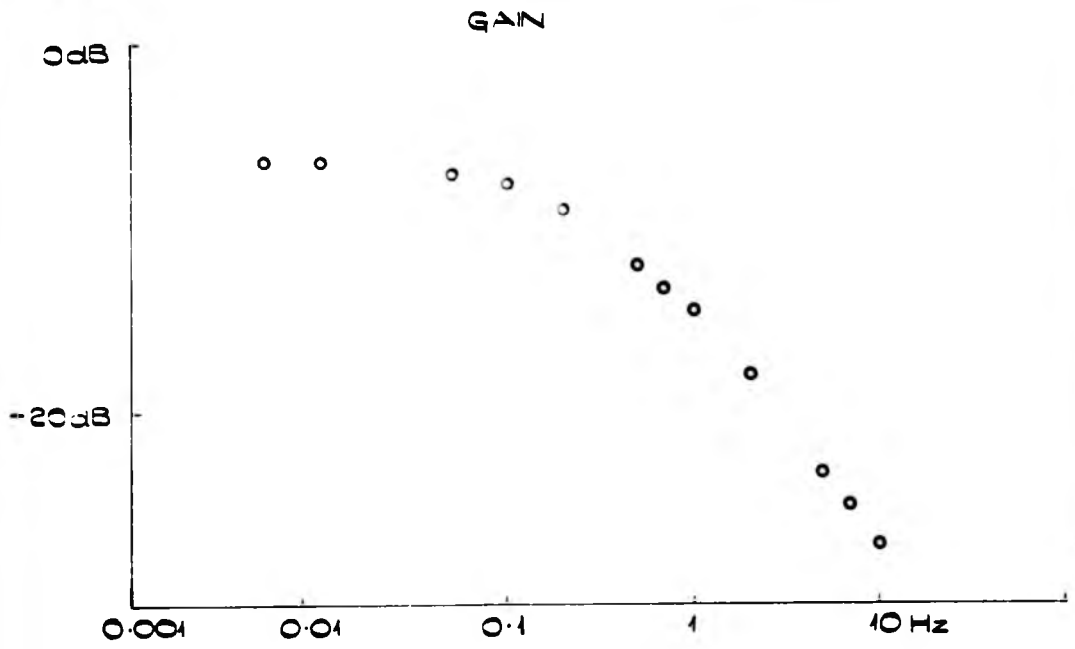

0dB = 1 VOLT PER 600 R.P.M.

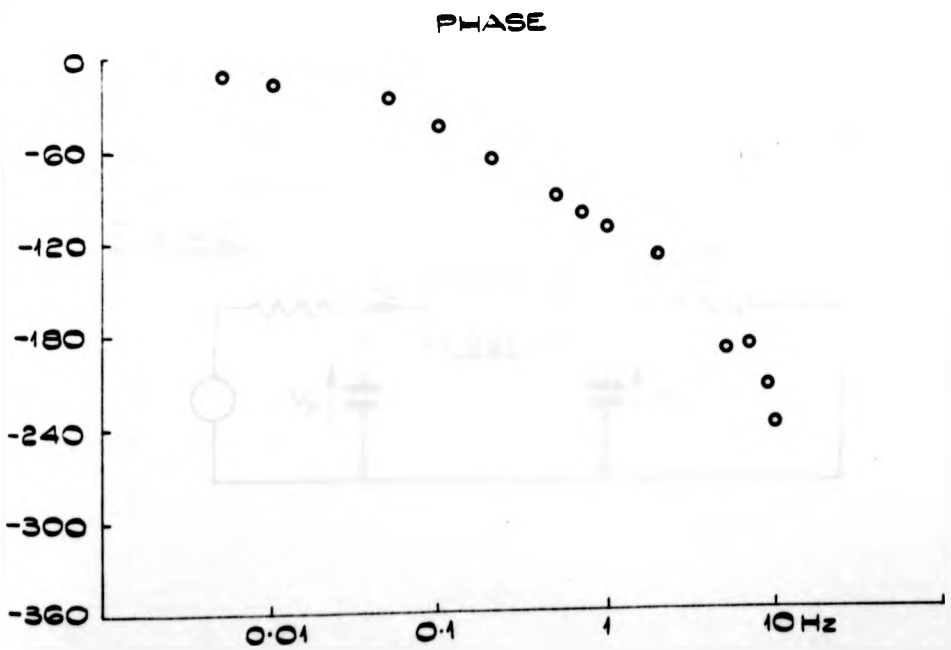

FIG. 4.2

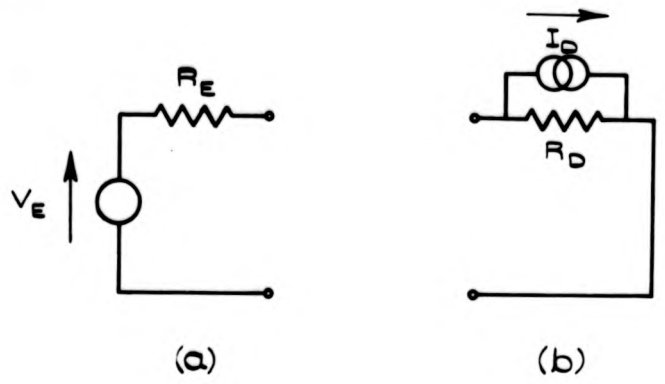

FIG. 4.5

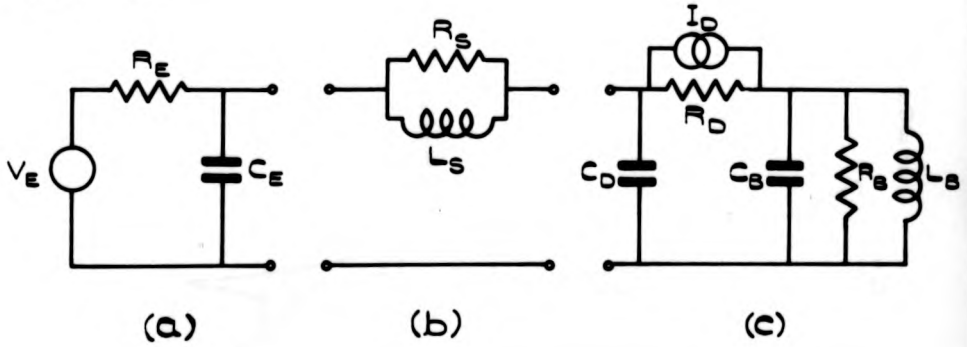

FIG. 4.6

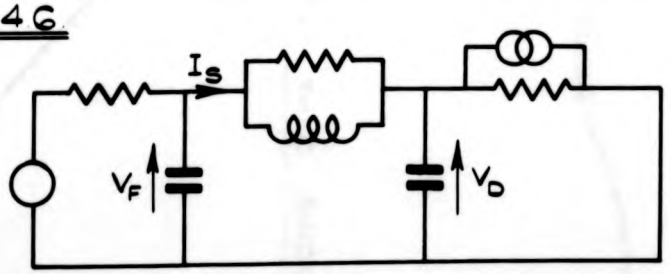

FIG 4.7

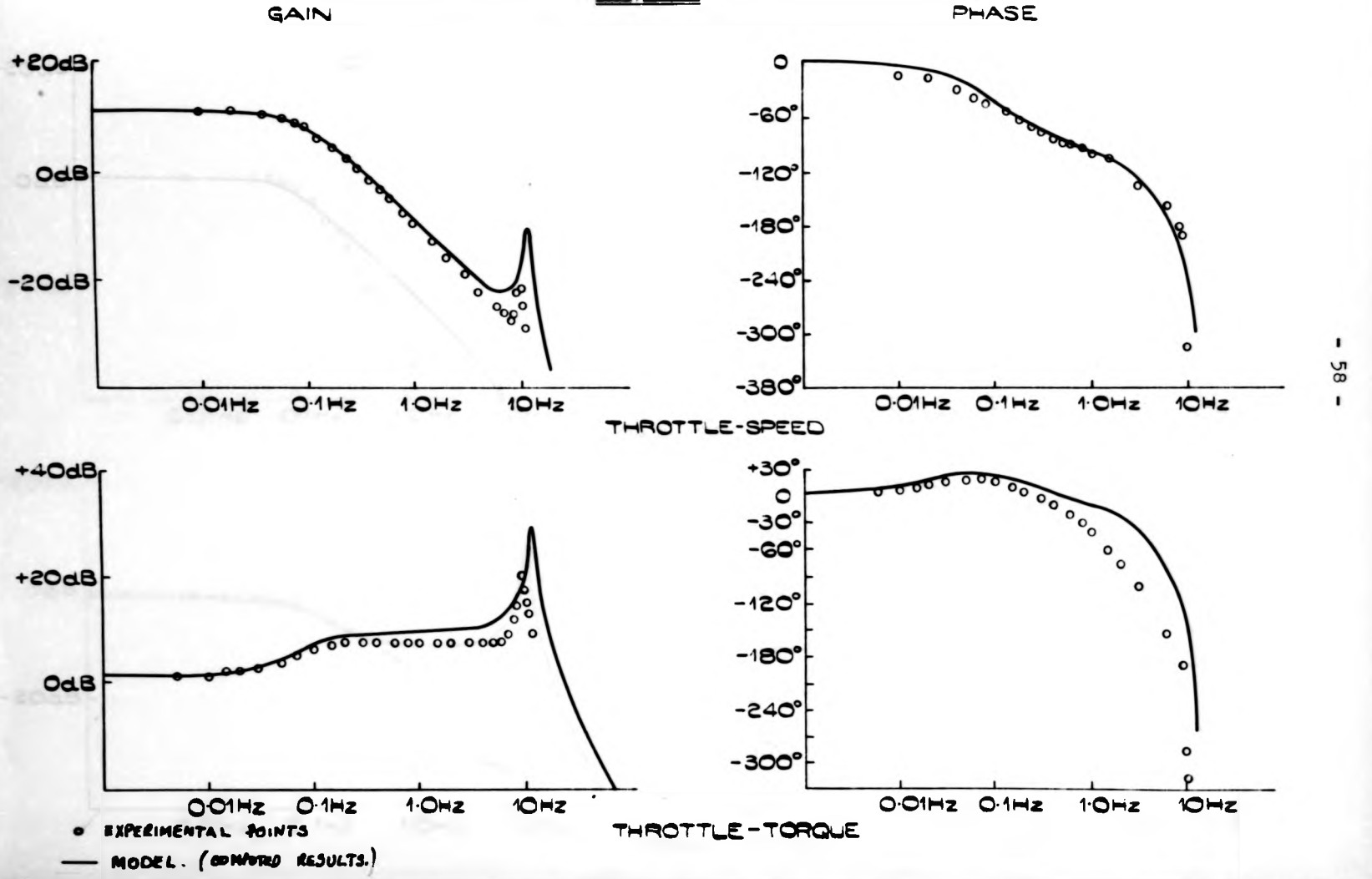
GAIN
PHASE
+20dB
0dB
-20dB
0
-60°
-120°
-180°
-240°
-300°
-380°
0·01Hz
0·1Hz
1·0Hz
10Hz
THROTTLE-SPEED
+40dB
+20dB
0dB
+30°
0
-30°
-60°
-120°
-180°
-240°
-300°
THROTTLE-TORQUE
o EXPERIMENTAL POINTS
— MODEL. (COMPUTED RESULTS.)

FIG. 4.8

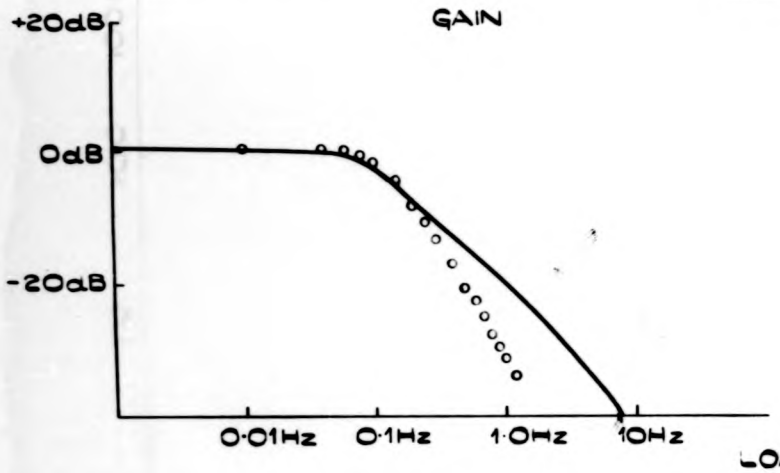

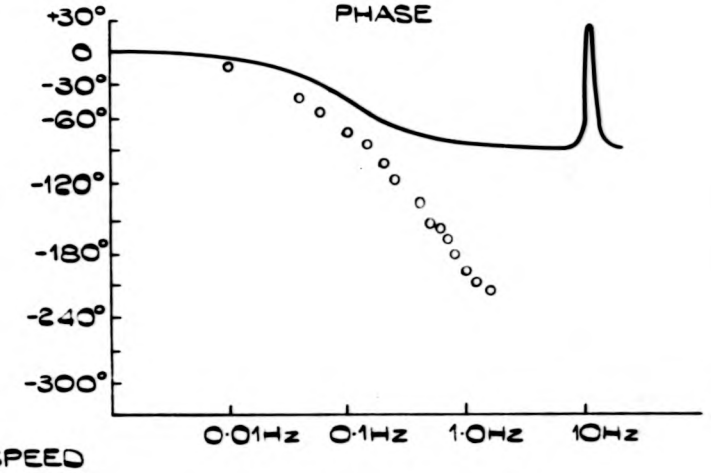

LOAD - SPEED

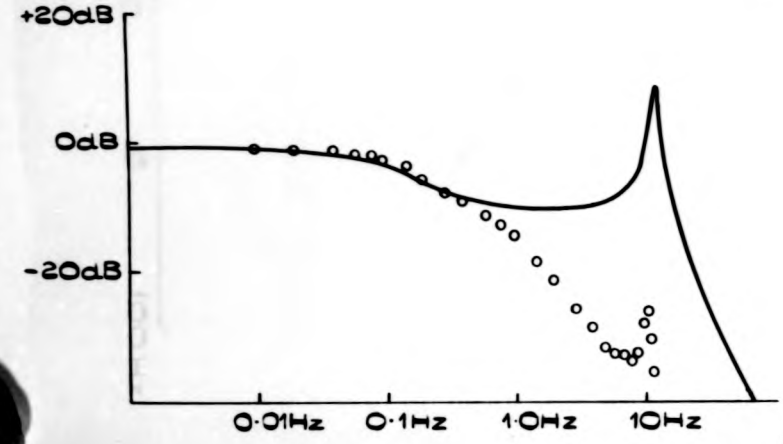

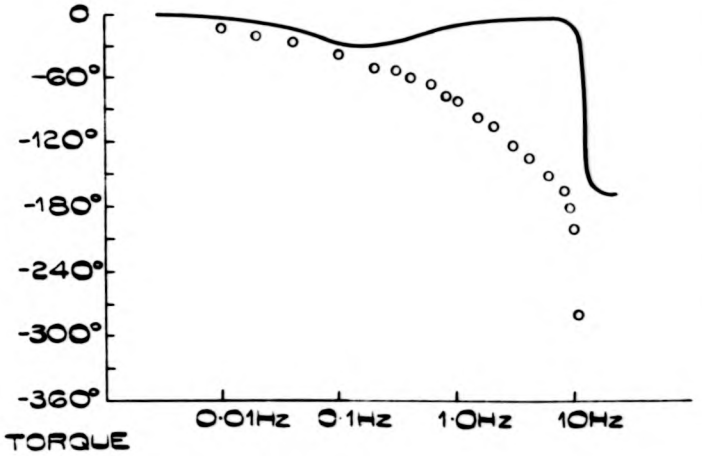

LOAD - TORQUE

FIG 4.9 CURRENT CONTROL INPUT VOLTAGE - FLUX

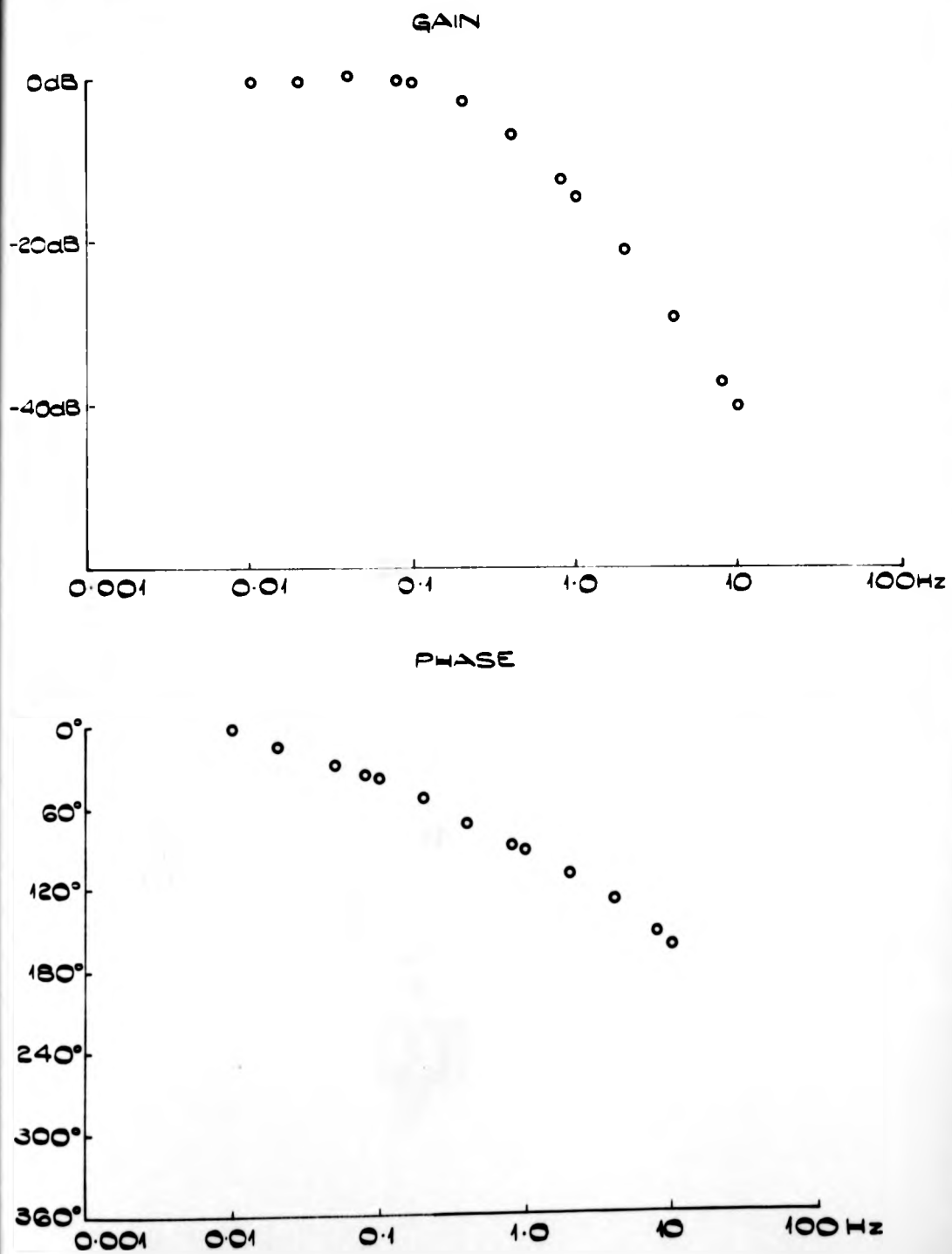

FIG 4.9 CURRENT CONTROL INPUT VOLTAGE - FLUX

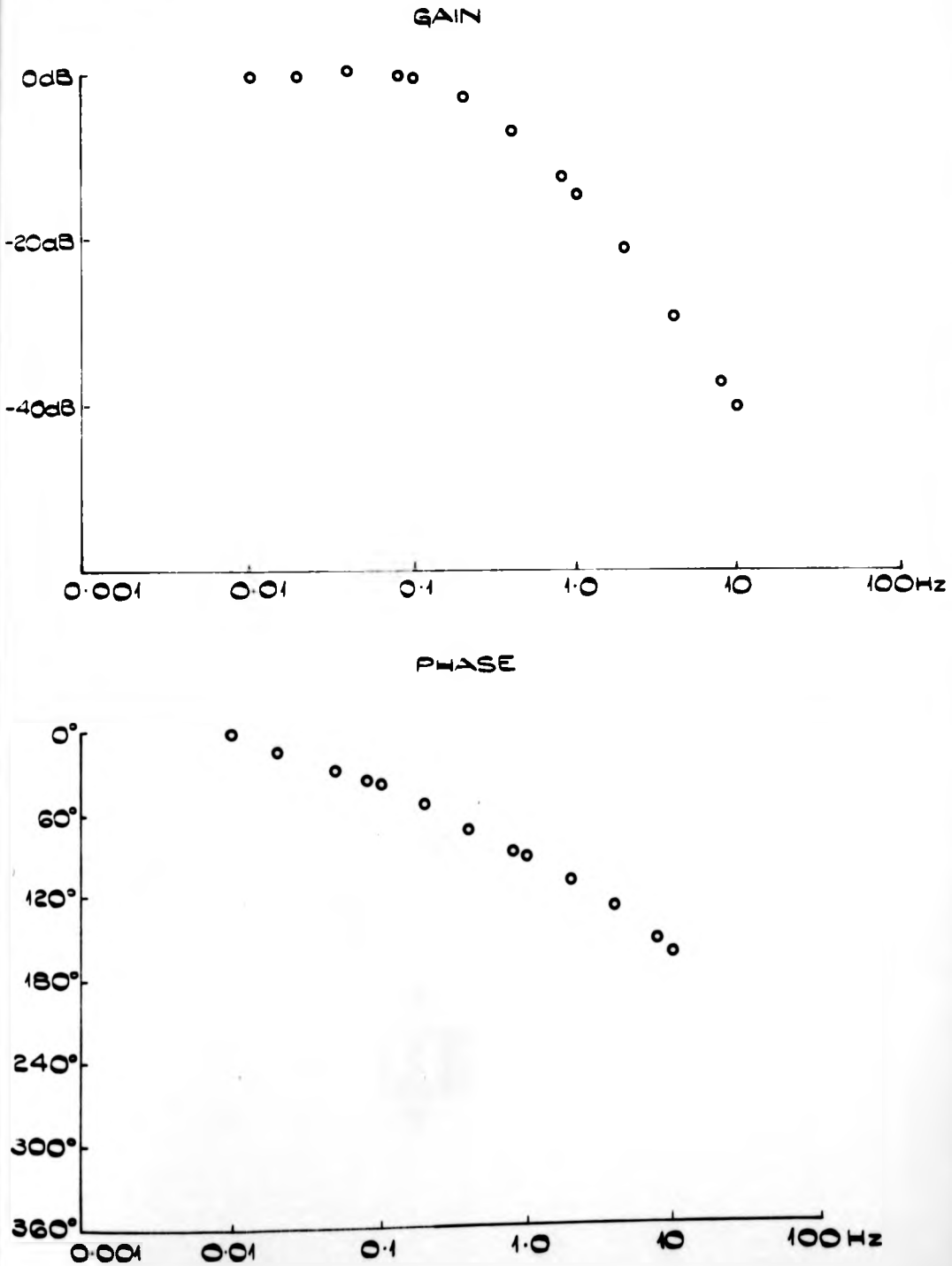

FIG 4.1

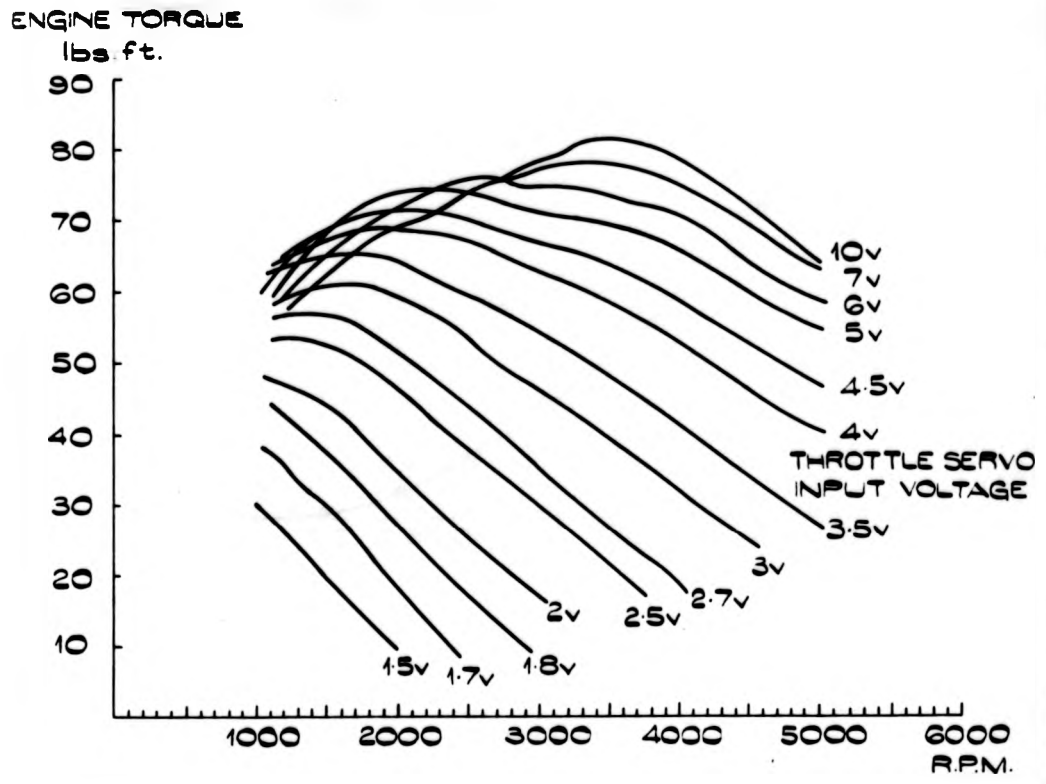
ENGINE TORQUE
lbs.ft.
90
80
70
60
50
40
30
20
10
10v
7v
6v
5v
4.5v
4v
THROTTLE SERVO
INPUT VOLTAGE
3.5v
3v
2.7v
2.5v
2v
1.8v
1.7v
1.5v
1000
2000
3000
4000
5000
6000
R.P.M.

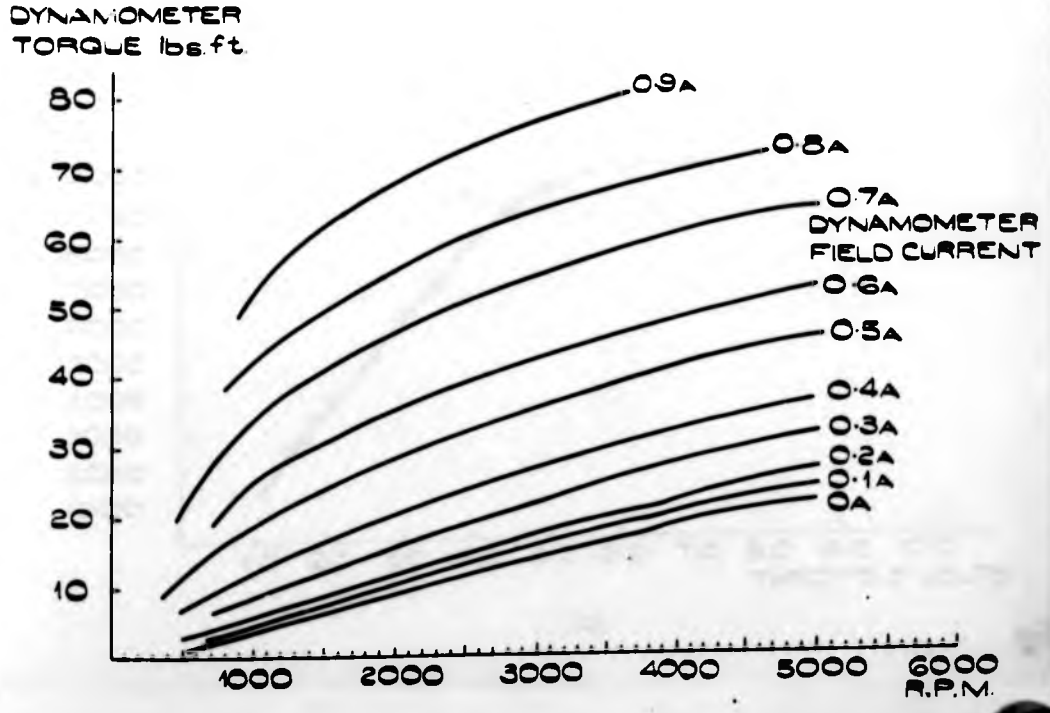
DYNAMOMETER
TORQUE lbs.ft.
80
70
60
50
40
30
20
10
0.9A
0.8A
0.7A
DYNAMOMETER
FIELD CURRENT
0.6A
0.5A
0.4A
0.3A
0.2A
0.1A
0A
1000
2000
3000
4000
5000
6000
R.P.M.

FIG 4.3

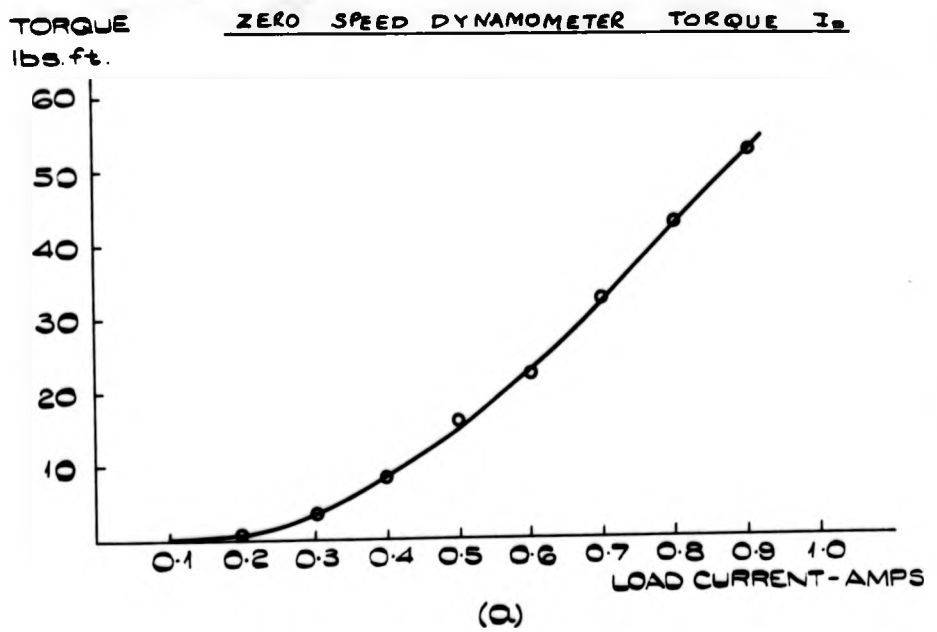
TORQUE
lbs.ft.
ZERO SPEED DYNAMOMETER TORQUE I_0
60
50
40
30
20
10
0·1 0·2 0·3 0·4 0·5 0·6 0·7 0·8 0·9 1·0
LOAD CURRENT - AMPS

(a)

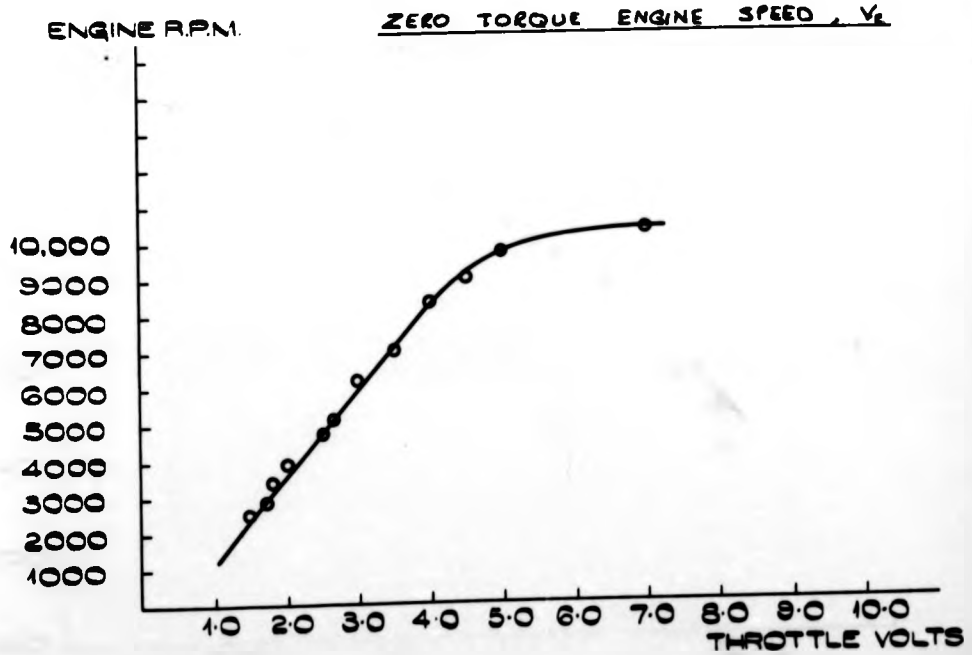
ENGINE R.P.M.
ZERO TORQUE ENGINE SPEED , V_E
10,000
9000
8000
7000
6000
5000
4000
3000
2000
1000
1·0 2·0 3·0 4·0 5·0 6·0 7·0 8·0 9·0 10·0
THROTTLE VOLTS

(b)

FIG 4.4 THROTTLE SPEED DYNAMOMETER DISCONNECTED.

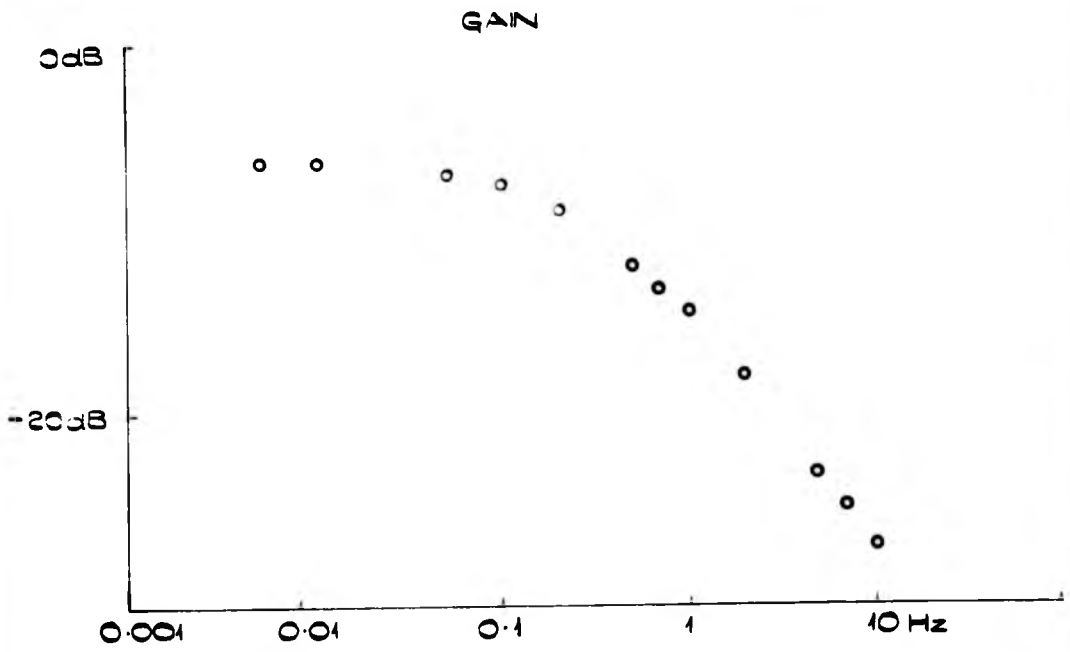

0dB = 1 VOLT PER 500 R.P.M.

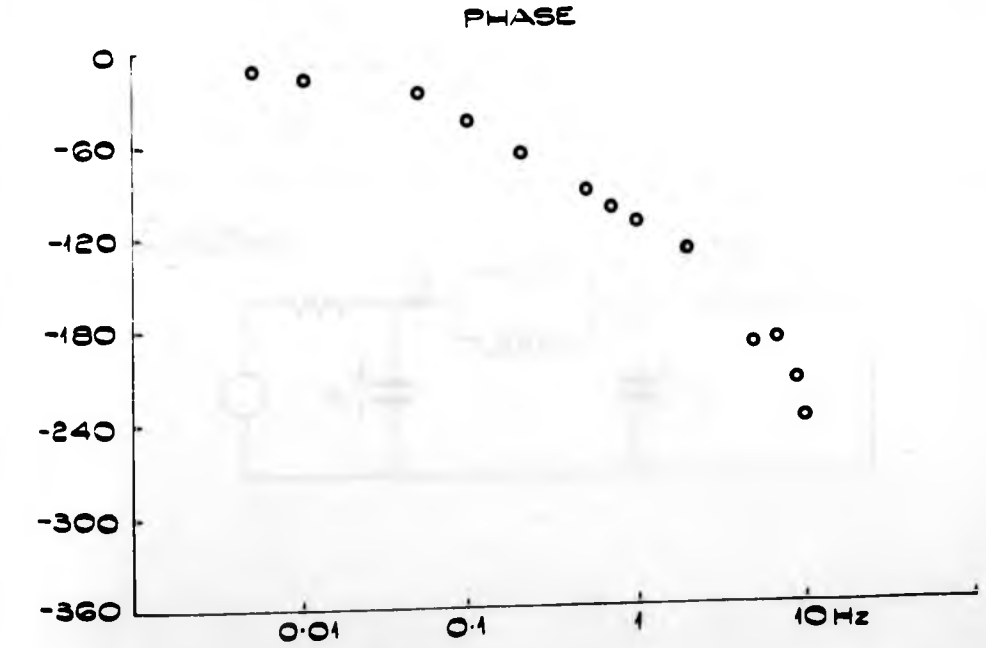

FIG 4.2

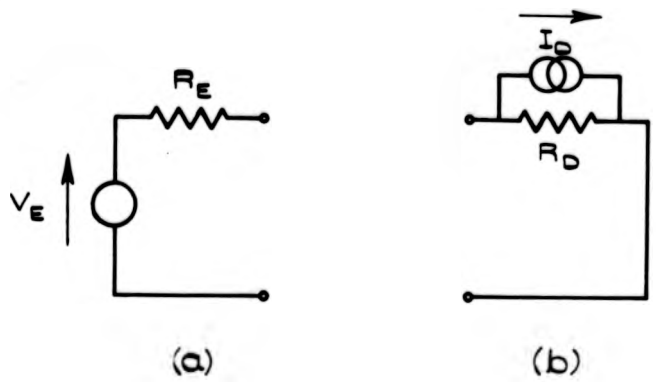

FIG. 4.5

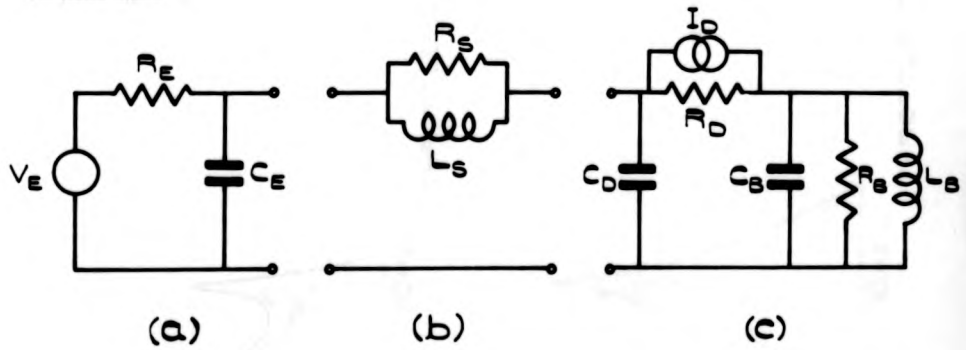

FIG 4.6

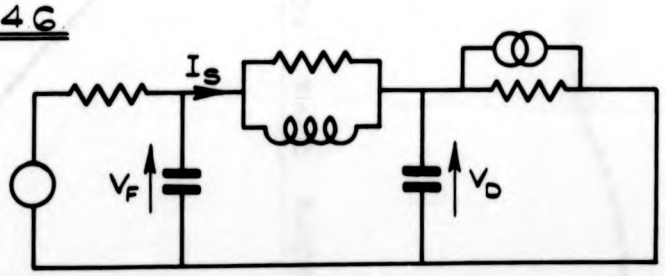

FIG 4.4 THROTTLE SPEED DYNAMOMETER DISCONNECTED.

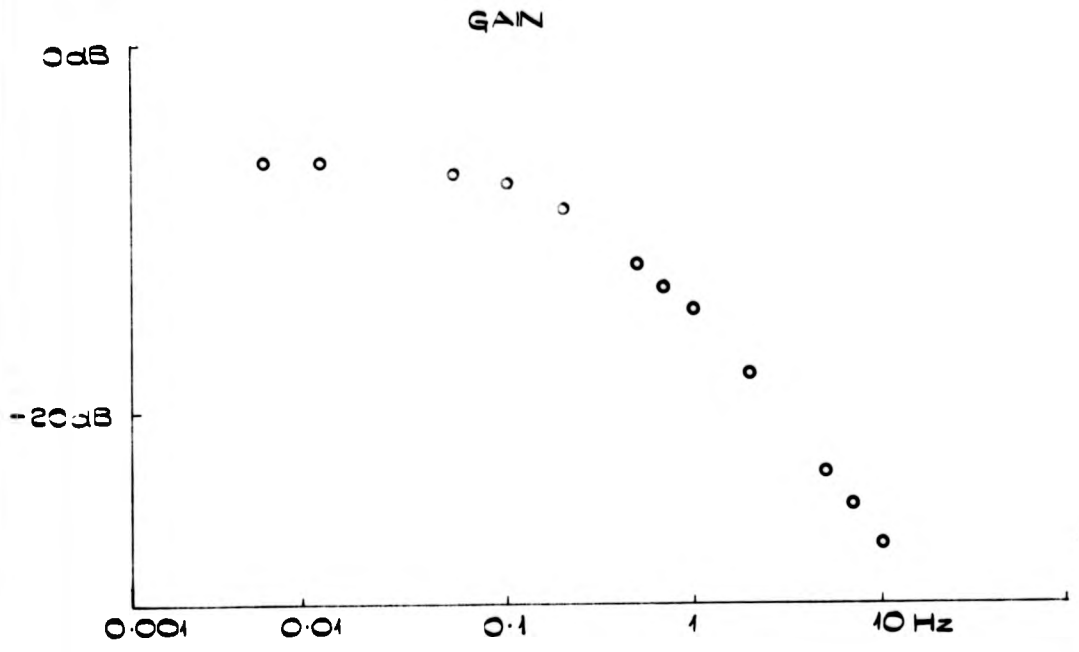

0dB = 1 VOLT PER 500 R.P.M.

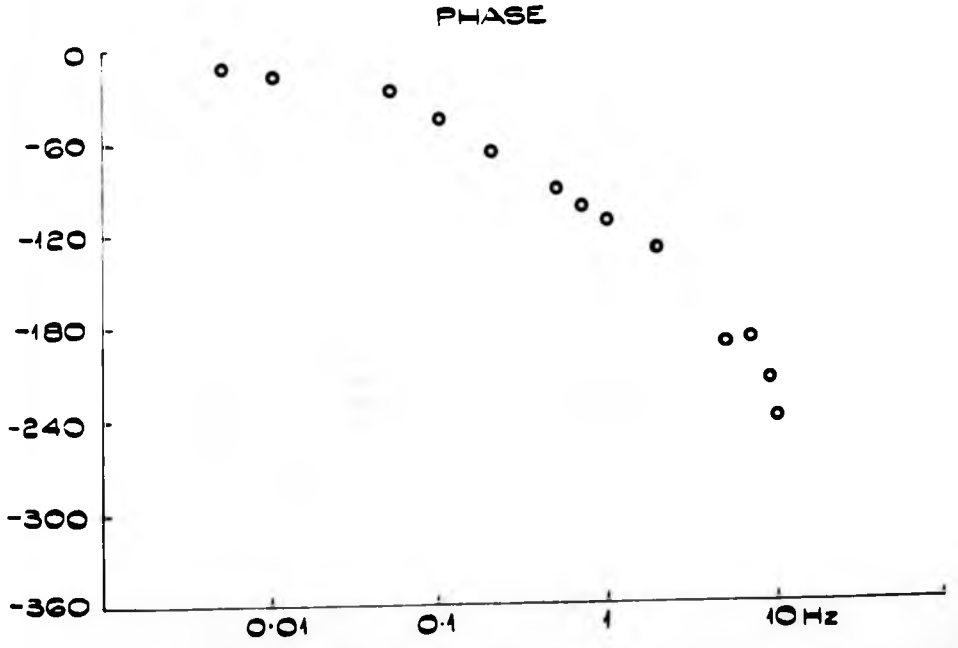

FIG 4.2

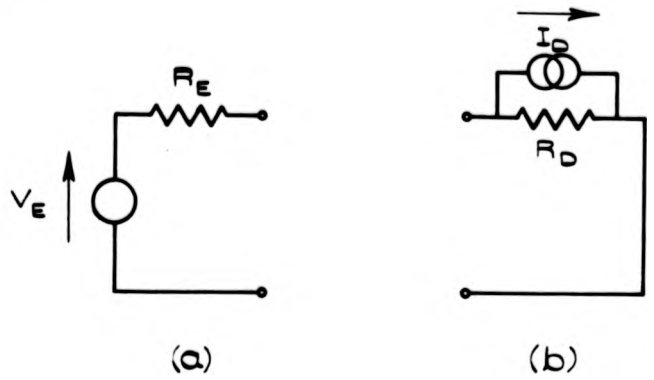

FIG 4.5

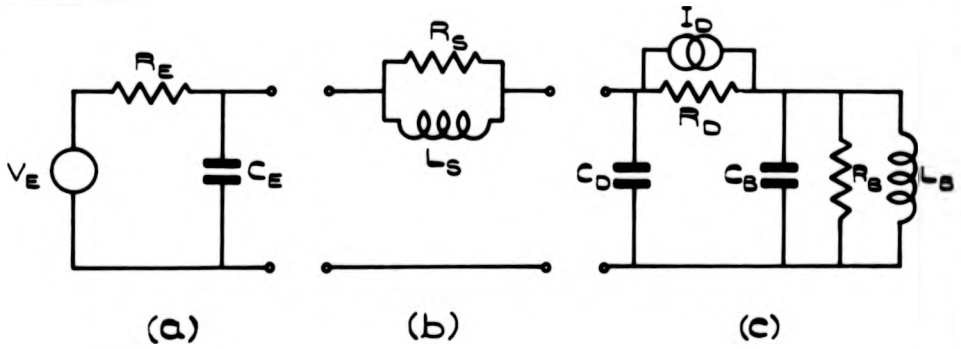

FIG 4.6

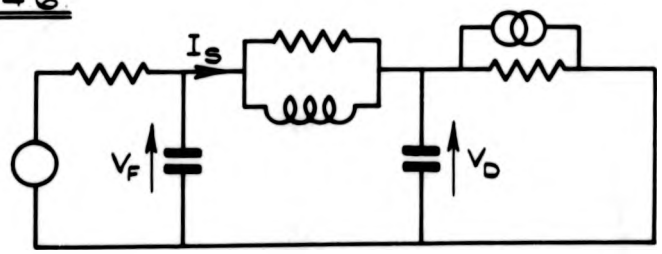

FIG. 4.7

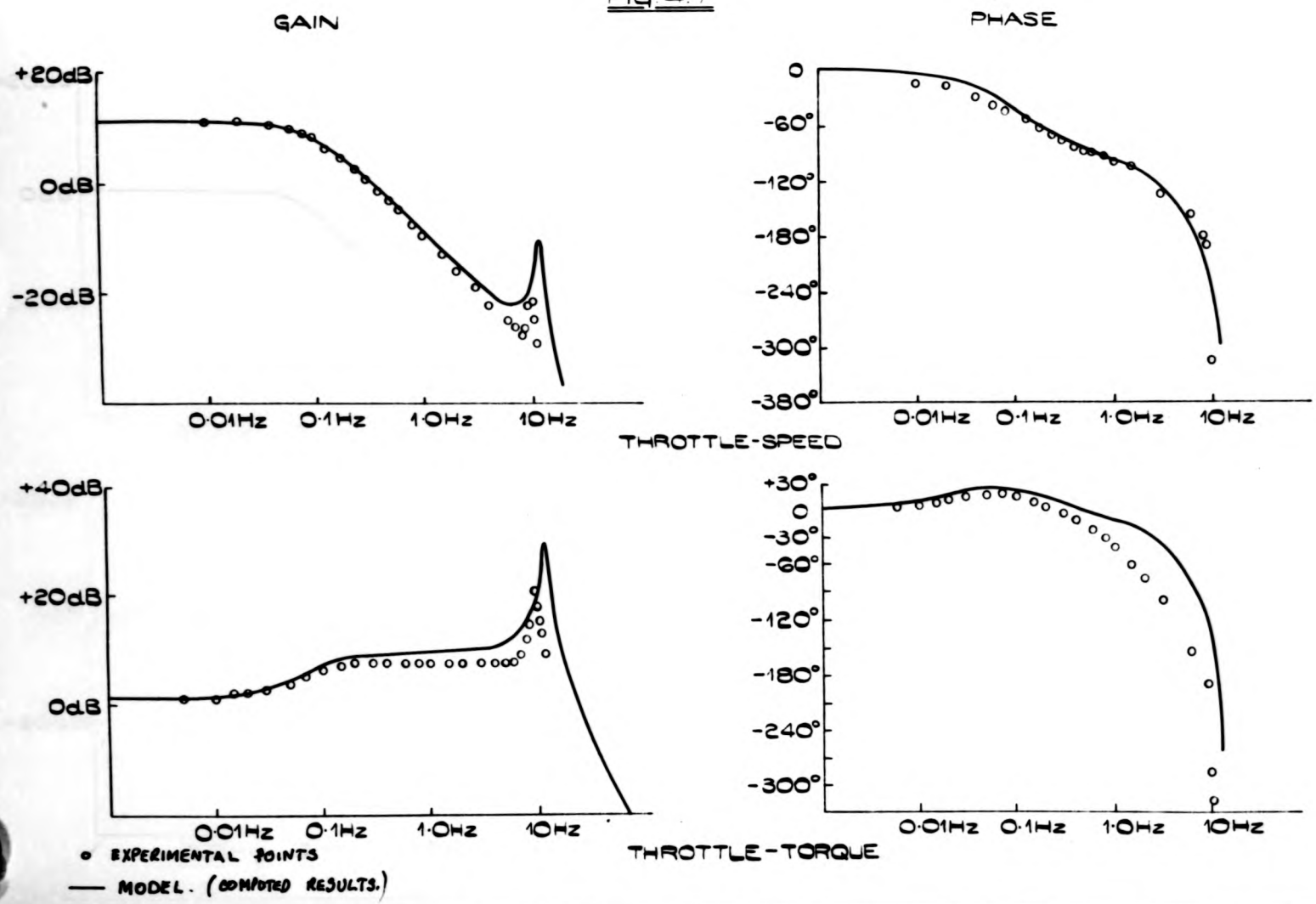
GAIN
PHASE
+20dB
0dB
-20dB
0
-60°
-120°
-180°
-240°
-300°
-380°
0·01Hz
0·1Hz
1·0Hz
10Hz
THROTTLE-SPEED
+40dB
+20dB
0dB
+30°
0
-30°
-60°
-120°
-180°
-240°
-300°
THROTTLE-TORQUE
o EXPERIMENTAL POINTS
— MODEL. (COMPUTED RESULTS.)

FIG. 4.8

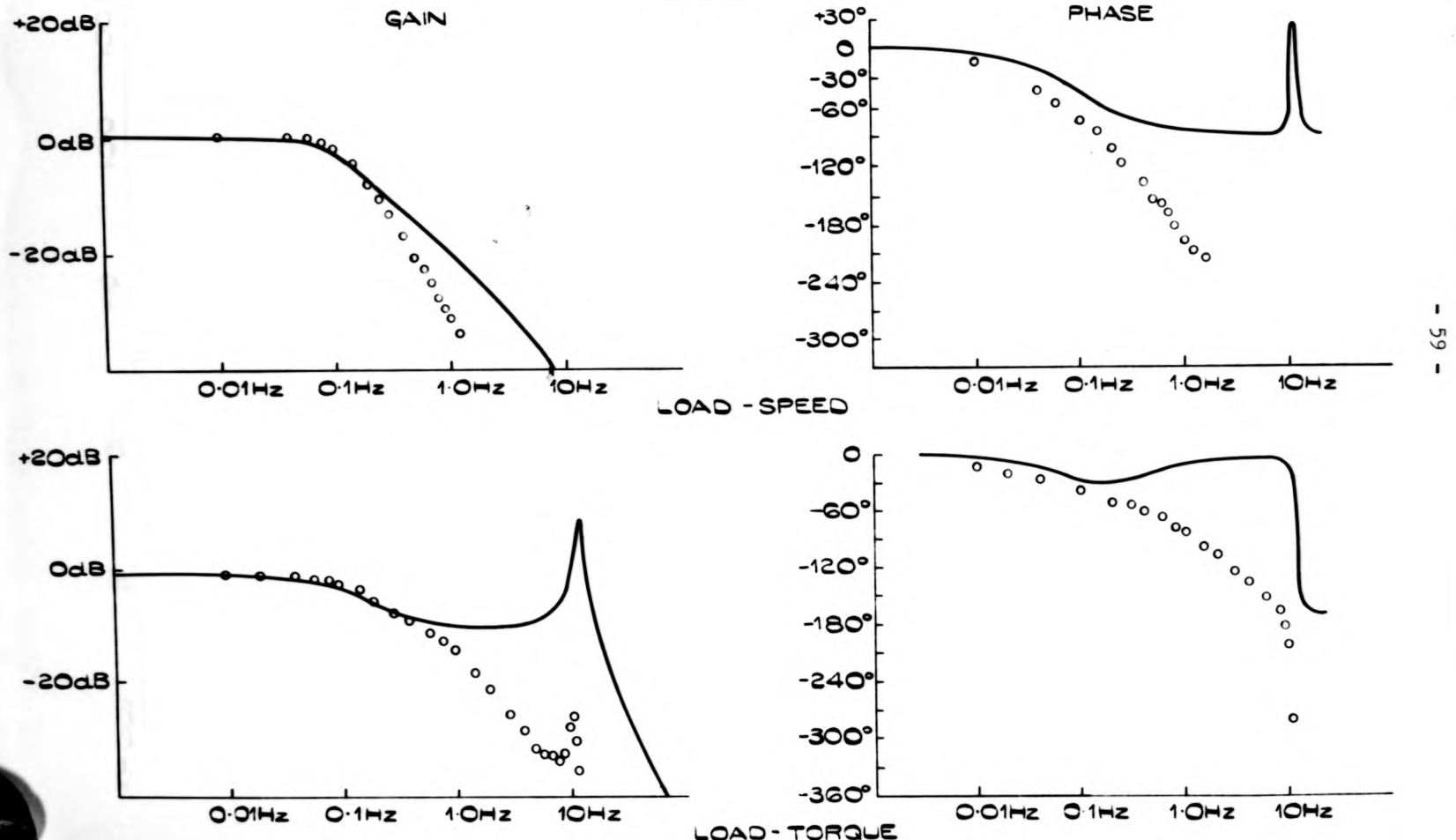
GAIN
+20dB
0dB
-20dB
0·01Hz
0·1Hz
1·0Hz
10Hz
PHASE
+30°
0
-30°
-60°
-120°
-180°
-240°
-300°
0·01Hz
0·1Hz
1·0Hz
10Hz
LOAD - SPEED
+20dB
0dB
-20dB
0·01Hz
0·1Hz
1·0Hz
10Hz
0
-60°
-120°
-180°
-240°
-300°
-360°
0·01Hz
0·1Hz
1·0Hz
10Hz
LOAD - TORQUE

FIG 4.9 CURRENT CONTROL INPUT VOLTAGE - FLUX

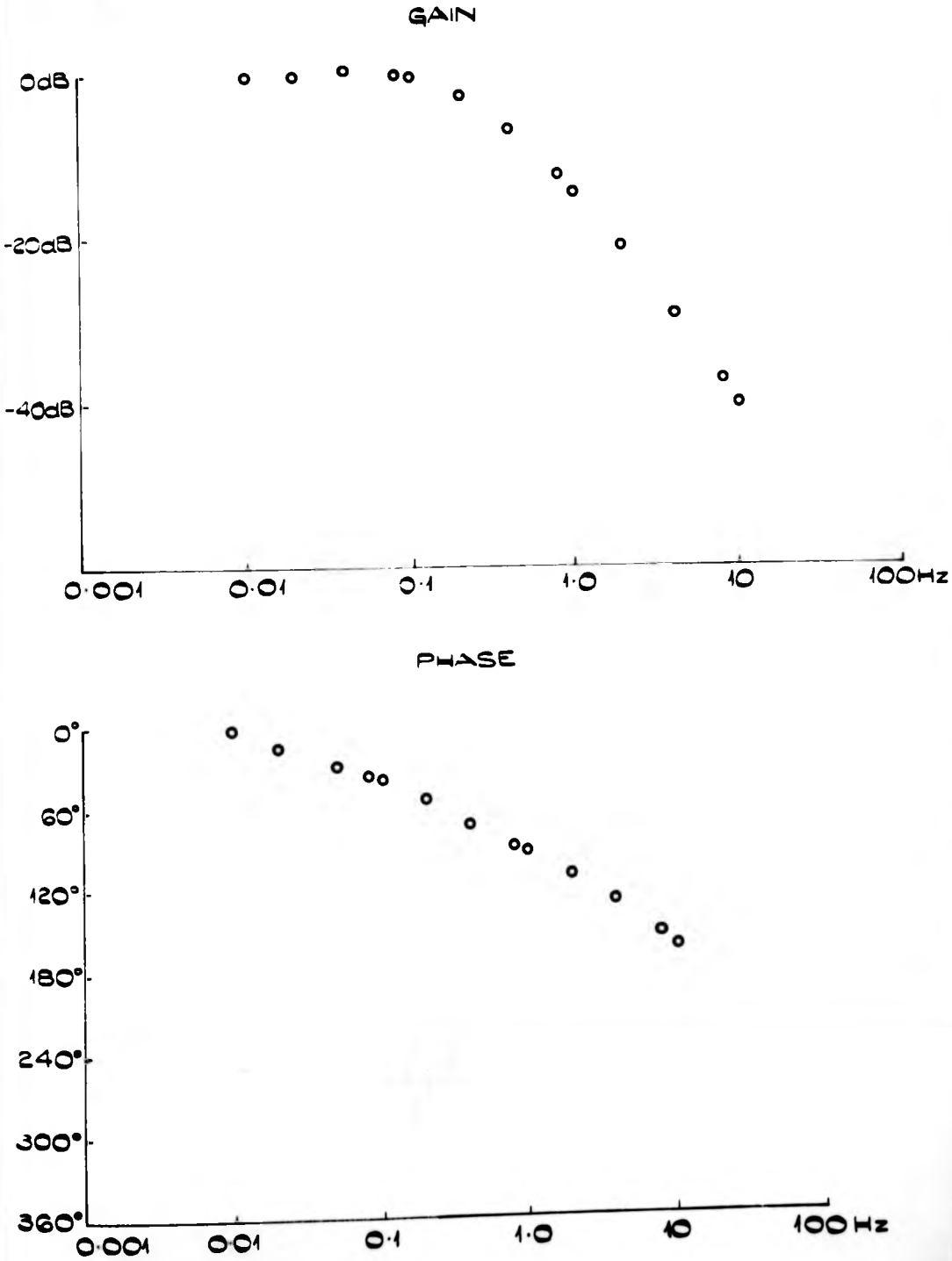

FIG 4.9 CURRENT CONTROL INPUT VOLTAGE - FLUX

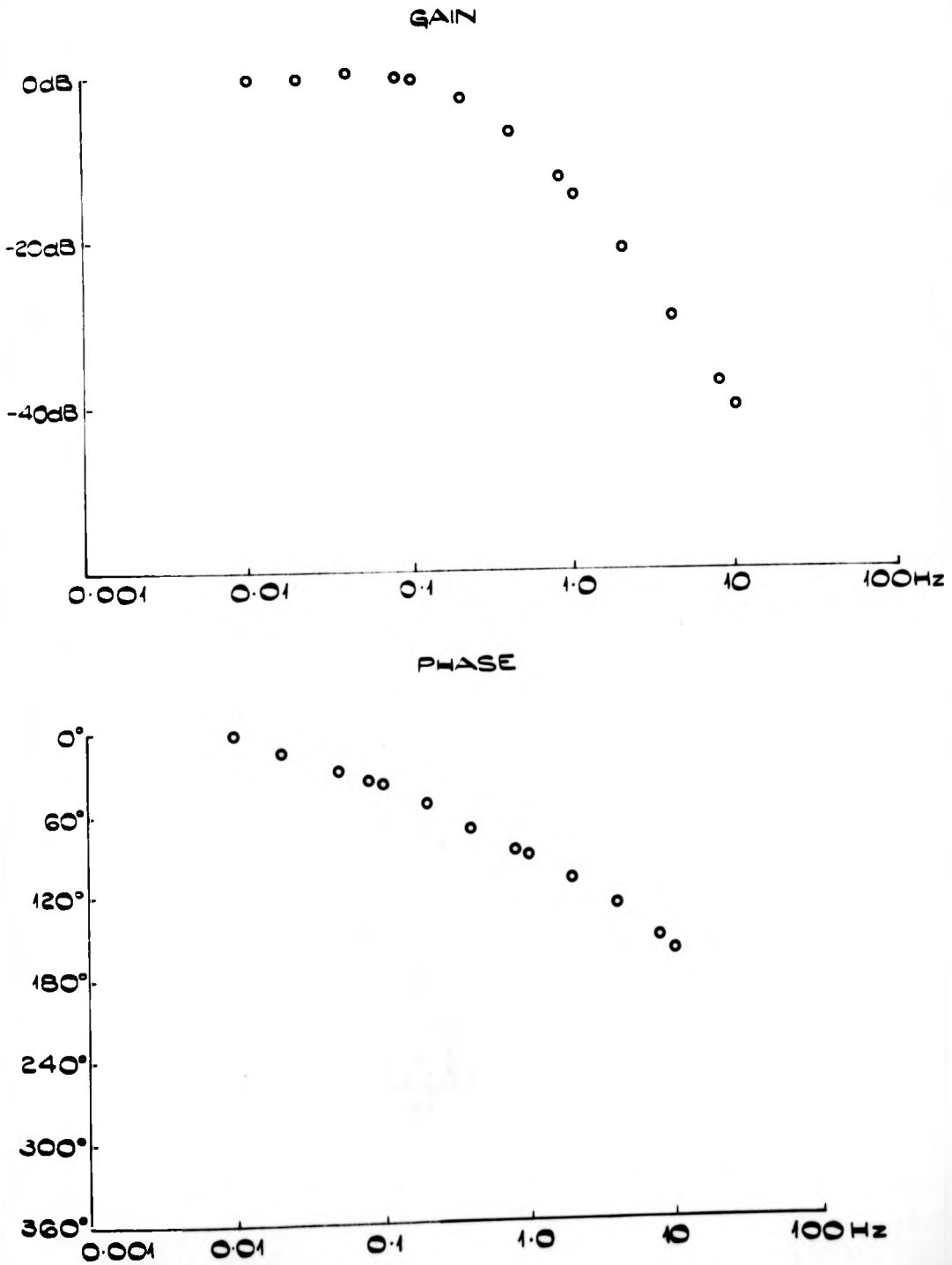

FIG. 4.10. REVISED MODEL

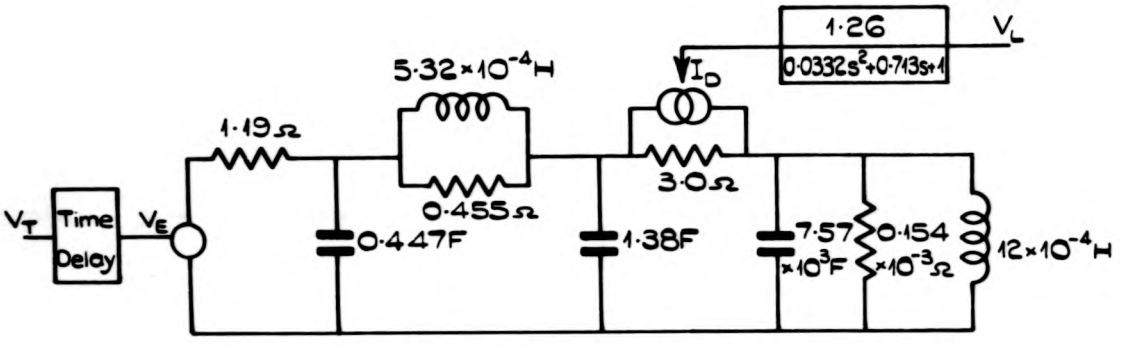

FIG. 4.11.

LOAD - SPEED

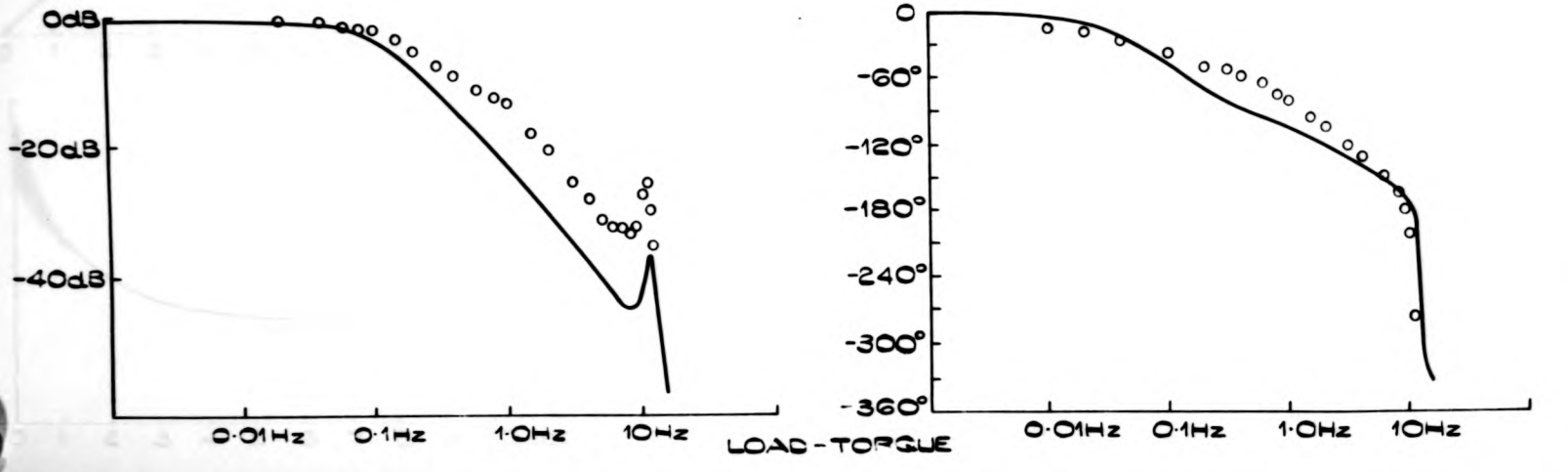

LOAD - TORQUE

FIG. 4.12. STEP RESPONSES:-

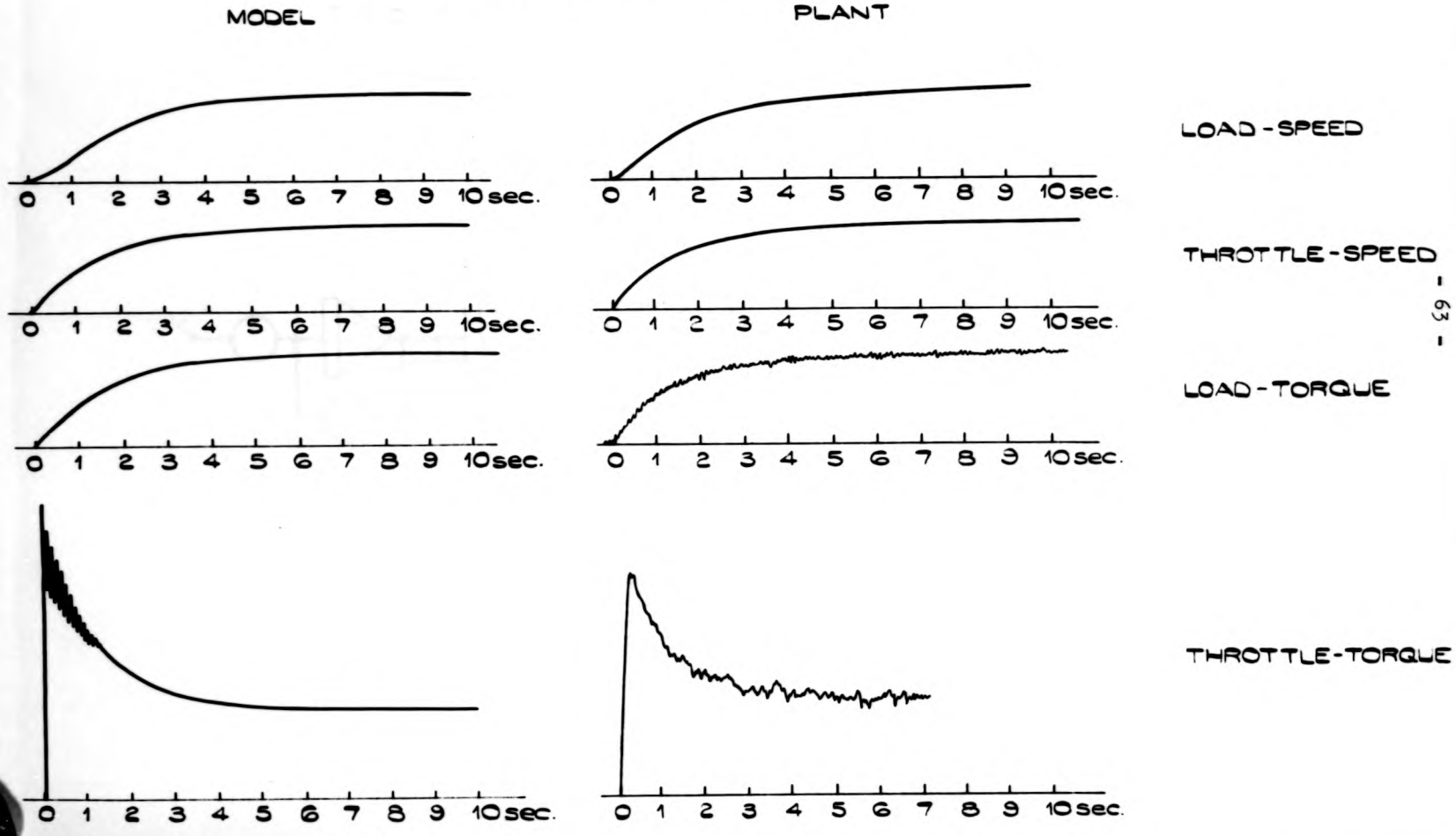

Fig 4.12. STEP RESPONSES:-

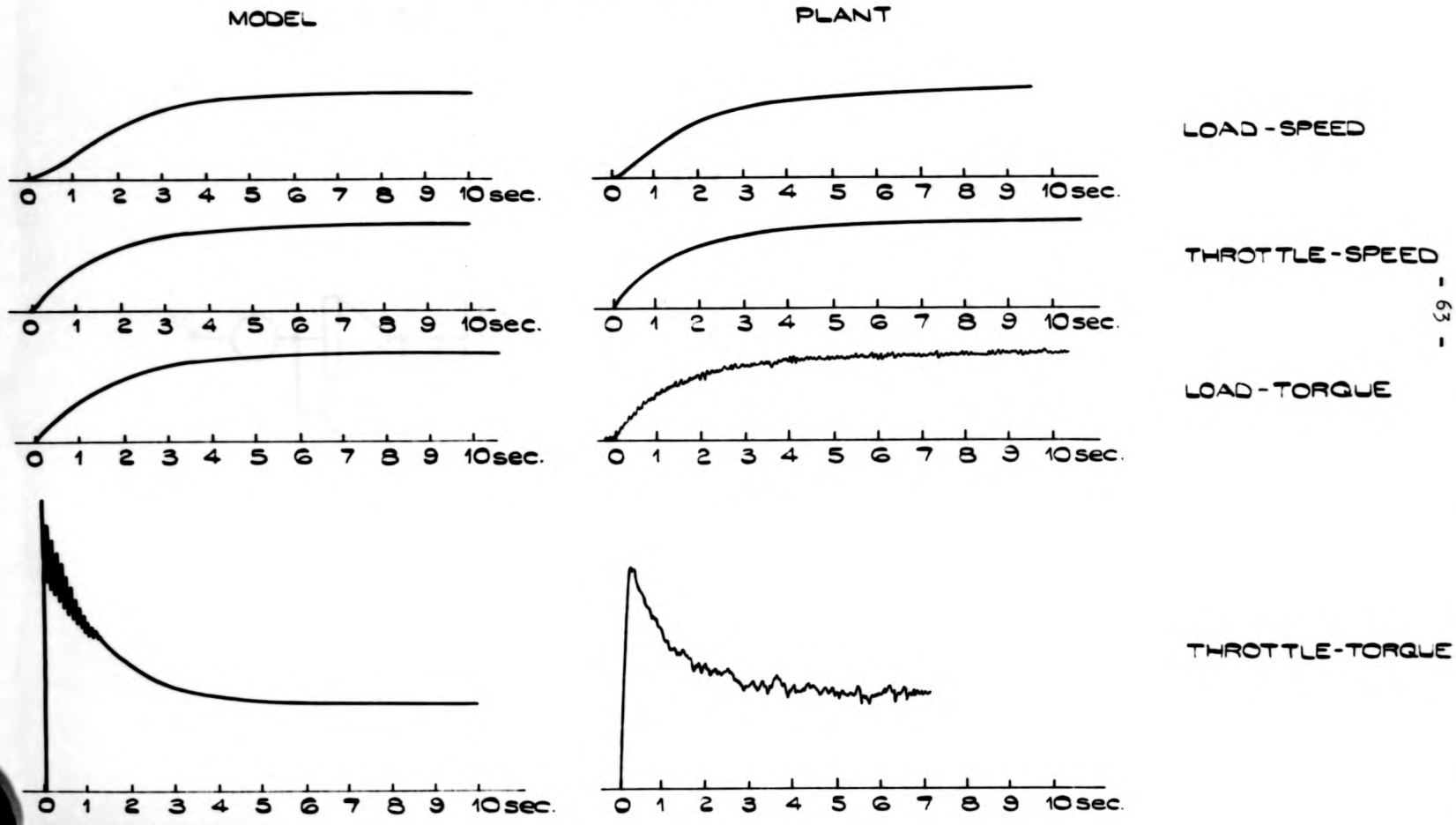

FIG. 4.13. ANALOG COMPUTER MODEL.

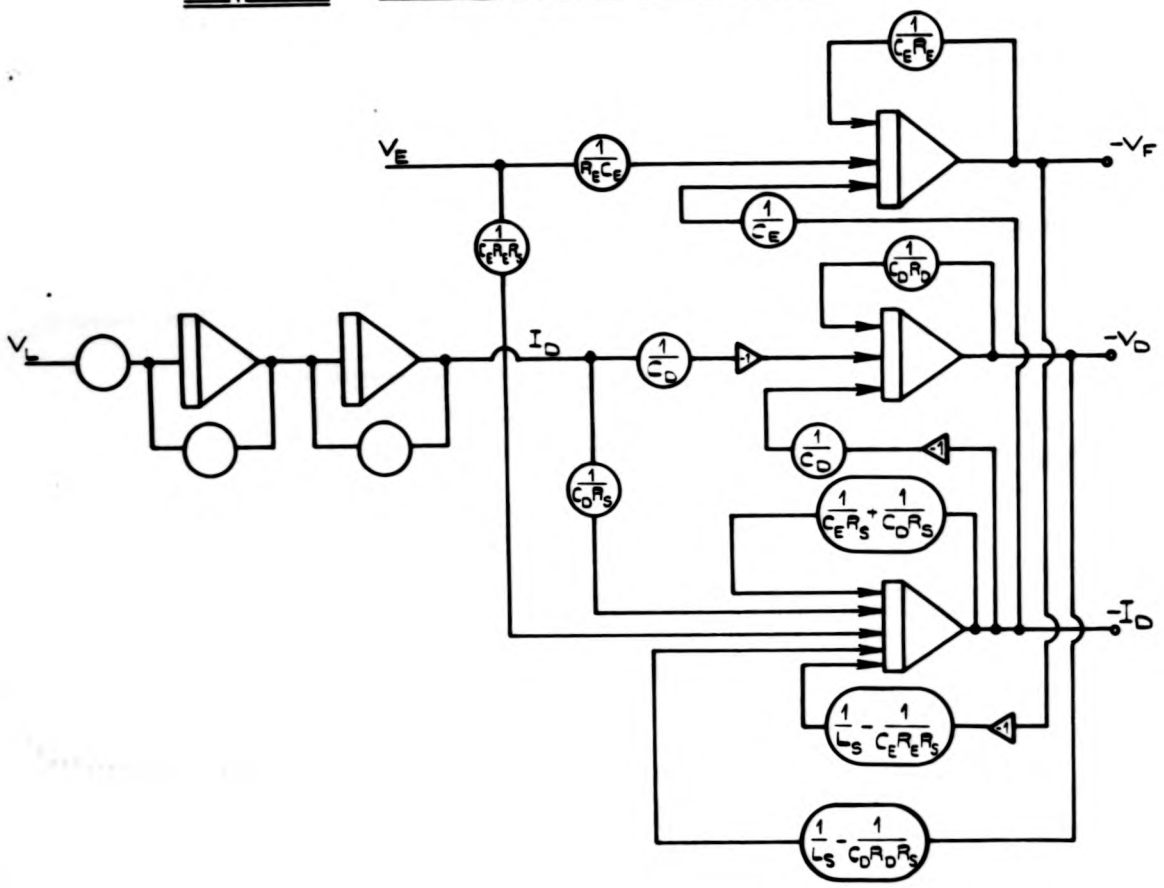

FIG. 4.14. IMPULSE RESPONSES

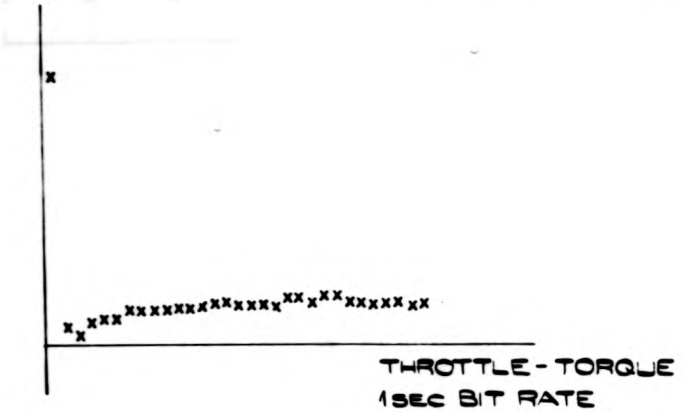

THROTTLE - TORQUE
1 SEC BIT RATE

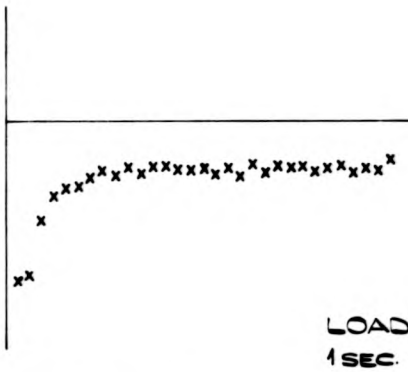

LOAD - TORQUE
1 SEC. BIT RATE

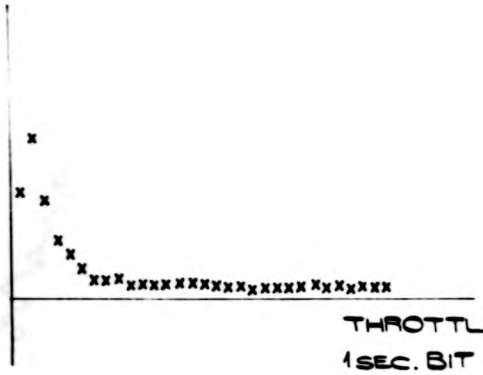

THROTTLE - SPEED
1 SEC. BIT RATE

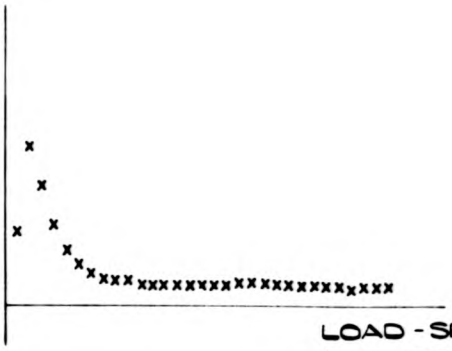

LOAD - SPEED
1 SEC. BIT RATE

FREQUENCY RESPONSE ESTIMATE FOR:-

THROTTLE - TORQUE

Fig. 4.15.

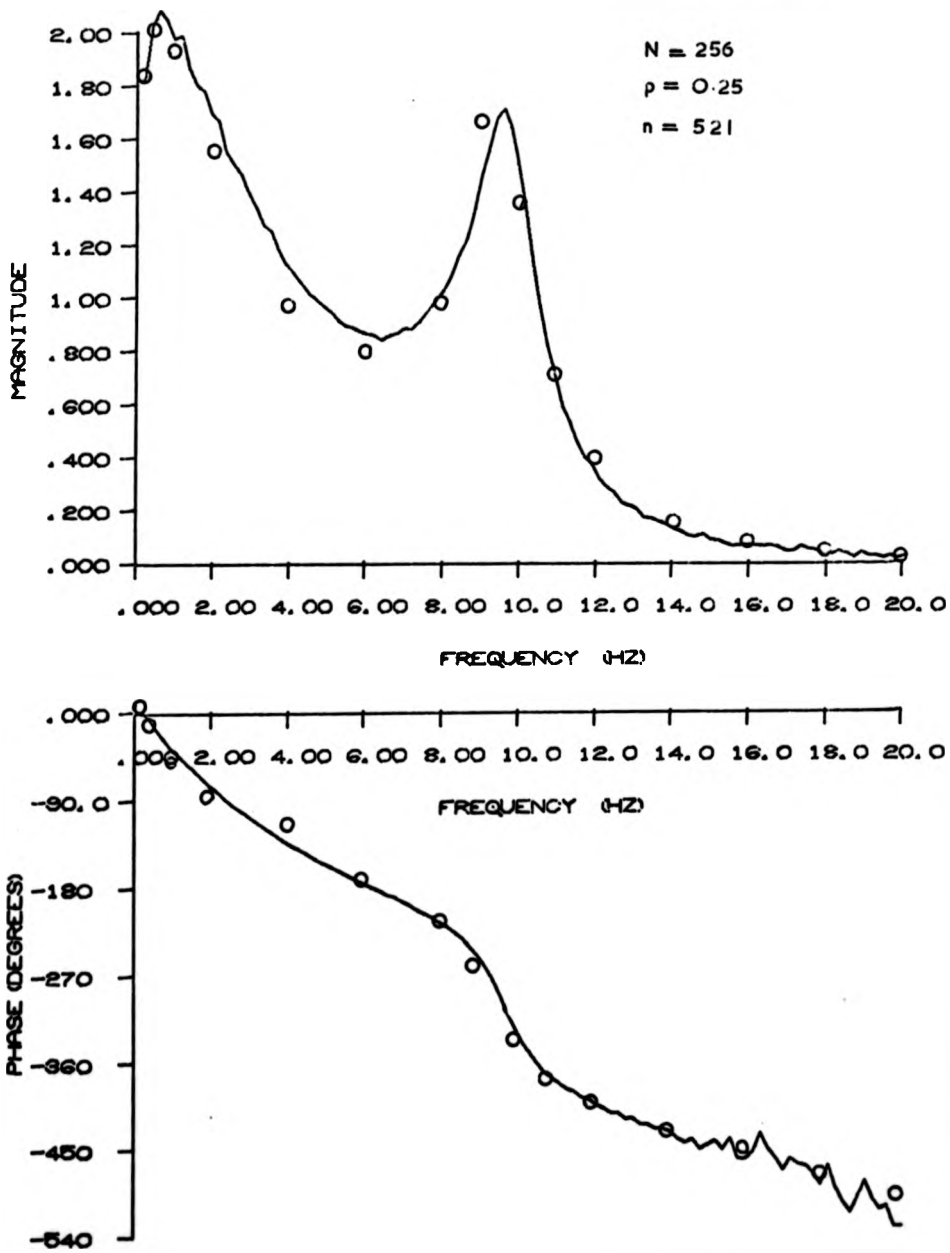

FIG. 4.11.

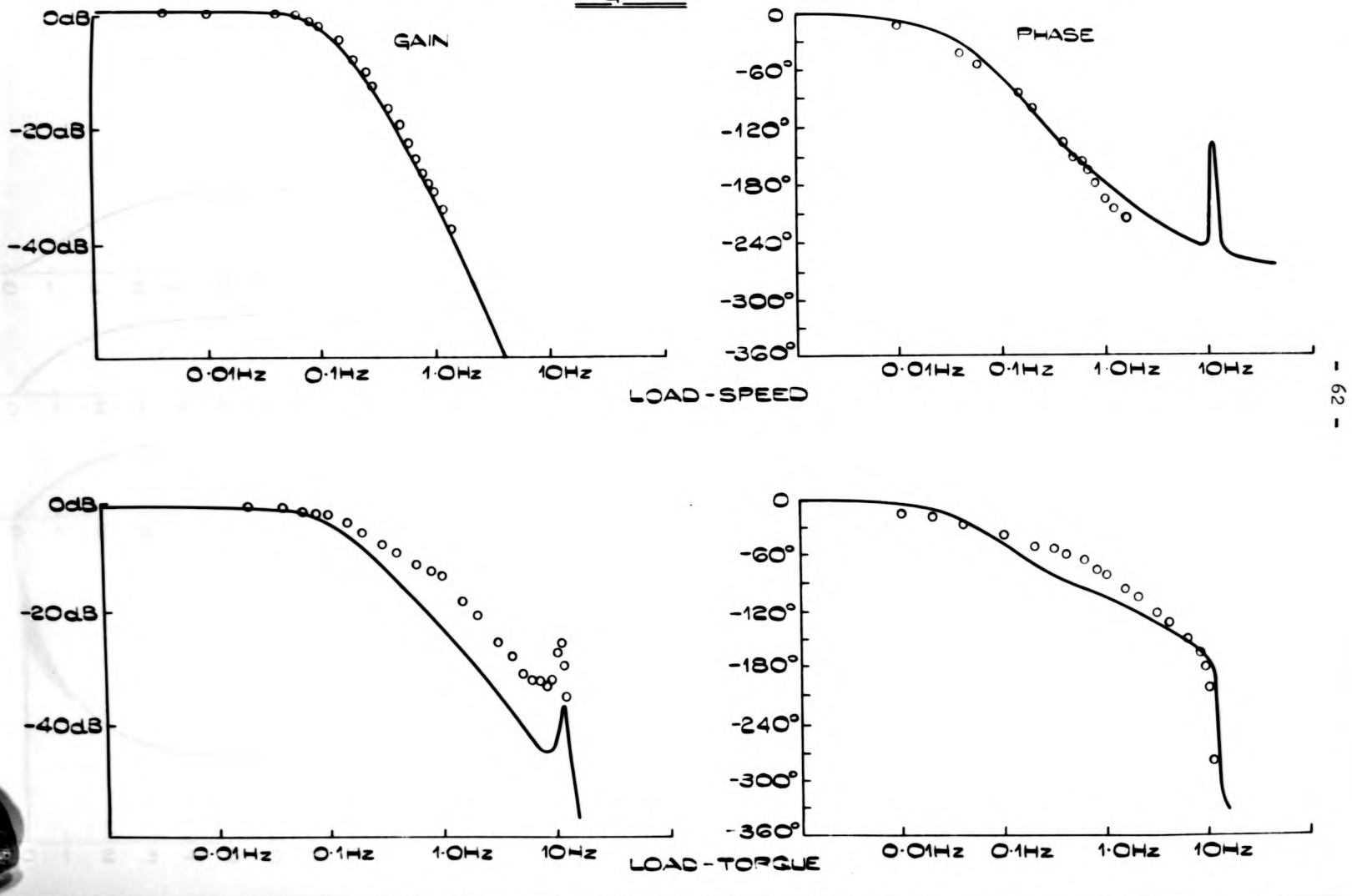
0dB
-20dB
-40dB
GAIN
0·01Hz
0·1Hz
1·0Hz
10Hz
LOAD - SPEED
0
-60°
-120°
-180°
-240°
-300°
-360°
PHASE
0·01Hz
0·1Hz
1·0Hz
10Hz
0dB
-20dB
-40dB
0·01Hz
0·1Hz
1·0Hz
10Hz
LOAD - TORQUE
0
-60°
-120°
-180°
-240°
-300°
-360°
0·01Hz
0·1Hz
1·0Hz
10Hz

FIG. 4.12. STEP RESPONSES:-

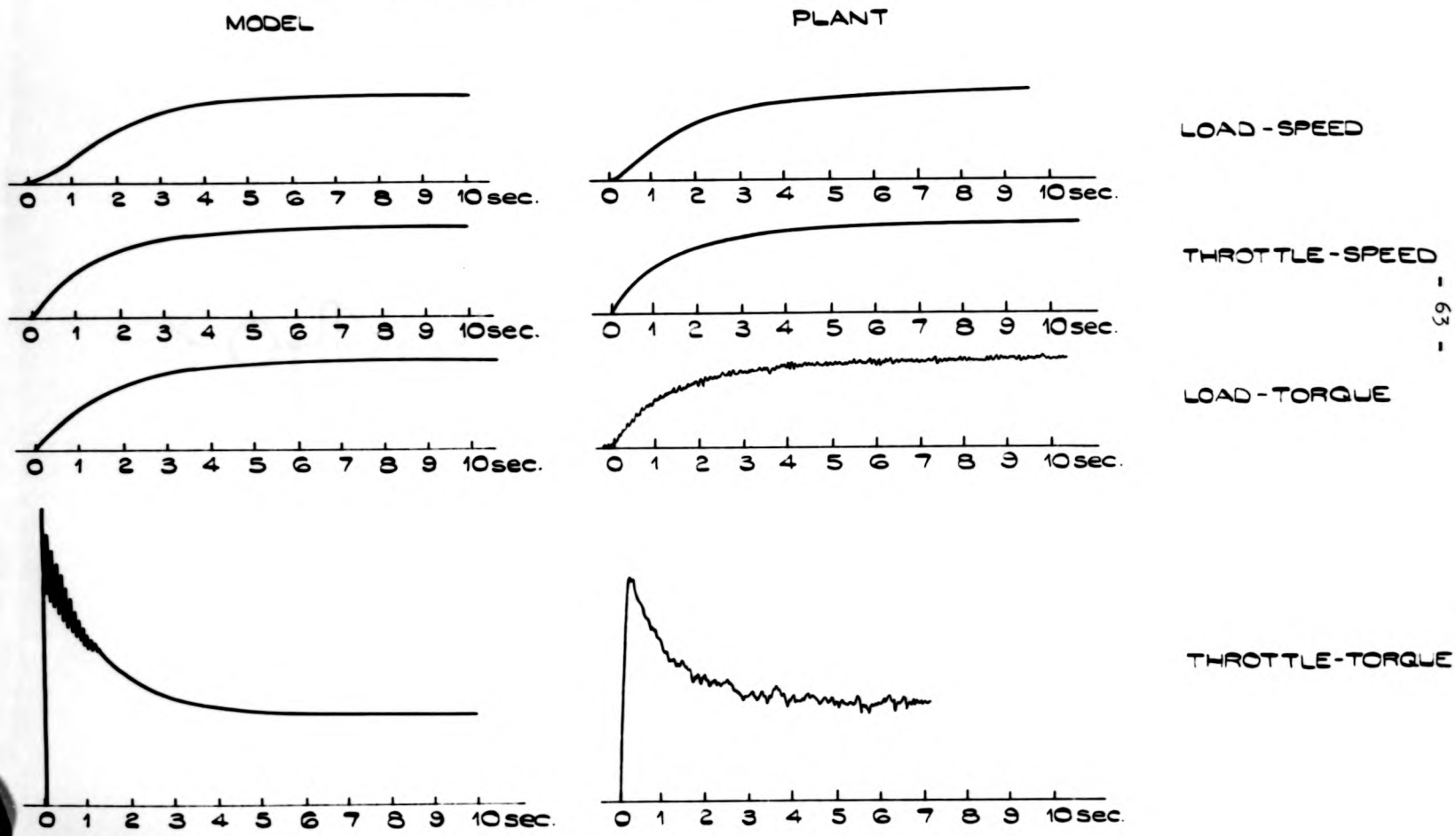

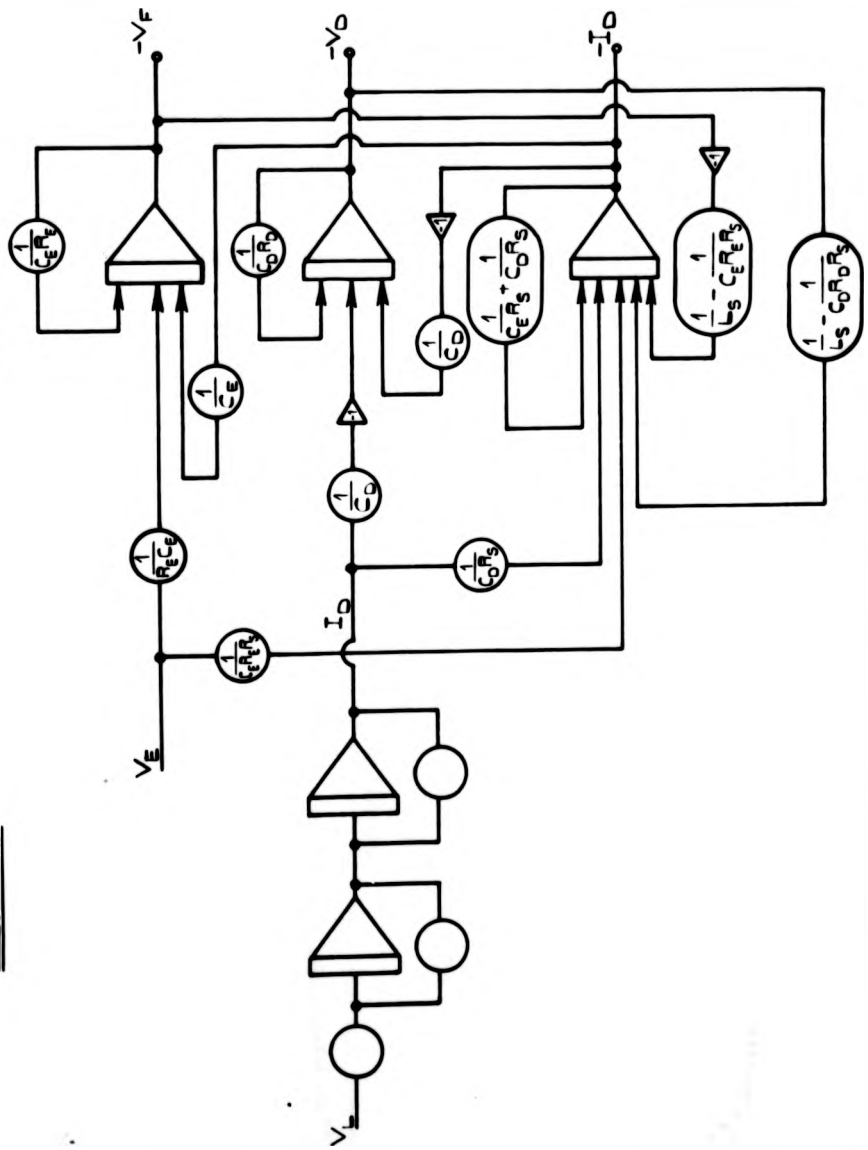

FIG 4.13 ANALOG COMPUTER MODEL

FIG. 4.14. IMPULSE RESPONSES

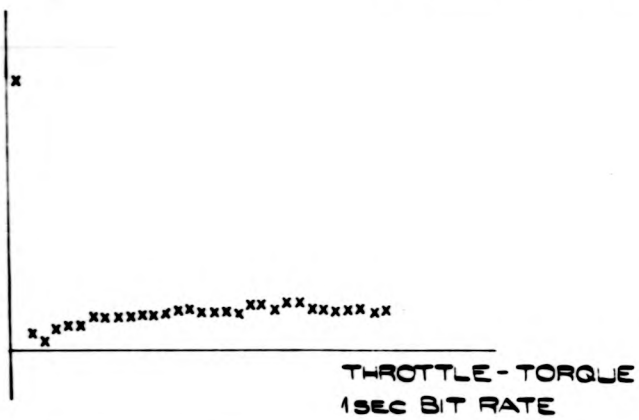

THROTTLE - TORQUE
1 SEC BIT RATE

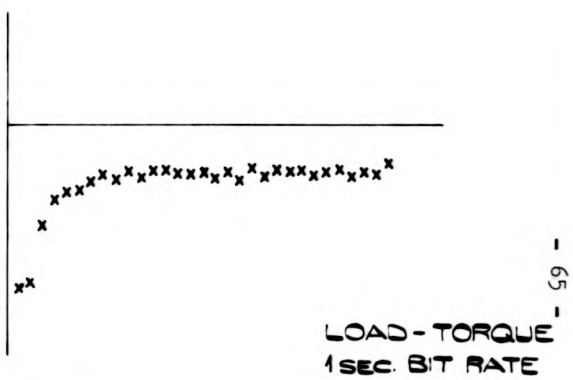

LOAD - TORQUE
1 SEC. BIT RATE

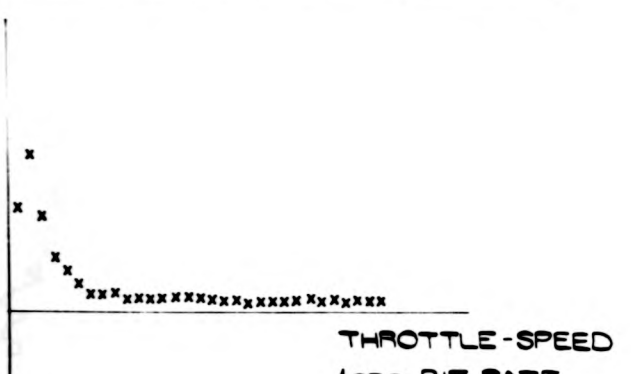

THROTTLE - SPEED
1 SEC. BIT RATE

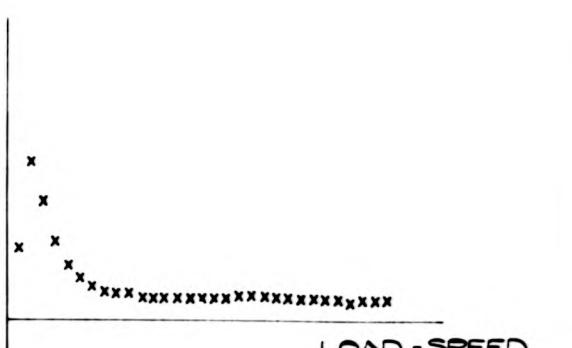

LOAD - SPEED
1 SEC. BIT RATE

FREQUENCY RESPONSE ESTIMATE FOR:-

THROTTLE - TORQUE

Fig. 4.15.

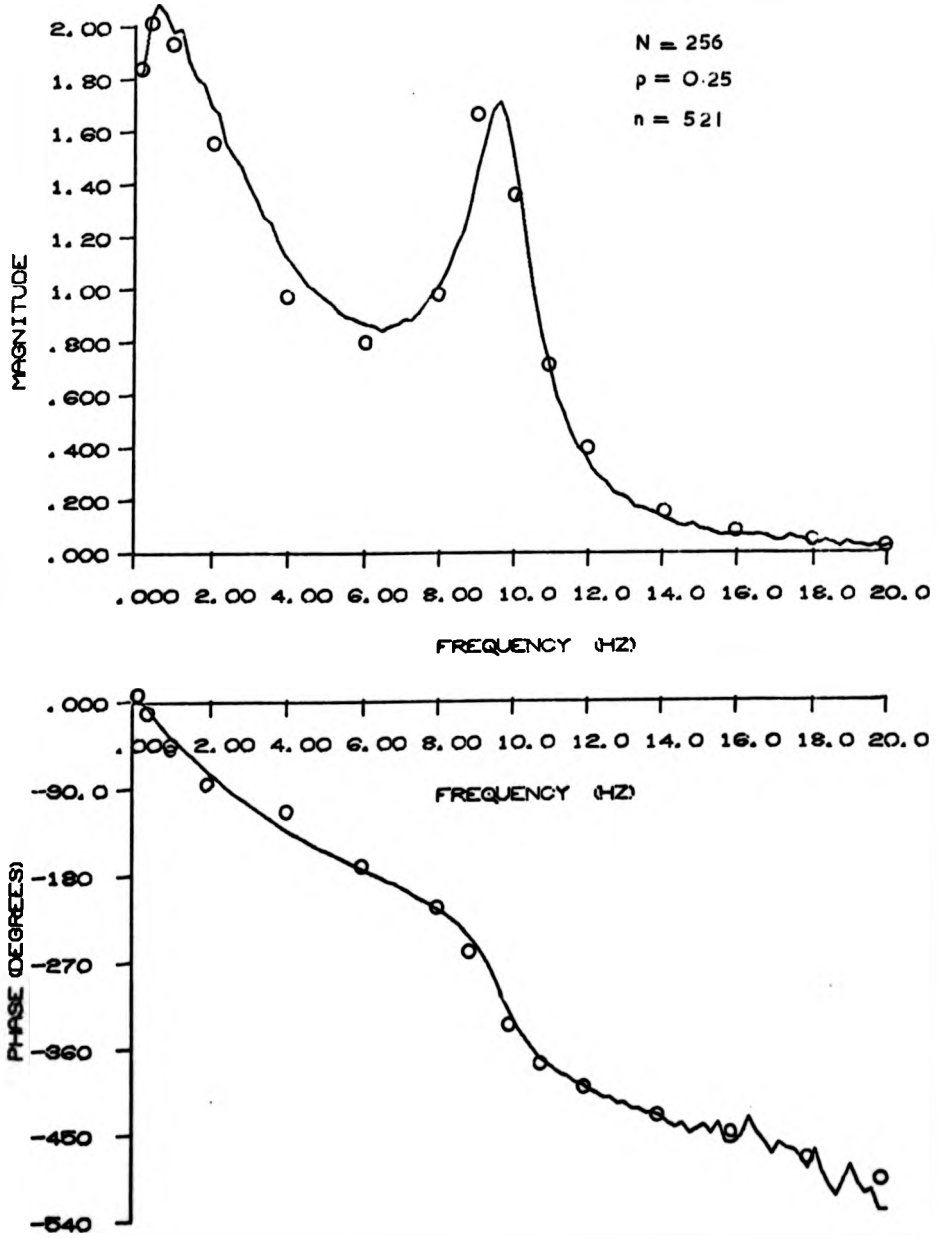

FREQUENCY RESPONSE ESTIMATE FOR:-

THROTTLE - SPEED Fig. 4.16.

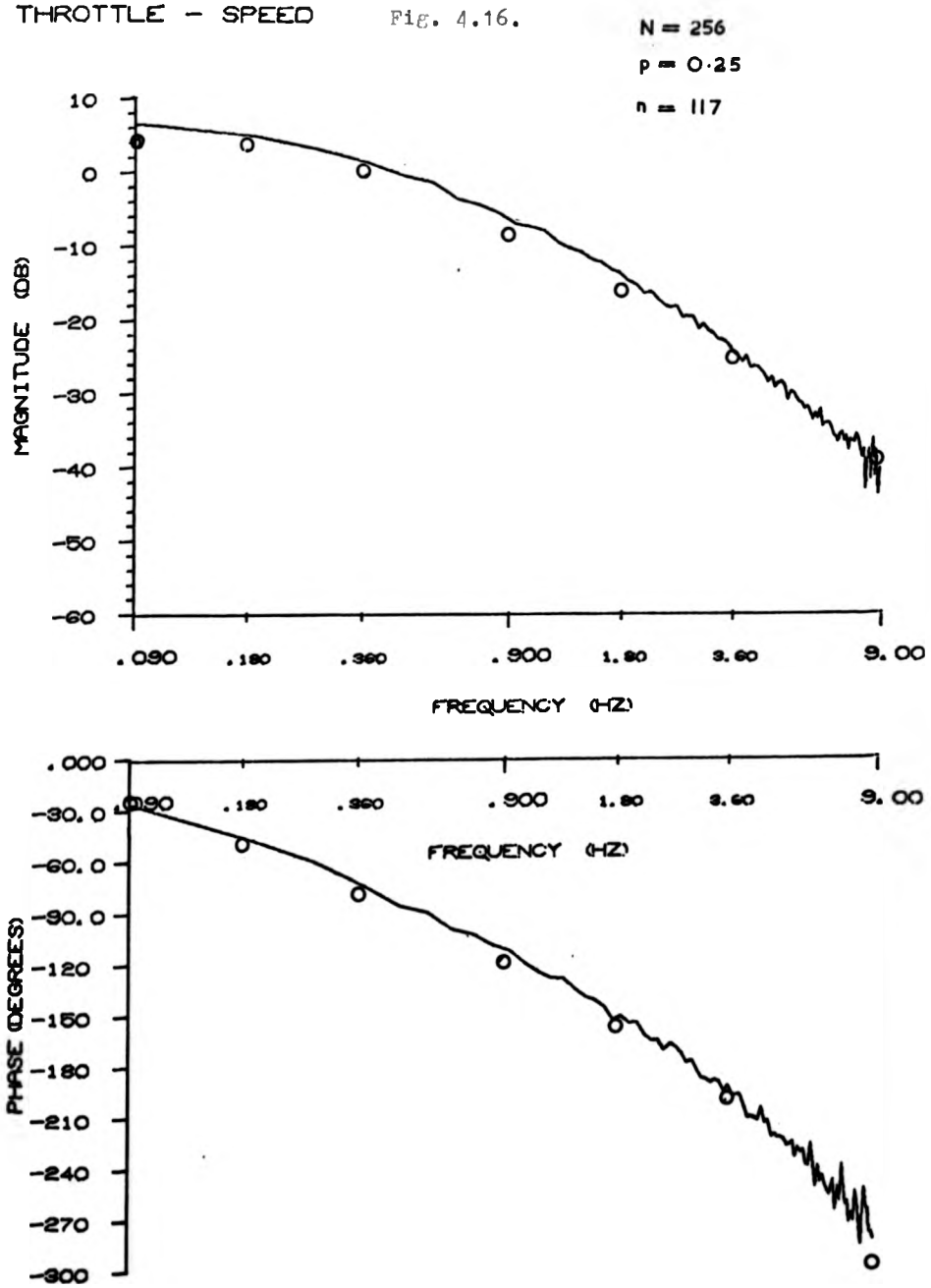

FREQUENCY RESPONSE ESTIMATE FOR:-

LOAD - TORQUE

Fig. 4.17.

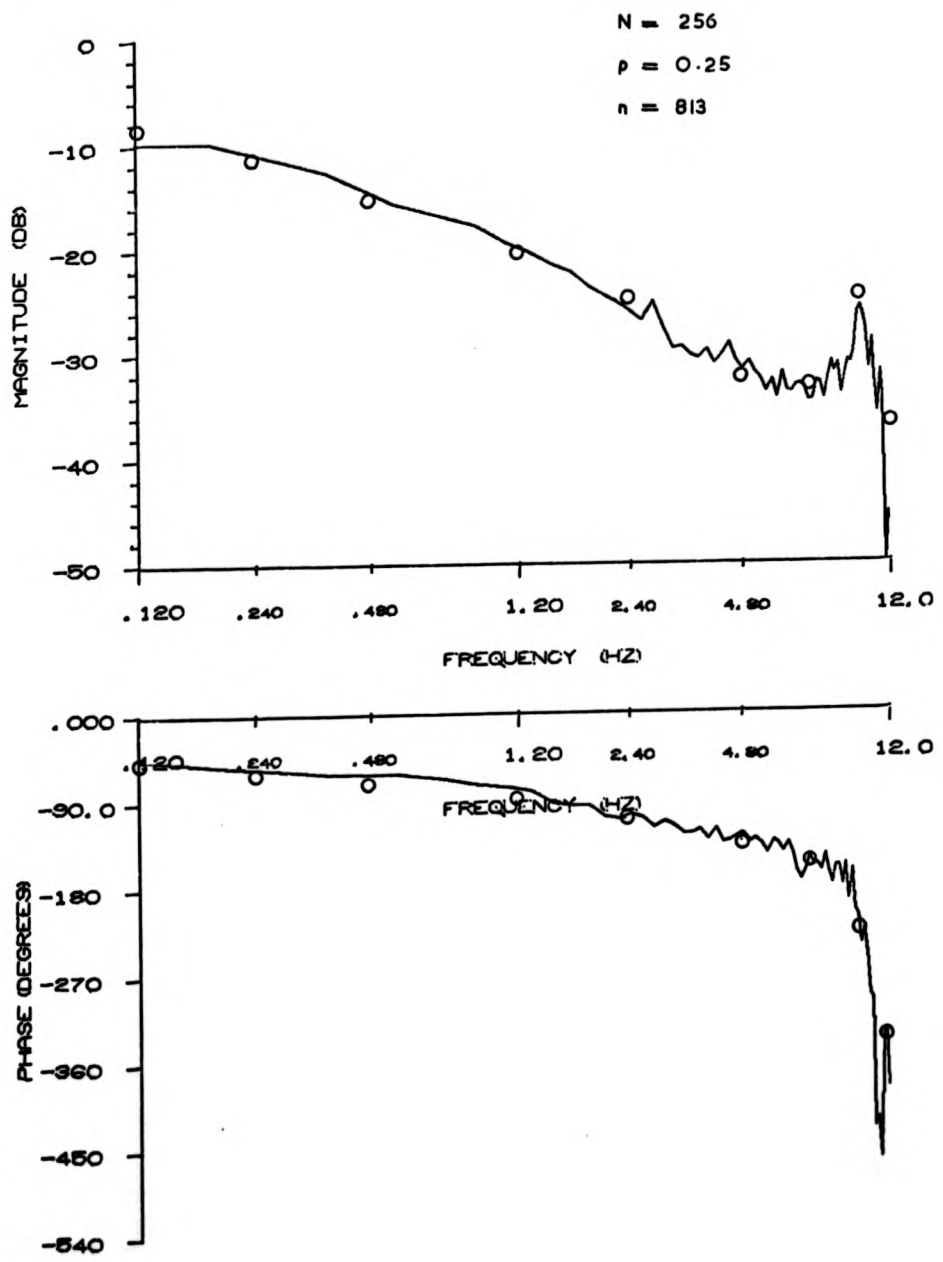

FREQUENCY RESPONSE ESTIMATE FOR:-

LOAD - SPEED

Fig. 4.18.

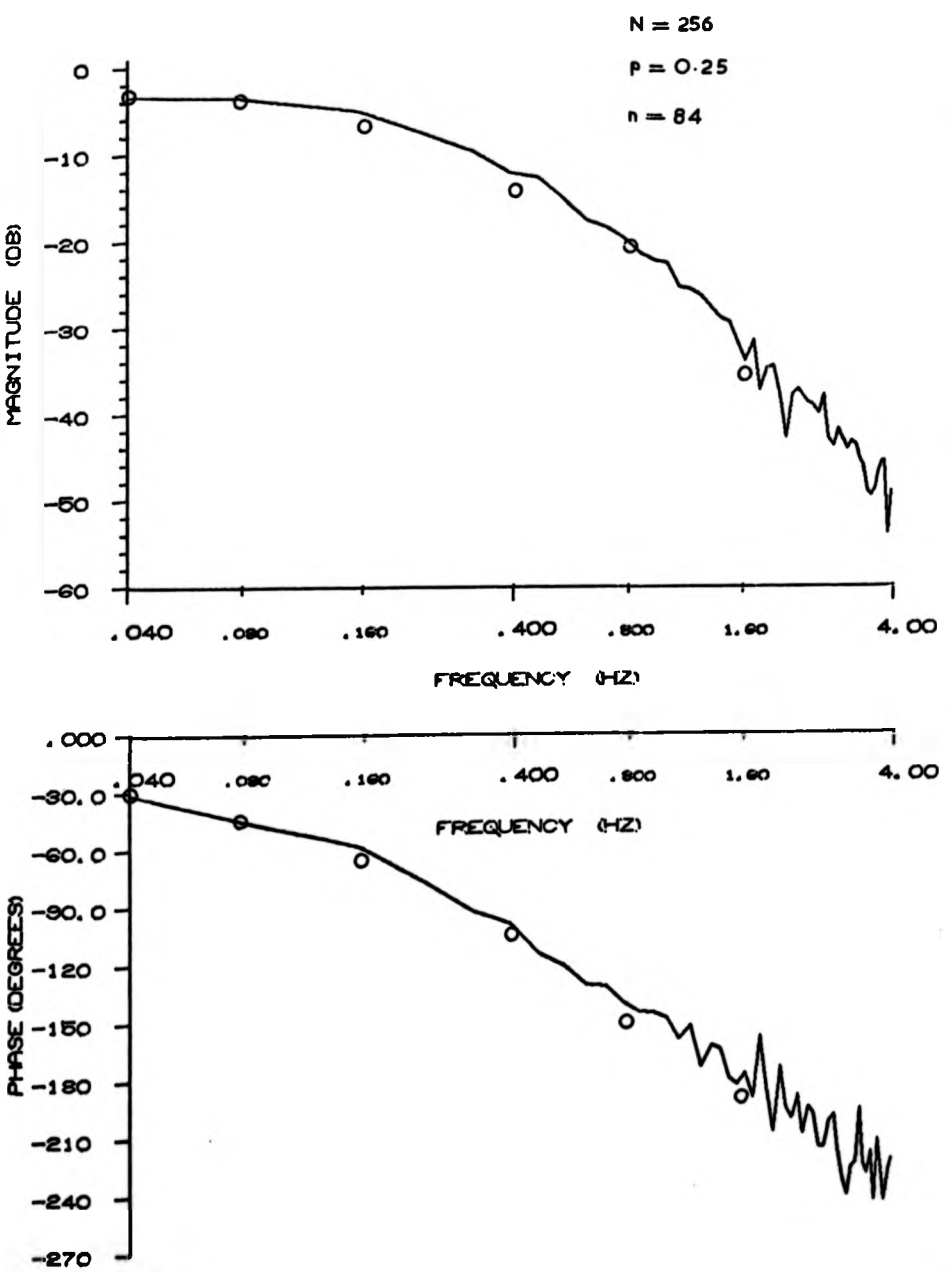

FIG. 4.19.

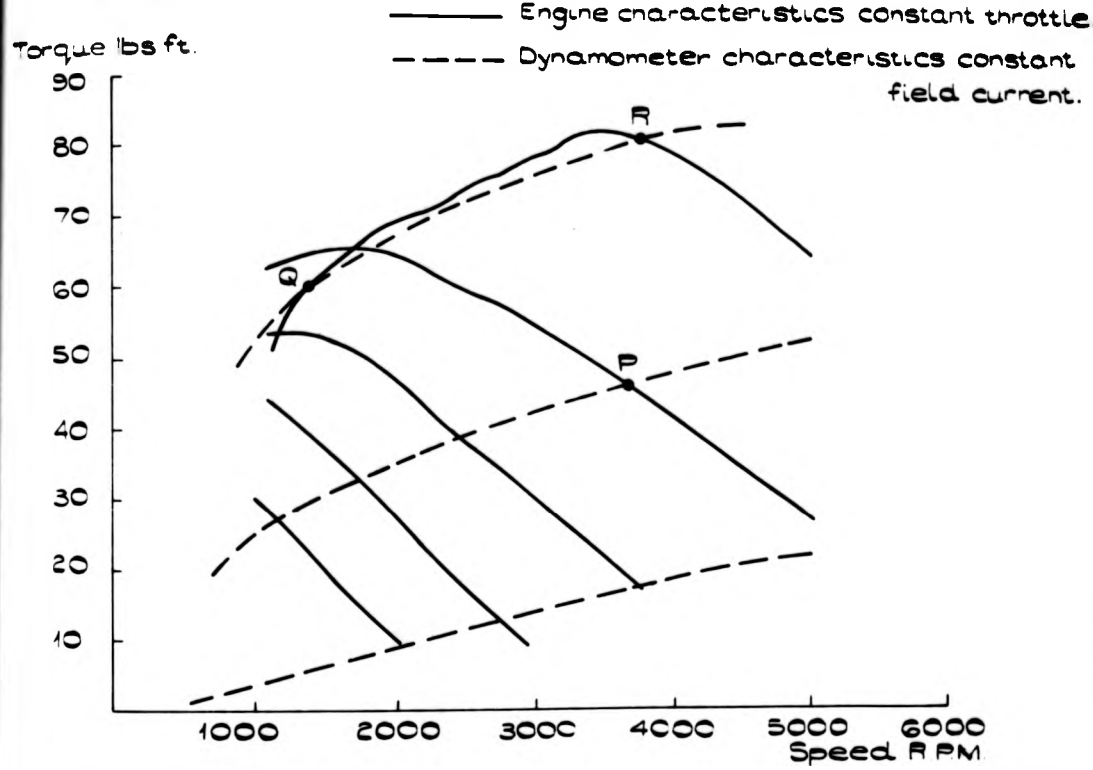

FIG. 4.20.

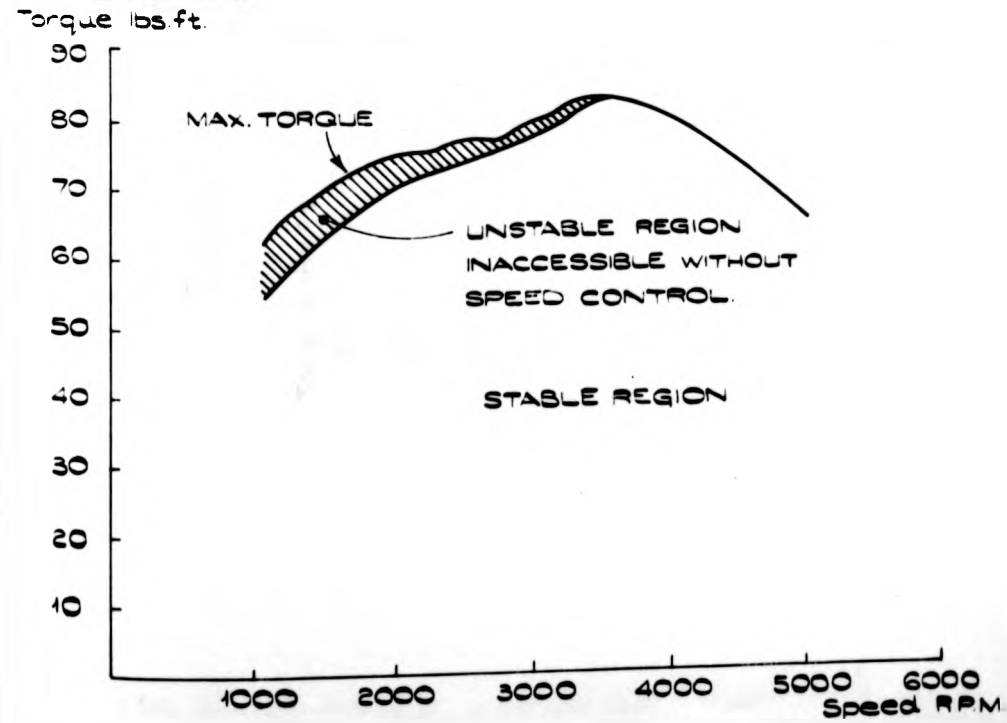

FIG. 4.21.

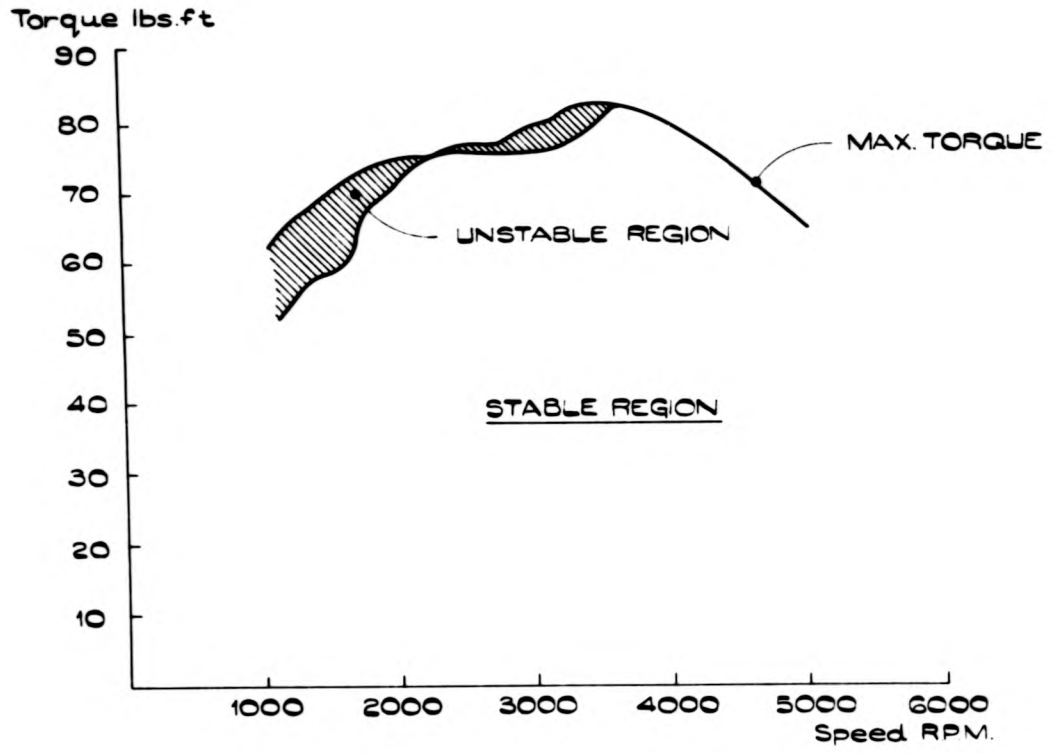
Torque lbs.ft
90
80
70
60
50
40
30
20
10
MAX. TORQUE
UNSTABLE REGION
STABLE REGION
1000
2000
3000
4000
5000
6000
Speed RPM.

CHAPTER 5.

CONTROL SYSTEMS.

1. Water and oil temperature controls.
2. The speed control system.
3. Fuel mass flow rate control.

1. Water and oil temperature controls.

Engine testing methods favour the use of the thermostat for the control of water temperature and a water to water heat exchanger is normally used in place of the vehicle radiator. The heat exchanger thermal capacity and flow resistance are matched to those of the vehicle radiator to provide a facsimile of the vehicle cooling system. An alternative method is to convert the vehicle radiator into a water to water heat exchanger.

Thermostatic temperature control suffers from two shortcomings, namely that a steady state error, which is a function of the heat rejection rate to the cooling system and the coolant flow rate will always exist, and setpoint changes require that the thermostat should be changed. To overcome these shortcomings a test bed system must be more sophisticated.

In order to formulate the performance specification for a controller the needs of motor vehicle manufacturers and oil companies were examined. As a result it was considered sufficient to control cooling water temperature, as measured in the thermostat housing to within $\pm \frac{1}{2}^{o}C$. The measurement may be averaged over 30 seconds and control was required between $60^{o}C$ and $90^{o}C$ for all engine operating conditions. The response to set point changes should achieve the specified accuracy within three minutes. (A considerably longer time than this is required to allow the thermal conditions within the engine to settle.)

The design of test bed cooling system is described with reference to fig.5.1. A motorised mixing valve was used as the control element. The vehicle radiator was replaced by a counter-current water-cooled heat exchanger.

The choice of heat exchanger is governed by its flow resistance and thermal capacity. (A general rule is to make the thermal capacity

slightly in excess of the maximum engine output power.) When determining the maximum acceptable flow resistance it is necessary to ensure that the minimum pressure at any point in the cooling system exceeds the saturated vapour pressure, otherwise boiling will occur locally and the coolant circulation will be impaired.

In the design adopted for the test bed the pressure drop through the heat exchanger at maximum flow rate was 4 p.s.i. The depression of the boiling point thus incurred was 8.7°C. Since the temperature drop through the heat exchanger exceeded this it was unnecessary to pressurise the system to prevent boiling unless the cylinder head outlet temperature was required to exceed 100°C.

A feedback position control was developed to actuate the motorised mixing valve. The valve was driven by a two-phase a.c. motor through a gearbox. Only one motor speed was available, but the motor was stopped by an electromagnetic brake immediately the current supply for either direction of rotation was turned off. This form of motor operation consequently limited the position control to an "on-off" type with a dead zone. The dead zone width was made slightly less than 1% of full travel. This width was determined by the quantisation of the position feedback potentiometer. The brake stopped the motor within this dead zone, thus enabling an extremely simple design of position control to be used. A circuit diagram for the position control is given in fig. 5.2. The response of the valve position controller was characterised by velocity limiting (10).

For the purposes of control design the system identification was carried out in two parts. The steady state gain between the valve angle and temperature was derived from step responses, whilst the system dynamics between 0.002Hz. and 0.2Hz. were identified using the digital transfer function analyser.

The results of the identification showed that the steady state accuracy requirements could not be satisfied with a proportional control. A gain of at least 25 would be required to achieve this and a Nyquist plot for the system showed that a gain of 10 would lead to unstable operation. A control employing proportional and integral action was therefore required.

The cylinder head outlet flow is not perfectly mixed and since the thermistor probe will measure instantaneous temperature, subject to its own thermal delay characteristics, it was considered undesirable to employ derivative action in the controller.

The control parameters were:-

Proportional gain 2.7

Time constant of integral action 6.3 seconds

The control circuit, which is shown in fig. 5.3. was based on an integrated circuit operational amplifier. The input impedance of the amplifier has been boosted with F.E.T. source followers to enable accurate integration to be performed at a rate normally associated with pneumatic controllers.

Under steady state performance the control maintained measured temperature to within $\pm \frac{1}{4}^{o}C.$ over the range $60^{o}C.$ to $90^{o}C.$ To settle to within $\pm \frac{1}{4}^{o}C.$ of final temperature for a step change in demand of $15^{o}C.$ took 150 seconds. Recovery to within $\pm \frac{1}{4}^{o}C.$ of final temperature from a full scale heat input change took the same time.

Lubricating oil temperature control is seldom applied to vehicle engines. Consequently reliance is placed upon the oil maintaining its lubricating properties over the wide range of temperatures encountered. With vehicle engines the sump is usually exposed to a draught of cold air by virtue of the vehicle's forward motion, hence some form of uncontrolled cooling will exist. With a test bed this does not occur so temperature regulation is necessary both from the

aspect of simulating normal running conditions and also for providing the adverse environments required for oil performance evaluation and engine endurance testing.

The design of the test bed oil temperature control system was very similar to that applied to the cooling water. The oil cooling circuit was placed between the oil pump and the feed to the main gallery. The temperature was measured at the return to the gallery.

Control performance was similar to that for the water temperature system but settling times were approximately doubled.

The control parameters were:-

Proportional gain 4.0

Time constant of integral action 5.5 seconds.

2. The speed control system.

The mathematical modelling studies indicated that a closed loop speed control operating on dynamometer field current provided the most useful test facility offered by any single or double loop control operating on either or both of the two system inputs. A speed control was initially available with the dynamometer but the performance of this control was unsatisfactory since it was not possible to achieve adequate regulation and at the same time maintain stability. (Regulation is defined as the change in controlled speed that occurs due to changes in throttle setting). It was decided in view of this that a replacement control should be developed.

The operation of the initial control system is examined in order to explain its inadequate performance. A block diagram of the system is given in fig. 5.4.

Dynamometer speed was measured by an integrally mounted a.c. tachometer. The output of this tachometer was rectified and smoothed to form an analog of speed. This speed measurement was compared with the speed reference voltage, set on a potentiometer, in a high gain

amplifier. This amplifier, termed "the speed error amplifier", controls the dynamometer field current through a power amplification stage. The amplification is achieved with thyratrons operating in the voltage follower mode.

The control system has a further feedback path to the speed error amplifier from a flux pick-up situated on the dynamometer stator. This feedback, which is a measure of the derivative of the field excitation current and also a measure of the derivative of load torque, acts so as to prevent rapid changes in the excitation current which would otherwise occur with the comparative action of the speed error amplifier.

Reduction of this inner loop of the control system provides useful insight into the overall control action. If the signal from the flux pick-up is assumed to be the derivative of excitation current then reduction of this inner loop and the assumption of linear operation will yield a predominantly first order transfer function between speed error and excitation current. (Speed error is defined as the difference between the speed reference and the measured speed.) The high gain of the amplifier in this inner loop will cause the first order transfer function to have a large time constant. This will cause the control action to be characteristically integral but with limited d.c. gain. This qualitative assessment was confirmed as accurate, since the regulation achieved with the control, albeit inadequate, was considerably better than could have been achieved with a stable proportional control.

A further inadequacy of the control system was the large overshoot in response to step inputs. The changes in loop gain between different operating points in the torque/speed plane made it difficult to adjust the control parameters to achieve stable control over all the torque/speed plane. The majority of speed changes which occur during testing take the form of step functions

and it is important that the response to these changes is without excessive overshoot, which otherwise could lead to overspeeding or stalling the engine.

The small signal transfer function between the input to the dynamometer field current amplifier and dynamometer speed provided a useful indication of the dynamics which were taken into account in the improved speed control design. The d.c. gain of this transfer function may also be derived from the slope of the dynamometer field current/dynamometer speed characteristics which are shown in fig. 5.5. These characteristics reveal an 8 : 1 variation in gain over the torque/speed plane. Furthermore, it can be seen from these characteristics that the dynamometer exhibits hysteresis. The effect of this was overcome by applying "dither" to the field current, the "dither" was conveniently provided by the ripple on the speed measurement. The variable time constant filter was adjusted to give a dither amplitude of about 0.05 amps.

The control system design policy was firstly to compensate for the system dynamics and provide a flat response up to the highest frequency possible. It was not practical to compensate for the dynamics at frequencies above 5 Hz. otherwise the field current control amplifier would have been driven into saturation even with the smallest step changes in speed demand. Secondly, by closing the compensated control loop with an integrator, the closed loop responses would be predominantly first order, with a time constant dependent on the position in the torque/speed plane.

An Algol 60 program was written to calculate the controller transfer function on this basis from the mathematical model of the system. An operating point in the middle of the torque/speed plane was chosen so as to define the model parameters and the control was designed so as to give a first order response with a time constant of 0.5 seconds. The calculated and practical controller transfer

functions are shown in fig. 5.6 and 5.7. The circuit diagram for the controller is shown in fig. 5.8. The input network to the field current amplifier (fig. 3.4) contains part of the loop compensation, so as to avoid the use of another integrated circuit amplifier. A diode between the output of the controller and the input to the field current amplifier prevents the reversal of field current with its attendant reversal of loop gain.

Some step responses of the control taken for 250 R.P.M. changes in speed over a range of throttle openings are shown in fig. 5.9. They show that the control response is predominantly first order with a time constant close to that predicted by the design.

3. Fuel mass flow rate control.

Some difficulty was experienced due to the output drift of the float chamber pressure control, the control being somewhat sensitive to pressure changes in the supply line to the mechanical regulator. This drift was nullified by including the control in another closed loop, the action of this loop was to operate on float chamber pressure to ensure a constant fuel flow rate in response to a setpoint. This control was only made possible by virtue of the continuous fuel flow measurement.

The control action of the loop was integral to ensure zero steady state error. The control circuit is shown in fig. 5.10. Use of the control required a prior knowledge of the approximate fuel flow rate at the operating point under consideration.

functions are shown in fig. 5.6 and 5.7. The circuit diagram for the controller is shown in fig. 5.8. The input network to the field current amplifier (fig. 3.4) contains part of the loop compensation, so as to avoid the use of another integrated circuit amplifier. A diode between the output of the controller and the input to the field current amplifier prevents the reversal of field current with its attendant reversal of loop gain.

Some step responses of the control taken for 250 R.P.M. changes in speed over a range of throttle openings are shown in fig. 5.9. They show that the control response is predominantly first order with a time constant close to that predicted by the design.

3. Fuel mass flow rate control.

Some difficulty was experienced due to the output drift of the float chamber pressure control, the control being somewhat sensitive to pressure changes in the supply line to the mechanical regulator. This drift was nullified by including the control in another closed loop, the action of this loop was to operate on float chamber pressure to ensure a constant fuel flow rate in response to a setpoint. This control was only made possible by virtue of the continuous fuel flow measurement.

The control action of the loop was integral to ensure zero steady state error. The control circuit is shown in fig. 5.10. Use of the control required a prior knowledge of the approximate fuel flow rate at the operating point under consideration.

FIG. 5.1. TEST BED WATER COOLING SYSTEM.

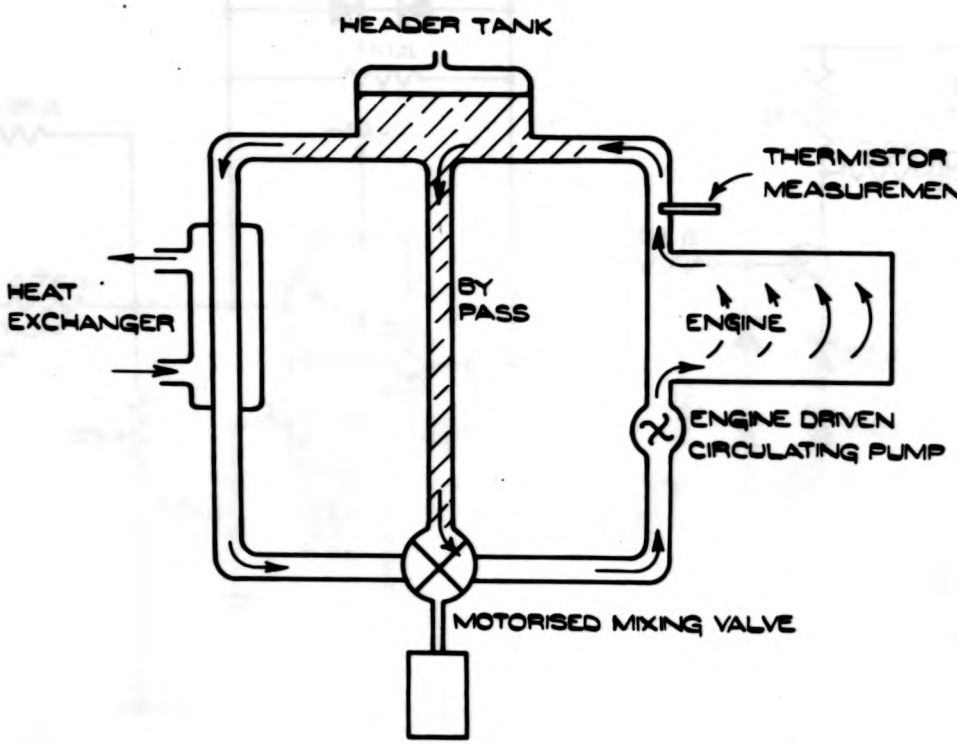

FIG. 5.2. VALVE POSITION CONTROLLER.

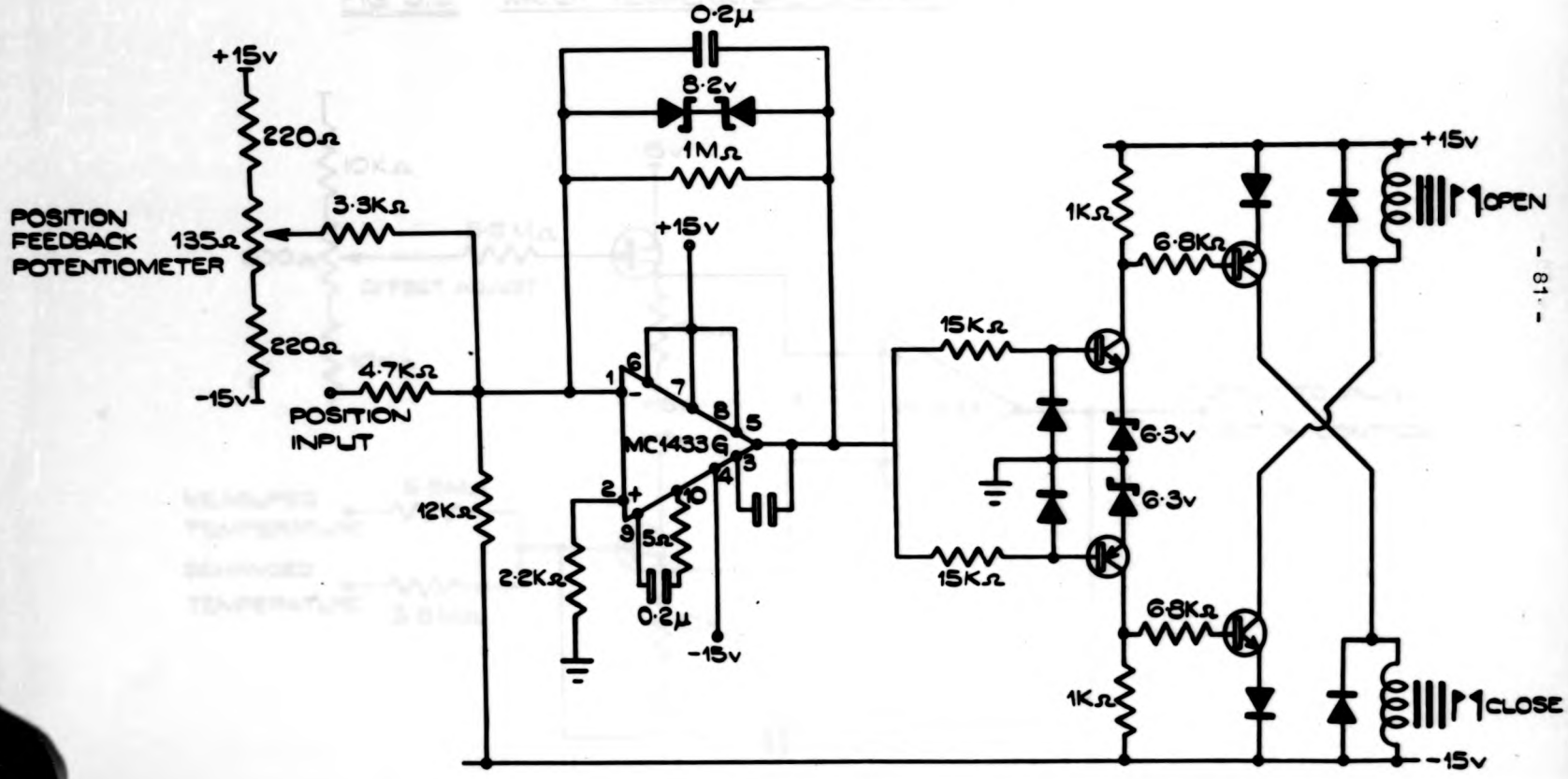

FIG. 5.3. WATER TEMPERATURE CONTROL.

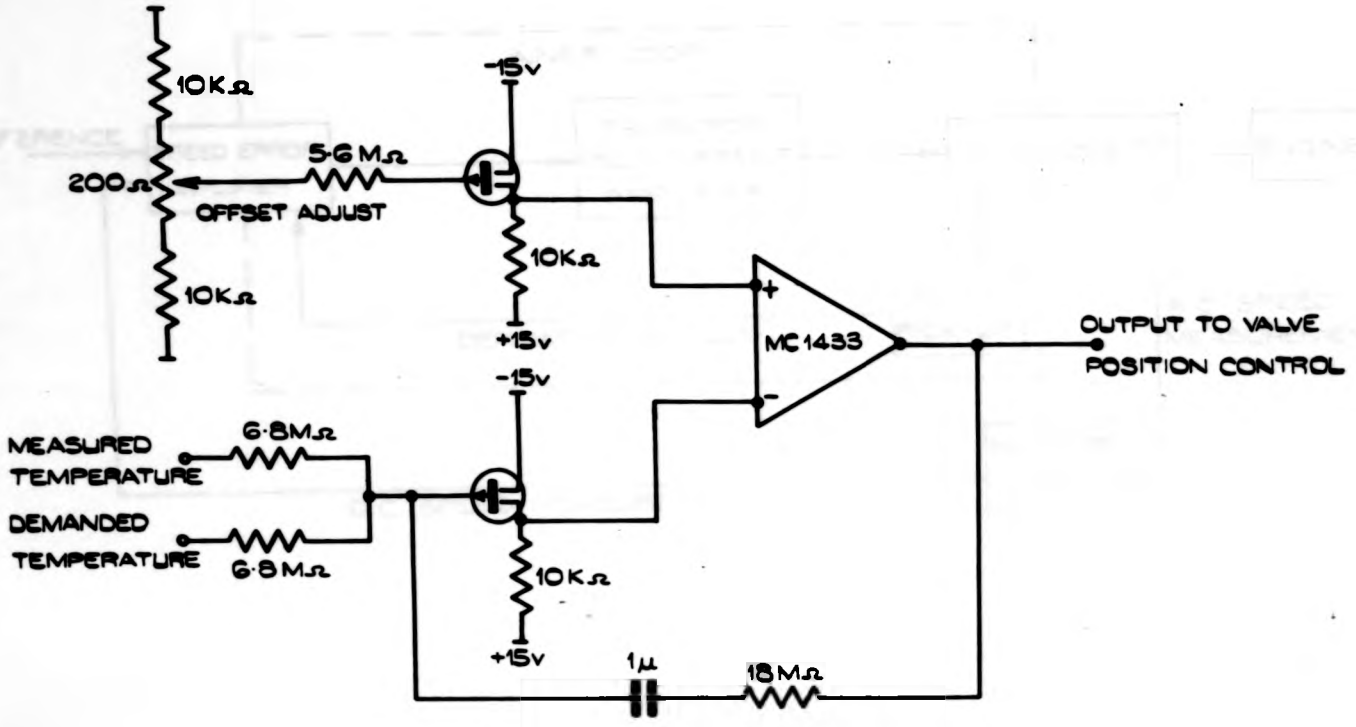

FIG. 5.4 INITIAL SPEED CONTROL SYSTEM

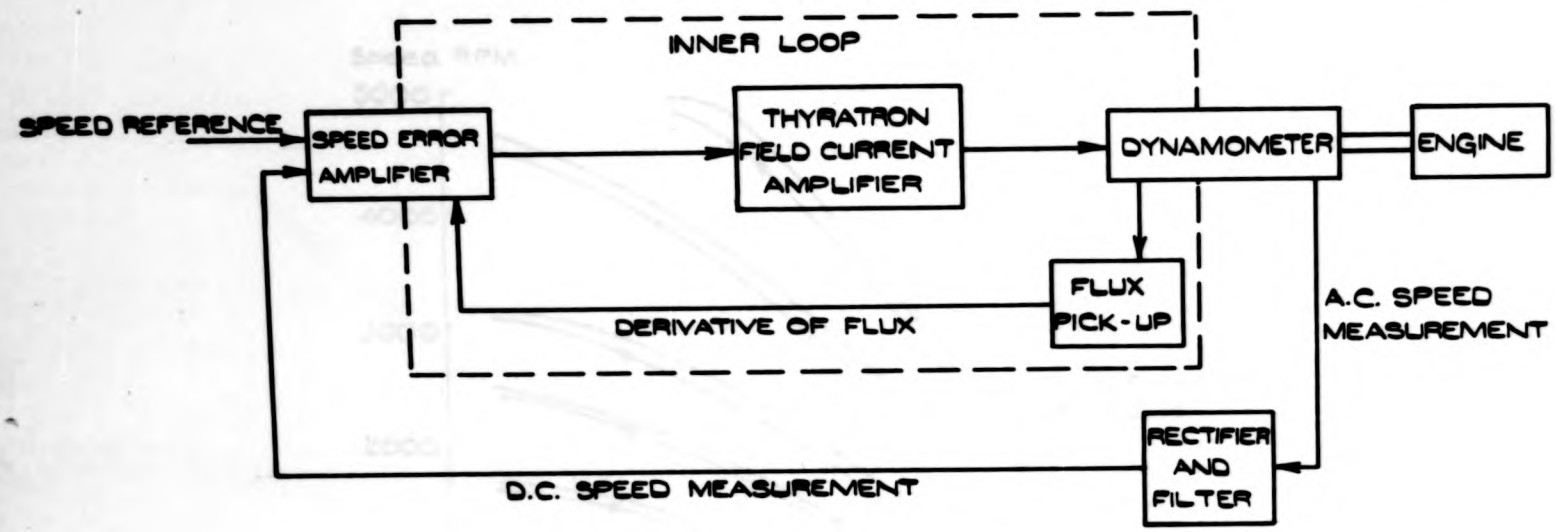

FIG. 5.5. DYNAMOMETER FIELD CURRENT/SPEED CHARACTERISTICS

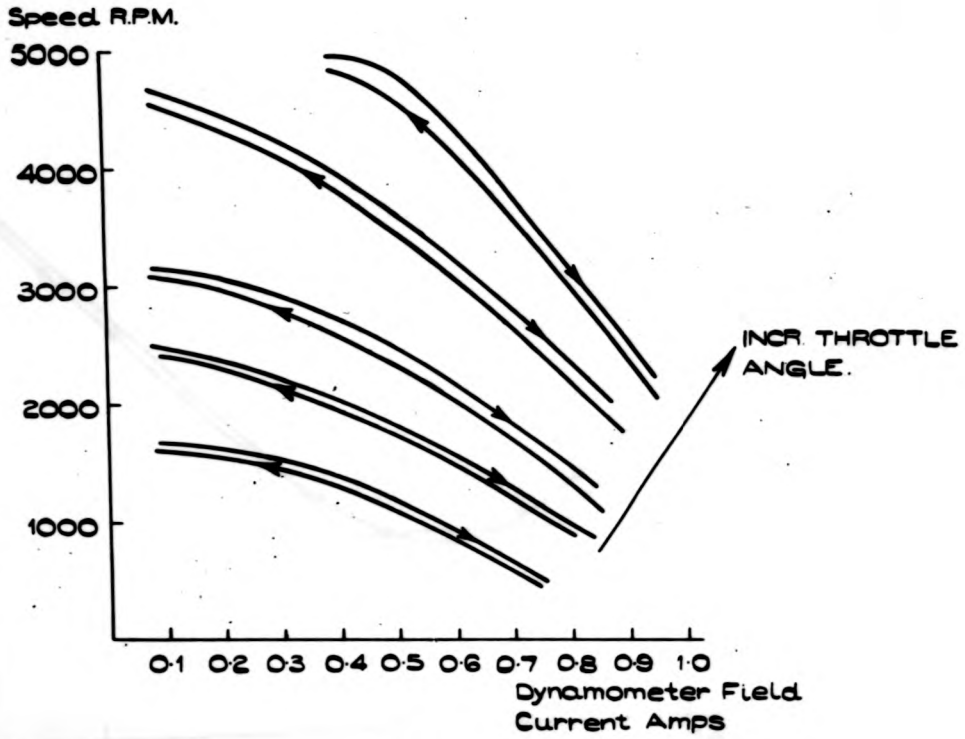

FIG. 5.6 CALCULATED AND PRACTICAL CONTROLLER TRANSFER FUNCTIONS - GAIN.

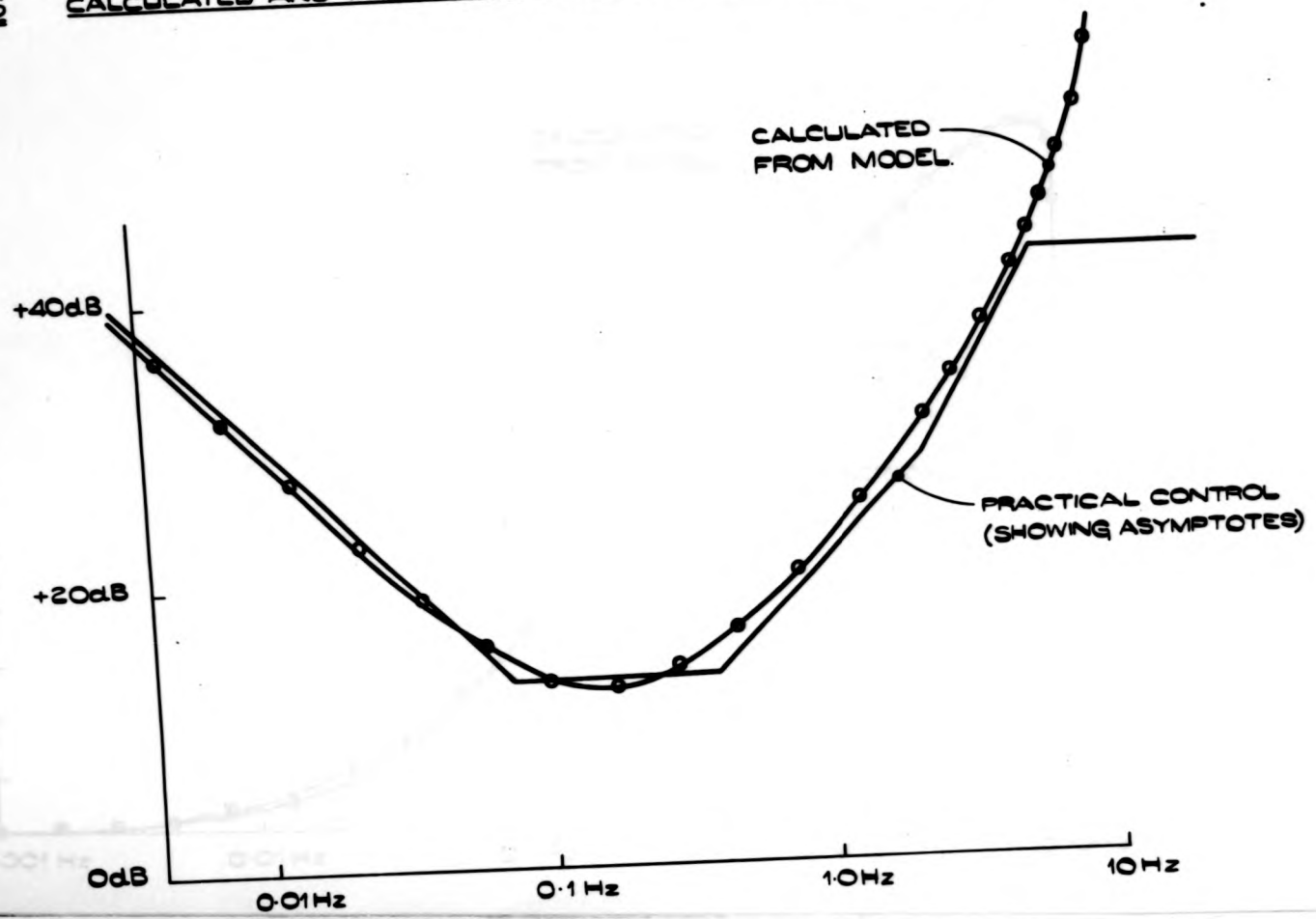

FIG. 5.7. CALCULATED AND PRACTICAL CONTROLLER TRANSFER FUNCTIONS - PHASE

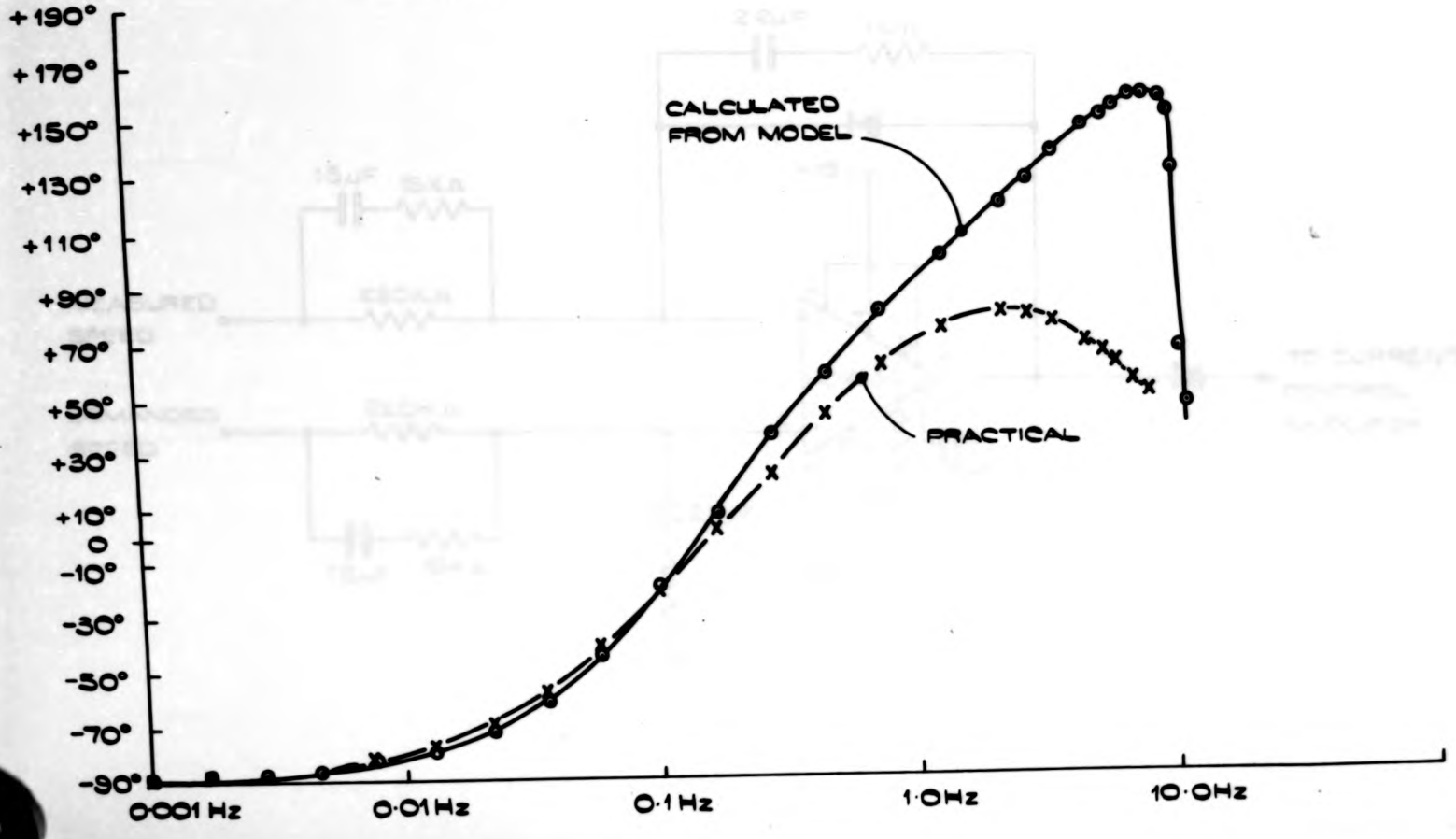

FIG. 5.8 SPEED CONTROL AMPLIFIER

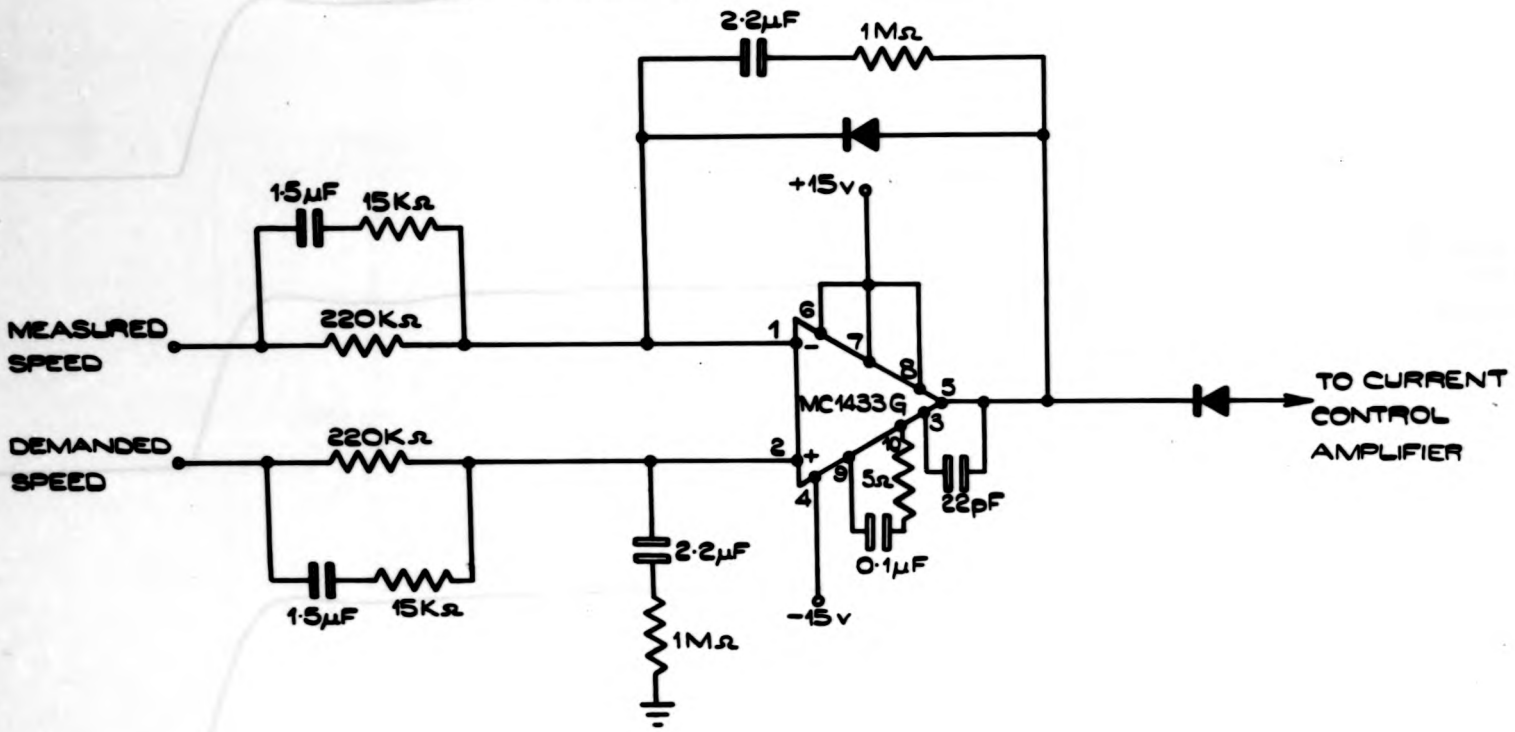

FIG. 5.9. SPEED CONTROL STEP RESPONSES
350 RPM CHANGES ABOUT 2500 RPM.

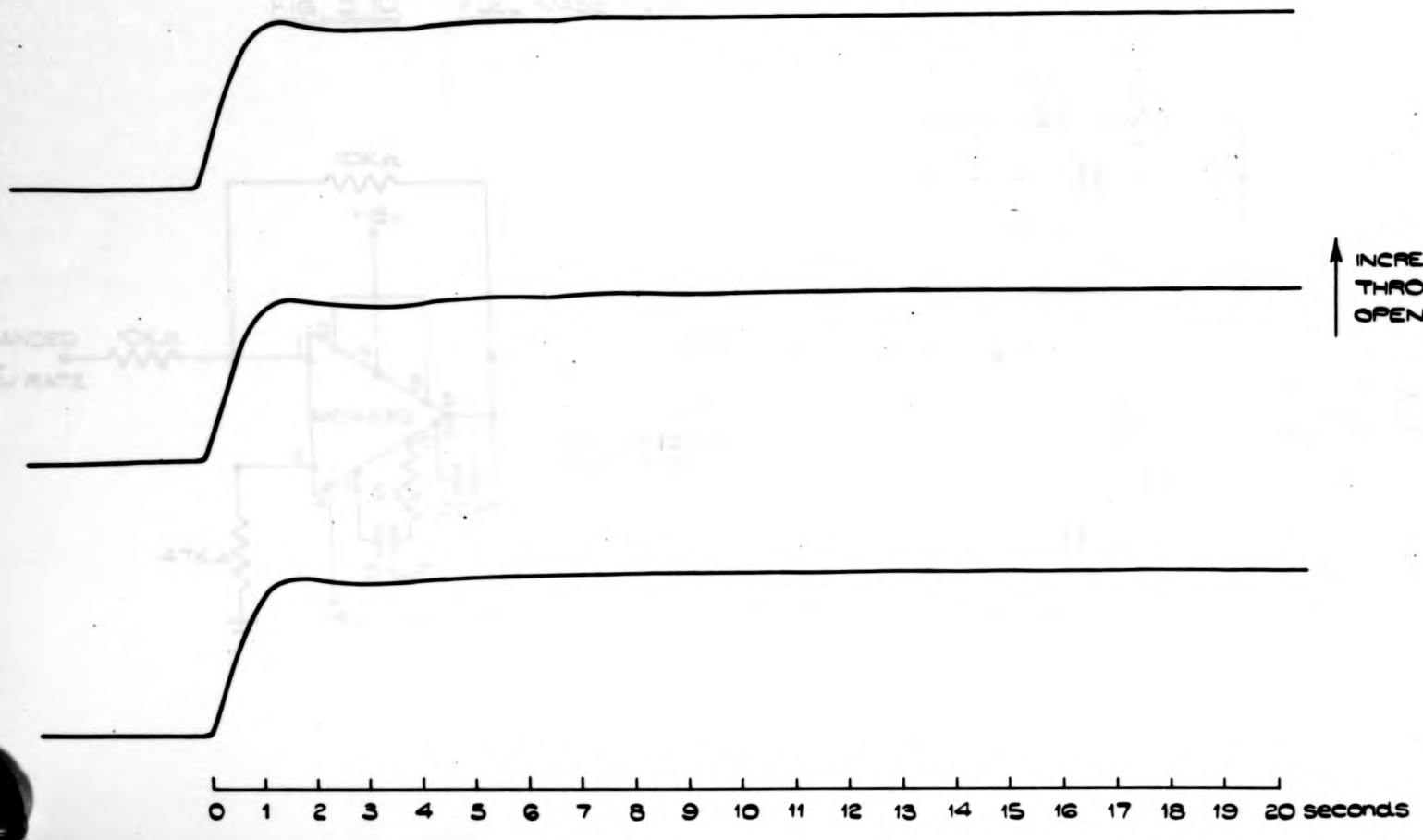

FIG. 5.10. FUEL MASS FLOW RATE CONTROL.

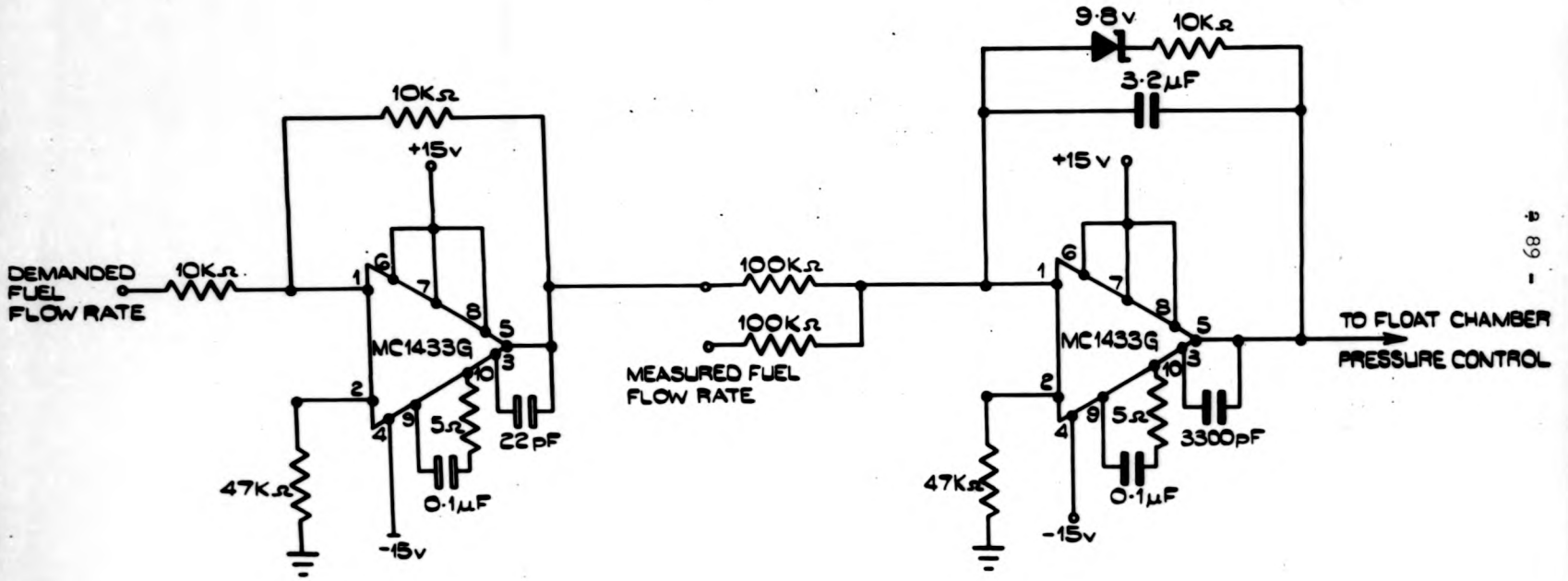

CHAPTER 6.

PROGRAMS FOR EXPLORATORY COMPUTER CONTROLLED TESTING.

1. The evolution of the program structure for computer controlled testing.
2. The assembly language S.D.S. Symbol.
3. The overall program structure.
4. The executive control program.
5. Program subroutine descriptions.

The section of the executive control program which handled the on-line typewriter input and output was written by the programmer for the school A.J.Hulme.

1. The Evolution of the program structure for exploratory testing.

Three basic essential qualities were required of the experimental on-line control programs, namely:-

1. The program structure should be as flexible as possible in order to permit the development of experimental test routines.
2. The program should enable the computer to execute the test activity with the minimum of reference to the test operator.
3. The interaction of the computer with the test operator should be at the highest possible level.

The function of the computer is essentially to service a channel of communication between the test operator and the engine, and at the same time maintain synchronism with a clock in order to permit the regular scanning of input variables and the timing of test operations. The scope of this communications channel is limited only by the data handling facilities of the computer and engine interfaces and by the speed of the computer's central processor.

In the experimental facility limitations were imposed by the scanning speed of the analog input multiplexer and by the data transfer structure between the computer and the typewriter, paper tape punch and paper tape reader which were connected on-line.

2. The assembly language S.D.S. Symbol.

The programming was carried out in the low level assembly language S.D.S. Symbol. This language provided a set of mnemonics for the range of machine instructions. The assembly operation translated these mnemonics into machine instructions on a one for one basis and output a program which could then be loaded into the machine.

Subroutines and interrupt servicing routines were handled by means of a "branch and mark place" type of instruction which operated by storing the address of the location to which the program would return in the first two locations of the subroutine. Direct re-entry into subroutines is not therefore possible and if this facility is required it must be programmed indirectly.

To simplify the problem of error checking programs were assembled in small blocks. The loading facilities made provision for this by co-ordinating the cross-referenced addresses between blocks at load time. The procedure adopted for compiling a complete test was to load the executive routine followed by the subroutines and the test routine. These were dumped on to paper tape together with a loader and could subsequently be re-loaded and run directly.

Although the use of a low level language gave a very versatile means of programming, learning the language proved relatively difficult and its efficient use demanded certain well-developed skills. Programs were therefore written in a form which aided error correction and to save core store space was deemed to be of secondary importance.

3. The overall program structure.

The program facilities developed for exploratory engine testing were centered around an executive control program which handled the on-line typewriter and analog input multiplexor in synchronism with a 50 Hz. clock. A library of subroutines provided the basic units from which the test programs were constructed. The engine test programs themselves consequently consisted largely of subroutine calls. The subroutines have been divided into groups according to their functions and are listed below.

Subroutine group functions.

1. To perform housekeeping operations for the executive control program. These subroutines were concerned with

handling input data from the on-line typewriter, and the transfer of program control to different locations in response to interrupts from the real time clock and the typewriter.

2. To start and stop the engine and set up running conditions.
3. To monitor the operation of the test facility and take appropriate action in the event of an emergency.
4. To handle the analog X-Y plotter and paper tape punch.
5. To process input data from the engine.

In addition a library of typewriter output messages was stored. A description of the subroutines is given later in the chapter.

4. The executive control program.

The timing structure of the executive control program was limited by the speed of the analog input multiplexor and by the speed of the on-line typewriter during character output. The input multiplexor had a maximum access scanning rate slightly in excess of 100 points per second and on output the typewriter took slightly less than 10 ms. to clear the input/output buffer of a character. The absolute maximum clock interrupt rate was therefore 100 Hz, since it was necessary to interlace the operation of the typewriter. For the convenience of program structure a 50 Hz. clock rate was used.

The on-line typewriter, real time clock and analog input multiplexor and converter were handled through the computer's priority interrupt system. When one of these devices became active an interrupt occurred, and program control was transferred to the appropriate location of the executive. After handling the peripheral the executive either transferred control to a new program location or returned it to the location at which the interrupt occurred.

The priority system ensured that the handling of a more important device took precedence - a high priority interrupt could therefore

interrupt the servicing routine of a device which had been assigned a lower priority. The interrupt priority order was not under the control of the programmer, and had been assigned when the interface was constructed.

The description of the executive control program which follows, has been divided into three sections, namely:- typewriter, clock and analog inputs.

Executive control program - typewriter.

The interrupt associated with the buffer between the computer and the typewriter, paper tape punch and paper tape reader had been assigned the highest priority. This interrupt occurred when the buffer collected a word or was cleared on the transmission of a word to the device. It also occurred when the typewriter was switched to the on-line output mode. When the paper tape punch was in use this interrupt was rendered temporarily inactive.

The normal state for the typewriter was awaiting an input. A location was maintained to store the current state of the typewriter. (This was necessary since the same interrupt occurred both on input and output). When a single character was input on the keyboard any synchronism with the interrupted program was cancelled by the immediate modification of the clock interrupt servicing routine. The character was then examined, and program control was transferred to the appropriate location. Single letters were used to define the test operator's requirements. These characters formed the beginning of a word - the computer supplied the remainder of the word from the store of messages, leaving a record of the current activity. Impermissible characters were questioned and the computer then awaited the input of a permissible character.

The output of characters was handled one at a time, so as to permit interlacing with the clock interrupt servicing routine. This

method of operation did not permit the normal form of indexing character lists, and it was necessary to head a list by its length. When the end of a list was detected the typewriter was returned to the state where it awaited another input, and the program sequence continued.

To call the character output subroutine from the main program a "branch and mark place" instruction was used, the subroutine being entered via the label "print". This branch instruction was followed by a dummy instruction which held the address of the character string. The dummy instruction was skipped over on the return to the main program. A flow diagram for the typewriter input/output section of the executive is given in fig. 6.1.

Executive control program - clock.

Second priority had been allocated to the clock interrupt. Each time a clock interrupt occurred the selection of and analog to digital conversion of one of five inputs was initiated in sequence. After all five inputs had been selected the sequence was reset. The servicing routine maintained a count of time in minutes, seconds and tenths of seconds. At the time the sequence was reset program control could be transferred to another previously defined location, (This is termed synchronous operation), alternatively, it was returned to the location where the interrupt occurred. (This is termed asynchronous operation). Synchronous operation was used where timing and data logging was required. A flow diagram for the clock interrupt servicing routine is given in fig. 6.2.

Executive control program - analog inputs.

Third priority had been assigned to the interrupt associated with the analog input multiplexor and converter. This interrupt occurred when the conversion was complete. The servicing routine transferred the input word to the appropriate store location.

The three sections of the executive control program together occupied 435 store locations.

5. Program subroutine descriptions.

The following headings are used in the description of program subroutines.

NAME :

REGISTERS : Details of locations and registers* used for data storage, flags etc.

PURPOSE : The action of the subroutine.

SUBROUTINES : Further subroutines called from within the subroutine.

NOTES :

STORAGE : Total number of core store locations occupied by the subroutine.

INTERFACE : Interface facilities utilised.

* The computer has two 12-bit registers, referred to as the A and B registers and one 1-bit register referred to as the F register.

A description of the subroutines follows:-

Subroutine functional group 1.

NAME : INTEX.

REGISTERS : A and B.

PURPOSE : To program all the exit instructions from the clock routine together. These consisted of a "branch and clear interrupt" instruction followed by the branch address.

NOTES : The common exit instruction and branch address were stored in the A and B registers respectively before entry into the routine.

STORAGE : 16.

NAME : RITU

REGISTERS : A and B.

PURPOSE : To return program control to the interrupted location at all exits from the clock routine.

SUBROUTINES : INTEX.

NOTES : This was used to asynchronise program control and was not interruptable.

STORAGE : 14.

NAME : KCK1.

REGISTERS : A and B.

PURPOSE : To program exits from the clock routine to transfer control at the end of 1/10th second periods.

SUBROUTINES : INTEX.

NOTES : This was used to synchronise program control and was not interruptable. The subroutine was entered with the transfer address in the B register.

STORAGE : 12.

NAME : KCK2.

REGISTERS : A and B.

PURPOSE : To program exits from the clock routine to transfer control at the end of 1 second periods.

SUBROUTINES : INTEX.

NOTES : This was used to synchronise program control and was not interruptable.

STORAGE : 16.

NAME : YESNO.

REGISTERS : B.

PURPOSE : To render the characters 'Y' and 'N' impermissible when input from the typewriter keyboard.

PURPOSE : To return program control to the interrupted location at all exits from the clock routine.

SUBROUTINES : INTEX.

NOTES : This was used to asynchronise program control and was not interruptable.

STORAGE : 14.

NAME : KCK1.

REGISTERS : A and B.

PURPOSE : To program exits from the clock routine to transfer control at the end of 1/10th second periods.

SUBROUTINES : INTEX.

NOTES : This was used to synchronise program control and was not interruptable. The subroutine was entered with the transfer address in the B register.

STORAGE : 12.

NAME : KCK2.

REGISTERS : A and B.

PURPOSE : To program exits from the clock routine to transfer control at the end of 1 second periods.

SUBROUTINES : INTEX.

NOTES : This was used to synchronise program control and was not interruptable.

STORAGE : 16.

NAME : YESNO.

REGISTERS : B.

PURPOSE : To render the characters 'Y' and 'N' impermissible when input from the typewriter keyboard.

NOTES : This subroutine caused the character input examination section of the executive to question these characters and was not interruptable.

STORAGE : 14.

NAME : ATAD.

REGISTERS : B.

PURPOSE : To render numerical characters impermissible when input from the typewriter keyboard.

NOTES : This subroutine caused the character input examination section of the executive to question numerical characters and was not interruptable.

STORAGE : 10.

NAME : DAX.

REGISTERS : B.

PURPOSE : To cause program control to be transferred to the appropriate location when numerical data was input from the typewriter keyboard.

NOTES : The subroutine was entered with the transfer address in the B register.

STORAGE : 10.

NAME : YAX.

REGISTERS : B.

PURPOSE : To cause program control to be transferred to the appropriate location when the character 'Y' was input from the typewriter keyboard.

NOTES : The character 'Y' indicated the answer 'yes' in reply to a question posed by the computer. The subroutine was entered with the transfer address in the B register.

STORAGE : 10.

NAME : NAX.

REGISTERS : B.

PURPOSE : To cause program control to be transferred to the appropriate location when the character 'N' was input from the typewriter keyboard.

NOTES : The character 'N' indicated the answer 'no' in reply to a question posed by the computer. The subroutine was entered with the transfer address in the B register.

STORAGE : 10.

Subroutine functional group 2.

NAME : ROCS.

REGISTERS : 5.

PURPOSE : To set up a list of running conditions, namely:- Throttle opening, demanded speed, ignition timing and float chamber pressure or fuel flow rate on the analog outputs.

NOTES : Running conditions were defined in the registers before entry into the subroutine and were preserved on exit. A spare location was reserved for timing.

STORAGE : 26.

INTERFACE : Analog outputs.

NAME : IDLCS.

PURPOSE : To set up light load running at 1250 R.P.M.

STORAGE : 22.

INTERFACE : Analog outputs.

NAME : STPP.

PURPOSE : To stop the engine.

NOTES : The engine was stopped by turning off the ignition.

STORAGE : 8.

INTERFACE : Relay outputs.

NAME : STAR.

REGISTERS : 6, E and F.

PURPOSE : To start the engine.

SUBROUTINES : RITU, MCH1.

NOTES : Five attempts were made to start the engine, during which time the starter was switched on for a maximum of five seconds. As soon as the engine fired and built up speed the starter was switched off. There was a five second wait in between the attempts to start the engine. A flow chart for this subroutine is given in fig. 6.3.

STORAGE : 139.

INTERFACE : Analog outputs, relay outputs and analog inputs.

NAME : START.

REGISTERS : E and F.

PURPOSE : To initiate engine starting from the typewriter keyboard by typing the letter 'S'.

SUBROUTINES : STAR, PRINT, YAX, MAX, RITU, YESNO.

NOTES : The operator was interrogated to establish if the choke was required for starting, and was informed of the success or failure of the starting operation.

STORAGE : 65.

INTERFACE : Analog outputs, relay outputs, analog inputs and the on-line typewriter.

NAME : IDLE.

REGISTERS : B.

PURPOSE : To initiate engine idling from the typewriter keyboard by typing the letter 'I'.

SUBROUTINES : IDLCS, PRINT, KCK1, CKS, USFD.

NOTES : The idling was monitored by the CKS subroutine.

STORAGE : 30.

INTERFACE : Analog outputs, analog inputs and the on-line typewriter.

NAME : HALT.

PURPOSE : To initiate engine stopping from the typewriter keyboard by typing the letter 'H'.

SUBROUTINES : STPP, PRINT.

STORAGE : 13.

INTERFACE : Relay outputs and the on-line typewriter.

NAME : BGN2.

PURPOSE : To arm and enable the interrupts and thereby initiate the running of a program after it had been loaded into the machine.

STORAGE : 13.

NAME : USFD.

PURPOSE : To inform the test operator that the engine has stopped involuntarily.

SUBROUTINES : PRINT.

STORAGE : 9.

INTERFACE : The on-line typewriter.

Subroutine functional group 3.

NAME : E'STP.

PURPOSE : To stop the engine in the shortest possible time when improper operation of the test facility was detected.

SUBROUTINES : RITU, PRINT.

NOTES : The engine was stopped by switching off the ignition, closing the throttle and applying full load. The cause of the emergency stop was indicated to the operator.

STORAGE : 72.

INTERFACE : Analog outputs, relay ouputs and the on-line typewriter.

NAME : WTCK.

REGISTERS : 1, B and F.

PURPOSE : To check upper and lower limits of the engine outlet water temperature.

SUBROUTINES : E'STP.

NOTES : An emergency stop occurred if either the lower or the upper limits were exceeded.

STORAGE : 31.

INTERFACE : Analog inputs.

NAME : SPCK.

REGISTERS : 1, B and F.

PURPOSE : To check the upper and lower limits of engine speed.

SUBROUTINES : E'STP, USFD.

NOTES : An emergency stop occurred on overspeed. Underspeed was recorded but no direct action taken.

STORAGE : 33.

INTERFACE : Analog inputs.

NAME : OPCK.

REGISTERS : 1 and F.

PURPOSE : To check the sense of the oil pressure warning switch.

SUBROUTINES : E'STP.

NOTES : Low oil pressure causes an emergency stop.

STORAGE : 11.

INTERFACE : S.E.S. 1-bit inputs.

NAME : CKS.

PURPOSE : To check water temperature, engine speed and oil pressure.

SUPROUTINES : WTCK, SPCK, OPCK, ABFS, ABFU.

NOTES : This subroutine combined WTCK, SPCK, CPCK. The A, B and F registers were preserved.

STORAGE : 14.

INTERFACE : Analog inputs, S.E.S. 1-bit inputs.

Subroutine functional group 4.

NAME : ABFS.

REGISTERS : 3.

PURPOSE : To store the contents of the A, B and F registers.

NOTES : This subroutine was used in conjunction with ABFU.

STORAGE : 13.

NAME : ABFU.

REGISTERS : 3.

PURPOSE : To reinstate the contents of the A, B and F registers.

NOTES : This subroutine was used in conjunction with ABFS. ABFS and ABFU were used at the beginning and end of programs when it was necessary to preserve the contents of these registers.

NAME : RZP.

PURPOSE : To raise the pen from the paper on the X-Y plotter.

STORAGE : 8.

INTERFACE : Relay outputs.

NAME : LZP.

PURPOSE : To lower the pen on to the paper on the X-Y plotter.

STORAGE : 8.

INTERFACE : Relay outputs.

NAME : SCW.

REGISTERS : 1 and F.

PURPOSE : To wait for one second.

SUBROUTINES : ABFS, ABFU, KCM1, RITU.

NOTES : Used as a means of wasting time. (For example it was used in between moving the plotter pen and lowering it on to or raising it from the paper on the X-Y plotter.)

STORAGE : 26.

NAME : ZZP.

PURPOSE : To move the X-Y plotter pen to the origin.

STORAGE : 14.

INTERFACE : Analog outputs.

NAME : AZX.

REGISTERS : 2.

PURPOSE : To draw the axes for a 2-dimensional plot.

SUBROUTINES : ABFS, ABFU, ZZP, LZP, RZP, SCW.

NOTES : A, B and F were preserved.

STORAGE : 88.

INTERFACE : Analog outputs, and relay outputs.

NAME : PTL.

PURPOSE : To punch a length of leader on the paper tape output.

SUBROUTINES : APFS, APFU.

STORAGE : 40.

INTERFACE : Paper tape punch.

NAME : PLG.

REGISTERS : 8.

PURPOSE : To punch a block of four characters on the paper tape output.

SUBROUTINES : APFS, APFU.

NOTES : The addresses of the characters were held in the subroutine.

STORAGE : 52.

INTERFACE : Paper tape punch.

Subroutine functional group 5.

NAME : AVGE.

REGISTERS : 4 lists of 65, A, B and F.

PURPOSE : To average a list of data.

NOTES : The length of the list was permitted to be 2^n, where n = 0,1,2,3,4,5 and 6. The length of the list was stored at the head of the block of data. The average was entered into the position of the first measurement.

STORAGE : 72.

NAMES: TORQAV, SPEEDAV, FLOWAV.

REGISTERS : A and B.

PURPOSE : To average a list of torque, speed or fuel flow measurements.

SUBROUTINES : AVGE.

STORAGE : 20.

NAME : POWER.

REGISTERS : 1, A and B.

PURPOSE : To compute power from torque and speed measurements.

STORAGE : 12.

NAME : SFC.

REGISTERS : 1, A and B.

PURPOSE : To compute the inverse of specific fuel consumption from torque, speed and fuel flow measurements.

STORAGE : 15.

FIG. 6.1.

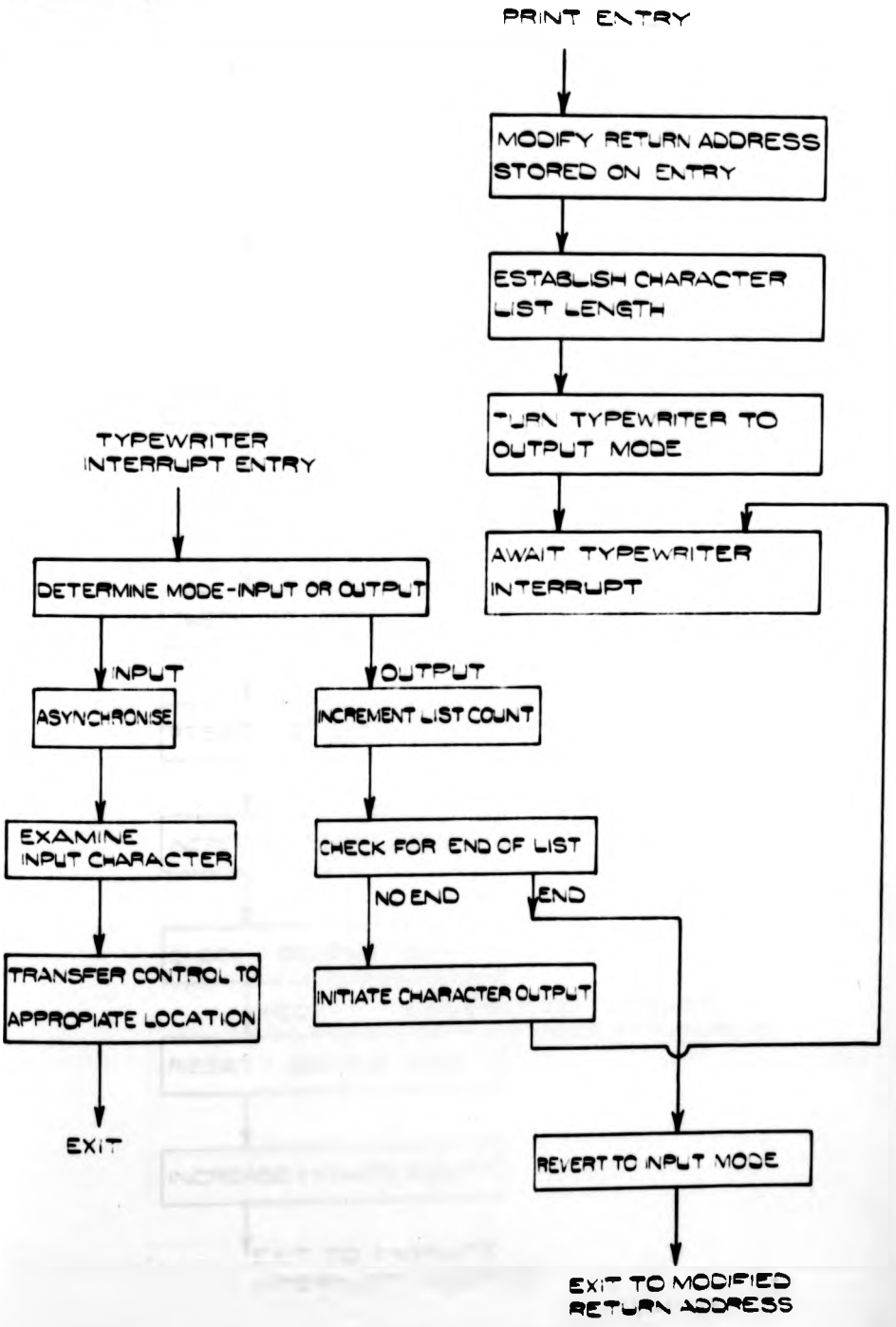

TYPEWRITER INPUT/OUTPUT.

Fig. 6.1.

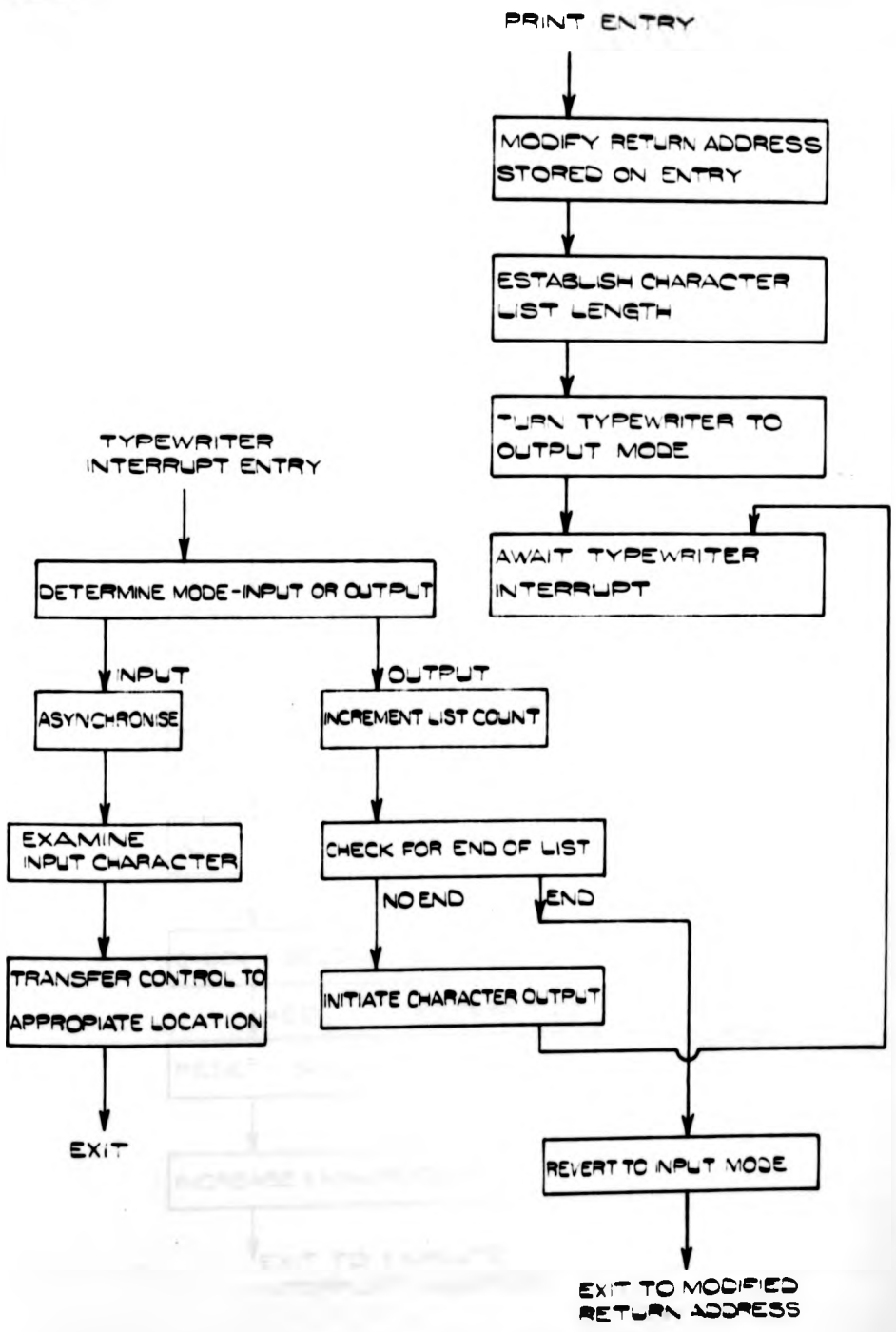

TYPEWRITER INPUT/OUTPUT

FIG. 6.2

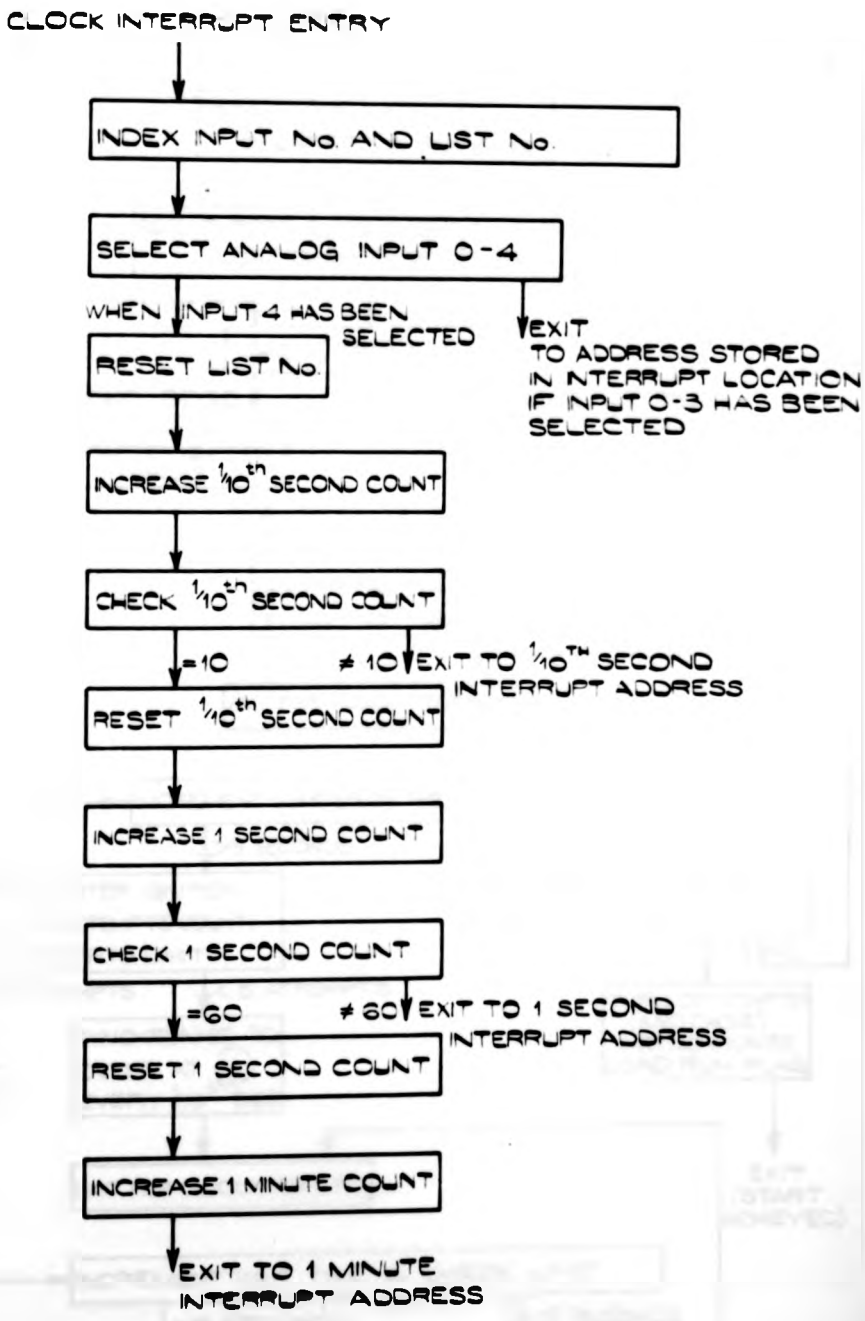
CLOCK INTERRUPT ENTRY
INDEX INPUT No. AND LIST No.
SELECT ANALOG INPUT 0-4
WHEN INPUT 4 HAS BEEN SELECTED
EXIT TO ADDRESS STORED IN INTERRUPT LOCATION IF INPUT 0-3 HAS BEEN SELECTED
RESET LIST No.
INCREASE 1/10th SECOND COUNT
CHECK 1/10th SECOND COUNT
=10
≠ 10 EXIT TO 1/10TH SECOND INTERRUPT ADDRESS
RESET 1/10th SECOND COUNT
INCREASE 1 SECOND COUNT
CHECK 1 SECOND COUNT
=60
≠ 60 EXIT TO 1 SECOND INTERRUPT ADDRESS
RESET 1 SECOND COUNT
INCREASE 1 MINUTE COUNT
EXIT TO 1 MINUTE INTERRUPT ADDRESS

CLOCK

FIG. 6.3.

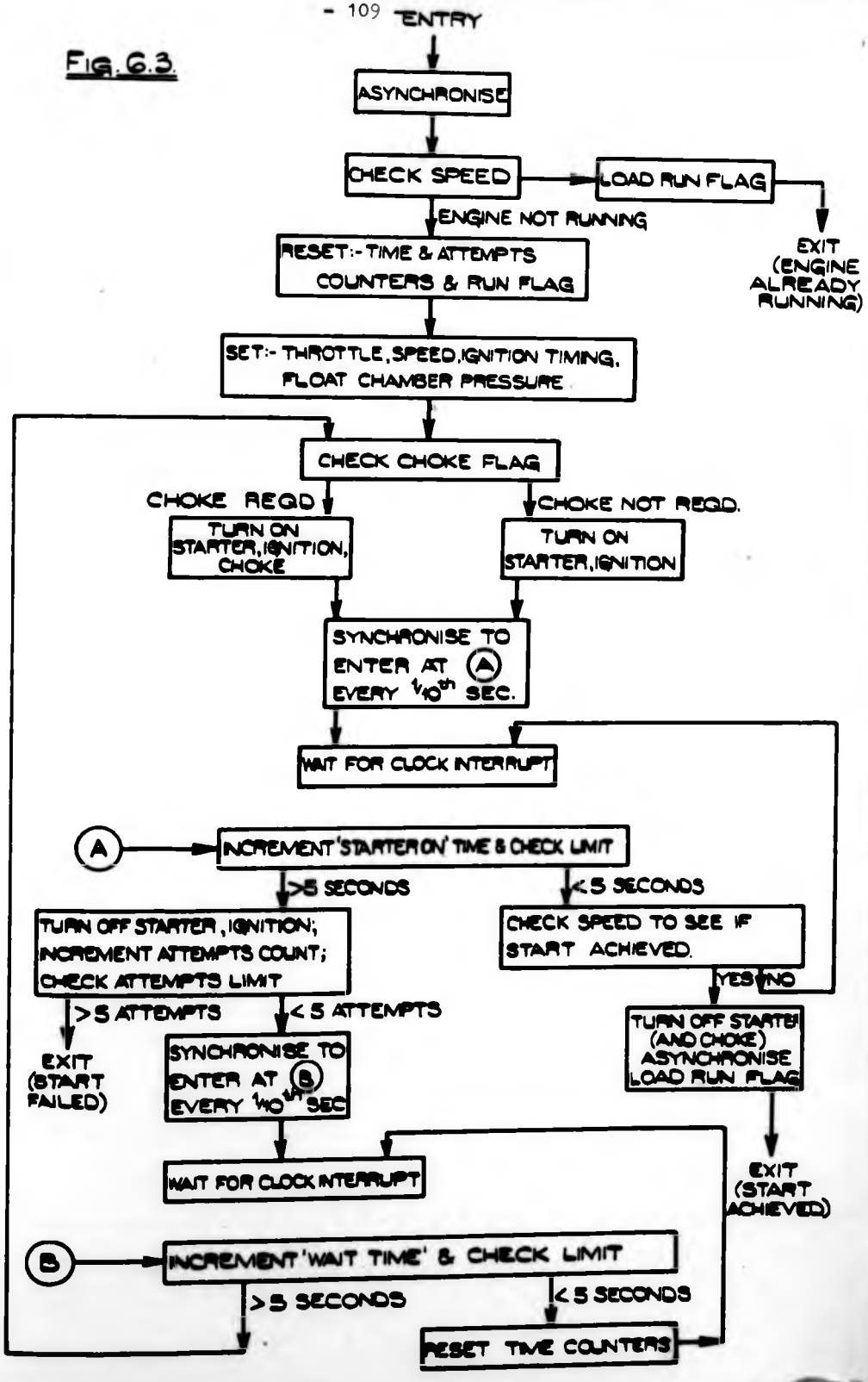

ENGINE STARTING.

CHAPTER 7.

OPTIMISATION STUDIES.

1. Optimisation in ignition distributor and carburettor design.
2. Consideration of the single parameter optimiser.
3. Further consideration of the single parameter optimiser under the influence of noise and asymmetric cost functions.
4. Manual ignition timing optimisation.
5. Perturbation limitations for ignition timing and air/fuel ratio optimisation.
6. An experimental sinusoidal ignition timing optimiser.

CHAPTER 7.

OPTIMISATION STUDIES.

1. Optimisation in ignition distributor and carburettor design.
2. Consideration of the single parameter optimiser.
3. Further consideration of the single parameter optimiser under the influence of noise and asymmetric cost functions.
4. Manual ignition timing optimisation.
5. Perturbation limitations for ignition timing and air/fuel ratio optimisation.
6. An experimental sinusoidal ignition timing optimiser.

1. Optimisation in ignition distributor and carburettor design.

The principle areas in which optimisation is already applied to i.c. engines is in the development of ignition timing and air/fuel ratio controls. These controls normally employ feed-forward techniques. The appropriate feed-forward transfer functions are determined during engine development.

The data from which these transfer functions are designed is acquired from testing which at present employs manually implemented optimisation processes. An attempt is made to satisfy two performance criteria in the design of the feed forward characteristics. The two performance criteria are defined:-

Under full throttle operation it is desirable to maximise torque so as to give maximum acceleration. Under part throttle operation specific fuel consumption is minimised to give economical running of the vehicle under cruising conditions.

The established practises of distributor and carburettor design make ignition timing a function of engine speed and manifold pressure, and air/fuel ratio a function of the differential pressure between the carburettor ventruri and atmosphere. Fairly lengthy test procedures are required to determine the optimum air/fuel ratio and ignition timing over a range of operating conditions. In particular, the forms of fuel flow measurement in common use for testing purposes at this time do not permit direct minimisation of specific fuel consumption (since this would be excessively time consuming) and the optimum must be interpolated by the test operator.

The design of these feed-forward transfer functions necessarily involves some compromise and to make this compromise a knowledge of the sensitivity of the various parameters close to the optimum is useful.

Ideally vehicle engines of the future will be equipped with closed loop controls to optimise ignition timing and air/fuel ratio. However, before any optimisation system is applied it is advisable to determine the factors that influence the optimiser's ultimate dynamic performance. These factors are considered by examining the response of a single parameter sinusoidal optimiser operating on a quadratic cost function. Subsequently the effects of a non-quadratic cost function and noise on the cost function output are examined in order to aid the choice of perturbation parameters and to estimate final accuracy.

The single parameter optimiser is shown schematically in fig 7.1.

The quadratic cost function, $y = -\alpha x^2$, is assumed to be without dynamics, and is free of noise. (i.e. $\Phi n(j\omega) = 0$). A perturbation $\delta \sin \omega t$ is applied to γ to form the input to the cost function. The resulting cost function output is given by $y = -\alpha(\gamma + \delta \sin \omega t)^2$

The d.c. component of y is removed by the high pass filter and the output of the multiplier is consequently

$$-\alpha \left(2\delta \gamma \sin \omega t + \frac{\delta^2}{2} \cos 2\omega t\right) \Delta \sin \omega t.$$

This is integrated with gain β to form the adjustment to γ, giving

$$\frac{d}{dt}(\gamma) = -\alpha\beta\delta\Delta\left[\gamma(1-\cos 2\omega t) + \frac{\delta}{2}(\sin 3\omega t - \sin \omega t)\right]$$

Taking expected values, denoted by E [ ]

$$E\left[\frac{d}{dt}(\gamma)\right] = -\alpha\beta\delta\Delta\, E[\gamma]$$

Since E [Cos 2 ωt]= E [Sin ωt]= E [Sin 3 ωt] = 0

The solution to this equation, which is recognisable as a first order exponential indicates that the expected value of γ approaches the optimum with a time constant of $\frac{1}{\alpha\beta\gamma\Delta}$. To minimise the periodic content of the response of γ the perturbation frequency should be as high as possible.

3. Further considerations of the single parameter optimiser under the influence of noise and asymmetric cost functions.

The analysis may now be extended to examine the case where the cost function is contaminated by noise. The noise is assumed to be additive to the cost function output. Operation close to the optimum is assumed in order to permit the assumption of stationarity. The noise on the cost function output, n(t), is described by its power spectrum $\Phi_n(j\omega)$. Close to the optimum it is assumed that the noise component of γ is attenuated by the cost function to a sufficient degree for its effect on the cost function output to be considered small compared with n(t).

The noise component of the cost function output, n(t), will contaminate γ, but its power spectrum will be significantly modified by the passage of n(t) through the high pass filter, multiplier and integrator. This sequence of operations on $\Phi_n(j\omega)$ is considered:-

The power spectrum of n(t) on the output of the high pass filter $\Phi_{n_1}(j\omega)$ is given by $\Phi_{n_1}(j\omega) = \Phi n(j\omega)|F(j\omega)|^2$

Where $F(j\omega)$ is the transfer function of the high pass filter.

The effect of the multiplier is most easily demonstrated by considering the input of a component in a small frequency band centered on ω_n with power $\lceil n$. The multiplier gives rise to components on its output centered around the frequencies $(\omega + \omega_n)$ and $(\omega - \omega_n)$ each with a power of $\frac{\lceil n \lambda^2}{4}$. The component at ω_n is removed. The overall effect of the multiplier is to apply a frequency shift to and attenuate $\Phi_{n_1}(j\omega)$, giving $\Phi_{n_2}(j\omega)$.

Finally the power spectrum of γ due to n(t), $\Phi_{n_3}(j\omega)$, is given by

$$\Phi_{n_3}(j\omega) = \Phi_{n_2}(j\omega)\left|\frac{\beta}{(j\omega)}\right|^2$$

Where β is the integrator gain. The variance of γ is obtained by integrating $\Phi_{n_3}(j\omega)$ over all frequencies.

This sequence of operations on $\Phi_n(j\omega)$ illustrates the importance of the choice of a suitable high pass filter characteristic and

perturbation frequency to minimise the variance of γ.

To achieve an advantageous signal to noise ratio in the case where noise is additive to the cost function output the perturbation amplitude should be as large as possible. Where the cost function is asymmetric, as will be the case in the majority of practical applications of any optimiser, the estimate of the optimum formed by a single derivative optimiser will be biassed. The bias is a function of the amplitude probability distribution of the perturbation waveform and the asymmetry of the cost function.

The case is considered where the cost function is represented by a fifth order polynomial. $P(\gamma) = \sum_{n=0}^{5} a_n (\gamma)^n$

The true optimum of the cost function is where

$$\sum_{n=0}^{5} n\, a_n(\gamma)^{n-1} = 0$$

The bias associated with the sinusoidal optimiser is determined by examining the change in correlator output over 1 cycle of the perturbation wave-form. The change in correlator output, c, is given by

$$c = \frac{\omega\Delta}{2\pi} \int_0^{\frac{2\pi}{\omega}} \sum_{n=0}^{5} a_n(\gamma + \delta \sin \omega t)^n \sin \omega t \, dt$$

Expanding this gives.

$$c = \frac{\omega\Delta\delta}{2\pi} (a_1 + 2a_2\gamma + 3a_3\gamma^2 + 4a_4\gamma^3 + 5a_5\gamma^4) \int_0^{\frac{2\pi}{\omega}} \sin^2 \omega t \, dt$$

$$+ \frac{\omega\Delta\delta^2}{2\pi} (a_2 + 3a_3\gamma + 6a_4\gamma^2 + 10a_5\gamma^3) \int_0^{\frac{2\pi}{\omega}} \sin^3 \omega t \, dt$$

$$+ \frac{\omega\Delta\delta^3}{2\pi} (a_3 + 4a_4\gamma + 10a_5\gamma^2) \int_0^{\frac{2\pi}{\omega}} \sin^4 \omega t \, dt$$

$$+ \frac{\omega\Delta\delta^4}{2\pi} (a_4 + 5a_5\gamma) \int_0^{\frac{2\pi}{\omega}} \sin^5 \omega t \, dt$$

$$+ \frac{\omega\Delta\delta^5}{2\pi} (a_5) \int_0^{\frac{2\pi}{\omega}} \sin^6 \omega t \, dt$$

Terms containing $\int_0^{\frac{2\pi}{\omega}} \sin^n \omega t \, dt = 0$ where n is odd. Evaluating the terms where n is even gives

$$c = \frac{\omega\Delta\delta}{2}(a_1 + 2a_2\gamma + 3a_3\gamma^2 + 4a_3\gamma^3 + 5a_5\gamma^4)$$

$$+ \frac{3\omega\Delta\delta^3}{8}(a_3 + 4a_4\gamma + 10a_5\gamma^2)$$

$$+ \frac{5\omega\Delta\delta^5}{16}(a_5)$$

The estimated value of the optimum is determined by where c = 0. The first term of the expression equals zero at the true optimum. The other terms are associated with the bias on the estimate of the optimum.

The bias for a square wave optimiser may be determined similarly for a perturbation of amplitude δ correlated with a square wave of amplitude Δ.

The change in correlator output after 1 cycle of period T is given by

$$c = \frac{\Delta\delta}{T}\int_0^{T/2} \sum_{n=0}^{5} a_n(\gamma + \delta)^n \, dt - \frac{\Delta\delta}{T}\int_0^{T/2} \sum_{n=0}^{5} a_n(\gamma - \delta)^n dt$$

$$= \Delta\delta \sum_{n=0}^{5} [a_n(\gamma + \delta)^n - a_n(\gamma - \delta)^n]$$

$$= \Delta\delta[a_1 + 2a_2\gamma + 3a_3\gamma^2 + 4a_4\gamma^3 + 5a_5\gamma^4]$$

$$+ \Delta\delta^3[a_3 + 4a_4\gamma + 10a_5\gamma^2]$$

$$+ \Delta\delta^5 a_5$$

By comparison a smaller bias will be associated with the estimate of the optimum formed by the sinusoidal optimiser using perturbations of the same amplitude.

4. Manual ignition timing optimisation.

During engine development ignition timing is adjusted manually so as to maximise output torque. This operation forms an important part of distributor design and is usually carried out with a constant speed control operating on dynamometer load torque to make the optimum more distinct to the test operator. Even with the use of a constant speed control the position of the optimum can still be very indistinct. The normal test practice therefore involves approaching the optimum by retarding the ignition until the first perceptable reduction in torque occurs. This is in order that any error in finding the optimum should be biassed towards the ignition being retarded.

The mechanical imperfections of the conventional distributor cause the ignition timing to wander about a mean level, causing a bias to be associated with the test operator's estimate of the optimum. The 'wander' is due to the run-out of the distributor cam and the clearance of the shaft bearings. It is present to a small extent even in a new distributor. The effect of this wander is considered for the case where the ignition has an equal probability of being fired anywhere within a band $2\delta^{o}$ wide. Again a fifth order polynomial $P(\gamma) = \sum_{n=0}^{5} a_n(\gamma)^n$ is used to represent the ignition timing torque cost function. The effect of the distributor "wander" is to modify $P(\gamma)$ to $P^*(\gamma)$ such that

$$E[P^*(\gamma)] = \frac{1}{2\delta}\int_{\gamma-\delta}^{\gamma+\delta} P(\gamma)dt$$

$$= \frac{1}{2\delta}\left[\sum_{n=0} a_n \frac{(\gamma+\delta)^{n+1}}{n+1} - a_n \frac{(\gamma-\delta)^{n+1}}{n+1}\right]$$

Expanding $E[P^*(\gamma)]$ gives

$$E[P^*(\gamma)] = a_0 + a_1\gamma + a_2\gamma^2 + a_3\gamma^3 + a_4\gamma^4 + a_5\gamma^5 + \frac{a_2\delta^2}{3} + \frac{a_4\delta^4}{5}$$
$$+ (a_3\delta^2 + a_5\delta^4)\gamma + 2a_4\delta^2\gamma^2 + \frac{10}{3}a_5\delta^2\gamma^3$$

Thus the maximum of $E[P^*(\gamma)]$ can be compared with the maximum of $P(\gamma)$

5. Perturbation limitations for ignition timing and air/fuel ratio optimisation.

Initial studies carried out by Draper and Li. (11) which were concerned with the optimisation of ignition timing and air/fuel ratio have demonstrated the feasability of such an operation using analog computing techniques. These and other investigators (12) failed to indicate two salient features of the combustion process which are of direct consequence to optimisation. Firstly, combustion is a discrete process. Any changes in operating conditions will not take effect until after the combustion cycle is initiated, and the results of these changes will not manifest themselves until after the combustion cycle is complete. Secondly the process is irregular, and any measurements associated with it may be considered as being contaminated by noise.

Optimisation consists of perturbing the parameters of the system and correlating the resulting outputs with the perturbation in order determine the adjustments to the parameters and maximise desired cost functions. The discrete nature of combustion can cause the distortion of perturbation waveforms, whilst the effect of the noise on output signals requires that they should be filtered before they can be used to evaluate performance criteria.

These two features of the combustion process must be considered in the design of any optimisation system. The discrete behaviour sets the absolute limit to perturbation frequency, whilst a speed limitation is imposed by the need for output signal filtering.

Mathematical models have been developed to aid the choice of perturbation waveforms and to indicate the absolute limits of optimiser speed.

Ignition timing.

Each time the ignition is fired the engine effectively samples the ignition timing and a pulse of torque is generated. This succession of pulses is filtered by the engine flywheel. Where the engine is running at constant speed and the ignition timing remains unaltered and the sampling rate is held constant. However, when perturbations are applied to the ignition timing the sampling instants will be advanced or delayed so that the sampling may no longer be regarded as periodic. The instantaneous sampling rate is a function of engine speed, perturbation amplitude and frequency.

A model for this aperiodic sampling process has been developed in order to define the distortion applied to the perturbation waveform. This is described with reference to fig. 7.2. The distortion may conveniently be considered by applying a phase displacement of the ignition timing signal so as to restore the periodicity of the sampling. The signal is then sampled at a constant rate and subsequently a reversed phase displacement is applied so as to restore the correct time relationship. The effect of the phase displacement is considered first.

Consider the engine to be running with an ignition advance of r radians at a speed of Ω radians per second. When the ignition timing is advanced by a further b radians the next spark to occur will take place $\frac{b}{\Omega}$ seconds earlier. To restore the even time spacing of ignition firing the timing waveform should itself be considered as being shifted back in time by $\frac{b}{\Omega}$ seconds at the instant the change was made.

This may be extended to cover the case where a sinusoidal perturbation, $b \sin \omega t$, is applied about a mean ignition advance of r. To restore the even time spacing of the ignition sampling and firing

instants the input waveform must become

$$r + b \sin (\omega t + \frac{b\omega}{\Omega} \sin \omega t).$$

This result is recognisable as a special case of frequency or phase modulation, where the modulation and carrier frequencies are equal.

Sin $(\omega t + \frac{b\omega}{\Omega} \sin \omega t)$ may be expressed in terms of Bessel functions giving:-

$$\begin{aligned}\text{Sin } (\omega t + \tfrac{b\omega}{\Omega} \sin \omega t) = {} & J_o (\tfrac{b\omega}{\Omega}) \sin \omega t \\ & + J_1 (\tfrac{b\omega}{\Omega}) \sin 2\omega t \\ & + J_2 (\tfrac{b\omega}{\Omega}) (\text{Sin } 3\omega t - \sin \omega t) \\ & + J_3 (\tfrac{b\omega}{\Omega}) (\text{Sin } 4\omega t + \sin 2\omega t) \\ & + \ldots\ldots\ldots\end{aligned}$$

Where $J_n (\frac{b\omega}{\Omega})$ is the Bessel function of the first kind and nth order with argument $(\frac{b\omega}{\Omega})$. The effect of the phase modulation is therefore to re-introduce the frequency components of the perturbation waveform at integer multiples of their frequency.

With sinusoidal perturbations very large amplitudes at relatively high frequencies and low engine speeds are required before the re-introduced components become at all significant. To illustrate this the Bessel function coefficients have been calculated for a 4-cylinder 4-stroke engine running at 1000 R.P.M. where a sinusoidal perturbation of amplitude 10° at 20 Hz. is applied. These are given:-

$$J_0 = 0.99$$

$$J_1 = 0.0049$$

$$J_2 = 0.00017$$

$$J_3 = 0.0000042$$

It can be seen that in this case the amplitudes of the sidebands introduced are insignificant.

Subsequent to the phase modulation the effects of periodic sampling must be considered. The effect of the sampling is to

re-introduce the now distorted perturbation frequency spectrum folded around multiples of the sampling frequency. A component with frequency f_p is re-introduced at $nf_s \pm f_p$, where f_s is the sampling rate, and n = 1,2,3..... ∞ The phase of the re-introduced components is arbitrary. As f_p is increased towards f_s distortion of this component will occur, and in the case where $f_p = f_s/2$ the sampling introduces a component at f_p of equal magnitude but arbitrary phase to the perturbation. To avoid the distortion of wideband perturbation signals by sampling the perturbation bandwidth should be less than half the sampling frequency.

To complete the model of the aperiodic sampling process the perturbation must be phase modulated in the reverse sense so as to restore the correct time relationship.

Mixture strength.

When each cylinder is filled during the induction stroke the contents of the induction pipe which are drawn into the cylinder are at the same time mixed. This has the effect of performing a running average of the mixture strength over each induction stroke. The transfer function of a running averager $R(j\omega)$, is given by

$$R(j\omega) = \frac{\sin \omega u/2}{\omega u/2}$$

where ω is the signal frequency and u the averaging time. Provided that the bandwidth of the perturbation remains substantially below $2/\omega u$ radians per second it will pass undistorted through the averager. For a 4-cylinder 4-stroke engine u = 30 ms. per 1000 R.P.M.

re-introduce the new distorted perturbation frequency spectrum folded around multiples of the sampling frequency. A component with frequency f_p is re-introduced at $nf_s \pm f_p$, where f_s is the sampling rate, and n = 1,2,3..... ∞ The phase of the re-introduced components is arbitrary. As f_p is increased towards f_s distortion of this component will occur, and in the case where $f_p = f_s/2$ the sampling introduces a component at f_p of equal magnitude but arbitrary phase to the perturbation. To avoid the distortion of wideband perturbation signals by sampling the perturbation bandwidth should be less than half the sampling frequency.

To complete the model of the aperiodic sampling process the perturbation must be phase modulated in the reverse sense so as to restore the correct time relationship.

Mixture strength.

When each cylinder is filled during the induction stroke the contents of the induction pipe which are drawn into the cylinder are at the same time mixed. This has the effect of performing a running average of the mixture strength over each induction stroke. The transfer function of a running averager R (jω), is given by

$$R(j\omega) = \frac{\sin \omega u/2}{\omega u/2}$$

where ω is the signal frequency and u the averaging time. Provided that the bandwidth of the perturbation remains substantially below $2/\omega u$ radians per second it will pass undistorted through the averager. For a 4-cylinder 4-stroke engine u = 30 ms. per 1000 R.P.M.

Experimental sinusoidal ignition timing optimiser.

A sinusoidal ignition timing optimiser to work under constant speed and throttle conditions was developed to permit the verification of theoretical performance evaluations and to compare its speed and accuracy with that of a human operator. The optimiser employed analog computing methods to form an estimate of the first derivative of the cost function, output torque. The rate of parameter adjustment was controlled by the computed local value of the gradient. A diagram of the optimiser is shown in fig. 7.3.

To obtain the fastest response to changes in ignition timing torque measurements were made on the coupling shaft between the engine and the dynamometer. Transfer function measurements between ignition timing and shaft torque indicated that accurate phase compensation of the perturbation signal could be applied at frequencies up to 8 Hz., at which point the transfer dynamics became dominated by the resonance associated with the rotating masses of the engine and dynamometer coupled by the elastic shaft.

A noise spectrum was derived from the shaft torque measurement at the optimum ignition timing. The measurement was taken at 2500 R.P.M. under part throttle operation. The spectrum was derived by performing a fast Fourier transform on the torque signal with the digital computer on-line.

The power spectrum obtained from these measurements is shown in fig. 7.4. The noise power was contained largely in the frequencies below 3 Hz., and consequently in this case it was advantageous to employ a perturbation frequency well above this so as to enable the low pass filter to minimise the noise power entering the correlator.

The ignition timing/torque cost function was measured at various operating conditions of speed and throttle, and fitted to fifth order polynomials in order that estimates of optimiser bias could be derived.

From these estimates it was concluded that even with a sinusoidal perturbation of amplitude 10° the bias would not exceed 0.5° for all operating conditions. In the experimental optimiser a perturbation of amplitude 5° at 8 Hz. was applied.

Under these conditions of amplitude and frequency the distortion imposed on the perturbation waveform by aperiodic sampling has been shown to be negligible. (At 1000 R.P.M. in a 4-cylinder 4-stroke engine the ignition timing will be sampled at 33⅓ Hz. and consequently a sinusoidal perturbation at 8 Hz. will pass into the system substantially undistorted.)

Some typical optimiser responses for a range of integrator gains are shown in fig. 7.5. The mean square error, theoretical time constant and experimental settling time taken to adjust over 30° from the optimum are compared in table 7.1.

The theoretical time constant was derived by assuming a quadratic fit for the cost function, and applying the theory derived earlier in the chapter. An Algol 60 program was written to estimate the mean squared adjustment error by performing the necessary filtering operations on the noise power spectrum and finally integrating over all frequencies to totalise the noise power.

TABLE 7.1.

Integrator gain.	M.S. error.	Time constant.	Experimental settling time.
2	1.2°	0.46 sec.	7 sec.
5	3.0°	0.125 sec.	2.8 sec.
20	12°	0.046 sec.	0.7 sec.

Fig. 7.1 SINGLE PARAMETER OPTIMISER

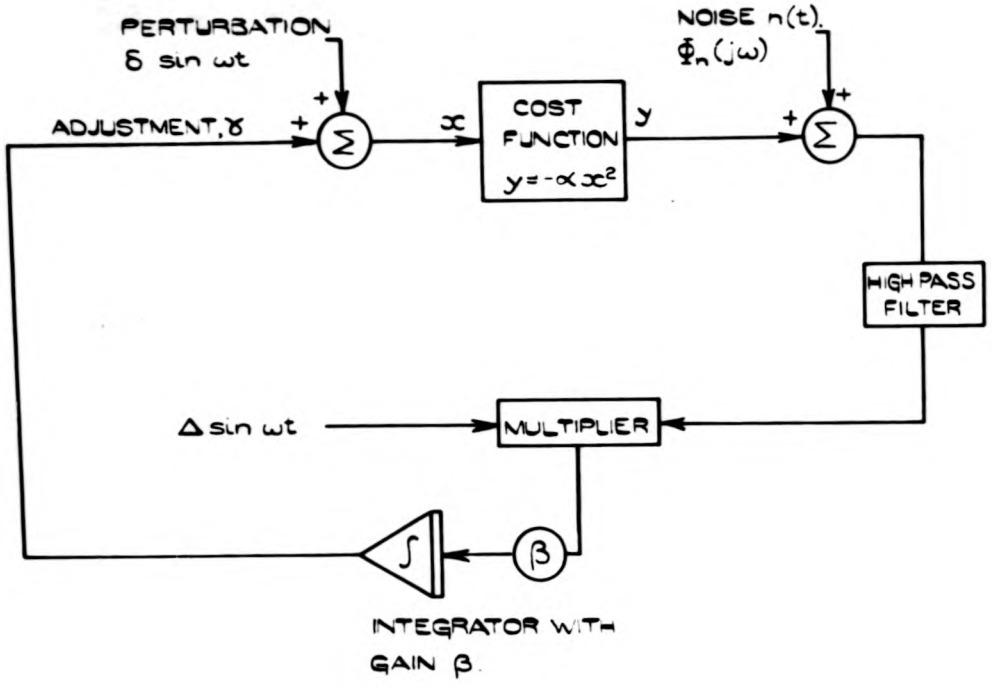

Fig. 7.2. APERIODIC SAMPLING PROCESS.

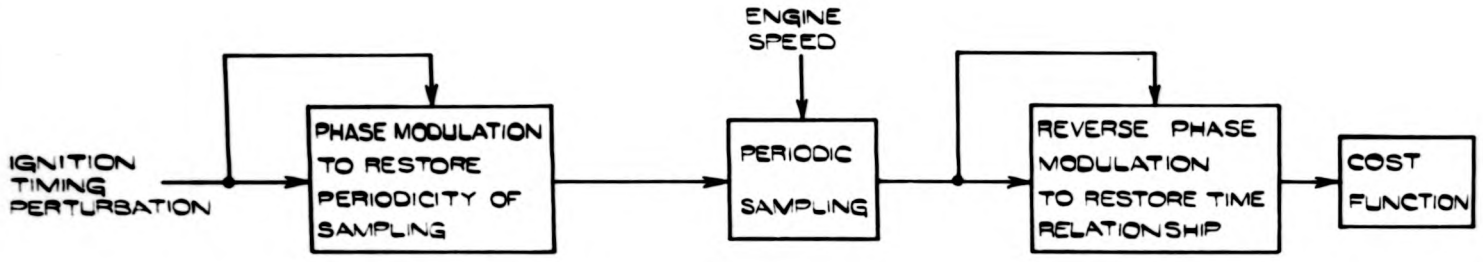

FIG. 7.3. SINUSOIDAL IGNITION TIMING OPTIMISER.

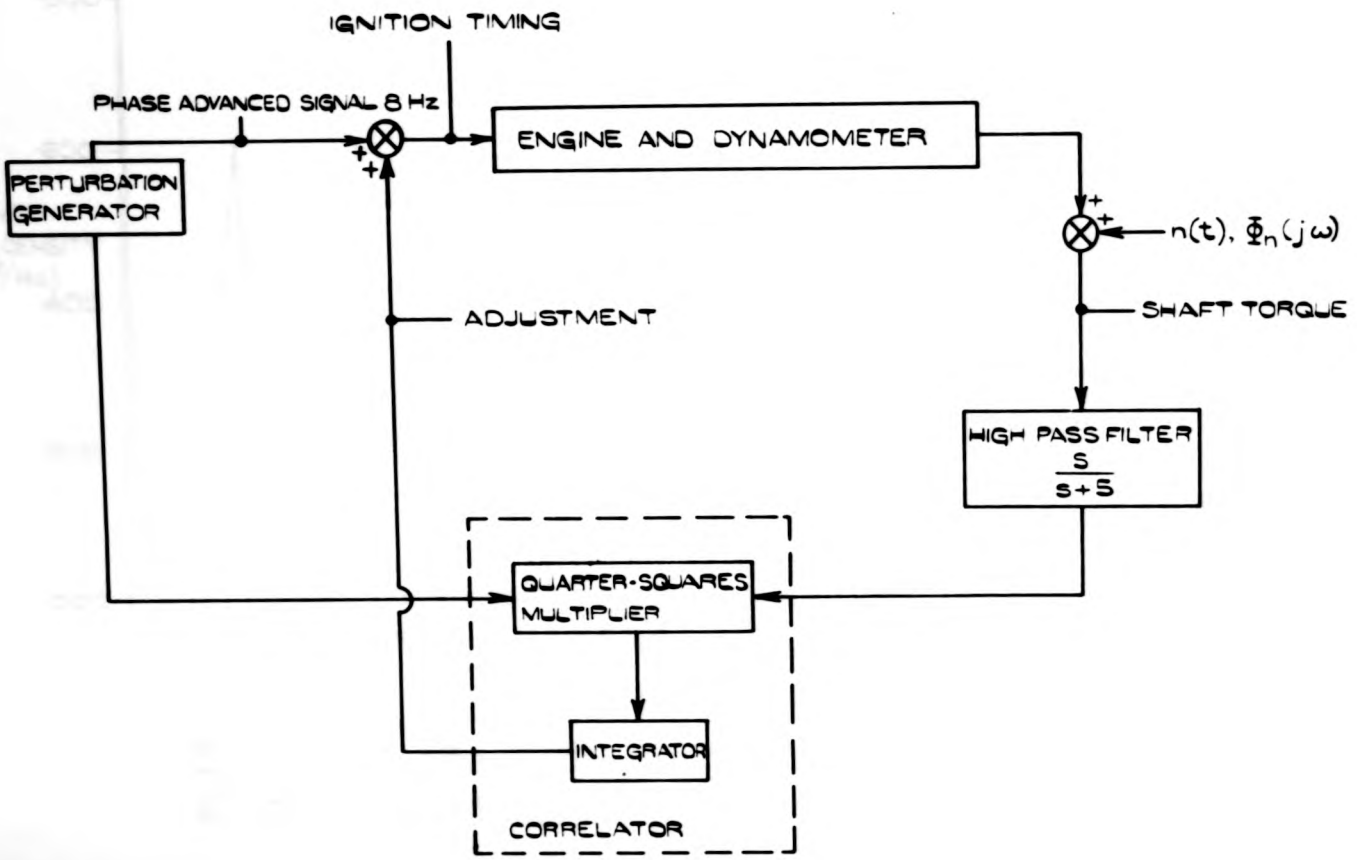

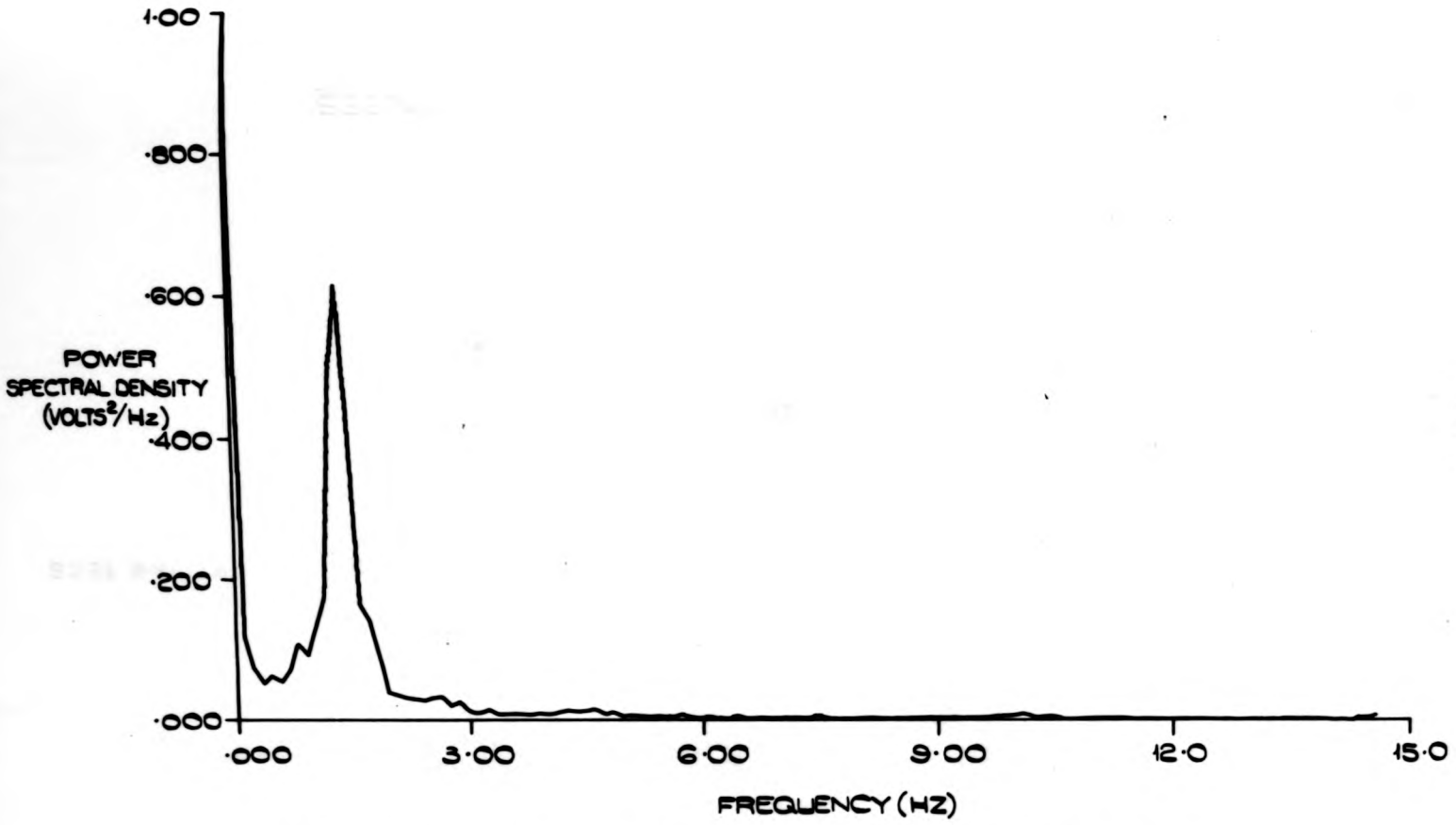

FIG. 7.4. MEASURED POWER SPECTRAL DENSITY OF NOISE COMPONENT ON SHAFT TORQUE MEASUREMENT.

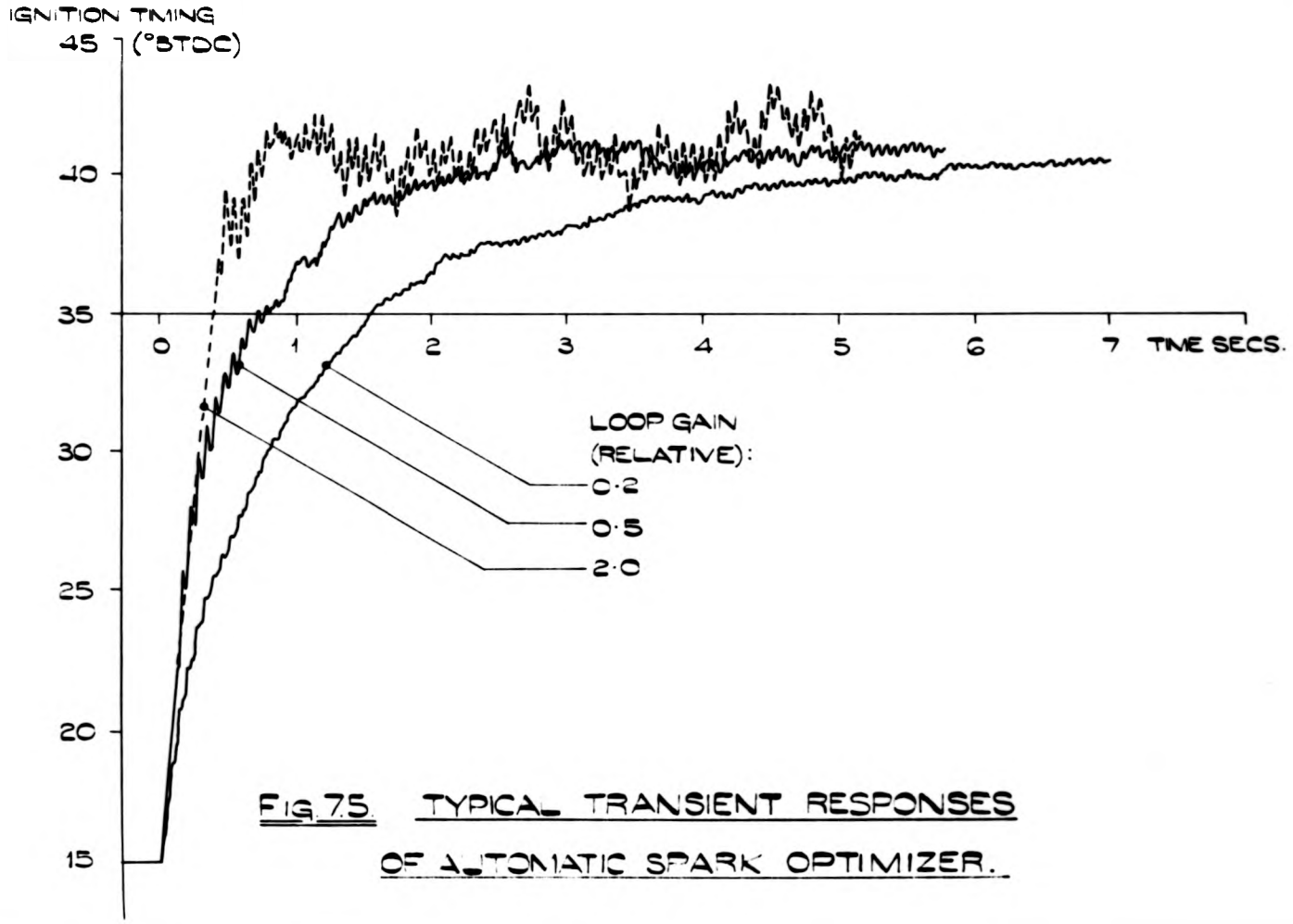

FIG. 7.5. TYPICAL TRANSIENT RESPONSES OF AUTOMATIC SPARK OPTIMIZER.

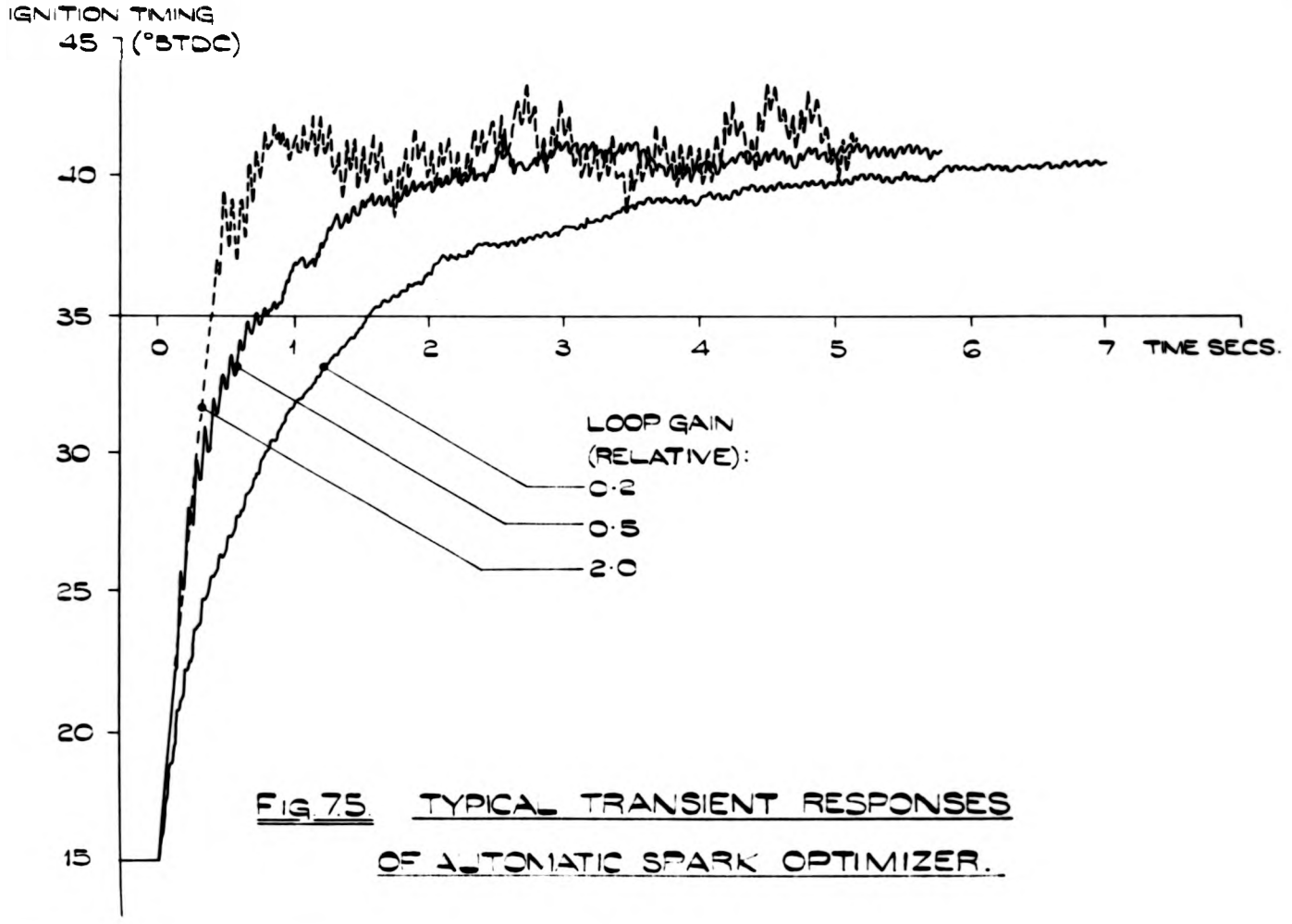

FIG 7.5. TYPICAL TRANSIENT RESPONSES OF AUTOMATIC SPARK OPTIMIZER.

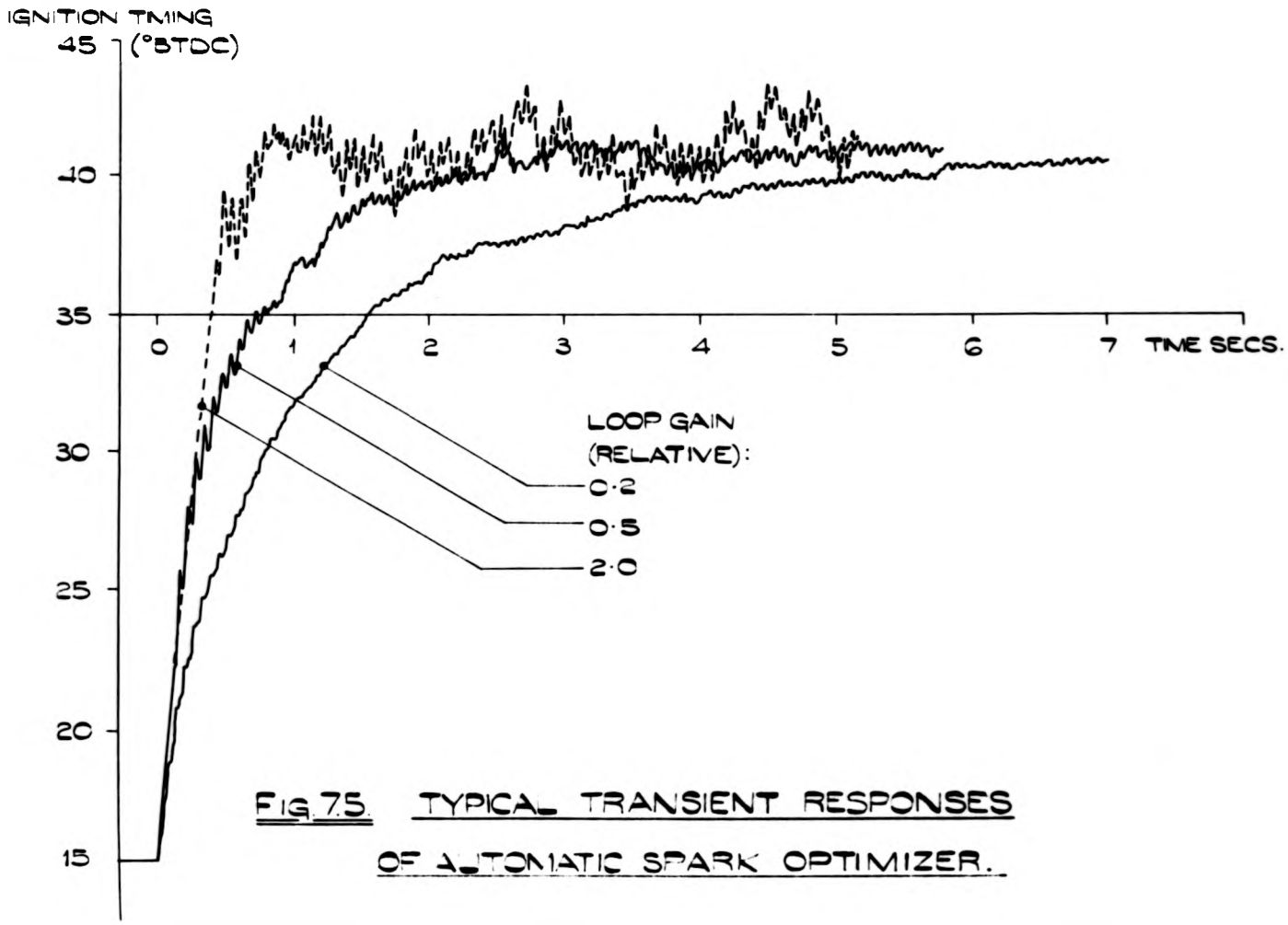

FIG 7.5 TYPICAL TRANSIENT RESPONSES OF AUTOMATIC SPARK OPTIMIZER.

CHAPTER 8.

COMPUTER CONTROLLED TESTS.

1. Control and measurement techniques for on-line tests.
2. List of interfacing utilised.
3. Torque and horsepower plots for a list of throttle openings.
4. Ignition timing sensitivity.
5. Air/fuel ratio sensitivity.
6. Mixture loops.
7. Ignition timing optimisation.
8. Ignition timing and mixture optimisation.

1. Control and measurement techniques for on-line tests.

All computer controlled tests were run with the closed loop speed control in operation, the speed setpoint being provided by the computer. Measurements were made with the setpoint held constant. The computer also controlled the throttle opening and the ignition and starter switches. Where appropriate control of the ignition timing and fuel flow rate or carburettor float chamber pressure were also utilised. The following measurements were sampled by the computer at 1/10th second intervals.

1. Engine speed.
2. Engine torque, measured as the dynamometer reaction.
3. Fuel flow rate.
4. Cylinder head water outlet temperature.
5. Oil temperature, measured on entry to the main gallery.

According to the requirements of the particular test the first three of these measurements were utilised in the calculation of output data. Where measurements contained any significant components above 5 Hz. they were filtered so as to minimise aliasing errors.

The procedure adopted for logging measurements at any running condition involved allowing the load and speed to settle, this taking up to 6 seconds, and then averages of the measurements were formed over up to 6.4 seconds. Averaging provided a useful means of reducing measurement noise which was due to the irregularities of combustion.

An algol 60 program was written to determine the effect of averaging time on the total noise power of torque measurements. The program utilised a measured power spectrum for the signal from the dynamometer weighing gear. In consequence it was concluded that the distribution of noise power was such as to require averaging times in excess of 2 seconds if any significant reduction in power was to be achieved.

Included in test programs were subroutines to examine measurements

and check that the limits of control setpoints were satisfied. Failure to satisfy these limits resulted in programmed action, or control being returned to the operator through the on-line typewriter.

If the engine stopped during a test an automatic starting routine was called. The test was re-entered if the starting routine was successful, otherwise control was returned to the operator and the test schedule abandoned.

2. List of interfacing utilised.

The interfacing utilised for on-line testing is listed below.

Computer ——→	Engine
Analog outputs.	Throttle opening. Closed loop speed. Ignition timing. Carburettor float chamber pressure or fuel flow rate.
Relay outputs.	Ignition switch. Starter switch.

Computer ——→	X - Y recorder.
Analog outputs.	X - axis. Y - axis.
Relay outputs.	Pen lift.

Engine. ——→	Computer.
Torque measured at the dynamometer weighing gear. Dynamometer speed. Fuel flow rate. Cylinder head water outlet temperature. Oil temperature on entry to main gallery.	Analog inputs.
Oil pressure switch. ——→	S.E.S. digital inputs.

3. Torque and horsepower plots for a list of throttle openings.

This test acquired the data for and plotted simultaneously torque or horsepower against speed for a list of throttle openings. The selection of torque or horsepower was achieved by setting a breakpoint switch on the front panel of the computer.

On entry to the test the axes of the graph were drawn and the engine started if it was not already running. The test itself was begun by selecting the smallest speed and throttle opening and was continued by stepping through the speed range with each member of the list of throttle openings.

Each set of running conditions was permitted to stabilise for 6 seconds before torque and speed were logged. The log consisted of 64 consecutive measurements of each of the two variables. On completion of the log measurements were averaged and a check was made to establish that the engine speed had remained within the prescribed limits of the setpoint. Under conditions where the engine was unable to reach the set speed due to an insufficient throttle opening the speed range traverse was terminated and the traverse with the next largest throttle opening initiated. A short period of idling was included in between each speed traverse.

When the list of throttle openings was exhausted the computer set the engine to idling and informed the operator that the test had been completed through the on-line typewriter.

At any time during the test the operator was able to abort from the schedule by idling or stopping the engine through the on-line typewriter. Alternatively it was possible to halt the test and re-enter at the beginning.

A flow diagram for the test is given in fig. 8.1.

An example of the graphical output is given in fig. 8.2.

The test took 22 minutes to execute during which time 105 points were plotted. The test program occupied 271 store locations.

3. Torque and horsepower plots for a list of throttle openings.

This test acquired the data for and plotted simultaneously torque or horsepower against speed for a list of throttle openings. The selection of torque or horsepower was achieved by setting a breakpoint switch on the front panel of the computer.

On entry to the test the axes of the graph were drawn and the engine started if it was not already running. The test itself was begun by selecting the smallest speed and throttle opening and was continued by stepping through the speed range with each member of the list of throttle openings.

Each set of running conditions was permitted to stabilise for 6 seconds before torque and speed were logged. The log consisted of 64 consecutive measurements of each of the two variables. On completion of the log measurements were averaged and a check was made to establish that the engine speed had remained within the prescribed limits of the setpoint. Under conditions where the engine was unable to reach the set speed due to an insufficient throttle opening the speed range traverse was terminated and the traverse with the next largest throttle opening initiated. A short period of idling was included in between each speed traverse.

When the list of throttle openings was exhausted the computer set the engine to idling and informed the operator that the test had been completed through the on-line typewriter.

At any time during the test the operator was able to abort from the schedule by idling or stopping the engine through the on-line typewriter. Alternatively it was possible to halt the test and re-enter at the beginning.

A flow diagram for the test is given in fig. 8.1.

An example of the graphical output is given in fig. 8.2.

The test took 22 minutes to execute during which time 105 points were plotted. The test program occupied 271 store locations.

4. Ignition timing sensitivity.

This test acquired the data for and plotted output torque or power against ignition timing for a given throttle opening and speed.

The test was initiated by the computer drawing the axes of the graph and interrogating the operator to determine the required speed and throttle setting. An automatic engine start was included. Measurements were made starting with the most retarded ignition setting which was increased in steps of approximately 2°. up to the most advanced setting. Since no changes in speed were required during the test a 4 second settling time was allowed in between making measurements and setting up new operating conditions. A data logging time of 6.4 seconds was used for each point. If the throttle opening was insufficient to enable the engine to reach the demanded speed an under speed message was output and control returned to the operator. This enabled a re-entry to be made with a larger throttle opening.

A flow diagram for the test is given in fig. 8.3.

An example of the graphical output is given in fig. 8.4.

The test plotted 20 points and took 2½ minutes to complete. The test program occupied 358 store locations.

5. Air/fuel ratio sensitivity.

This test acquired the data for and plotted output torque against carburettor float chamber pressure. The procedure adopted was exactly similar to that for determining the sensitivity to ignition timing. Similar interfacing was utilised except that the control of float chamber pressure was substituted for that of ignition timing.

An example of the graphical output is given in fig. 8.5.

6. Mixture loops.

This test acquired the data for and plotted the inverse of specific fuel consumption against torque for a pre-defined speed

4. Ignition timing sensitivity.

This test acquired the data for and plotted output torque or power against ignition timing for a given throttle opening and speed.

The test was initiated by the computer drawing the axes of the graph and interrogating the operator to determine the required speed and throttle setting. An automatic engine start was included. Measurements were made starting with the most retarded ignition setting which was increased in steps of approximately 2°. up to the most advanced setting. Since no changes in speed were required during the test a 4 second settling time was allowed in between making measurements and setting up new operating conditions. A data logging time of 6.4 seconds was used for each point. If the throttle opening was insufficient to enable the engine to reach the demanded speed an under speed message was output and control returned to the operator. This enabled a re-entry to be made with a larger throttle opening.

A flow diagram for the test is given in fig. 8.3.

An example of the graphical output is given in fig. 8.4.

The test plotted 20 points and took 2½ minutes to complete. The test program occupied 358 store locations.

5. Air/fuel ratio sensitivity.

This test acquired the data for and plotted output torque against carburettor float chamber pressure. The procedure adopted was exactly similar to that for determining the sensitivity to ignition timing. Similar interfacing was utilised except that the control of float chamber pressure was substituted for that of ignition timing.

An example of the graphical output is given in fig. 8.5.

6. Mixture loops.

This test acquired the data for and plotted the inverse of specific fuel consumption against torque for a pre-defined speed

and throttle angle. The test was carried out with the fuel flow rate control in operation, the fuel flow set point being provided by the computer. The test required a prior knowledge of the range of fuel flow rates to be covered for the particular speed and throttle setting.

Operation under constant fuel flow rate precluded on-line starting of the engine, so the test was initiated without computer control of fuel flow. When the engine had been started and the initial operating conditions set up the constant fuel flow rate control was brought into operation. At this stage the logging of data and graphical output was begun.

A flow diagram of the test is given in fig. 8.6.

An example of the graphical output is given in fig. 8.7.

The test plotted 100 points and took 23 minutes to complete. The test program occupied 251 store locations.

7. Ignition timing optimisation.

Optimisation of ignition timing using square wave perturbations was implemented utilising the torque measurements from the dynamometer weighing gear. By comparison with the sinusoidal optimiser, which utilised shaft torque measurements, a lower perturbation frequency was necessary.

As with sinusoidal perturbations the variance of the final estimate of the optimum will depend on measurement noise levels, perturbation amplitude and frequency, and parameter adjustment rate. Since the perturbation frequency is very low compared with the frequency at which the noise power is concentrated it may be considered as d.c. for the purposes of calculating the variance of the estimate of the optimum.

The variance will be a function of the noise power spectrum, the averaging time and the adjustment rate. The effect of averaging

time was considered and it was concluded that no significant reduction in total noise power could be achieved with averaging times of less than 3 seconds.

The adjustment rate was determined from the ignition sensitivity data. It was selected so as to give the fastest response free from overshoot. Measurements of the total noise power yielded an R.M.S. level of 75 mV. at the optimum. No significant change in this value or in the shape of the power spectrum occurred for non-optimal ignition timing. With the adjustment rate chosen averaging times below 3 seconds gave a variance in the estimated value of the optimum of approximately 1°. The perturbation amplitude was 4°. A flow diagram of the optimisation routine is given in fig. 8.8. Some typical optimiser responses are shown in fig. 8.9. The optimisation program occupied 300 store locations.

A more developed form of this optimisation routine was utilised in a test which plotted ignition timing for maximum torque against speed for a given throttle setting. An example of the graphical output of this program is given in fig. 8.10. To traverse the speed range and plot 20 points took approximately 15 minutes. This program occupied 362 store locations.

8. Ignition timing and mixture optimisation.

The optimisation routine which was applied to ignition timing and maximised output torque was extended to the control of mixture strength. The two parameters were perturbed sequentially and an adjustment made after each perturbation.

On entry to the optimisation routine engine speed was checked to establish that it was within the prescribed limits of the setpoint. Failure to satisfy this condition resulted in the engine being returned to idling and the output of an "underspeed" message on the on-line typewriter.

The optimisation was begun by applying one cycle of perturbation to the ignition timing. This was followed by an adjustment. Subsequently one cycle of perturbation was applied to the carburettor float chamber pressure and a further adjustment made. Each cycle of perturbation took 8 seconds and the adjustments were plotted on the X - Y recorder. Perturbations and adjustments to each parameter were continued in turn until both adjustments fell below the specified limits, whence the optimisation was terminated. Using limits of $\pm$ 0.11" of water for the carburettor float chamber pressure and $\pm \frac{1}{2}^{o}$ for ignition timing some specimen optimiser trajectories were obtained. An example which involved four adjustments to each variable to reach the optimum is shown in fig. 8.11.

The program occupied 615 store locations.

FIG. 8.1. TORQUE AND HORSEPOWER PLOTS

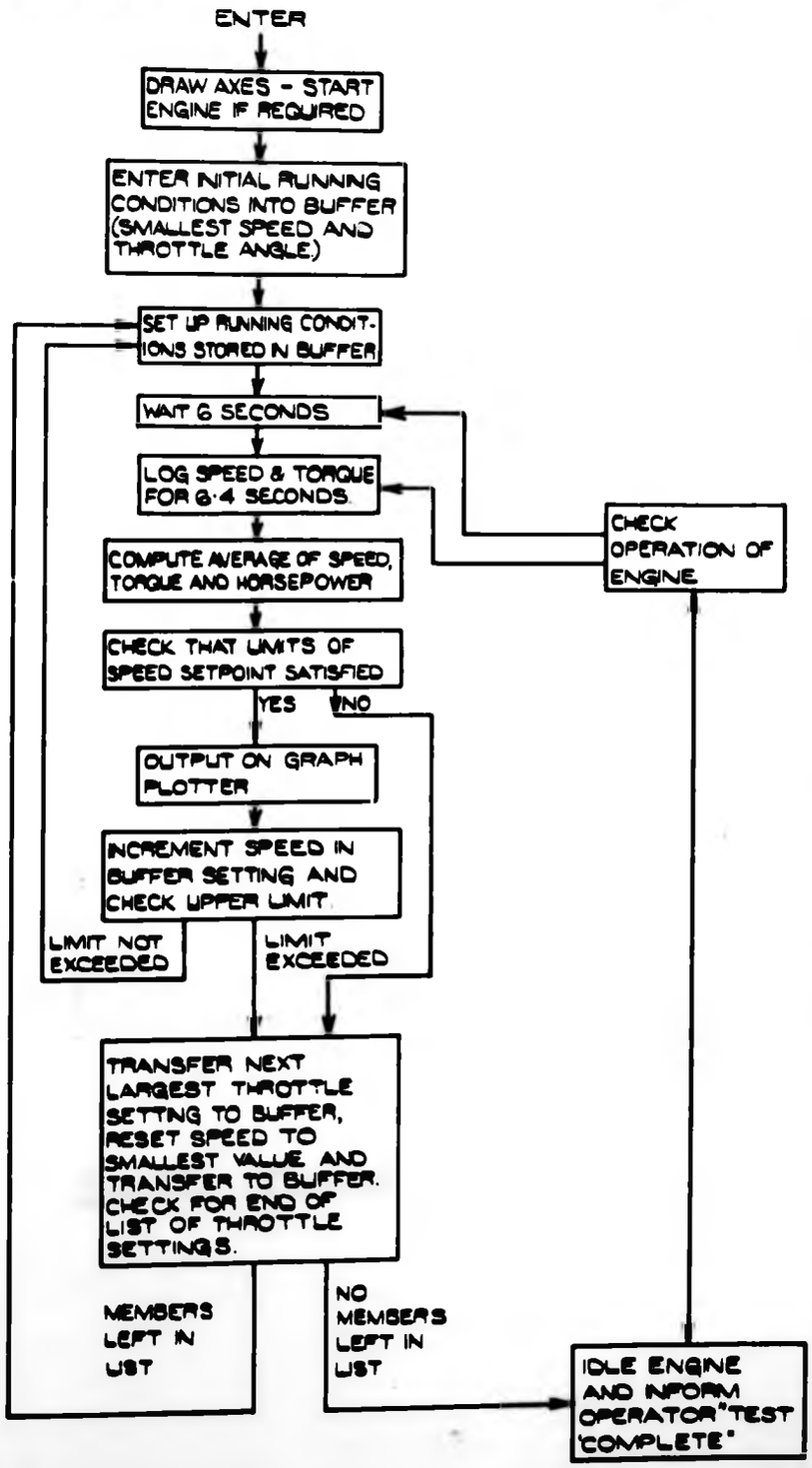

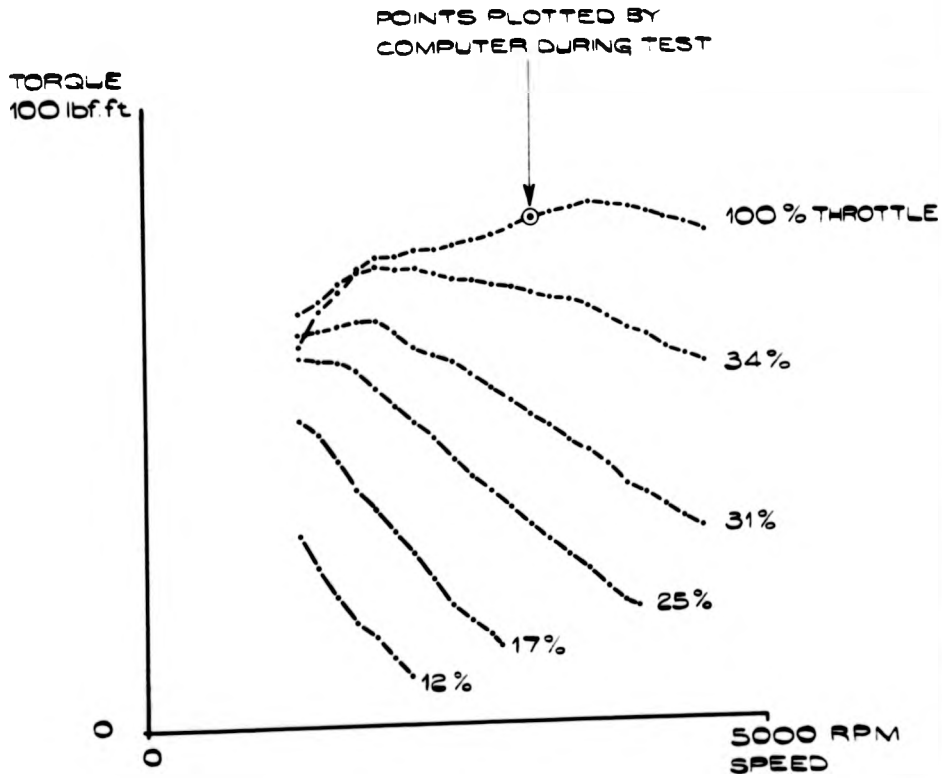

FIG. 8.2. TORQUE vs SPEED

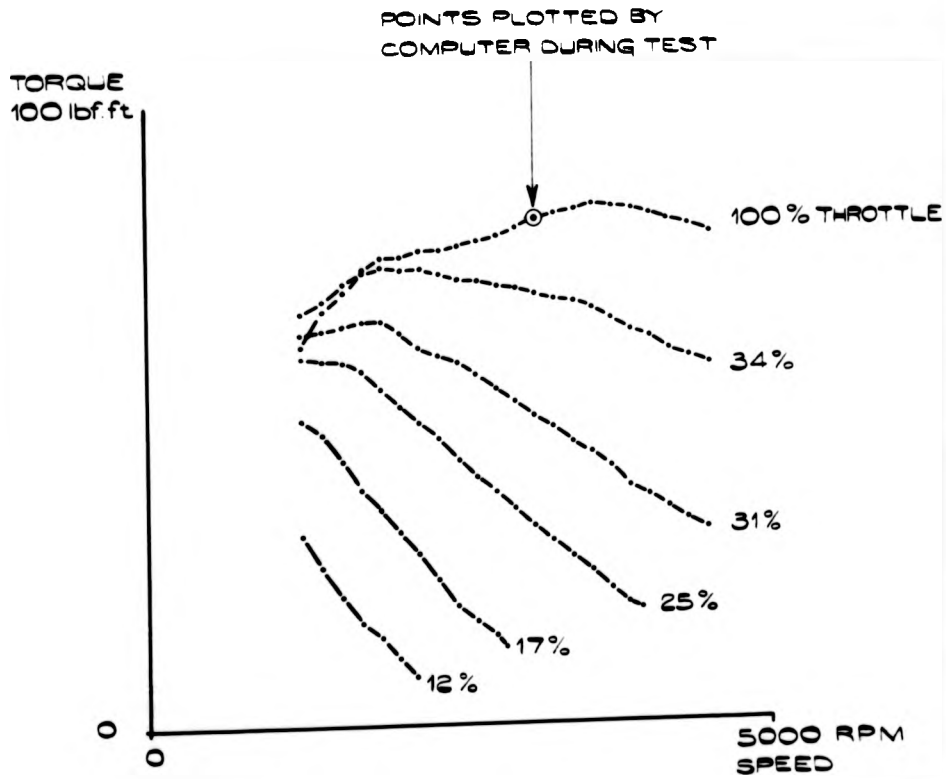

Fig. 8.2. TORQUE vs SPEED

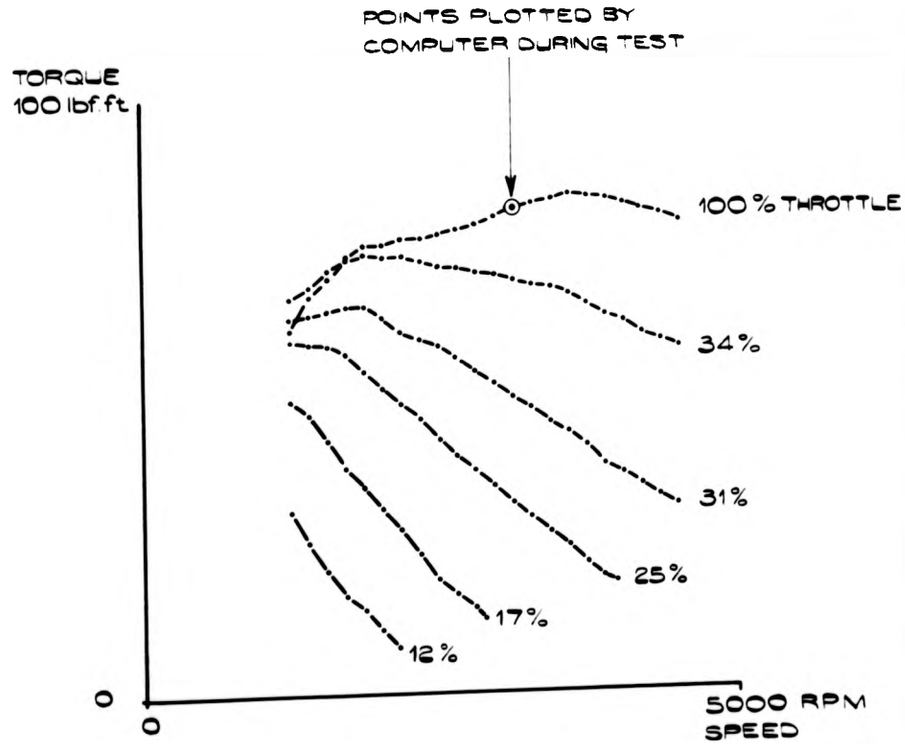

Fig. 8.2. TORQUE vs SPEED

FIG 8.3 IGNITION TIMING SENSITIVITY.

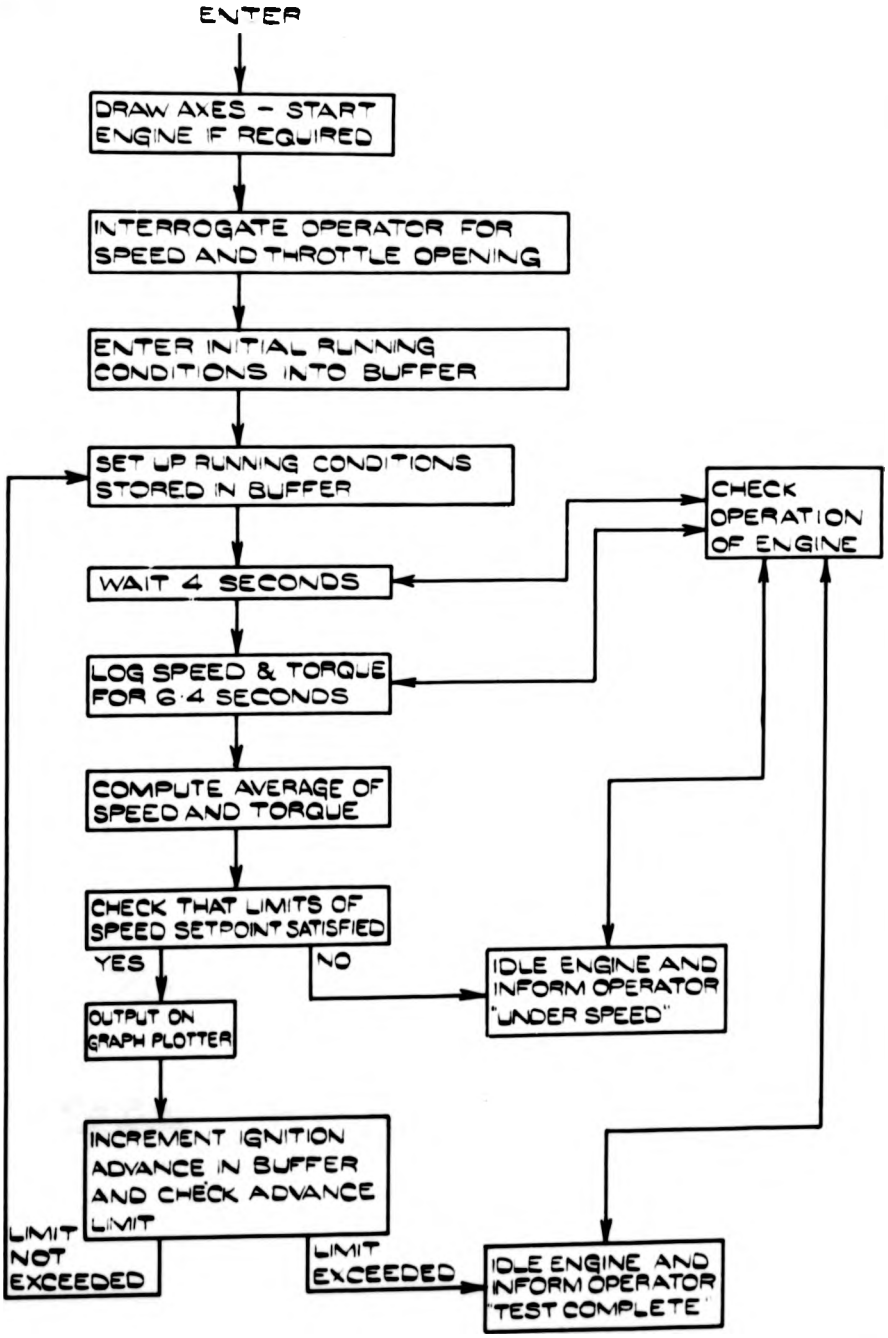

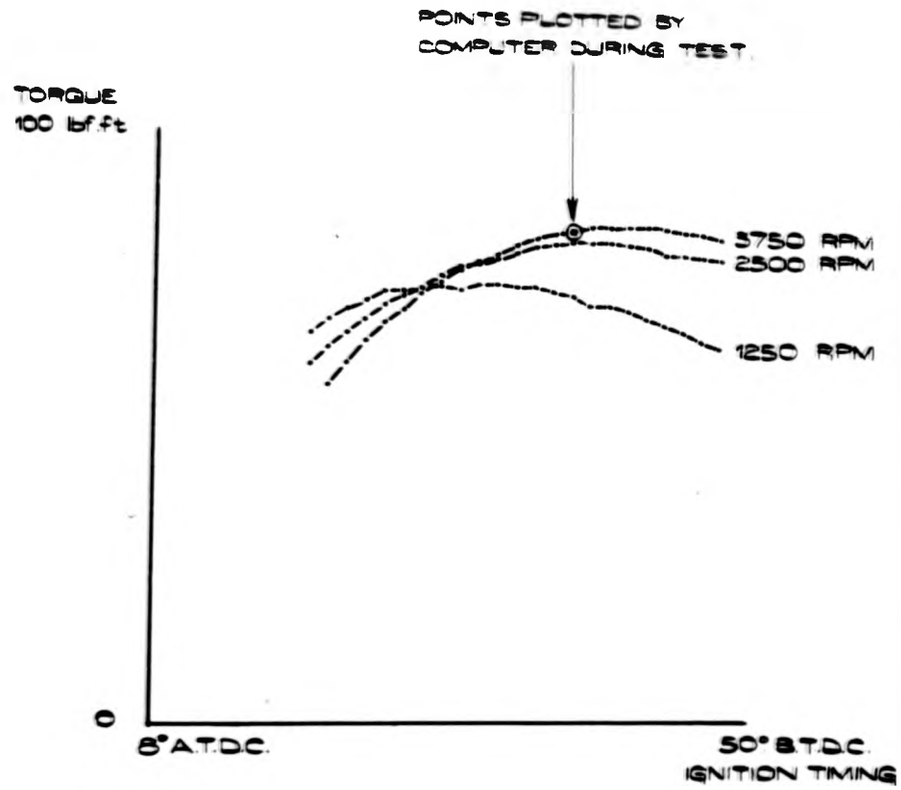

FIG. 8.4 IGNITION TIMING SENSITIVITY AT FULL THROTTLE

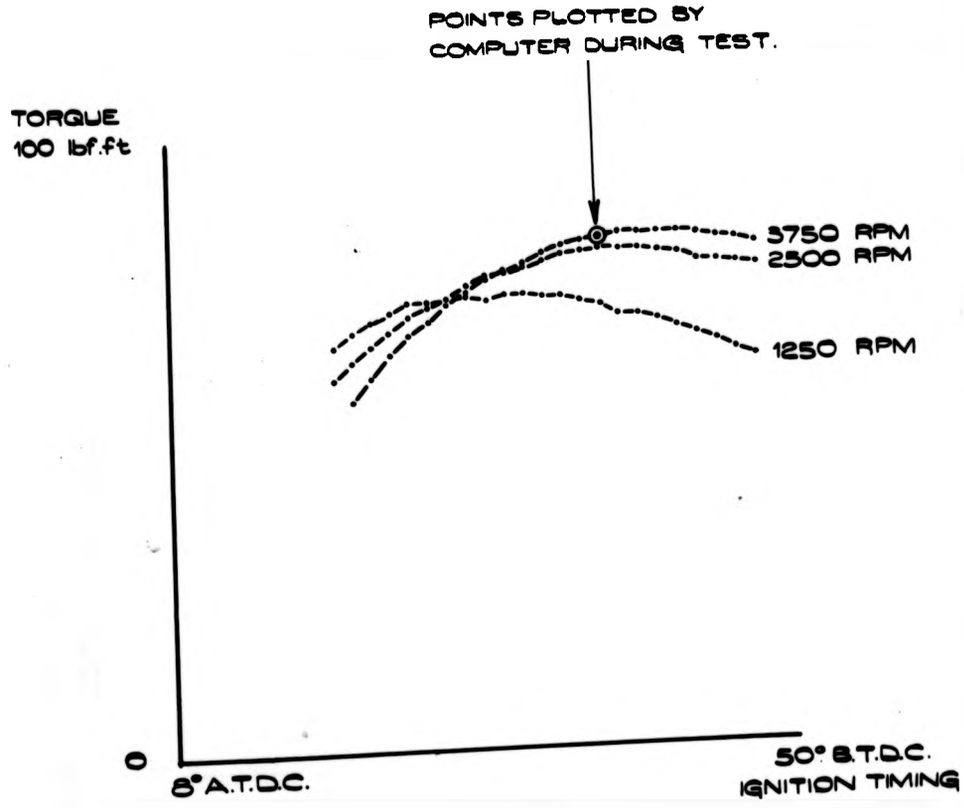

Fig. 8.4. IGNITION TIMING SENSITIVITY AT FULL THROTTLE.

FIG. 8.5. AIR/FUEL RATIO SENSITIVITY.
2500 R.P.M. FULL THROTTLE.

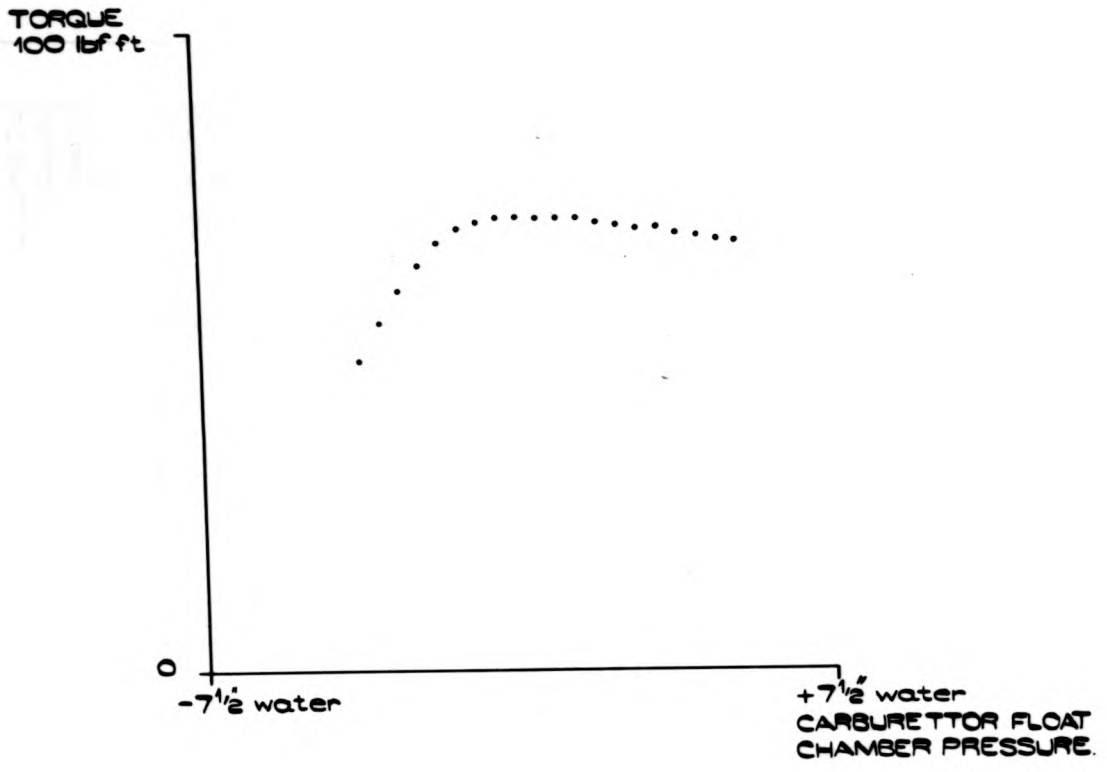

FIG 8.6 MIXTURE LOOPS.

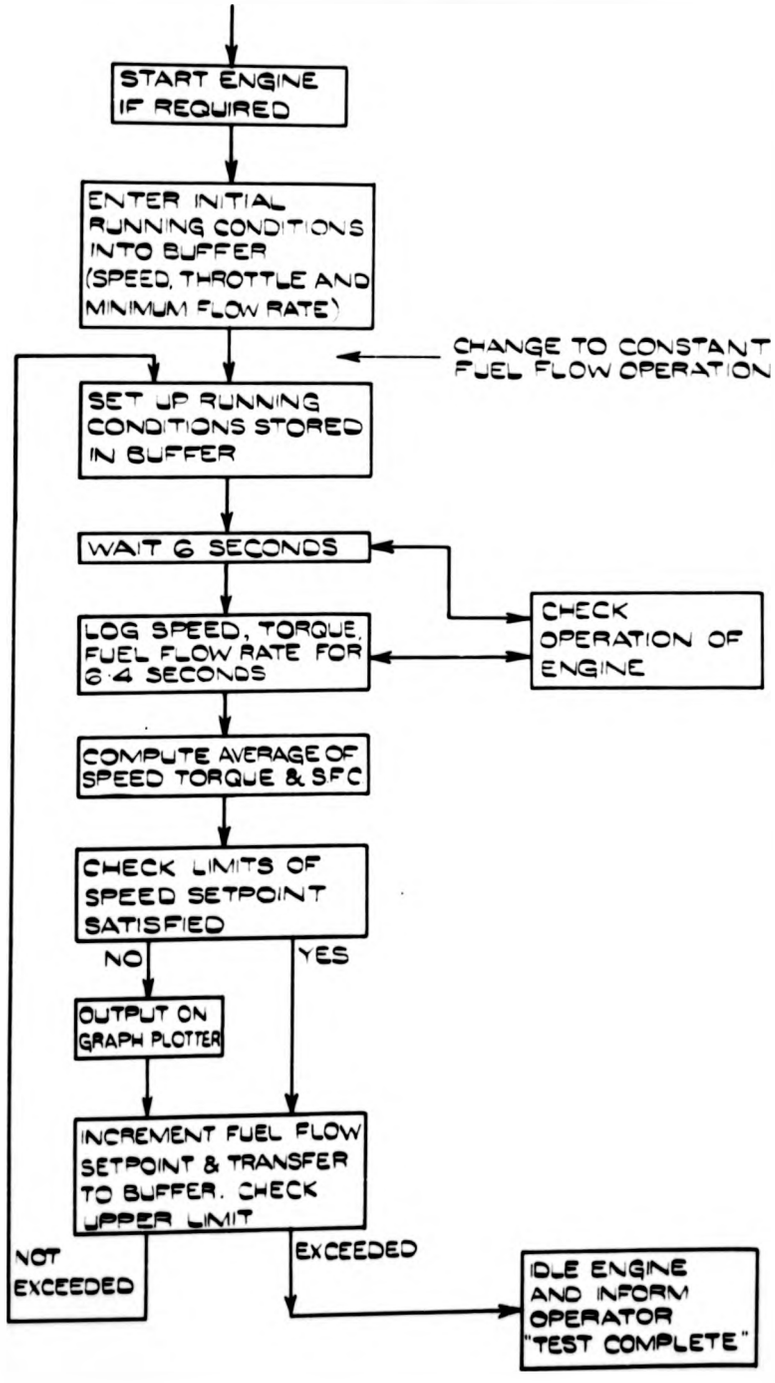

FIG. 8.6 MIXTURE LOOPS.

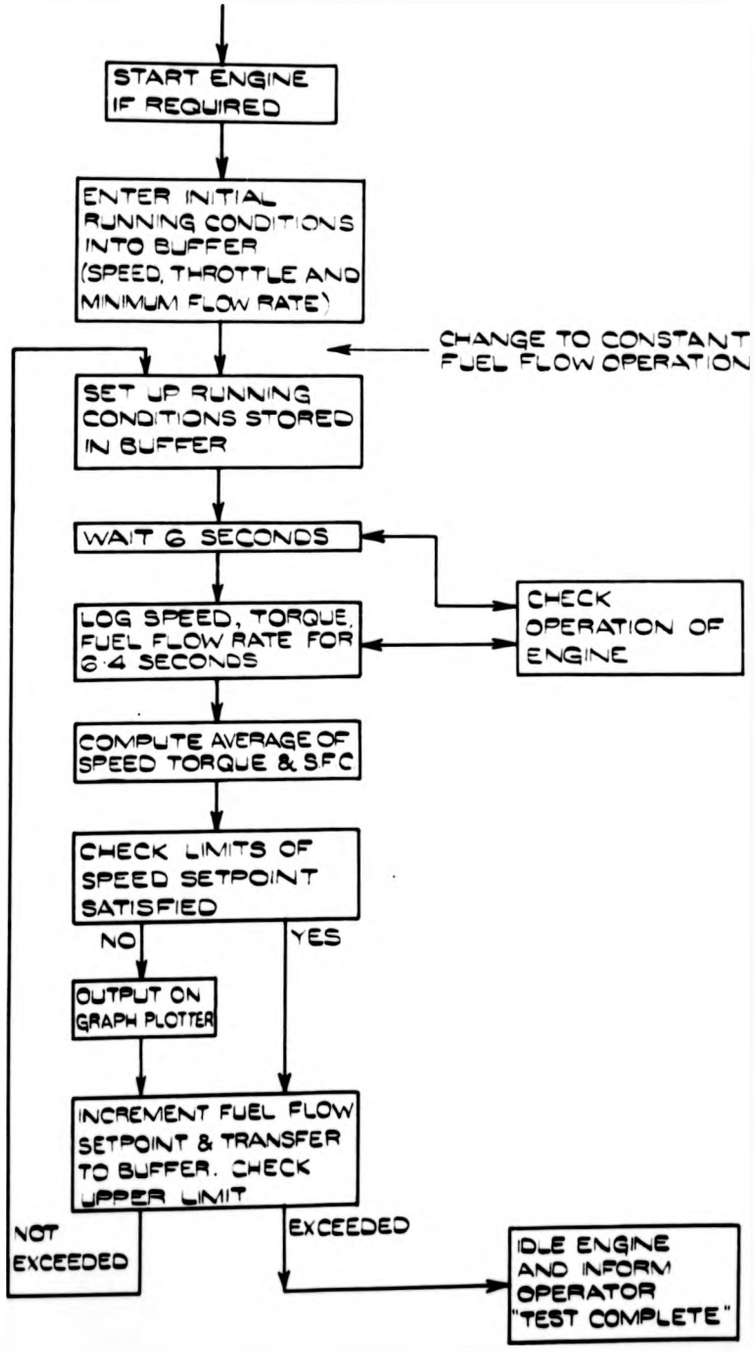

FIG. 8.7. MIXTURE LOOP.
2500 R.P.M. FULL THROTTLE

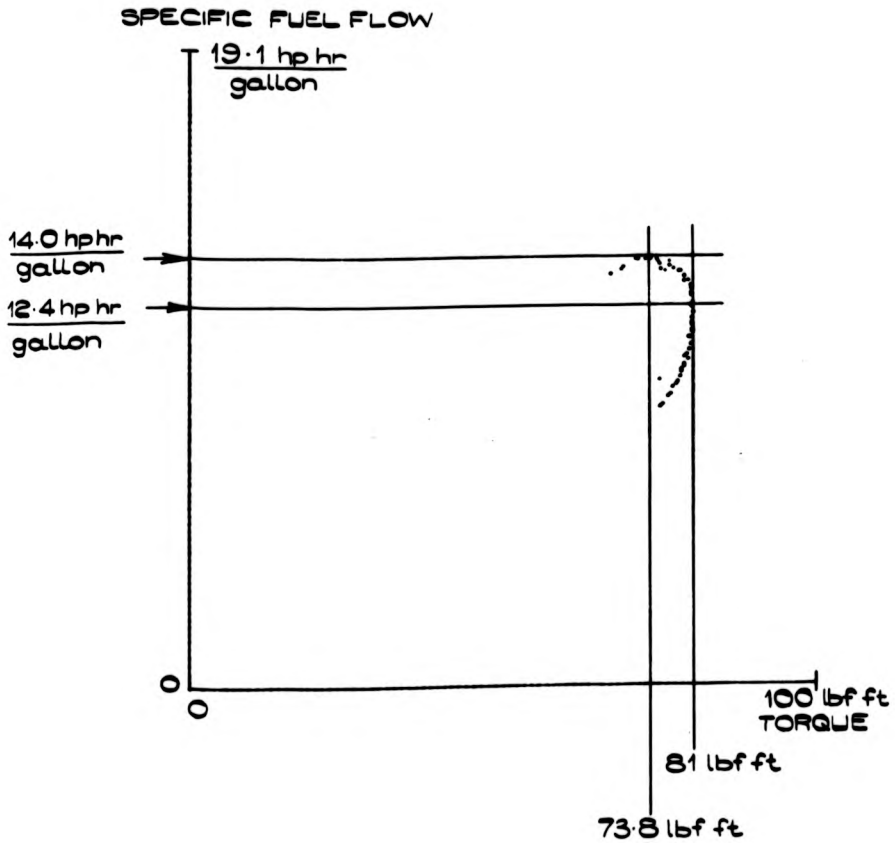

FIG. 8.8 IGNITION TIMING OPTIMISATION.

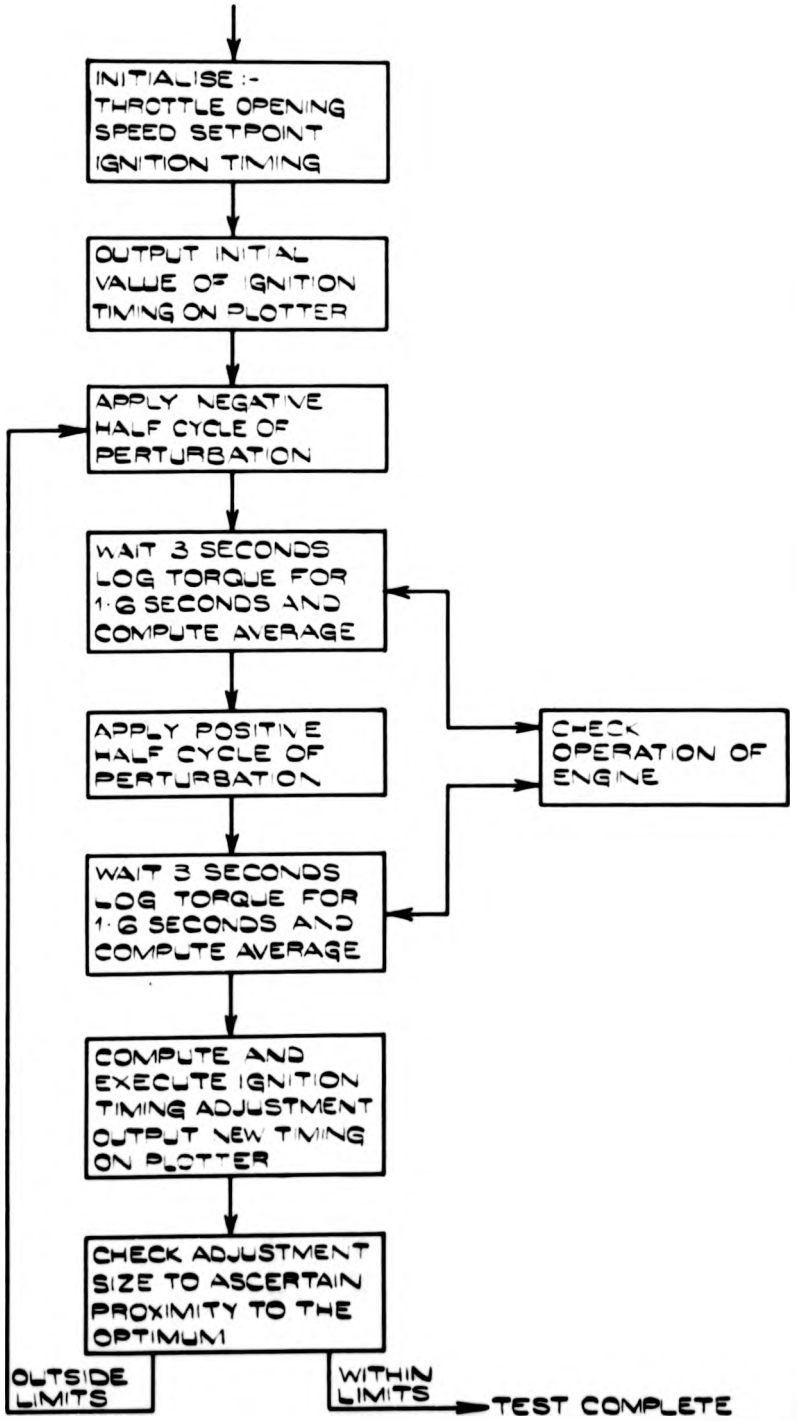

FIG. 8.9. IGNITION OPTIMISER RESPONSES

3750 R.P.M. 75% THROTTLE

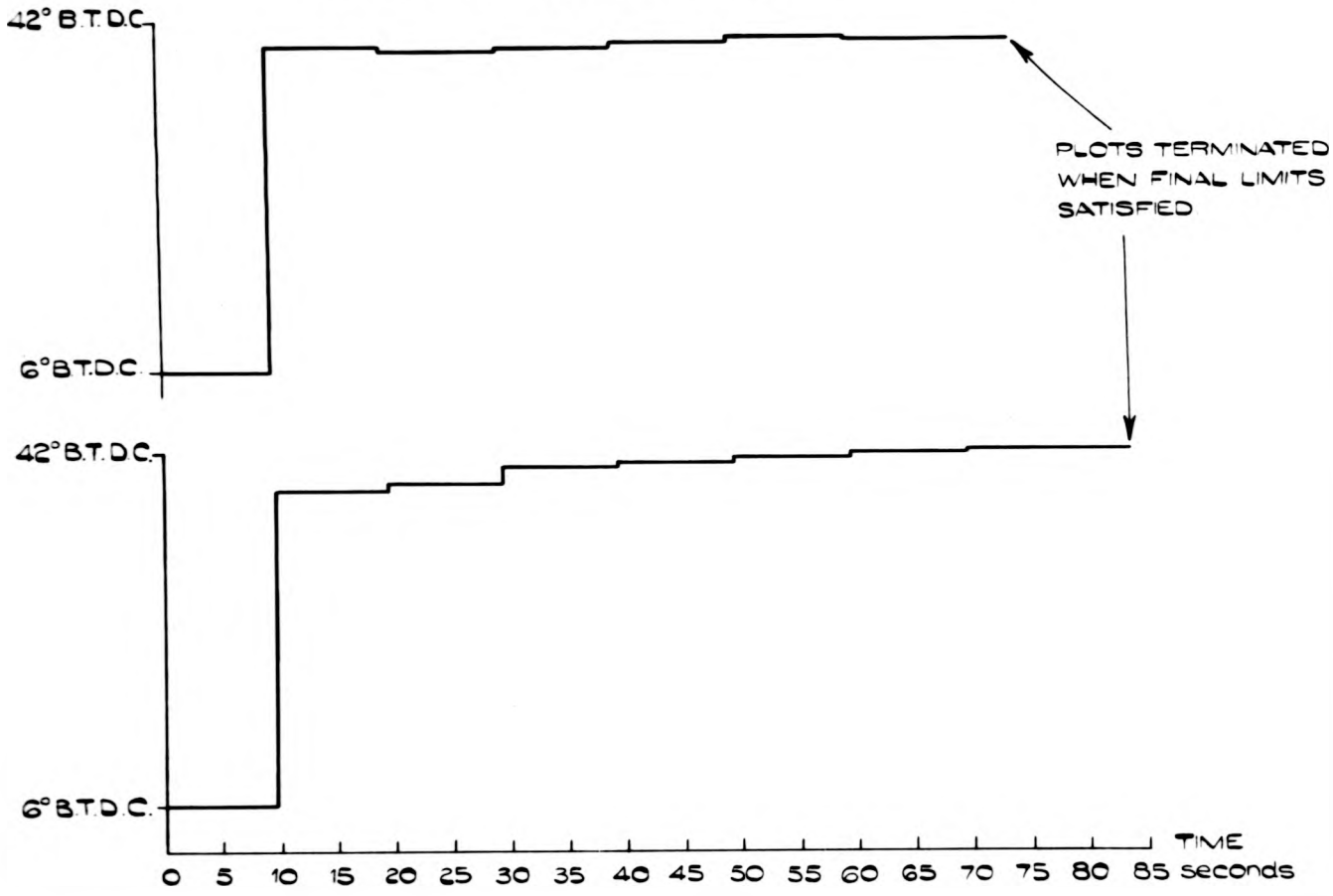

FIG. 8.9. IGNITION OPTIMISER RESPONSES

3750 R.P.M. 75% THROTTLE

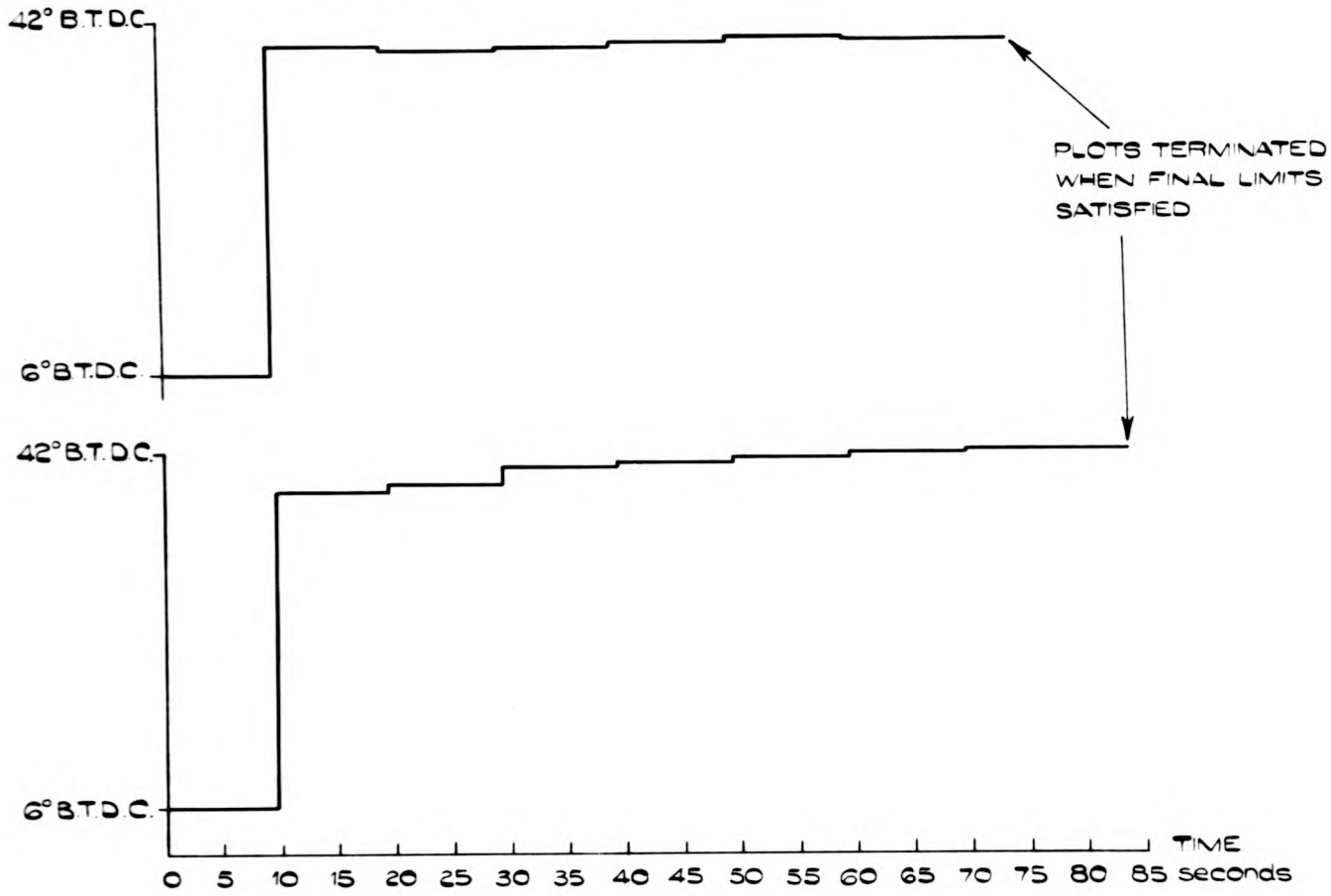

Fig 8.10. IGNITION TIMING V.S. SPEED FOR MAXIMUM TORQUE.

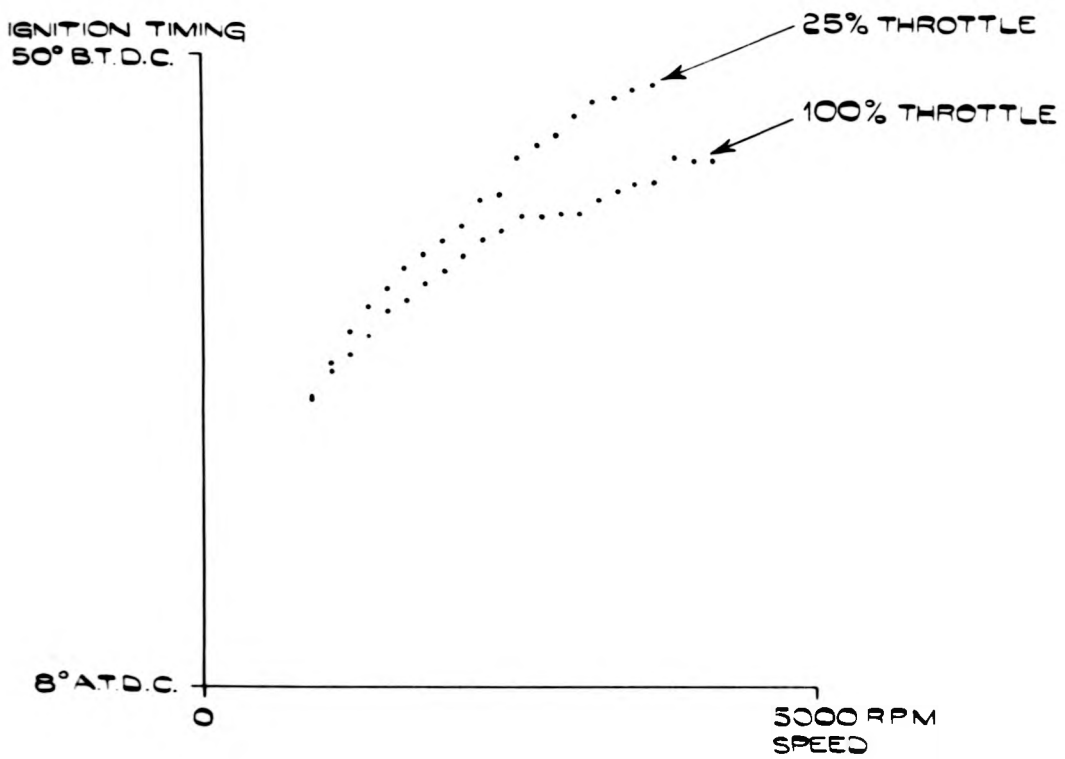

FIG. 8.11. IGNITION TIMING AND MIXTURE OPTIMISER RESPONSE

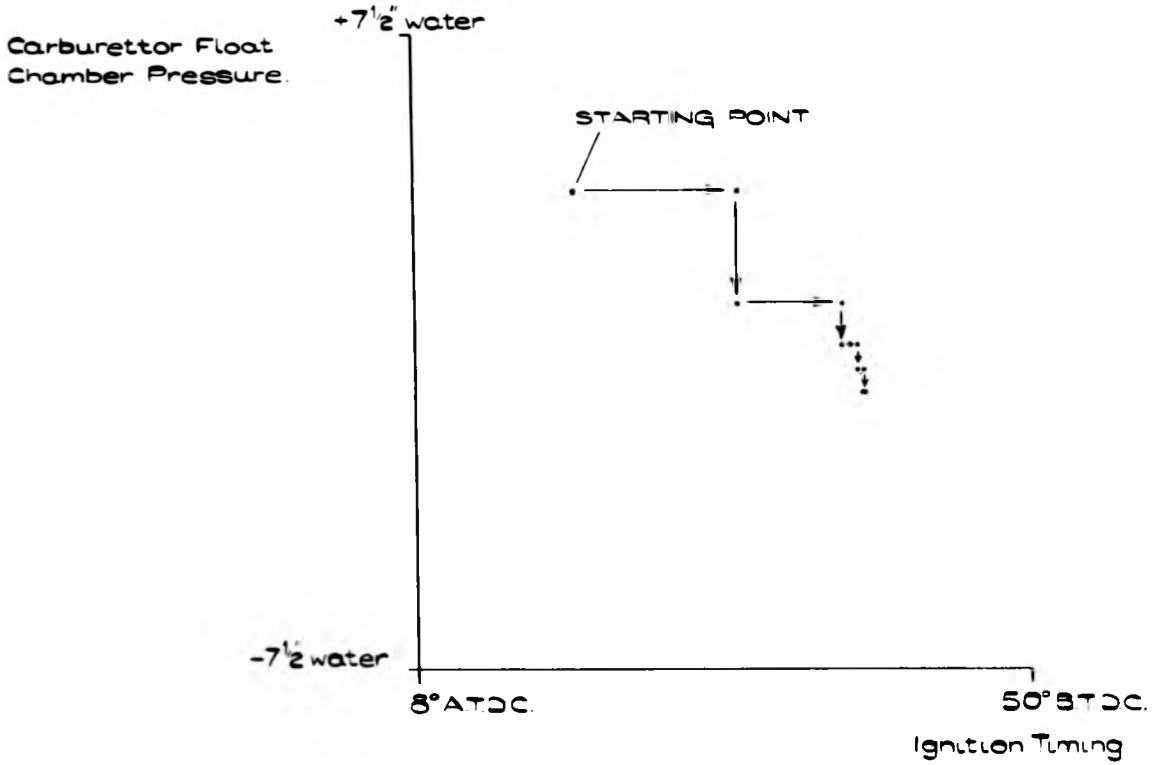

CHAPTER 9.

CONCLUSION.

1. Interfacing and programming.
2. Measurement techniques.
3. Controls and instrumentation.
4. Dynamic load simulation.
5. The future of on-line testing.

1. Interfacing and programming.

In the design of the engine interface of the exploratory test rig it was essential to cater for off-line operation as well as making the instrumentation compatible with the existing interface of the G.E.C. 90/2 computer. Since this interface was constructed interfacing for process control computers has become available with a wider range of capabilities and consequently more scope is offered to the system designer to satisfy the engine interface, data transmission and economic requirements. The interfacing for the exploratory test rig was consequently far from ideal.

It is anticipated that engine test specifications will continue to change and as a result new instrumentation and test programs will always be required. The need for adaptability underlines the basic requirement that programming methods and instrumentation should have sufficient flexibility to enable changes to be made relatively easily. Computer languages must enable the test engineer to communicate his requirements directly to the computer, and to aid the commissioning of new routines manual operation of the test facility must be possible. It is also important that wherever possible the computer should calibrate and check the operation of the interfacing and data transmission.

Programming test routines for the exploratory test facility in the assembly language 'Symbol' proved extremely tedious. Assembly languages for real time applications are not easy to learn and demand of the programmer an intimate knowledge of the workings of the computer interface before any useful results can be achieved.

It was interesting to note that a subroutine block structure for constructing the test programs evolved naturally. Whenever it was found that a new series of instructions were used frequently they were assembled to form a new subroutine block. As the art of programming became more developed the test programs became more a series of

subroutines calls and consequently the programming method began to resemble that of a high level language. This natural evolution of program structure underlines the need for the formal development of such a language.

2. Measurement techniques.

The transfer of data from analog to digital form essentially involves a sampling operation. Sampling rates must be made high enough to prevent frequency aliasing or alternatively the bandwidth of the signal must be reduced before the sampling takes place. Before any measurement procedure which involves analog to digital conversion is adopted a knowledge of the frequency spectrum of the variable to be measured is required.

With the exploratory test rig the choice of sampling frequency was limited by the speed of the analog input multiplexor and the need to maintain a fairly simple program structure. Measurement bandwidths were therefore limited in the cases where the frequency spectrum contained significant components above 5 Hz. Where measurements derived from steady state operation were used to generate output data noise components due to combustion irregularities were attenuated by digital filtering.

3. Controls and instrumentation.

The closed loop speed control system.

The transfer dynamics of the speed control loop were a function of the characteristics of the engine as well as of the dynamometer. It was therefore essential to take into account the dynamics of both in the design of the speed control. This is the price that must be paid for the increased accessibility to the operating range of the engine that is afforded by such a control.

The limitations in performance of the speed control were imposed by the inductance of the dynamometer field windings. To overcome this limitation a field current control amplifier with an excessively large output voltage swing is required. The design of the amplifier for the exploratory system was essentially a compromise, the objective being to provide an adequate output voltage range for steady state operation and for small step changes in speed (i.e. under 500 R.P.M.) The speed control gave very adequate performance, demonstrating that loop gain changes as large as 8 : 1 could be accommodated where the changes in dynamics are not too severe.

Ignition timing control.

Although considerable accuracy of ignition timing was achieved by the digital measurement of engine rotation this measurement proved difficult to make, particularly in the confined space where an engine is tested with the gearbox in situ. Furthermore, the system as used on the exploratory test rig involved unnecessary digital to analog and analog to digital conversions as the computer interface was not equipped with fast digital outputs.

A simpler form of control could be achieved by the provision of a controllable time delay dependent on engine speed. Comparable accuracy over a speed range could be achieved with analog circuits and it would then only be necessary to provide a single transducer to initiate the time delay.

Carburettor float chamber pressure control.

The carburettor float chamber pressure control was itself used as a means of controlling mixture strength. However, with this mode of operation carburettor design data will be presented to the engineer in the form of float chamber pressures relative to jet sizes.

A more useful mode of operation of the control was within a constant fuel flow rate loop. By adjusting the demanded fuel flow rate until the desired operating conditions are achieved design data is made more directly available to the carburettor designed.

The constant fuel flow rate operation was achieved with integral control. There is scope for further investigation of the dynamics of this control loop. The advantages of this mode of operation, made possible by the continuous fuel flow measurement, warrant a more extensive study in order to optimise control system design.

Continuous fuel flow rate measurement.

The hot-film fuel flow rate measurement indicated very large pulsations in the flow rate at a frequency corresponding to that of cylinder firing. These pulsations were present under all operating conditions of the engine and their amplitude was of the order of half the mean flow rate.

The performance of the measurement system was checked under these conditions over the range 0-2 gallons/hour by comparing its time average with a volumetric flow rate measurement. As a result of this comparison it was concluded that the instrument satisfied the manufacturer's claims which specified an accuracy of 2% of full scale or 5% of the reading (whichever is the smaller).

For making measurements under steady state operation gravimetric or volumetric methods appear to be more suitable, since time averaging is inherent and the equipment is more rugged. The expense and sophistication of hot film measurements is only justifyable where a continuous measurement of fuel flow is required, such as for operation with a fuel flow rate control or to study performance under transient conditions.

Throttle control.

The quantisation of the throttle movement proved to be the main disadvantage associated with the stepping motor drive. The effect

A more useful mode of operation of the control was within a constant fuel flow rate loop. By adjusting the demanded fuel flow rate until the desired operating conditions are achieved design data is made more directly available to the carburettor designed.

The constant fuel flow rate operation was achieved with integral control. There is scope for further investigation of the dynamics of this control loop. The advantages of this mode of operation, made possible by the continuous fuel flow measurement, warrant a more extensive study in order to optimise control system design.

Continuous fuel flow rate measurement.

The hot-film fuel flow rate measurement indicated very large pulsations in the flow rate at a frequency corresponding to that of cylinder firing. These pulsations were present under all operating conditions of the engine and their amplitude was of the order of half the mean flow rate.

The performance of the measurement system was checked under these conditions over the range 0-2 gallons/hour by comparing its time average with a volumetric flow rate measurement. As a result of this comparison it was concluded that the instrument satisfied the manufacturer's claims which specified an accuracy of 2% of full scale or 5% of the reading (whichever is the smaller).

For making measurements under steady state operation gravimetric or volumetric methods appear to be more suitable, since time averaging is inherent and the equipment is more rugged. The expense and sophistication of hot film measurements is only justifyable where a continuous measurement of fuel flow is required, such as for operation with a fuel flow rate control or to study performance under transient conditions.

Throttle control.

The quantisation of the throttle movement proved to be the main disadvantage associated with the stepping motor drive. The effect

of quantisation was particularly noticeable at small throttle openings where the gain of the throttle was highest. In a practical engine test facility a motor drive system which is built around the carburettor body is not acceptable. The control system must assume a form such that it can easily be transferred from one carburettor to another.

Torque measurement.

Although the shaft torque measurements provided valuable data for the mathematical modelling study their usefulness in routine testing is considered doubtful in view of the practical difficulties involved. A more reliable and accurate form of torque measurement can be achieved by using a load cell to measure dynamometer reaction. This method also increases the stiffness of the dynamometer reaction support compared with the spring balance method of measurement.

4. Dynamic load simulation.

Vehicle test procedures which involve measuring performance after several thousand miles of road use are not uncommon. They are difficult to execute for the simple reason that there is a severe risk that the vehicle will be irreparably damaged before the requisite number of miles have been covered. It is also easier to apply sophisticated instrumentation to an engine on a test bed than to a vehicle on a chassis dynamometer. There is a need therefore to simulate vehicle loads on a test bed. For the loading to be representative the loading system must exhibit the appropriate inertia and dissipative characteristics.

Inertial characteristics can be achieved by analog simulation or simply by the use of a rotating mass. The former is more complex to apply since the loading device must be capable of regeneration, but changes in inertia can be made relatively easily and quickly. The use of a rotating mass offers a simpler solution since it then

is only necessary for the load to be a function of speed. Regeneration is still required to simulate over-run conditions. Where inertia is simulated load torque will necessarily be a function of both speed and its derivative. The simulating control loop should in both cases derive its torque measurement from the coupling shaft, but shaft torque measurement can be avoided if sufficient compliance is built into the dynamometer reaction supports.

5. The future of on-line testing.

On-line computer control of engine testing has shown itself to be a particularly powerful means of aiding the task of the development engineer by performing calculations, and by executing supervisory and decision making processes. The importance of providing the engineer with test data in the most easily assimilated form immediately the test is complete cannot be over-emphasised. The computer has the inherent capability of doing just this.

The majority of the author's time during the research project was spent on the design, development and construction of interfacing for the engine. The resulting interfacing was far from ideal in its mode of operation or comprehensive in its coverage. Experience has shown the simplest approaches to instrumentation to be the most effective even if their use involves some loss of time during tests. It is felt that this is the area where most of the research effort is still required.

REFERENCES.

1. 'Dynamometer testing under computer control.'
L.S.Leonard and F.E.LaVerghetta. S.A.E. paper No. 680131.

2. 'Two applications of an on-line data acquisition and reduction system.'
The International Harvester Co. S.A.E. paper No. 690498.

3. 'Test bed automation in the United Kingdom.'
Ricardo and Co. U.K. Ministry of Technology. July 1969.

4. 'Dynamometer endurance tests for petrol engines.'
B.L.M.C. (Austin-Morris) test specification No. 14.

5. 'Dynamic transfer characteristics of reciprocating engines.'
D.E.Downs. Bath University of Technology School of Engineering internal report No. 127. July 1968.

6. 'Correlation analysis of process dynamics using pseudo-random binary test perturbations.'
P.A.N.Briggs, P.H.Hammond, M.T.G.Hughes, G.O.Plumb.
Proc. Inst. Mech. Engrs. 1964-65. 179 pt 3H.

7. 'Automatic feedback control system synthesis.' p 395.
J.G.Truxal. McGraw-Hill.

8. 'A digital transfer function analyser based on pulse rate techniques.'
C.S.Elsden and A.J.Ley. Automatica. Vol. 5. No. 1. January 1969.

9. 'The theory and design of eddy-current slip couplings.'
W.J.Gibbs. Beama Journal. 1946. pp 123-28, 172-77, 219-25.

10. 'Limiting in feedback control systems.'
R.J.Kochenburger. Trans. A.I.E.E. Pt 11 Vol. 72 (1953)
pp 180 - 192.

11. 'Principles of optimalising systems and an application to an internal combustion engine.'
C.S.Draper and L.T.Li. A.S.M.E. publication 1967.

12. 'Adaptive control for prime movers.'
P.H.Schweitzer and C.Volz. A.S.M.E. publication 1967.

APPENDIX.

Papers to which the author has contributed whilst registered for a higher degree at the University of Warwick.

'Mathematical Model of an Internal Combustion Engine and Dynamometer Test Rig.'
J.Monk and J.Comfort. Journal of the Institute of Measurement and Control. Volume 3. Number 6. June 1970.

'The Fundamentals of Electrohydraulic Servo-controlled Fatigue Test Rig Design.'
R.C.Fisher and J.V.Comfort. Instrument Practice. Volume 24. Number 6. June and July 1970.

'The application of on-line optimisation to spark ignition engine development.'
J.V.Comfort. Paper presented at a conference on 'Optimisation Techniques in Circuit and Control Applications' organised by the Institution of Electrical Engineers. 29-30 June 1970.

Mathematical Model of an Internal Combustion Engine and Dynamometer Test Rig

*J. Monk and J. Comfort

An electrical circuit model and an analog computer simulation have been developed to represent the dynamic behaviour of an IC engine and eddy current dynamometer system. Various refinements to the model are introduced and its performance is compared with that of the real system using pseudo-random binary sequence and sinewave testing techniques. A brief description of the necessary instrumentation and interfacing is included.

1. INTRODUCTION AND AIMS

The model was developed to clarify, and suggest solutions to the control problems that exist with IC engine/dynamometer test rigs. The overall aim was to promote an increase in the efficiency of IC engine performance evaluation. The model is developed in terms of a lumped electrical circuit analogy. This is an established and convenient form for representing the interconnections between the various physical components of the system. In order to carry out control studies a linearised version of the model has been programmed for simulation on an analog computer. An essential part of the study has been to compare the theoretical results from the model with those obtained from the test rig itself. This is carried out using pseudo-random binary sequence, step, and sinewave testing techniques. In order to carry out measurements and interface the test rig with a digital computer, a digital transfer function analyser and controllers, it has been necessary to develop instrumentation and control systems. These are briefly described.

2. PLANT AND INSTRUMENTATION

The engine is a 1725 cc petrol engine representative of the type currently used to power medium-sized passenger cars. The engine is coupled to an eddy current dynamometer with power dissipation capabilities which comfortably exceed the output of the engine. The power absorption is controlled by adjusting the field excitation current. Energy absorbed is converted into heat in the dynamometer casing which is cooled by a constant stream of water, delivered under pressure from a pump. The dynamometer casing is free to swing in trunion bearings and is fitted with weighing gear as a means of measuring the torque supplied to it. Because of its mode of operation the dynamometer is not capable of supplying power to the engine under steady state conditions.

Heat is removed from the dynamometer cooling water circuit, the engine cooling water circuit, and the lubricating oil by heat exchangers. Safety circuits shut down the plant and turn off the engine ignition in the event of a dynamometer cooling water or lubrication failure, or in the event of a mains power failure.

The instrumentation of the engine test rig has been designed to be compatible with the voltage range of the digital computer interface.

Integrated circuit operational amplifiers, around which much of the instrumentation is based, work linearly over this voltage range.

The carburettor is equipped with a feedback angular position controller to actuate the throttle. The throttle is moved by a directly connected stepping motor and the throttle opening angle is measured by a directly connected potentiometer. For small amplitude sinusoidal inputs up to 5 per cent. of fsd, the servo has a flat response up to 15 Hz.

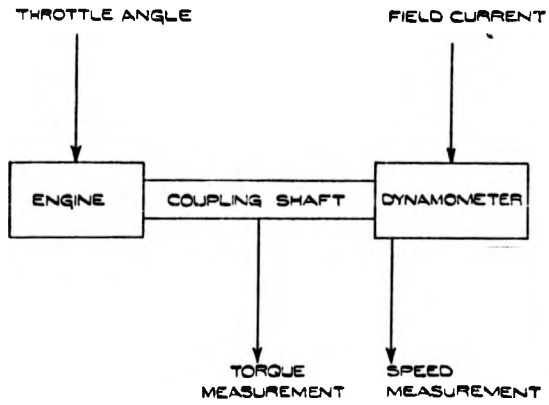

Fig. 1 Block diagram of the plant.

A feedback controller controls the dynamometer field current. Small signal step changes in demanded field current give rise to actual changes with a rise time of 4 ms.

The torsional strain in the coupling shaft between the engine and dynamometer is measured with resistance strain gauges. These are connected in a bridge configuration. The change in resistance of the gauges modulates the frequency of an oscillator, which is located on the coupling shaft. The output of the oscillator and power supplies are fed through slip-rings. The frequency output is demodulated and converted into an analog voltage signal.

Dynamometer speed is measured by an ac tachometer. The output of the tachometer is rectified, smoothed and appropriately scaled in a buffer circuit.

Engine cooling water and lubricant temperatures are measured by thermistor probes, and are under electronic closed loop control.

A block diagram of the system showing the positions of inputs and outputs is given in Figure 1.

3. THE PLANT MODEL

The basis of the electro-mechanical analogy used in the plant model is the formal similarity of the mathematical equations describing the properties of the two physically diverse systems The analogy is defined in Table 1. It will be appreciated that the choice of current to represent torque and voltage to represent angular velocity is arbitrary, and could equally well have been reversed, in which case an inductance would be used to represent a moment of inertia and a capacitance flexibility.[1]

The model is developed initially to represent the system under steady state conditions about a chosen operating point in the middle of the torque and speed ranges. To extend the model so that it will represent the system under dynamic conditions at this point the energy storage elements and time delays are added. Their interactions and magnitudes are evaluated by structural

*School of Engineering Science, The University of Warwick.

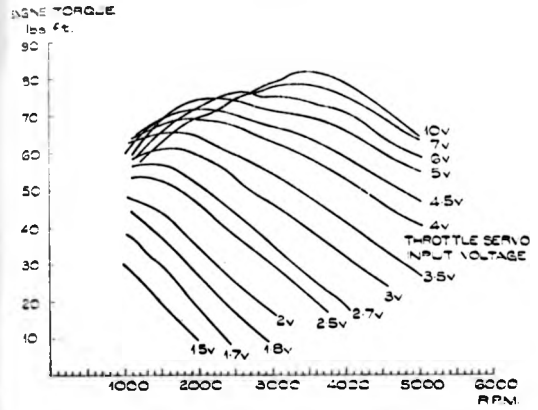

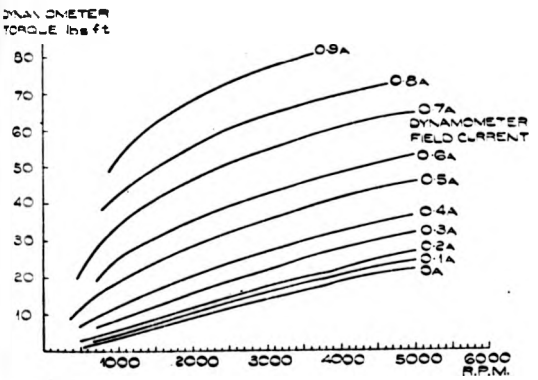

Fig. 2 Engine and dynamometer torque-speed characteristics.

considerations and dynamics measurements.

The engine torque/speed curves for the full range of throttle servo inputs are given in Figure 2. Difficulties were encountered in obtaining the curves in the low speed and high torque regime due to unstable operation. The curves in this regime were obtained using a proportional speed control which acted upon the dynamometer field current. The engine is represented by a voltage source, V_E with internal resistance, R_E, shown in Figure 3a. The slope of the torque/speed curves remains substantially constant for the full range of throttle settings. V_E is given by the intercept of the tangent to the torque/speed curve with the speed axis. The slope of this tangent equals $-1/R_E$. The model structure is valid throughout the torque/speed range of the engine. At low speeds with large throttle openings the slope of the characteristic changes sign. Under these conditions R_E becomes negative. V_E is a function of throttle opening, which is governed by the input voltage to the throttle servo V_T.

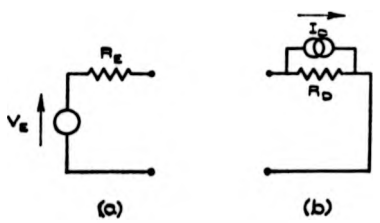

Fig. 3 (a) Engine steady state model.
(b) Dynamometer steady state model.

TABLE 1

Definition of the analogy.

Mechanical Quantity	*Electrical Quantity*	*Mechanical Units*	*Electrical Units*
Torque	Current	Poundal Feet	Amps
Angular Velocity	Voltage	Radians/Second	Volts
Inertia	Capacitance	lbm.ft²	Farads
Viscous Damping	Resistance	Rads/sec.ft.pdl.	Ohms
Compliance	Inductance	Rads/pdl.ft.	Henrys

The relationship between V_T and V_E is shown in Figure 4. If the low speed high torque regime is excluded the relationship between V_T and V_E is substantially linear.

The dynamometer torque/speed curves are given in Figure 2. The small signal model for the dynamometer is given by a resistance R_D in parallel with a current generator I_D, and is given in Figure 3b. The values are obtained in a similar manner to those for the engine. The small signal effect of a change in field current I_F is to change the value of I_D. For larger signals it is not possible to make the assumption that R_F is constant and I_D is linearly related to field current.

In the analogy the coupling shaft is represented by a short-circuit coupling, as no velocity difference exists across it in the steady state.

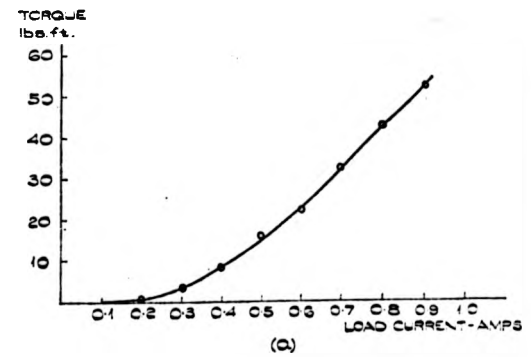

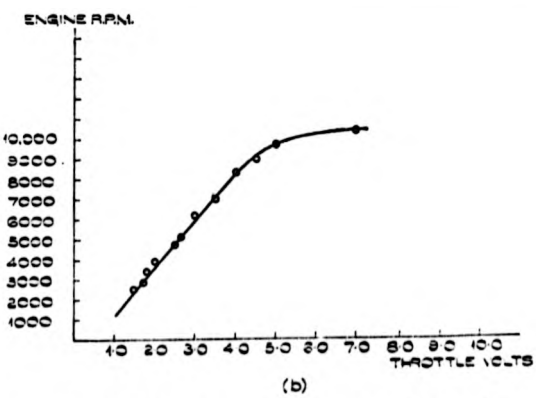

Fig. 4 Throttle and dynamometer steady state transfer characteristics.

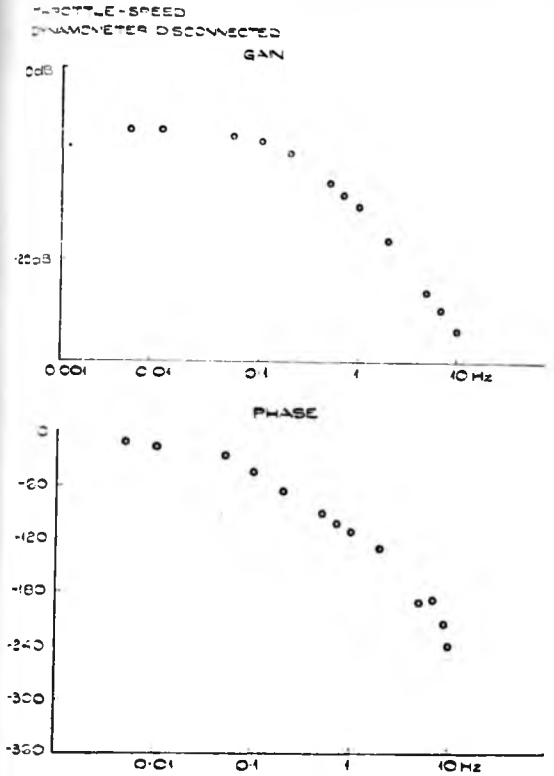

Fig. 5 Throttle-Speed frequency response of the engine.

Extension to the model to include dynamics

A consideration of the detailed structure of the engine would lead to a model including energy dissipation elements due to service, pumping thermodynamic and mechanical losses, energy storage elements due to the various reciprocating and rotating parts which would all contribute to the dynamic behaviour. (Service losses are those due to such items as the dynamo and cooling fan drive.) Because of this, the most significant dynamics of the engine were revealed by experimental investigation. This was carried out by decoupling the engine flywheel from the shaft connecting it to the dynamometer and obtaining a series of transfer functions between input voltage to the throttle servo and engine speed. The transfer functions were measured over a range of mean speeds using a digital transfer function analyser, a typical result is shown in Figure 5. Examination of the amplitude plots of the transfer function revealed the dynamics of a first order system. The phase plots correspond to a first order system with a time delay. The time delay was found to be proportional to the inverse of engine speed and is given by (104/engine speed in rpm) seconds. This would be accounted for by the average time taken to inhale and ignite a charge. The capacitor C_E is introduced into the model to represent the lumped inertia of the engine. Its value is derived from the engine source resistance R_E

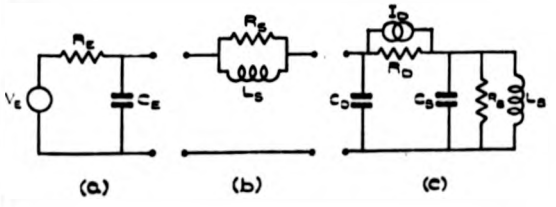

Fig. 6 (a) Engine dynamic model.
(b) Shaft dynamic model.
(c) Dynamometer dynamic model.

TABLE 2

Numerical values for the electrical analogy.

1 volt = 52.4 rads s (10 v = 5000 rpm)

1 amp = 322 pdl ft (10 v = 100 lbf ft)

R_E	1.19 Ω
C_E	0.447 F
L_S	5.32×10^{-4} H
R_S	0.455 Ω
C_D	1.38 F
R_D	3.00 Ω
C_B	7.57×10^{3} F

and the time constant of the first order system. The dynamic model of the engine is given in Figure 6a.

Examination of the mechanical structure of the dynamometer reveals a large rotor inertia. Energy absorption is carried out between the rotor and the outer casing. The rotor inertia giving the value of C_D, was evaluated by carrying out simple mechanical tests. The outer casing of the dynamometer is connected to the weighing gear through a lever arm. The weighing gear is comprised of a spring and dashpot system, connected at one end to the inertial frame of reference and at the other to the lever system. The component values associated with the dynamometer outer casing and weighing gear were evaluated from physical measurement of the spring and lever arm and a step response of the system. Hence C_B, R_B and L_B were determined. The dynamic model of the dynamometer is given in Figure 6c.

To complete the model the connecting shaft is represented by an inductor in parallel with a resistor, since it behaves like a torsional spring with internal damping. The shaft stiffness was measured physically, and the internal damping was derived from inspection of the transient response of the anchored shaft attached to the dynamometer rotor. The model of the shaft is shown in Figure 6b. Table 2 assigns the equivalent electrical values to the model.

4. EXPERIMENTAL VERIFICATION OF THE MODEL

To reduce the order of the model and simplify the problem of comparing the model with the plant the dynamometer casing was clamped to the inertial frame of reference. This operation also permits the design of closed loop torque and speed control systems with a marginally greater bandwidth than would be otherwise possible. This simplified form of the model is given in Figure 7.

The initial verification of the model was carried out using sine-wave testing techniques. Subsequently on-line identification techniques using pseudo-random binary sequences (PRBS) were employed. Finally step responses for the plant were compared with those obtained from the analog computer model.

The measured variables available were dynamometer speed, V_D, and shaft torque, I_S, and the input variables were the voltages applied to the throttle servo, V_T, and the dynamometer field current controller, V_L. Four transfer functions would therefore define the small signal dynamic performance. An ALGOL 60 program was written to calculate the theoretical frequency responses for the model, and these are compared with those obtained with the digital transfer function analyser (TFA)[2] in

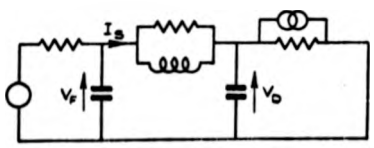

Fig. 7 Simplified dynamic model of the rig.

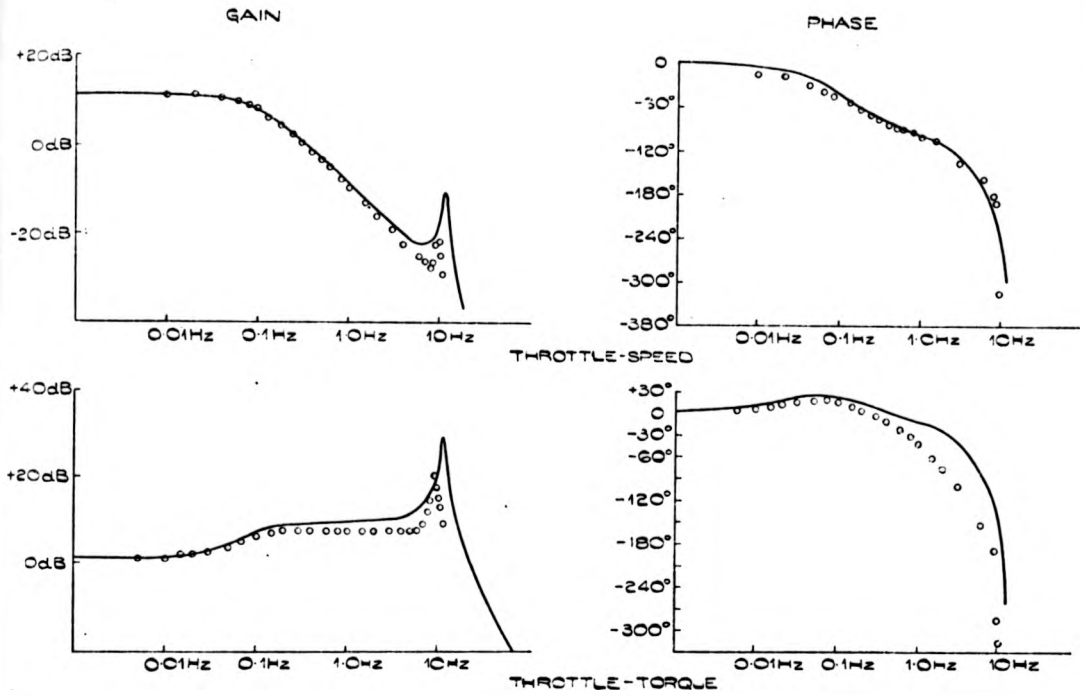

Fig. 8 Frequency response of torque and speed to throttle perturbations. Solid line shows the computed results.

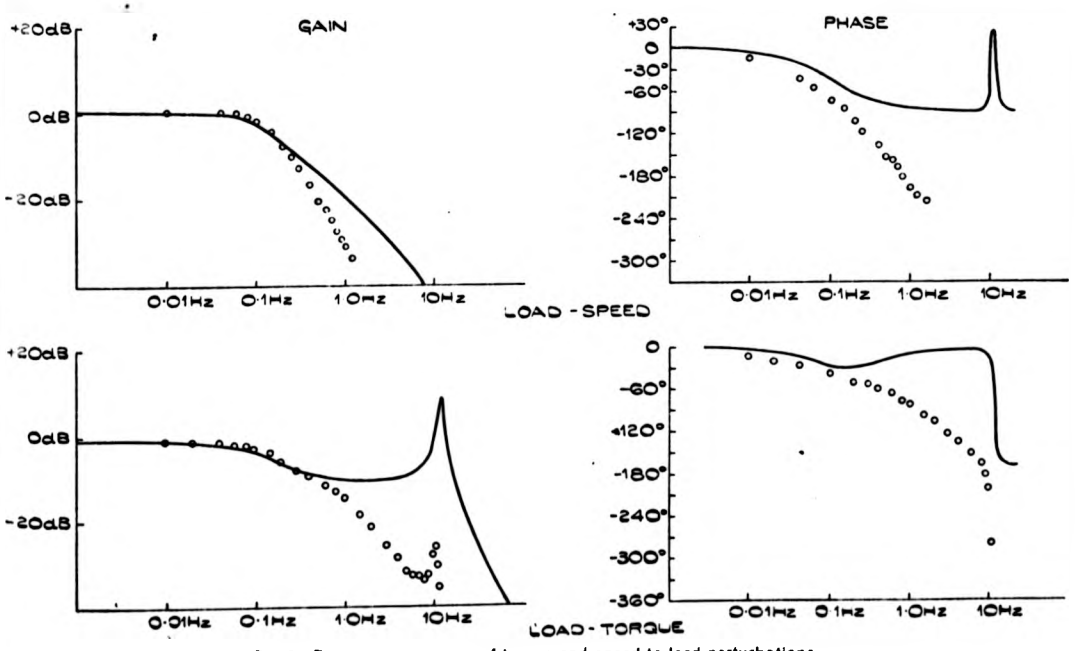

Fig. 9 Frequency response of torque and speed to load perturbations.

Figures 8 and 9. Measurements over the range 0.001 to 15 Hz were taken with the TFA. In this range the experimental and theoretical transfer functions between the throttle servo input and dynamometer speed and shaft torque show favourable agreement. However the responses of shaft torque and dynamometer speed to inputs to the dynamometer field current control show poor agreement. These responses are compared in Figure 9. It was suggested that the extra attenuation at high frequencies of the plant was due to the flux build-up associated with the dynamometer casing and rotor. To investigate this, the frequency response between the field current control input voltage and flux was examined using a search coil. This response is given in

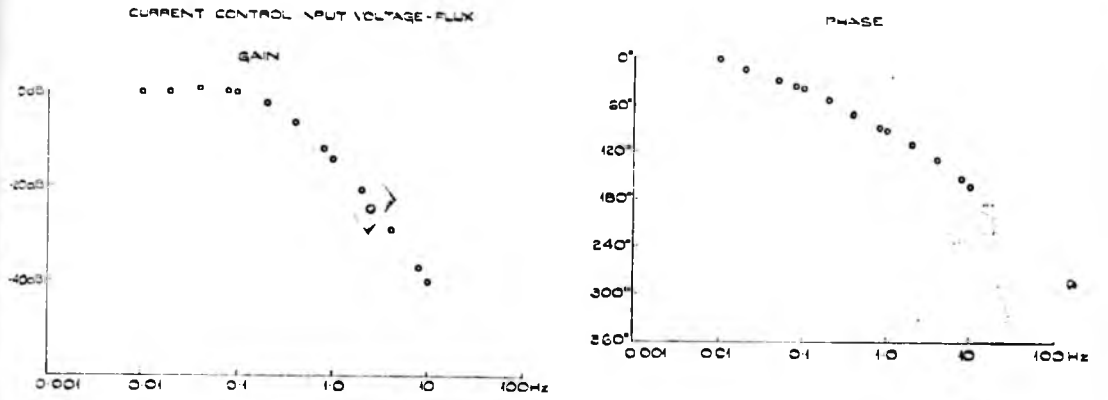

Fig. 10 Frequency response of flux in the dynamometer to field current perturbations.

Figure 10. The experimental result has been modified to remove the differentiating action of the search coil. From examination of this response it was deduced that the flux build up contributed two cascaded first order lags. The revised model including these lags is shown in Figure 11. The revised frequency responses of shaft torque and dynamometer speed to the input to the dynamometer field current control showed considerably better agreement. These are shown in Figure 12.

A now established method of system identification using PRBS[3] was examined as a comparison with sine wave testing. The advantages of using non-sinusoidal perturbations is that many frequencies can be excited simultaneously. A PRBS has the further advantage that its power is spread evenly over the lower harmonics of the spectrum. The test rig was operated on-line by a digital computer, all measurements being available to the computer on analog inputs. Correlation methods using PRBS, which are particularly suited to digital computers, were used to evaluate the impulse responses of the system. To ensure a flat power spectrum over the frequency range of interest the PRBS bit rate was made twice the highest frequency concerned with in the identification. The slowest time constant to be identified defines the period of the sequence. A bit frequency of 25 Hz and a period of 150 s would be required to cover the range of engine time constants. The nearest available sequence to fit this specification has 4095 bits and with a period of 150 s the harmonics are spread every 0.0066 Hz. This would give excellent frequency resolution but requires excessive computer time and space for computation of all the shifts necessary to describe the system. To avoid this, high, low and mid frequency experiments were carried out. In the lower and mid-frequency experiments high

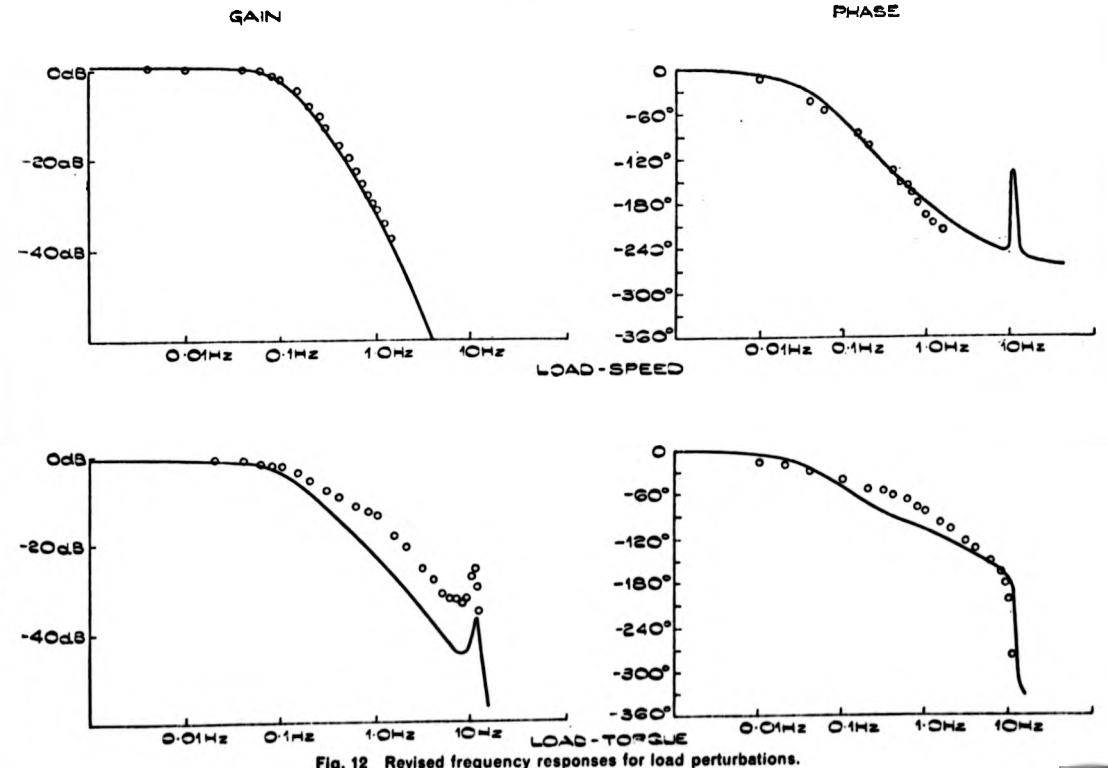

Fig. 12 Revised frequency responses for load perturbations.

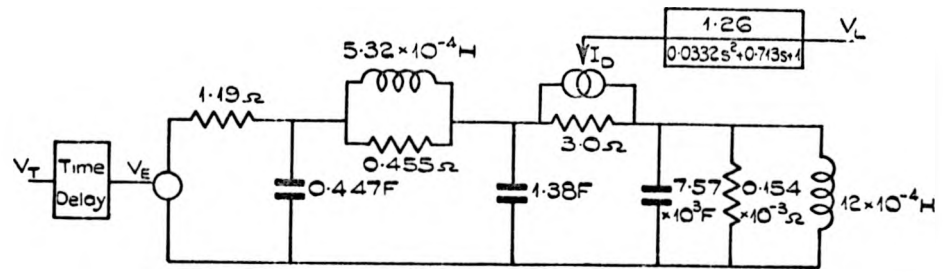

Fig. 11 Revised dynamic model.

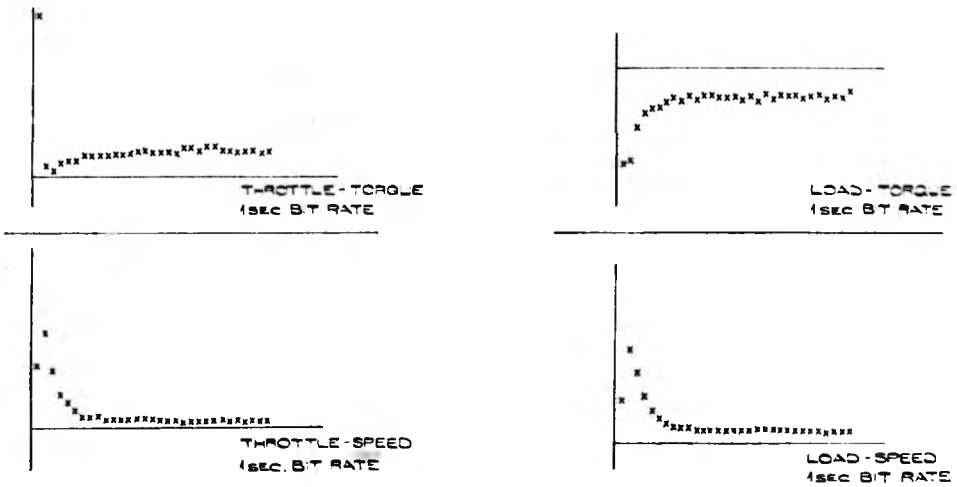

Fig. 13 Estimates of impulse response obtained using PRBS and correlation techniques.

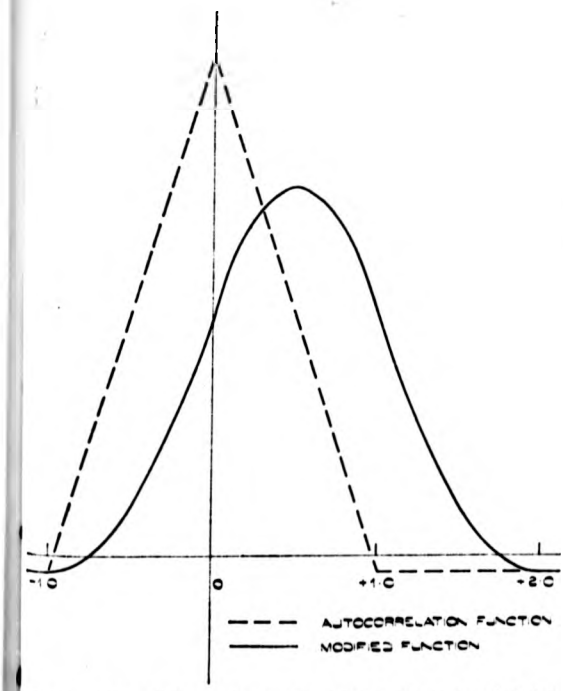

Fig. 14 Effect of the running average filter on the auto-correlation function of the PRBS.

frequencies were excluded with a digital filter. A 31 bit sequence was used for perturbation at three different clock rates. For the high and mid frequency experiments identification of the lower frequencies was avoided since no components of the perturbations exist at frequencies below the fundamental. The bit rates for the three experiments were 10 s, 1 s and 1/25th s. With a 31 bit sequence this leads to different fundamental frequencies and different harmonic spacings, so that in the fastest sequence frequency resolution is in steps of 0.806 Hz. This is marginally satisfactory for identification of the system resonance which has a bandwidth of the same order.

Impulse responses obtained from PRBS perturbations are shown in Figure 13. The effect of the filter used to attenuate the high frequencies can be taken into account by assuming a modified autocorrelation function of the PRBS[4]. For the running average filter used the effect on the autocorrelation function is shown in Figure 14. The impulse responses obtained from the high frequency perturbations were noisy. For all responses except that from the throttle servo input to torque the plant heavily attenuates high frequencies and the swamping of signals by noise makes identification at these frequencies difficult. The throttle servo suffers from velocity limiting when following a two level signal. This has the same effect as operating on the throttle input signal with a running average filter. With the velocity limit and the PRBS amplitudes involved significant attenuation occurred at 8 Hz and above, due to the sharp cut-off of the running averager frequency characteristic. An improved result for the impulse response of shaft torque to throttle perturbations was obtained by perturbing the ignition advance in place of the throttle angle. The results are shown in Figure 15.

Step responses for the plant and analog computer model are shown in Figure 16. The throttle velocity limit will significantly affect the high frequency components of a large step input, therefore it is difficult to identify the high frequency performance of the rig from these responses.

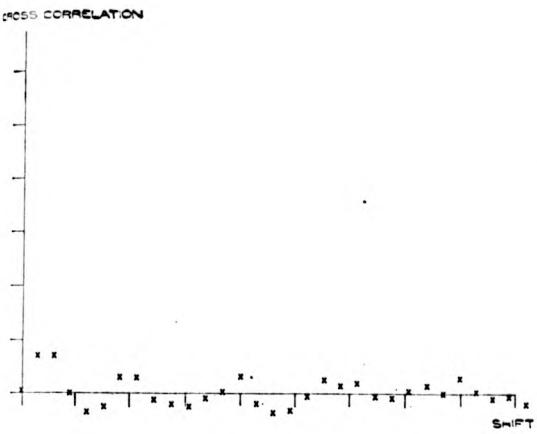

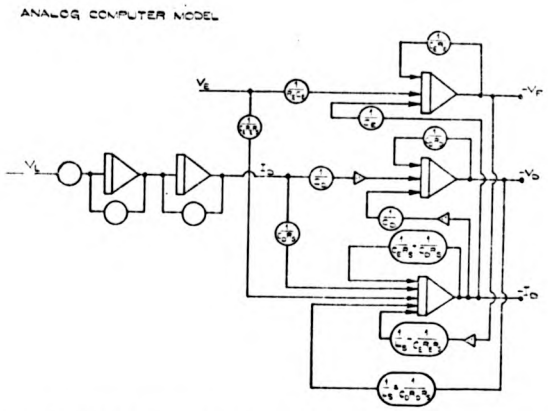

Fig. 15 (Left) Estimate of impulse response from ignition advance setting to torque using PRBS.

Fig. 17 (Above) Interconnections for the analog computer simulation.

Dynamic equations and analog computer simulation

The three state variables chosen for the electromechanical model were the engine speed V_F the dynamometer speed V_D, and the shaft torque I_S.

The state space matrix equations for the system, assuming linear operation are:

$$\begin{bmatrix} (d/dt)V_F \\ (d/dt)V_D \\ (d/dt)I_S \end{bmatrix} = \begin{bmatrix} -1/C_E R_E & 0 & -1/C_E \\ 0 & -1/C_D R_D & 1/C_D \\ (1/L_S - 1/C_E R_E R_S)(1/C_D R_D R_S - 1/L_S)(1/C_E R_S - 1/C_D R_S) \end{bmatrix} \begin{bmatrix} V_F \\ V_D \\ I_S \end{bmatrix} + \begin{bmatrix} 1/R_E C_E & 0 \\ 0 & -1/C_D \\ 1/C_E R_E R_S & 1/C_D R_S \end{bmatrix} \begin{bmatrix} V_E \\ I_D \end{bmatrix}$$

Where $V_E = 4.86\ V_T$

and $0.0332\ d^2/dt^2(I_D) + 0.713\ d/dt(I_D) + I_D = 1.26\ V_L$

V_T = throttle servo input voltage

V_E = engine source voltage

V_L = load current amplifier input voltage

I_D = dynamometer source current

The analog computer diagram for the above equations is given in Figure 17.

5. CONCLUSIONS

The frequency responses of the model and rig show good

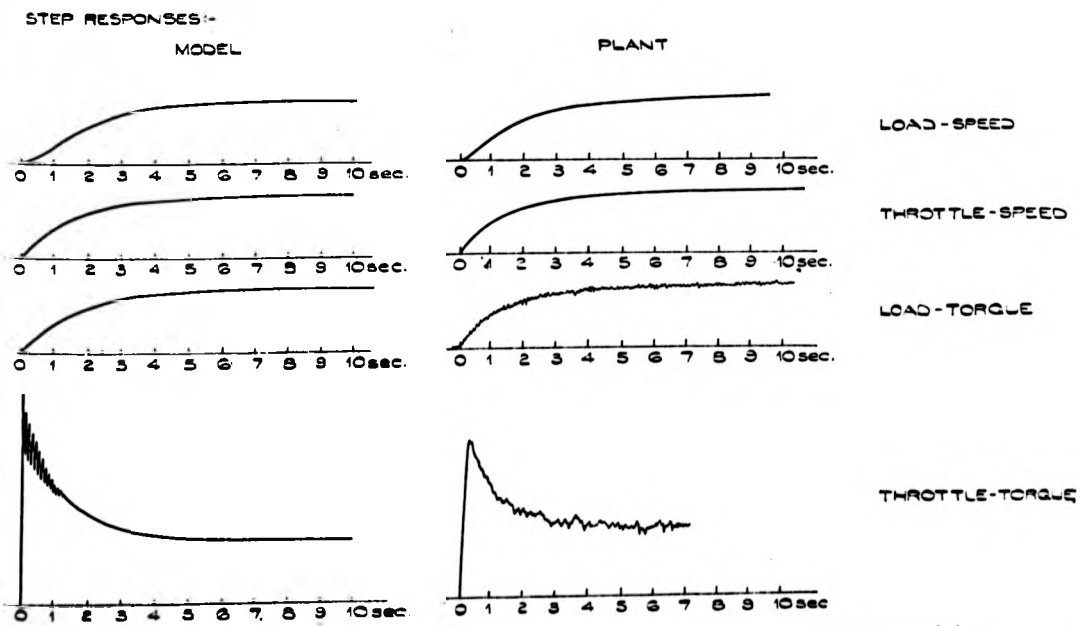

Fig. 16 Step responses obtained from the rig compared with the responses of the analog computer simulation.

agreement over the frequency range 0.001 to 10 Hz. The model can be used in transfer function or state space form for control system design. The analog computer model has already proved useful in the evaluation of control schemes; control performance can be studied without the risk of damage to the rig by over speeding.

With the rig, sinewave testing did not prove unduly time consuming, since the system time constants are moderately short Special equipment, in the form of a digital transfer function analyser, was required in order to derive the results quickly. Step responses gave rapid results when examining the slowest system time constants with a minimum of *a priori* knowledge. Without the knowledge of the time constants involved gained from the sinewave testing the design of experiments using PRBS perturbations for dynamic system identification proved most difficult. The velocity limiting of the throttle servo rendered identification of the high frequency response of the plant difficult when using PRBS and step perturbations.

The slope of the torque/speed characteristics of the engine alter significantly in certain regimes of operation. For the model to be representative its parameters should also be changed. In particular R_E, the equivalent source resistance of the engine becomes negative in the high torque and low speed regime. Under some operating conditions the other energy absorption elements in the model fail to swamp this, and the system becomes unstable causing the engine to stall. The use of a feedback speed control operating on dyamometer field current stabilised the operation of the rig which allowed the plotting of torque/speed curves in this regime.

The resonance associated with the rig has been found to impose limits on the performance of control and optimising systems associated with the rig.

FURTHER WORK

The analog computer is to be extended to simulate as far as possible the non-linearities of the system.

Computer programs have been developed to evaluate the noise spectra of the rig output. It is intended to use these to improve the accuracy of the PRBS and step responses, using a generalised least squares technique.

To alleviate the problems associated with the coupling shaft it is intended to replace this with a type incorporating universal joints with a greater compliance. In this way it is hoped to extend the useful frequency range of torque measurements.

ACKNOWLEDGEMENTS

The authors wish to acknowledge the support and advice given to them by Rootes Ltd., the Thornton research centre of Shell Research Ltd., Mr. D. Hurtley, Professor J. L. Douce and Dr. M. T. G. Hughes.

REFERENCES

1. Truxall, J. G., 'Automatic feedback control system synthesis'. McGraw-Hill.
2. Elsden, C. S., and Ley, A. J., 'A digital transfer function analyser based on pulse rate techniques'. *Automatica*, 1, 5, January, 1969.
3. Briggs, P. A. N., Hammond, P. H., Hughes, M. T. G., and Plumb, G. O., 'Correlation analysis of process dynamics using pseudo-random binary test perturbations'. Proc Inst. Mech Engrs. 1964–65. 179 Pt. 3H.
4. Godfrey, K. R., and Murgatroyd, Prof. W., 'Input-transducer errors in binary cross-correlation experiments'. Proc. IEE, 3, 112, March 1965.

The Fundamentals of Electrohydraulic Servo-controlled Fatigue Test Rig Design—Part 1

By **B. C. FISHER**, *Senior Research Associate, and*
J. V. COMFORT, *Research Graduate, School of Engineering Science, University of Warwick.*

THE DEVELOPMENT of the electrohydraulic servo system was stimulated by the demands of the aerospace industry to solve control problems such as those presented by radar antenna drives and rocket steering systems. Low power level electrical signals are processed electronically to control high power, rapid response hydraulic equipment. The component which is vital to the closed loop chain is the servo valve, which transforms the electrical control signal into an hydraulic flow. Over the past few years the difficulties associated with the production of these valves have been overcome and the electronic techniques associated with closing the loop have been understood. This, backed by the flexibility of control offered by electrohydraulic servo systems has brought their use to other fields. Commercial electrohydraulic fatigue testing equipment has been available for several years for mechanical testing. The capabilities of this type of equipment have been outlined in Ref. 1.

The design and performance of an electrohydraulic servo-controlled fatigue test rig can be established from certain basic mechanical, electronic and control engineering principles without resorting to complex mathematics. The control system can be designed to allow for a considerable variety of test rig/component layouts. Frequency responses flat from d.c. to about 25Hz are not uncommon.

The loop transfer function is the combined effect of the individual transfer functions of the mechanical and electrical components within the loop. The system design is simplified if these components have flat frequency responses and do not introduce significant phase lags within the frequency range mentioned. When this is the case, loop design and closed loop performance evaluation is relatively simple. Where significant phase lags do occur, the closed loop response can often be improved by closed loop transfer function measurement, which is used for the design of phase lead networks.

An extensive treatment of the analysis and design of hydraulic servo systems is given in Ref. 2, while the subject is treated more generally in Ref. 3. The basic electrohydraulic servo loop with component force as the controlled parameter is shown in Fig. 1.

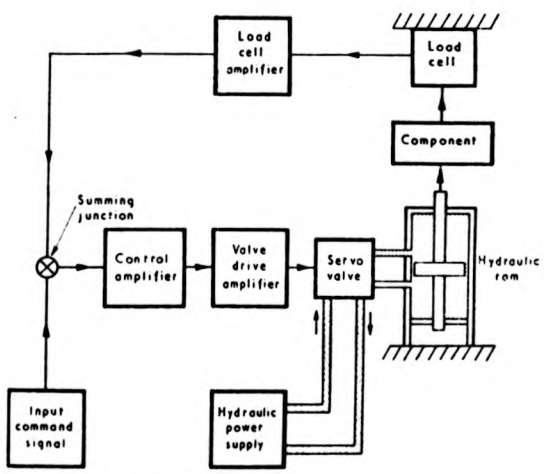

Fig. 1. Basic electrohydraulic servo loop

Hydraulic Circuit Considerations

By far the largest number of hydraulic power supply units in electrohydraulic servo systems maintain a fixed pressure level regardless of the flow demand placed upon the supply by the load. Constant pressure supply units have the advantage that several loads can be paralleled from one supply unit, and they afford more linear characteristics from the servo valve. Self-contained hydraulic power packs can be bought from hydraulic equipment manufacturers complete with accumulators, microfilters, pressure relief valves, dump valves, *etc.*, and fail-safe systems which cut out with excessive variations in oil temperature, level and pressure.

Most systems operate with 3000lbf/in^2 supply pressure.

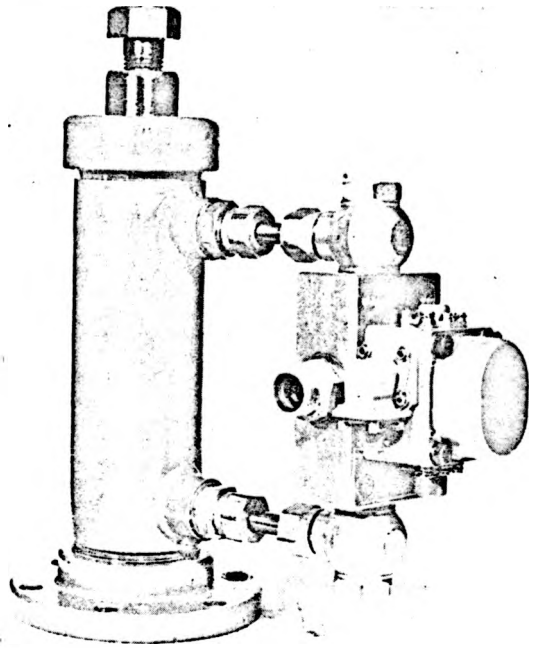

Fig. 2. Hydraulic ram and servo valve 2in dia. ram. Moog Series 21 servo valve. (Courtesy Keelavite Hydraulics Ltd., Dowty Hydraulic Units Ltd.)

The maximum required delivery is dictated by the flow capacity of the servo valve. The power pack, servo valve and hydraulic ram should be compatible with the same hydraulic oil and supply pressure. The ram can be subjected to full supply pressure during slow cycling and static operation because then there is little pressure drop through the servo valve.

Oil system cleanliness is of utmost importance. The servo valve is most susceptible to particle contamination because of the small clearances between the spool and sleeve[4]. The chosen servo valve will dictate the system filtration level, usually of the order of 10μ. A recommended practice is to install a filter in the pressure line, as near to the servo valve as practicable, in addition to that on the power pack, because particle contamination can originate in high pressure lines between the pump and servo valve.

Standard hydraulic pressure tube and couplings can be used to connect a servo valve mounting block to the ram, and the servo valve is then easily bolted to the mounting block, (Fig. 2). Alternatively, some ram bodies are drilled to provide fluid galleries which terminate in ports at a machined face and which mate with similar ports on the servo valve manifold. The ram/servo valve assembly is then connected to the power pack with standard flexible, hydraulic pressure hose and couplings to complete the hydraulic circuit.

Any disconnexions in the hydraulic circuit should be followed by a thorough circuit flushing. This involves replacing the servo valve with a flushing block and running at reduced pressure for about one hour to ensure that any particle contaminants are filtered from the oil supply.

Servo Valves

There are many types of servo valve and an extensive review has been made by Kinney and Weiss[5]. The criteria which determine the performance specification of a servo valve are given in Ref. 6.

The basic servo valve is one in which the output flow to a constant load is proportional to the electrical input current. The most common arrangement consists of a low power electrical motor with two windings, known as the valve coils, and two stages of hydraulic power amplification, (Fig. 3). A signal applied to the motor deflects the flapper to provide a pressure difference proportional to the input signal which controls the second stage, consisting of a spool-sleeve assembly. A large group of valves use this principle. Valve weights are about 1lb and their flow capacities vary between 2 and 60in³/s for 3000 to 4000lbf/in² supplies, with internal leakage flows from 0·25 to 1·5in³/s. Electrical input powers are of the order 0·05 to 0·2W and 90° phase shift frequencies 100 to 200Hz. The servo valve and ram together form an integrating component and cannot be used in an open loop without null shift. In fatigue testing it is usual to use this type of valve in a closed loop with component force feedback.

The required valve flow capacity can be determined from the maximum values of test frequency, ram displacement and net ram piston area. Reference 7 gives the necessary guide lines to be followed for the servo valve/hydraulic ram specification, but note that flows are expressed in U.S. gallons. Errors introduced by the servo valve dead zone, hysteresis, null-shift and resolution characteristics are not usually significant in the overall system accuracy. However, the valve flow capacity should not be excessively greater than the maximum required flow since these errors will be roughly proportional to the valve flow capacity.

The next step is to establish the approximate dynamic response for the servo valve from the manufacturer's data. The frequency response between output flow at zero load pressure and a sinusoidally varying input current can be approximately described by a first order transfer function for the limited frequency range given by:

$$G_v(s) = \frac{K_v}{1 + sT}$$

T = servo valve time constant: dictates the valve dynamics and is largely determined by valve flow capacity (seconds).

K_v = servo valve static flow gain; determined from valve rated flow and input current (in³/s/mA).

s = Laplace operator.

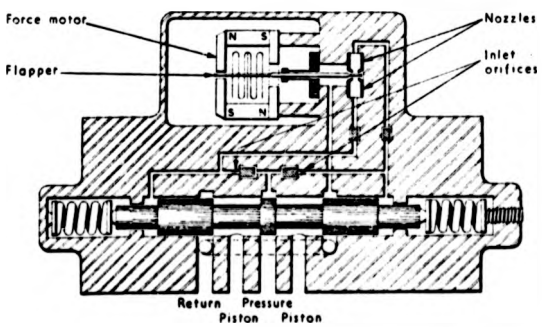

Fig. 3. Two-stage electrohydraulic flow control servo valve. (Courtesy of Moog Servo Controls Inc.)

This approximation holds providing the resonant frequency of the valve load combination (*i.e.* oil compressibility and damping, and load mass and stiffness) is high. A dominant non-linearity in the system will be the force rate of change limit (or velocity limit) introduced at maximum valve flow. This non-linearity will be amplitude and frequency dependent and will produce behaviour substantially like a first order system. Correct specification of the servo valve flow capacity avoids introducing this non-linearity within the test frequency range. Thus, for the initial design in the frequency range of interest here, $G_v(s)$ can be considered frequency independent, and:

$$G_v(s) = K_v$$

The characteristics which affect the servo valve drive amplifier are the nominal maximum demand current, the maximum current which can be applied without damaging the valve coils, and the values of coil-resistances and inductances.

In practice, a servo valve proves to be a highly non-linear device whose actual dynamic response varies with operating conditions, *e.g.* hydraulic supply temperature and pressure, signal input level, valve loading, *etc.* These effects are usually negligible for performance about the valve design operating point, and linear analysis techniques are adequate for inputs of the order of 25% rated current. A more complete account of servo valve dynamic performance with empirical approximations which can be used in system design is given in the publication, Ref. 8.

Hydraulic Rams

The hydraulic ram dimensions are determined from the maximum force to be applied to the component, the ram differential pressure, and the ram stroke. Thus:

$F = A\,P$ lbf.

F = output force (lbf).

A = net piston area (in²).

P = differential pressure (lbf/in²).

Oil-column resonant frequency is an important consideration in the use of hydraulic rams and can represent a limitation on the performance of the servo system. The overall apparent bulk modulus of the valve/ram combination will be considerably lowered by using flexible tubing between the valve and ram. The oil column stiffness combined in parallel with the component stiffness forms a resonant frequency which should be considerably higher than the desired system frequency response limit to avoid creating a closed loop stability problem. The ram stroke should in general be kept to a minimum in order to reduce the volume of oil enclosed in the ram. Neglecting load and piston damping, and assuming a rigid ram cylinder and valve connexions, the oil column stiffness is given:

$$K_o = \frac{A^2B}{V} \text{ lbf/in}$$

B = oil bulk modulus (lbf/in²).

V = total half volume of the ram, provided that piston movements are small and about the stroke centre position (in³).

The resonant frequency is:

$$F_n = \frac{1}{2\pi}\sqrt{\frac{(K_O + K_L)}{M}} \text{ Hz}$$

K_L = component stiffness (lbf/in).

M = load and piston effective dynamic mass (lb).

Usually the hydraulic stiffness is greater than the load stiffness, and the resonant frequency is well outside the frequency range of interest here.

Fig. 4. Fatigue test rig. Frequency response up to 40Hz dynamic force ±3½tonf. (School of Engineering Science, University of Warwick.)

Dynamically the ram acts as a pure integrator, providing there is no excessive seal or bearing oil leakage from the ram cylinder. Thus:

$$G_R(s) = \frac{1}{sA}$$

Since the load combination will not affect the frequency range of interest, the gain of the hydraulic ram for the system design is:

$$K_R = \frac{1}{A}\left(\frac{1}{\text{in}^2}\right)$$

Differential area rams can be used and compensation of the unequal area is made by the closed loop control action. Static and dynamic forces can be applied together. The application of a static force gives a hydraulic pressure difference across the piston and thus the peak value of

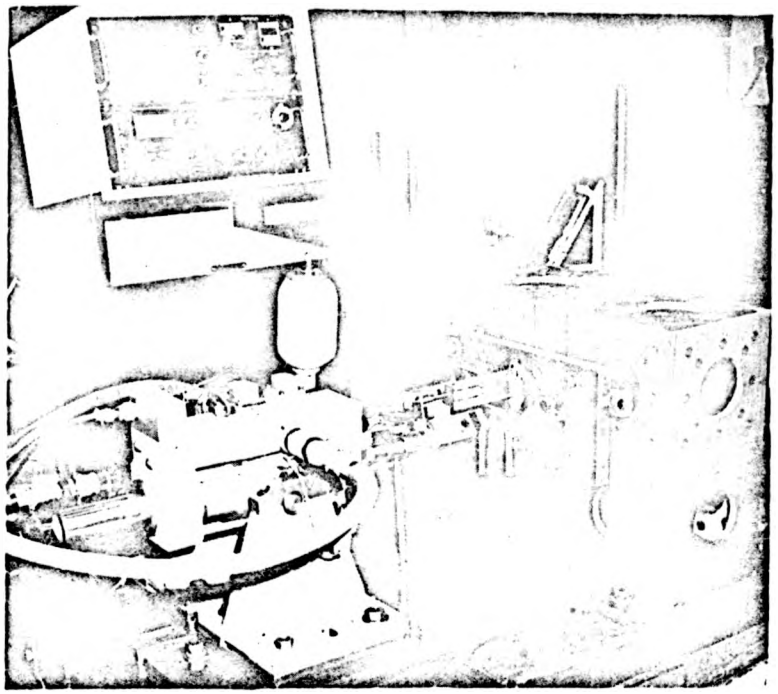

Fig. 5. Fatigue test rig. Trunnion mounted hydraulic ram driven by two servo valves in parallel. (Courtesy Ford Motor Co. Ltd.)

the dynamic load which can be applied about this static load is reduced. A wide range of commercial hydraulic rams with various types of mounting are available. Cylinder damping is recommended to prevent shock loading. Two other factors influence the choice of the hydraulic ram, *viz* ram friction and asymmetric load reaction forces

Seal and bearing friction is important. It is preferable to use a combination of rubber wiper seals with p.t.f.e. lined bearings and p.t.f.e. piston seals. Excessive friction will cause non-linear stick-slip piston rod movement. The amount of friction does effect the system response to small input signals, *i.e.* system resolution, which is mentioned in Ref. 6. System resolution can be improved by dithering the valve. Four hundred Hertz is the usual order of valve dither frequency.

The other main factor is the severity of the component load reaction forces experienced by the ram. Ram performance is best when driving into structurally symmetrical loads, *i.e.* in the axial push-pull mode, when industrial rams can usually be employed. Alignment of the component drive with the ram is important to avoid excessive side loading. Satisfactory performance under cantilever loading is not easy to achieve because the ram is subjected to side loads and bending moments which have to be counterbalanced by the ram bearings. Special ram designs may have to be made to suit these conditions and the ram mounted on a swivel or pivot so that it can "follow" component deformation.

Test Frame/Component Drive Considerations

The main point about the design of the test frame is to ensure that any mechanical resonant frequency falls outside the desired servo system frequency response limit by a factor of about ten. This avoids creating a closed loop stability problem from the test frame dynamic behaviour.

Normally components are not designed to resonate within the test frequency range. The component itself will form a resonant frequency:

$$F_c = \frac{1}{2\pi}\sqrt{\frac{K_c}{M_c}}\ \text{Hz}$$

K_c = component stiffness (lbf/in).

M_c = effective component mass (lb).

There are two approaches to the test frame design. The hydraulic ram and component can be mounted in a structural steel frame standing on an anti-vibration mounting. The framework can be welded and constructed from standard hollow tubular steel sections, making it stiff and light to give high natural frequencies, (Fig. 4). Alternatively, the design of mounting fixtures which can be clamped to a machined and keywayed base may be justified to give various component/ram layouts when many different components have to be tested (Fig. 5).

The component can be fixed between the ram and load cell, or the loadcell can be mounted on the piston rod. The load cell range determines the force capacity of the control system, and it should be closely matched to the test force range. Axial load cells should be compensated to eliminate any signal from bending due to misalignment. Achieved test rig component stresses are best measured by strain gauging the critical test areas and using a component static calibration to check the stresses achieved dynamically and calculated from the load cell output.

Difficulties with component drive attachments usually arise when loading is from tension to compression and allowance has to be made for rotational movement.

Backlash and waveform distortion can result from bearing drives. A spring steel strip clamped at both ends and designed to act as a strut is flexible and gives a solution under these conditions. With axial loading the component can be rigidly bolted in position but alignment is important to avoid inducing high clamping stresses. Useful design data is given in Ref. 9.

Assuming that the test frame is very stiff compared with the component stiffness, and that its dynamics do not contribute to the frequency range of interest, then the control loop design will only be affected by the load cell sensitivity and the component stiffness. The component is within the loop in a force control system. The load cell/component transfer function can be assumed frequency independent for the frequency range of interest here, so that for the system design:

K_c = component gain or stiffness; slope of load/deflexion graph (lbf/in)

K_L = load cell gain or sensitivity; depends on bridge supply volts (μV/lbf).

Trip Circuits

Trip circuits shut down equipment at component failure.

The microswitch is a reliable electromechanical trip which is triggered from component deflexion, either directly or by a lever or cam to amplify component movement. A plunger opens or closes electrical contacts which make or break an electrical circuit to shut down timers, hydraulic power pack, signal excitation, *etc.*

Thin wire can be included in a trip circuit and glued to the component surface to be broken as a fatigue crack propagates, although it is important to ensure that the gluing process does not affect the test results.

Another method is to pass a d.c. voltage through the component, providing it is held in grips which are electrically insulated from the test rig, and component fracture breaks the circuit.

A reliable electronic circuit which works from the fall in load cell dynamic signal at component failure is shown in Fig. 6, and can be used except for very slow cycling tests. The load cell signal is rectified and amplified by a differential input operational amplifier to drive a transistor which provides the necessary current to energize a number of reed relay coils. The trips are set at the start of a test by a d.c. voltage and held by the dynamic signal. Low frequency signal components are blocked. For sinewave testing the time constant of the feedback resistor/capacitor can be set to about 1s but for random signals it may need to be higher, perhaps between 5 and 10s, to prevent the circuit from tripping as the amplifier voltage falls during a period of low load signal.

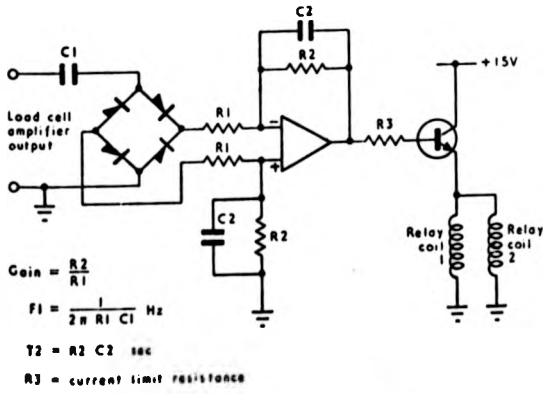

Fig. 6. Trip amplifier circuit

References

(1) Butzow, G. N. and Churchill, R. W. Electro-hydraulic Fatigue-Test-Systems Capabilities. Oct. 1964. MTS Systems Corporation, Minneapolis, Minnesota.

(2) Guillon, M. and translated by Griffiths, R. T. Hydraulic Servo Systems. Published by Butterworth & Co. Ltd., London. 1969.

(3) Morse, A. C. Electrohydraulic Servomechanisms. Published by McGraw-Hill. 1963.

(4) Osgood, R. E. How Contamination Affects Servo Valve Design. *Applied Hydraulics & Pneumatics*. Feb. 1959. Vol. 12, No. 2, p. 79-82.

(5) Kinney, W. and Weiss, P. What You Can Get in Electrohydraulic Servo Valves. *Applied Hydraulics & Pneumatics*. Feb. 1959. Vol. 12, No. 2, p. 67-78.

(6) Holzbock, W. G. Principles of Servo Valves—Part 1. *Hydraulics and Pneumatics*. Oct. 1960, Vol. 13, No. 10, p. 68-73.

(7) Johnson, H. C. Application of Electro-Hydraulic Servo Control to Physical Testing. Proceedings of National Conference on Fluid Power. 1964. Vol. 18, p. 125-136.

(8) Thayer, W. J. Transfer Functions for Dowty-Moog Servo Valves. Jan. 1965. Dowty Hydraulic Units Ltd., Tewkesbury, Gloucestershire.

(9) Heywood, R. B. Designing Against Fatigue. Published by Chapman & Hall Ltd., London. 1962.

SIMA Metrication Guide

THE Scientific Instrument Manufacturers' Association, (SIMA), have published a "Metrication Guide" for the use primarily of member companies.

The guide was compiled by the Metrication Working Party at the request of the Sima technical and standardization committee and is based on an extremely practical and comprehensive approach to the problems.

The guide, which is extensively illustrated, is divided into five major sections:

(1) Introduction to metric working.
(2) Drawing office practice.
(3) Reference material.
(4) Managerial, commercial and clerical information.
(5) Training and education.

Although the guide was produced as part of the service provided by Sima to all its members, it is considered that in view of the general interest throughout British industry in the complex issues involved, it should be made available to other organizations.

The price per copy to non-members of Sima, including packing and postage is 50/-d. Orders for single or multiple copies, which shou'd be accompanied by the necessary remittance, should be addressed in writing to Scientific Instrument Manufacturers' Association, 20, Peel Street, London, W.8, and should be endorsed "Metrication Guide".

The Fundamentals of Electrohydraulic Servo-controlled Fatigue Test Rig Design—Part 2

By B. C. FISHER, *Senior Research Associate and*
J. V. COMFORT, *Research Graduate, School of Engineering Science, University of Warwick.*

AN ELECTROHYDRAULIC servo system has a high performance with an overall quick response. The hydraulic system operates at high power levels while the electrical system carries low energy signals, but both systems have rapid response speeds. The electrical system is flexible, and the overall system response may be compensated by additional electrical circuits rather than by their more complex hydraulic equivalents.

The availability of monolithic and integrated circuit operational amplifiers has greatly simplified the electronic design problems in electrohydraulic servo systems. Manufacturers' data sheets include recommended balancing and stabilization circuits for a range of feedback configurations and performance figures aid the choice of a suitable amplifier for different applications. Reference 1 gives a useful guide for the design and application of operational amplifier circuits.

The regulation of commercially available power supplies permits their direct use for amplifier drive and load cell excitation. Once designed, the electronic equipment can be arranged in separate modules—control amplifier, valve drive amplifier, power supply, *etc.*—and mounted in standard racks (Fig. 1). Multiway screened electrical cable is used to connect the remote load cell and servo valve to this equipment.

The electronics of the basic electrohydraulic servo loop with component force sensed by a strain gauge bridge are shown in Fig. 2.

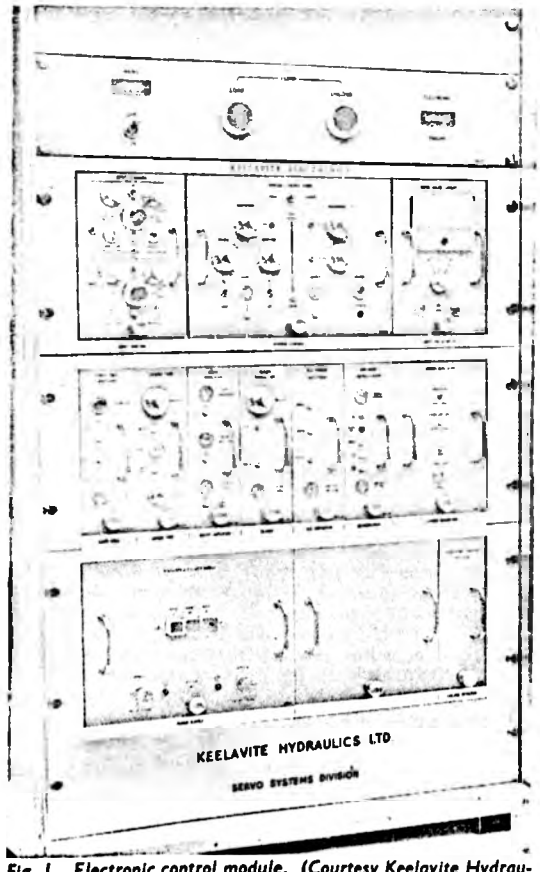

Fig. 1. Electronic control module. (Courtesy Keelavite Hydraulics Ltd.)

Stabilized Voltage Power Supply

The power supply provides the electronic component supply voltages, a voltage reference for the static load level, and the strain gauge bridge excitation for the load cell. Power supply rating is usually ±15V about earth with a current capacity up to 3A. The main factor to be considered in the specification of voltage stability is its effect on load cell measurement accuracy. Force measurement accuracies are normally in the region of 1% because of hysteresis and linearity errors of the load cell. Voltage changes on the load cell must not, therefore, cause a significant increase in this figure.

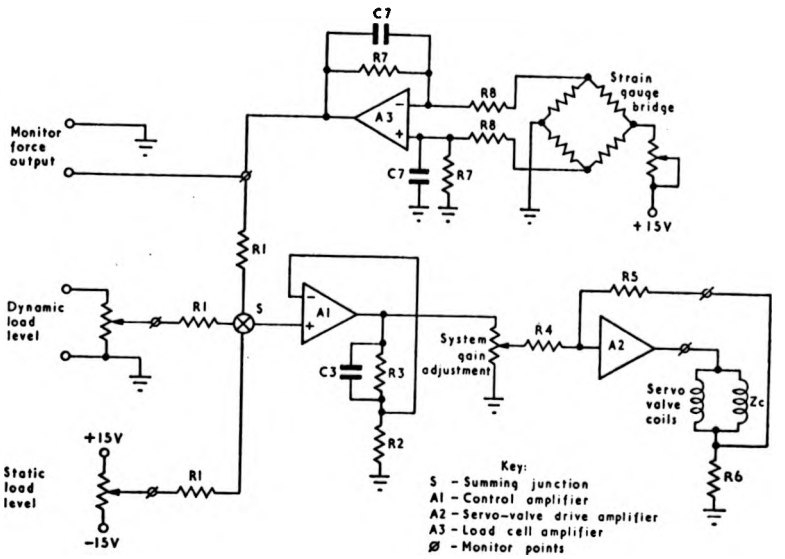

Fig. 2. Basic electronics of servo loop

Variations in stabilized voltage supply are due to:—

(a) *mains voltage fluctuations*;
(b) *ripple and noise in regulating circuits;*
(c) *load regulation caused by the supply having a finite output impedance*;
(d) *temperature changes which affect supply reference voltages and control circuits within the power supply itself.*

Their cumulative effect should be less than 0·25%. For a typical precision power supply available commercially the corresponding figures are:—

(a) 0·001% *for* ±10% *change in mains supply voltage*;
(b) 0·002%;
(c) 0·01% *no load to full load*;
(d) 0·2% *for* 10*degC temperature change.*

No design problems should be encountered here.

Load Cell Amplifier/Load Cell

The accuracy of the control loop is principally determined by the accuracy of the force measurement. The use of strain gauges for force measurement involves a high gain differential input operational amplifier in order to increase the measurement signal level to that comparable with the control loop command signal. Adequate consideration must be given to the effects of temperature, electrical interference and noise, amplifier gain and the feedback configuration if acceptable accuracy of force measurement is to be achieved[2]. Drift at the load cell amplifier is seen at the summing junction as an error in the static load level. This error causes the servo system to alter the static load level until the drift signal has been cancelled. To achieve accurate results it will be necessary to use a low drift, chopperless, differential input operational amplifier to amplify the load cell signal, together with metal film or metal oxide resistors which define the amplifier closed loop gain.

For the system design here, the frequency invariant amplifier gain is:

$$K_{A3} = \frac{R7}{R8}$$

K_{A3} = amplifier gain, usually 500 to 1000.

The strain gauge bridge resistance is usually about 250Ω. The bridge can be balanced by paralleling one arm with a variable resistance, usually of the order of 100kΩ. When the load cell amplifier output is monitored the input resistance of the monitoring equipment should be high, *e.g.* an oscilloscope; otherwise, the equipment causes electrical loading effects. A differential amplifier oscilloscope is required to monitor servo valve voltage. A voltage follower[1] is a useful buffer amplifier to insert between the control loop and monitoring equipment.

Control Amplifier

The control amplifier forms the difference or error between the input signal, which is the demanded force, and the measured force. The input may be the sum of a mean force level and a time varying demand. Similar considerations to those in the load cell amplifier design apply but since smaller gains are usually required, conditions are less stringent.

For the system design here the gain of the amplifier transfer function is:

$$K_{A1} = 1 + \frac{R3}{R2}$$

K_{A1} = control amplifier gain, usually 1 to 10.

Adjustment of the system gain potentiometer fixes the level of the amplified error voltage signal available at the servo valve drive amplifier input.

Servo Valve Drive Amplifier

The servo valve drive amplifier uses current feedback as opposed to voltage feedback. Operation in this mode helps to swamp any changes in coil resistance and inductance that occur due to changes in the temperature and reflected impedance of the hydraulic load. The purpose of this is to stabilize control loop gain and minimize the phase shift through the amplifier/valve combination. To protect the servo valve from excessive currents, a current limit should be incorporated in the amplifier design. Connecting the valve coils in parallel reduces their effective impedance and hence the drive current limitation due to amplifier output voltage saturation. However, this condition should not occur during normal testing.

Any small high frequency current demand, *e.g.* amplifier chopper frequency or signal carrier frequency, causes a high voltage across the valve coils. This affects the valve drive amplifier only, and if this voltage is limited by the amplifier supply voltages non-linear amplifier behaviour can result. Dither frequency and amplitude should be chosen so as not to cause amplifier voltage saturation.

The amplifier gain is expressed:

$$K_{A_2} = \frac{R5}{R4}\,\frac{10^{-3}}{R6}\left(\frac{mA}{V}\right)$$

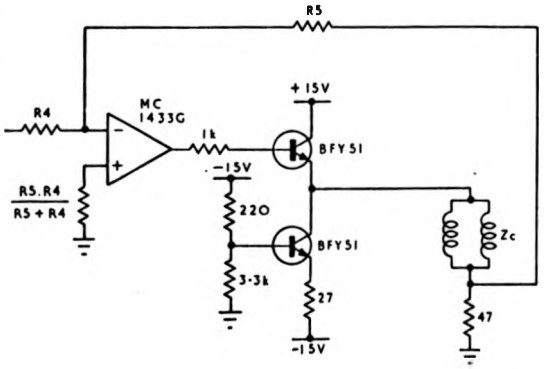

Fig. 3. Simple current amplifier circuit

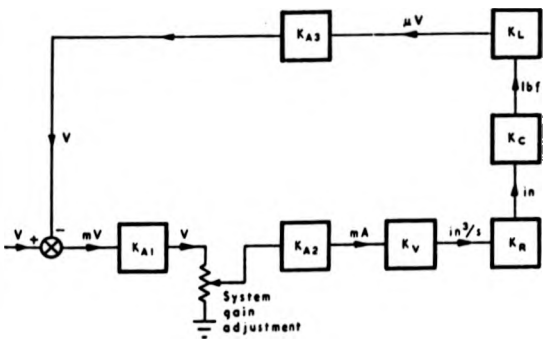

Fig. 4. Simplified block diagram of servo system

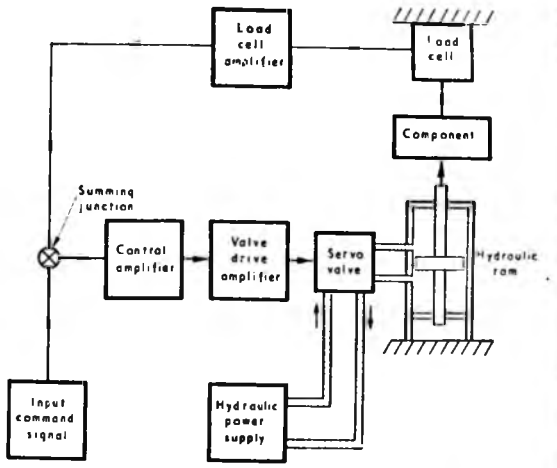

Fig. 1 (Part I). Basic electrohydraulic servo loop

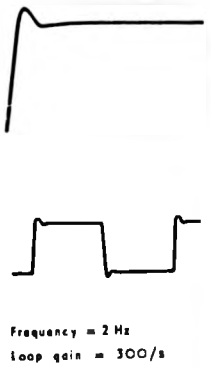

Fig. 5. Traces of servo system square wave response

Integrated circuits by themselves cannot normally be used to drive servo valves because of their limited output current. A useful circuit which will provide about ±15mA is shown in Fig. 3. This consists of an integrated circuit amplifier with a booster stage to supply the necessary current. The booster consists of a constant current emitter follower. The amplifier and booster stage is in itself a current control system and should be designed so as to ensure closed loop stability and an adequately damped transient response.

Servo valve manufacturers supply standard amplifier units to drive servo valves. The components in these amplifiers are readily accessible and adjustments to suit load impedance and gain are easily made.

Initial Loop Gain Setting

The initial loop gain is set to the highest value to give an adequately damped transient response. An approximate method for obtaining this value is given by:

$$K = \frac{1}{T}$$

Servo Valve Drive Amplifier

The servo valve drive amplifier uses current feedback as opposed to voltage feedback. Operation in this mode helps to swamp any changes in coil resistance and inductance that occur due to changes in the temperature and reflected impedance of the hydraulic load. The purpose of this is to stabilize control loop gain and minimize the phase shift through the amplifier/valve combination. To protect the servo valve from excessive currents, a current limit should be incorporated in the amplifier design. Connecting the valve coils in parallel reduces their effective impedance and hence the drive current limitation due to amplifier output voltage saturation. However, this condition should not occur during normal testing.

Any small high frequency current demand, *e.g.* amplifier chopper frequency or signal carrier frequency, causes a high voltage across the valve coils. This affects the valve drive amplifier only, and if this voltage is limited by the amplifier supply voltages non-linear amplifier behaviour can result. Dither frequency and amplitude should be chosen so as not to cause amplifier voltage saturation.

The amplifier gain is expressed:

$$K_{A_2} = \frac{R5}{R4}\,\frac{10^{-3}}{R6}\left(\frac{mA}{V}\right)$$

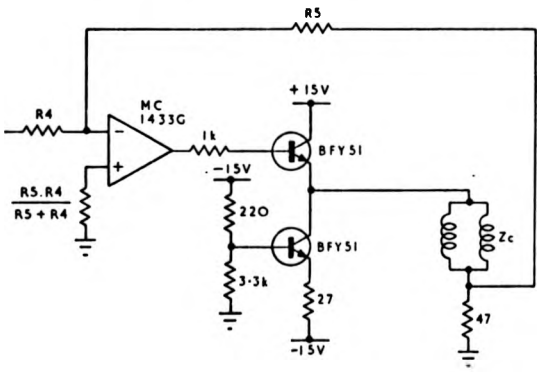

Fig. 3. Simple current amplifier circuit

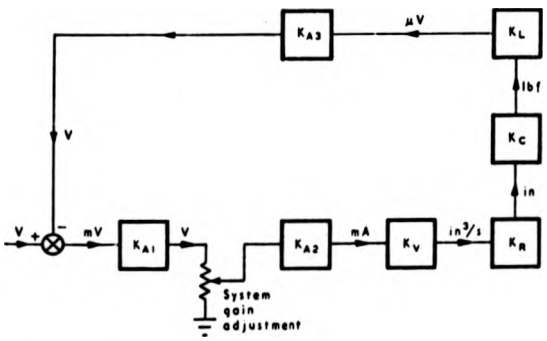

Fig. 4. Simplified block diagram of servo system

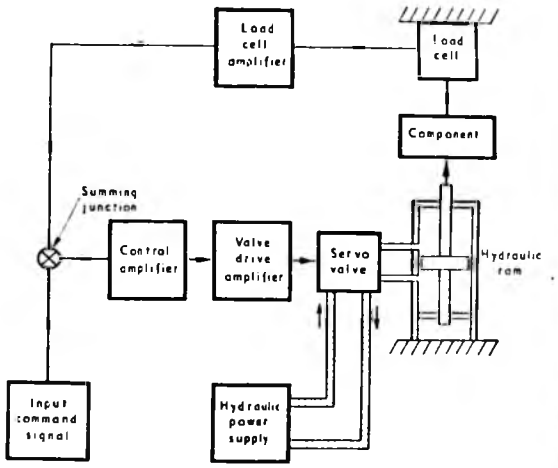

Fig. 1 (Part I). Basic electrohydraulic servo loop

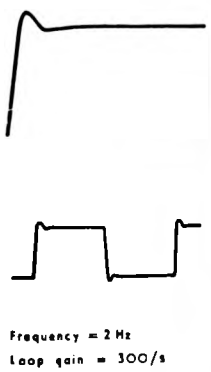

Fig. 5. Traces of servo system square wave response

Integrated circuits by themselves cannot normally be used to drive servo valves because of their limited output current. A useful circuit which will provide about ±15mA is shown in Fig. 3. This consists of an integrated circuit amplifier with a booster stage to supply the necessary current. The booster consists of a constant current emitter follower. The amplifier and booster stage is in itself a current control system and should be designed so as to ensure closed loop stability and an adequately damped transient response.

Servo valve manufacturers supply standard amplifier units to drive servo valves. The components in these amplifiers are readily accessible and adjustments to suit load impedance and gain are easily made.

Initial Loop Gain Setting

The initial loop gain is set to the highest value to give an adequately damped transient response. An approximate method for obtaining this value is given by:

$$K = \frac{1}{T}$$

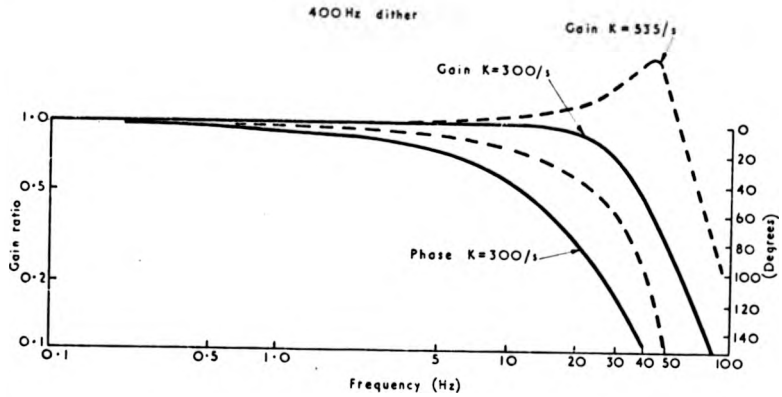

Fig. 6. Closed loop response (without compensation)

K = loop gain.
T = servo valve time constant obtained from manufacturer's data.

The units of loop gain are s^{-1} since the loop contains an integrating element. The loop gain is given (Fig. 4) by:

$$K = R \times K_{A_1} K_{A_2} K_V K_R K_C K_L K_{A_3}$$

R = attenuation factor of the system gain potentiometer.

Subsequent to the closed loop identification, compensation can be designed to extend the frequency response.

To check correct operation of the control system the pressure is set at about 500lbf/in² and with the system gain potentiometer at about a quarter full turn, mean loads are applied to the component from the static level control. It is important to ensure negative feedback of the load cell voltage. Once correct control operation has been established, the full 3000lbf/in² supply pressure can be used and the final adjustment of the system gain made to provide a well damped transient response from a step input (Fig. 5).

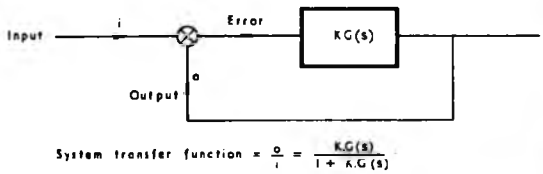

Fig. 7. Simplified operational flow diagram of servo system

Design Example

A dynamic response from the fatigue test rig (Fig. 1, Part 1), was required which would substantially reproduce a random signal input with a frequency content from d.c. to 25Hz, and peak dynamic forces of 7000lbf about a mean tensile load of 1000lbf.

The hydraulic power supply working pressure is 3000lbf/in². The differential area hydraulic ram has a 2·5in dia. bore with a 1in dia. piston rod and 2in stroke. The servo valve is a Moog Series 22 with a rated flow of 40in³/s and a time constant of approximately 0·0026s. The gains of the loop components were given values:

$K_C = 2 \times 10^4$lbf/in
$K_{A_1} = 2$
$K_{A_2} = 37$mA/V
$K_V = 2{\cdot}67$in³/s/mA
$K_L.K_{A_3} = 1{\cdot}25$mV/lbf
$K_R = 0{\cdot}22 \frac{1}{\text{in}^3}$

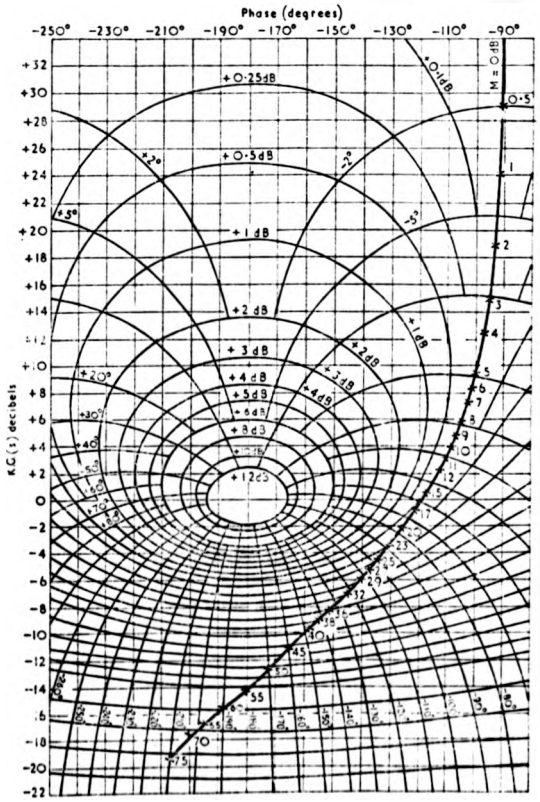

Fig. 8. (right) Open loop—closed loop conversion (contours of constant gain and phase of $\frac{K.G(s)}{1 + K.G(s)}$ *for input KG(s)*

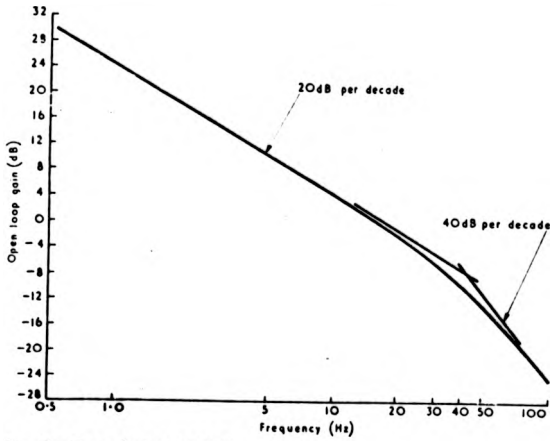

Fig. 9. Open loop response

The total loop gain is:

$$K = R \times 11\,000 \frac{1}{s}$$

Adjustment of R gave the closed loop response shown in Fig. 6.

To substantially reproduce a random input signal in a test rig, a loop transfer function is required which has a flat amplitude response and a phase lag not greater than about 45° within the input signal frequency range. The servo system performance was improved to meet these demands by introducing electrical compensation networks. In force feedback systems the open loop transfer function is such that a simple compensating network can usually be employed, *e.g.* phase advance compensation. The required form of compensation is derived from the open loop transfer function.

For the purposes of analysis the assumption of linear operation can be made. The inherent integrating action of the servo valve/hydraulic ram combination makes it necessary for the open loop identification to be made under closed loop conditions. This was achieved using a digital transfer function analyser[3]. If a transfer function analyser is not available, accurate measurements of the voltage feedback input signal amplitude ratio (dB) and phase displacement (degrees) can be made using an oscilloscope with time delay facilities, or from ultra-violet recordings of the input and feedback signals.

The open loop transfer function can be quickly derived from the closed loop transfer function using the Bode-diagram-phase-angle-Nichols-chart method. The servo system can be represented by the operational diagram shown in Fig. 7, a form which can be directly analysed using a Nichols chart, where K is the loop gain and G(s) the frequency dependence of the loop transfer function.

The flat closed loop response of Fig. 6 is plotted for specific frequencies on the Nichols chart, (Fig. 8), using the contour gain and phase lines.

The open loop response is determined by reverse use of the Nichols chart by reading the gain and phase for each frequency from the cartesian scale. This response is shown in the form of a Bode diagram, (Fig. 9).

Neglecting effects below 0·1Hz where measurements were difficult the loop consisted of an integrator (the hydraulic ram) and a first order lag with a break frequency of about 40Hz (the servo valve). These were the only significant dynamics in the frequency range of interest.

To compensate for this lag a lead term is introduced into the control amplifier with a breakpoint frequency of 40Hz. This was done by paralleling the summing point feedback and dynamic input resistors with a capacitor. With a small increase in loop gain the closed loop response shown in Fig. 10 was achieved. Lags which are introduced into the measurement and control amplifiers to attenuate noise prevent any further extension of the frequency response.

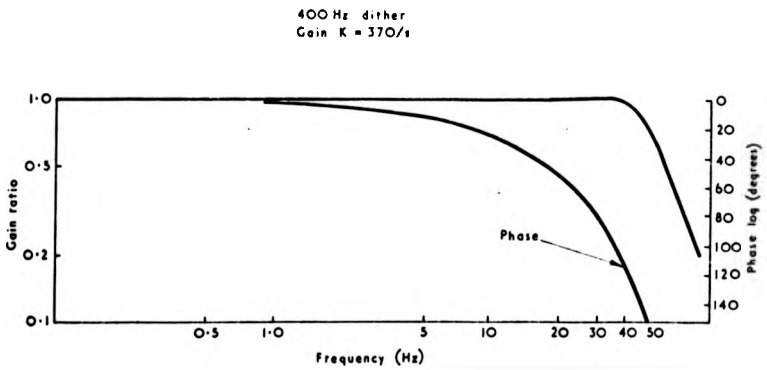

Fig. 10. Closed loop response (with compensation)

References

(1) Handbook of Operational Amplifier Applications. Published 1963, copyright Burr Brown Research Corporation. General Test Instruments Ltd., Huccleote, Gloucester.

(2) FISHER, B. C. Application of Strain Gauge Transducers to Electrohydraulic Test Systems. *Instrument Practice*. Vol. 24, No. 4. April, 1970.

(3) ELSDEN, C. S. AND LEY, A. J. A Digital Transfer Function Analyser Based on Pulse Rate Techniques. *Automatica*, Vol. 5, No. 1. January, 1969.

THE APPLICATION OF ON LINE OPTIMISATION TO SPARK IGNITION ENGINE DEVELOPMENT

J.V.Comfort

While it is not anticipated that on line optimisation will in the near future be applied directly to vehicle engine control, its use in the automotive industry as a development engineer's aid is expected to become well established. Indeed, regulations concerning vehicle exhaust emissions are becoming so demanding that it is impossible to foresee how the development engineer will be able to execute his duties efficiently without the aid of on line computational facilities, part of whose function will be optimisation.

Already in routine engine testing applications the on line digital computer has shown itself to be a valuable tool (2) Although very few computer controlled engine test installations have been commissioned the more ambitious schemes are sufficiently flexible to allow the running of off-line programs on a time shared basis. This facility permits the development of optimisation routines. A logical step forward from the present situation is to delegate more of the engine development work load to the computer, and this will necessarily involve optimisation.

A further advantage in computer control of engine testing is that test procedures must be defined far more rigorously than is necessary with manually controlled testing. As a result decisions can now be based upon more reliable data and the subjective element in testing is eliminated. The tremendous time saving in test data processing makes optimisation realisable where previously it would never have been attepted.

Initial studies concerned with the optimisation of ignition timing and air/fuel ratio to maximise output torque using analog computation techniques have demonstrated the feasibility of such an operation (1). Early investigators failed to point out two salient points concerning the combustion process. Firstly combustion is a discrete process. Any changes in operating conditions will not take effect until the combustion process is initiated, and the results of these changes will not manufest themselves until after the combustion cycle is complete. Secondly, the process is irregular, and any measurements associated with it may be considered as being contaminated by noise. This necessitates the filtering of output data if they are to be used in the evaluation of performance criteria.

J.V. Comfort is with the I.U.I.E.C. at The University of Warwick.

These two facets of the combustion process must be considered in the design of any optimisation system. The discrete behaviour sets the absolute limit to optimiser speed. Other limitations are imposed by actuator and measurement dynamics as well as any other dynamic behaviour associated with the engine test bed and the requirement for output data filtering.

The most obvious application of optimisation to the spark ignition engine is in the control of spark timing to maximise output torque. The application of this to an experimental test bed is considered.

Computer controlled engine test facility. A computer controlled engine test facility has been developed at the University of Warwick to facilitate the study of control and optimisation problems. The control programs which execute the optimisation described also provide alarm monitoring and automatic starting and stopping of the engine In the case where maximal length sequence and square wave perturbations are applied the computer also services a d.d.c. algorithm to control dynamometer field current and maintain constant speed operation. Where sinusoidal perturbations are applied the optimisation is achieved with a small analog computer and a local analog speed control.

Ignition timing control. A digital system was developed to control ignition timing (3). The control introduced no dynamics into the optimisation system, since it was possible to make full scale changes in ignition timing between adjacent firings. The mode of operation of the control is described with reference to fig.1. At 50° B.T.D.C. a count of each degree of crankshaft rotation is initiated. The count is converted into an analog voltage. When this voltage exceeds the input voltage the ignition is fired electronically and the counter reset and inhibited until the next count is required. Crankshaft rotation is monitored by photoelectric transducers.

Torque measurement. The engine output torque was measured on the coupling shaft between the engine and the dynamometer. This method provided a faster measurement than from the dynamometer weighing gear. A strain gauge bridge controls the frequency of an oscillator, both being fitted to the shaft. The frequency signal is transmitted from the shaft via slip rings and demoduated. The final analog voltage measurement has a flat frequency response up to 10Hz, as against 0.2Hz for the dynamometer weighing gear.

Experimental results. Some examples of ignition timing/torque hills, obtained under constant speed and throttle operation, are shown in fig.2. The results were plotted by the computer during an on-line test. (In this case the torque measurements were derived from the dynamometer weighing gear which was fitted with a potentiometer.) Although each curve has a single maximum, the various maxima are not sharply defined. The curve plotted at 1250 R.P.M. shows this tendency.

All the methods employed formed only an estimate of the first derivative of the function to be maximised. The problem of measurement noise precluded the use of methods which utilised higher derivatives. The perturbation methods applied were 2 and 3-level maximal length sequences, square waves and sine waves.

Both the 2 and 3-level sequences were used as a means to determine the local impulse response. Integration of this impulse response yielded the step response and hence an estimate of the first derivative of the function. The 2-level sequence had a length of 31 bits and a period of 0.6 seconds while the 3-level sequence had a length of 26 bits and a period of 0.5 seconds. The effect of perturbation amplitude was most marked and the results obtained with larger perturbations showed a correspondingly smaller variance.

The most promising result obtained using maximal length sequences was obtained with the 3-level sequence. In this particular case the impulse response was estimated by averaging over two periods of the perturbation waveform. The response obtained with this method was estimated to have a variance of 3° and took 12 seconds to reach the optimum with an adjustment of 35°.

Square wave perturbations are advantageous in so much as they are considerably easier to apply than pseudo-random sequences. Square wave perturbations were applied with periods of 5 and 2.5 seconds and under the same conditions the optimum was reached in 120 seconds. This time a smaller variance of approximately 1° was ascribed to the final result.

The analog optimiser using sinussoidal perturbations was subject to integrator drift. When care was taken to ninimise the effect of this some quite encouraging results were obtained. Again under similar conditions the optimum was reached in 7 seconds with an estimated variance of 1°. Faster results were attainable, but at the expense of increased variance. Fig. 3 shows the responses of 3-level m-sequence and sinusoidal optimisers.

The initial studies suggest that gradient estimation techniques based on pseudo-random perturbations need to be applied with caution. Gradient estimates must be derived from the averaged results of several periods of perturbation. An adequate knowledge of the noise power spectrum of the torque signal was deemed essential and was later obtained by performing a fast Fourier Transform on line. The power spectrum was used to predict the accuracy of the sinusoidal optimiser. The predicted accuracy gave favourable agreement with that of the system using sinusoidal perturbations. The power spectrum contained significant components around 1 Hz. These must be taken into account by any filtering system.

The bias associated with the estimates of the optimum under noise free conditions was evaluated for various perturbation waveforms and amplitudes. This was achieved by fitting

a polynomial to the ignition timing/torque hill. Surprisingly large perturbation amplitudes are required to attach a significant bias to the estimate of the optimum. Perturbation amplitudes of 10^{0} were quite acceptable and gave rise to bias errors of less than 0.25^{0}.

Further on line optimisation will apply digital filtering to the torque signal from the dynamometer weighing gear, which in itself performs mechanical filtering. Parameter adjustment will be based on gradient estimates from torque measurements sampled over several seconds as a result of step perturbations. This technique is simply a formal execution of the methods used by the manual optimisation process.

Further studies to investigate the simultaneous optimisation of ignition timing and mixture strength to minimise specific fuel consumption are proceeding at this time. It is felt that the implementation of this two parameter optimisation can show a tremendous time saving compared with manual testing methods.

References.

1.C.S.Draper and Y.T.Li. 'Principles of optimalising systems and an application to an internal combustion engine.' A.S.M.E. publication 1951.

2.G.Williams and E. Muir. 'A study of closed loop control and data acquisition for engine test cells.' S.A.E. paper no. 680134.

3.'Electronic Ignition timing'. The Chartered Mechanical Engineer. November 1969

Acknowledgements. The on line optimisation experiments using pseudo-random and square wave perturbations were performed by J.Monk and the fast Fourier Transforms were programmed and executed by P.E.Wellstead. The author wishes to acknowledge the help and encouragement of colleagues associated with this research program.

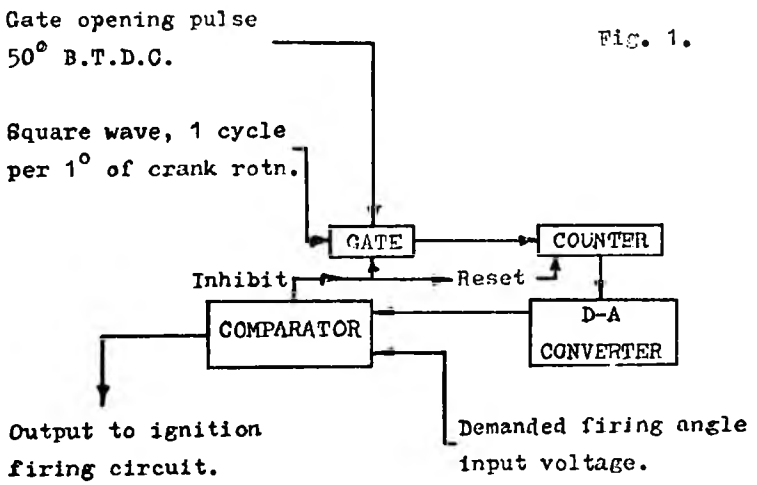

Fig. 1.

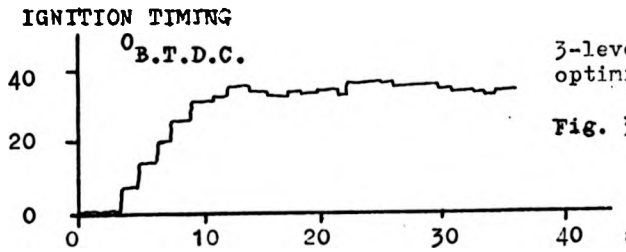

3-level m-sequence optimiser response.

Fig. 3a.

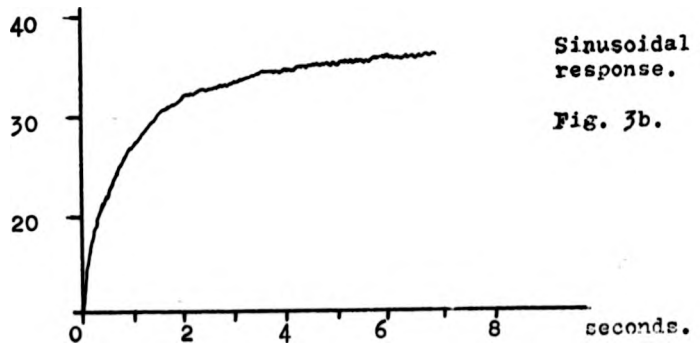

Sinusoidal optimiser response.

Fig. 3b.

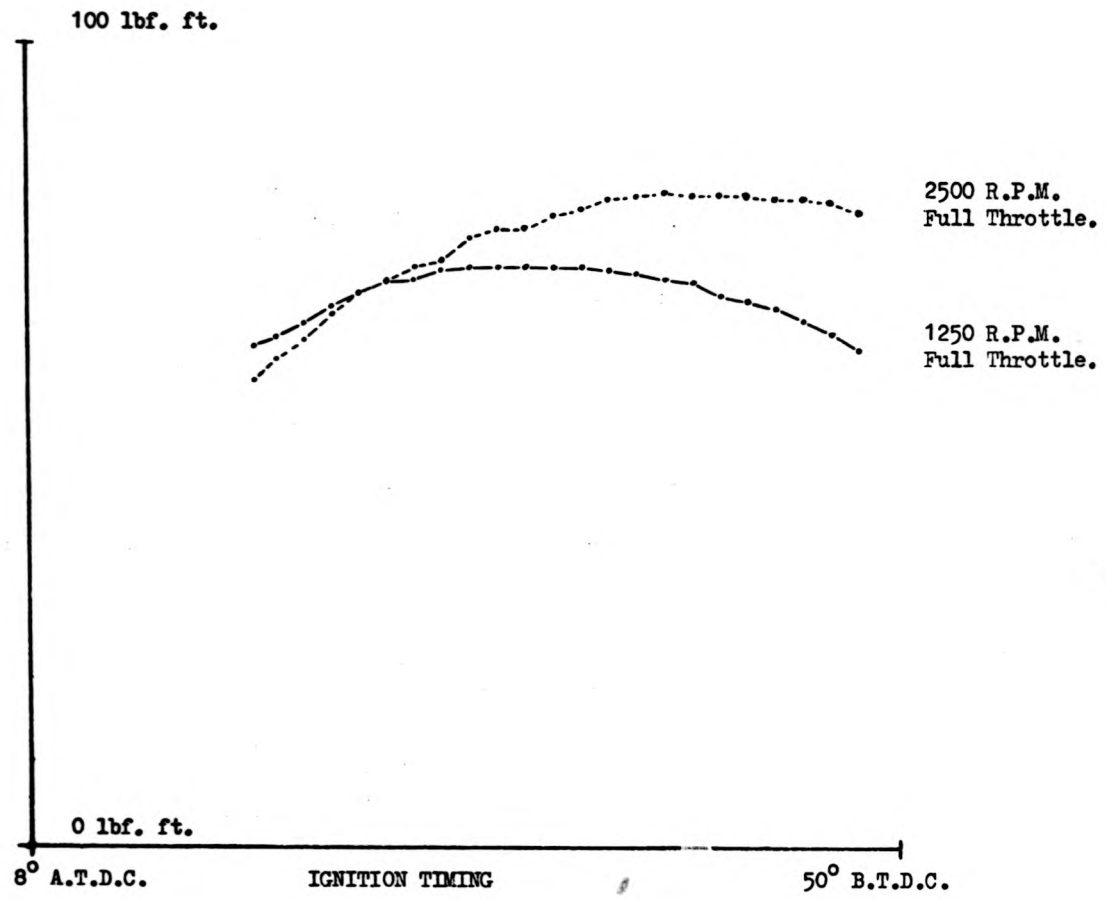
TORQUE
100 lbf. ft.
2500 R.P.M.
Full Throttle.
1250 R.P.M.
Full Throttle.
0 lbf. ft.
8° A.T.D.C.
IGNITION TIMING
50° B.T.D.C.

Fig. 2.

3

D30198 '8

END